DISSERTATION

SYNTHESE UND REAKTIVITÄT NEUER EISEN-, MOLYBDÄN- UND WOLFRAMKOMPLEXE

Ausgeführt zum Zwecke der Erlangung des akademischen Grades eines Doktors der technischen Wissenschaften

unter der Leitung von

Prof. Dr. Karl Kirchner

Institut für Angewandte Synthesechemie 163/AC

eingereicht an der Technischen Universität Wien

Technische Chemie Fakultät

Von

DI Özgür Öztopcu

Matr. Nr: 526954

Aloisgasse 1/3, 1020 Wien

18.10.2013

Kurzfassung

Im ersten Teil der Arbeit wurden die Komplexe [FeCp(CO)(κ^2(*C,P*)-(C=O)-N*i*Pr-PPh_2)], [FeCp(CO)(κ^2(*C,P*)-(C=O)-N*t*Bu-PPh_2)] und [FeCp(CO)(κ^2(*C,P*)-(C=O)-NCy-P*i*Pr_2)] mit den Amidophosphin Liganden Li[R_2PNR'] (R = Ph, *i*Pr, R' = *i*Pr, *t*Bu, Cy) hergestellt. Diese Komplexe besitzten einen viergliedrigen Carboxyamido-phosphazyklus, welche durch einen nucleophilen Angriff von Stickstoff auf den Kohlenstoff der Carbonylgruppe entsteht. Wenn diese Komplexe mit dem Elektrophil [Me_3O]BF_4 umgesetzt werden, entsteht ein Aza-phospha-carbenkomplex vom Typ [FeCp(CO)(κ^2(*C,P*)=C(OMe)-N*i*Pr-PPh_2)]$^+$. Durch Umsetzung der Komplexe *cis,trans,cis*-[Fe(Ph_2PNH*i*Pr)$_2$(CO)$_2$($Br)_2$] und *cis,trans,cis*-[Fe(Ph_2PNH*t*Bu)$_2$(CO)$_2$($Br)_2$] mit KO*t*Bu entstehen ebenfalls Verbindungen mit einem viergliedrigen Carboxyamido-phosphazyklus, wie zum Beispiel *trans*-[Fe(Ph_2PNH*i*Pr)(CO)$_2$(κ^2(*C,P*)-(C=O)-N*i*Pr-PPh_2)Br] und *trans*-[Fe(Ph_2PNH*t*Bu)(CO)$_2$(κ^2(*C,P*)-(C=O)-N*t*Bu-PPh_2)Br].

Im zweiten Teil der Arbeit wurden die oktaedrischen Mo(0) und W(0) Komplexe [M(PNP)$(CO)_3$], sowie die oktaedrischen neutralen und siebenfach-koordinierten kationischen Mo(II) und W(II) Komplexe [M(PNP)(CO)X_2], [M(PNP)$(CO)_3$Br]$^+$, [M(PNP)$(CO)_3$H]$^+$ mit dreizähnigen PNP Pincer Liganden hergestellt (X = Br, I und Cl). Die Synthese von Mo(0) Komplexen erfolgte durch Umsetzung von [$Mo(CO)_3(CH_3CN)_3$] mit PNP Liganden. Die W(0) Komplexe wurden durch die Reduktion von den Komplexen [W(PNP)$(CO)_3$Br]$^+$ mit NaHg hergestellt, welche durch Umsetzung vom zweikernigen Komplex [$W(CO)_4(\mu$-Br)Br]$_2$ mit den PNP Liganden hergestellt wurden. Die Synthese von den Hydridocarbonylkomplexen erfolgte durch Umsetzung von den Mo(0) und W(0) Komplexen mit HBF_4. Diese Komplexe sind in der Lösung dynamisch und können mit Basen, z.B. NEt_3, vollständig zu [M(PNP)$(CO)_3$] deprotoniert werden. Wenn die Mo(0) Komplexe mit Halogenen in Anwesenheit des Sauerstoffs umgesetzt werden, entstehen kationische Monooxo-Molybdänkomplexe vom Typ [Mo(PNP)(O)X]$^+$. Diese Reaktion verläuft über koordinativ ungesättigte mono CO Komplexe [M(PNP)(CO)X_2].

Abstract

In first part of this study the complexes [FeCp(CO)(κ^2(*C,P*)-(C=O)-N*i*Pr-PPh_2)], [FeCp(CO)(κ^2(*C,P*)-(C=O)-N*t*Bu-PPh_2)] and [FeCp(CO)(κ^2(*C,P*)-(C=O)-NCy-P*i*Pr_2)] were produced with adding 1 equiv of the amidophosphine ligands Li[R_2PNR'] (R = Ph, *i*Pr, R' = *i*Pr, *t*Bu, Cy) to [FeCp$(CO)_2$Cl]. Complex [FeCp(CO)(κ^2(*C,P*)-(C=O)-N*i*Pr-PPh_2)] was also formed when [FeCp(PPh_2NH*i*Pr)$(CO)_2]^+$ was reacted with 1 equiv of KO*t*Bu. These complexes feature an unusual four-membered carboxamido-phospha-ferracycle as a result of an intramolecular nucleophilic attack of the amidophosphine ligand on coordinated CO. Upon treatment of [FeCp(CO)(κ^2(*C,P*)-(C=O)-N*i*Pr-PPh_2)] with the electrophile [Me_3O]BF_4 the aminocarbene complex [FeCp(CO)(κ^2(*C,P*)=C(OMe)-N*i*Pr-PPh_2)]$^+$ was obtained bearing an aza-phospha-carbene moiety. Upon treatment of *cis,trans,cis*-[Fe(Ph_2PNH*i*Pr)$_2(CO)_2(Br)_2$] and *cis,trans,cis*-[Fe(Ph_2PNH*t*Bu)$_2(CO)_2(Br)_2$] with KO*t*Bu the carboxamido-phospha-ferracycles *trans*-[Fe(Ph_2PNH*i*Pr)$(CO)_2$(κ^2(*C,P*)-(C=O)-N*i*Pr-PPh_2)Br] and *trans*-[Fe(Ph_2PNH*t*Bu)$(CO)_2$(κ^2(*C,P*)-(C=O)-N*t*Bu-PPh_2)Br] were formed.

In the second part a series of Mo(0) and W(0) complexes [M(PNP)$(CO)_3$] as well as seven coordinate cationic hydridocarbonyl and halocarbonyl Mo(II) and W(II) complexes of the type [M(PNP)$(CO)_3$H]$^+$ and [M(PNP)$(CO)_3$X]$^+$ and octahedral neutral [Mo(PNP)(CO)X_2] featuring PNP pincer ligands were prepared. The synthesis of Mo(0) complexes [Mo(PNP)$(CO)_3$] was accomplished by treatment of [Mo$(CO)_3(CH_3CN)_3$] with the respective PNP ligands. The analogous W(0) complexes were prepared by reduction of the bromocarbonyl complexes [W(PNP)$(CO)_3$Br]$^+$ with NaHg. These intermediates were obtained from the known dinuclear complex [W$(CO)_4$(μ-Br)Br]$_2$, prepared in situ from W$(CO)_6$ and stoichiometric amounts of Br_2. Addition of HBF_4 to [M(PNP)$(CO)_3$] resulted in clean protonation at the molybdenum and tungsten centers to generate cationic Mo(II) and W(II) hydride complexes [M(PNP)$(CO)_3$H]$^+$. The protonation is fully reversible and upon addition of NEt_3 as base the Mo(0) and W(0) complexes [M(PNP)$(CO)_3$] are regenerated quantitatively. All heptacoordinate complexes exhibit fluxional behavior in solution. Treatment of Mo(0) complexes with halogens in the presence of oxygen afforded cationic monooxo complexes of the type [Mo(PNP)(O)X]$^+$. This Reaktion proceeds via the Mo(II) intermediates [Mo(PNP)(CO)X_2].

Mein Dank gilt

Prof. Kirchner für die Unterstützung bei der Umsetzung eigener Ideen, für viele Anregungen und interessante Diskussionen und die Freude an der Chemie, die er allen vermittelt und für die Durchführung der DFT Berechnungen, die meine Arbeit bereichert haben.

Prof. Mereiter für die Durchführung vieler Röntgenstrukturanalysen und die vielen wissenschaftlichen und auch nichtwissenschaftlichen Diskussionen.

Prof. Weil und Dr. Stöger für die Durchführung von Röntgenstrukturanalysen.

Dr. Puchberger für die Durchführung von Tieftemperatur-NMR Messungen.

Dr. Sven Barth für die gute Freundschaft.

Meine Kollegen DI Christian Holzacker, DI Bernhard Bichler, DI Nikolaus Gorgas, Mathias Glatz und Matthias Mastalir für die gute Zusammenarbeit.

Meinen Eltern und meinen Schwestern für ihr Verständnis und ihre Unterstützung.

Inhaltsverzeichnis

Allgemeiner Teil

Spezieller Teil

Experimenteller Teil

Anhang

Literaturverzeichnis

Allgemeiner Teil

Einleitung und Problemstellung (Eisenkomplexe)

Aminophosphinliganden PR_2NHR' sind multifunktionelle Liganden mit einer polaren P(III)-N Bindung und werden häufig als vielseitige Liganden für Übergangsmetalle verwendet.[1] Für die Synthese werden primäre oder sekundäre Amine und PR_2Cl verwendet. Um sterischen und elektronischen Eigenschaften zu variieren, können die Liganden durch Alkyl oder Arylgruppen beliebig modifiziert werden. Wegen der „soft/hard“ Atomkombination und dem aciden NH zeigen diese Liganden eine Vielzahl von unterschiedliche Koordinationsmöglichkeiten (Schema 1).

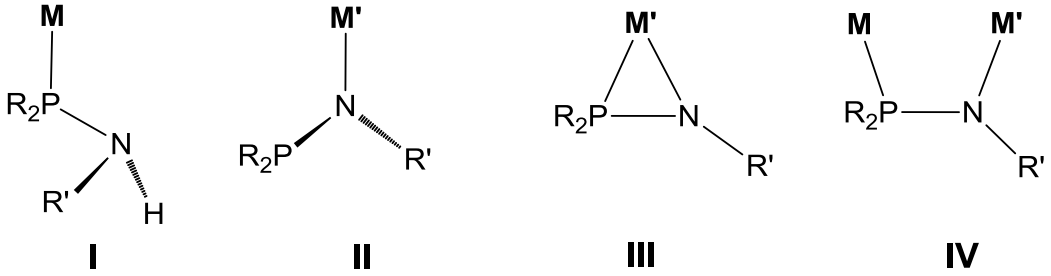

Schema 1: Häufige Koordinationsmöglichkeiten von PR_2NHR'-Liganden

Bei mittleren und späten Übergansmetallen findet man in der Regel eine $\kappa^1(P)$-Koordination **(I)**. Bei deprotonierten PR_2NHR' Liganden findet man eine $\kappa^1(P,N)$ **(III)** und $\kappa^1(N)$ **(II)** Koordination (Schema 1). In Kombination mit frühen und späten Übergansmetallen gibt es μ^2-gebrückte Komplexe vom Typ **(IV)**.[3,4]

Überdies zeigen PR_2NHR' Liganden eine Vielzahl von intramolekularen Reaktionen. Vinyliden und Allenyliden Ruthenium Komplexe vom Typ $[RuCp(PPh_2NHR)_2(=C=(C)_n=CHR')]^+$ und $[RuTp(PPh_2NHR)_2(=C=(C)_n=CHR')]^+$ (n = 0, 1; R = Ph, *n*-Pr; R' = alkyl, aryl), kommt es zu einer intramolekularen Addition von NHR' an den α-Kohlenstoff und es bildet sich ein viergliedriges Aza-phospha-carben (Schema 2, 3, **A**).[5]

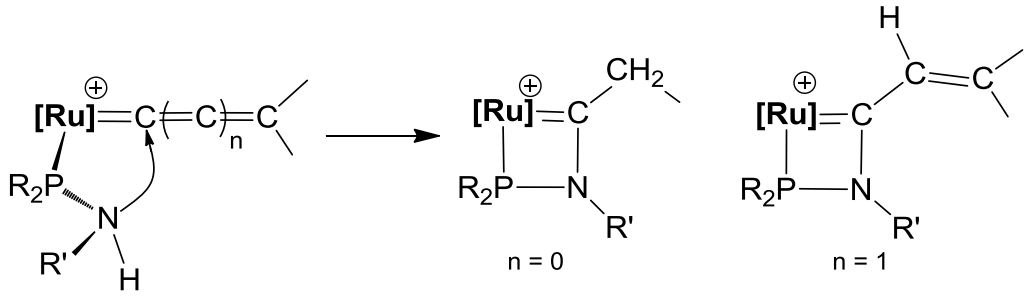

[Ru] = RuCp(PR_2NHR'), RuTp(PR_2NHR')

Schema 2: Intramolekulare Addition von NHR' am α- Kohlenstoff

Weiters gibt es einige Amidobutadienkomplexe vom Typ $[RuCp(PPh_2NHPh)(CH_3CN)_2]^+$ und $[RuCp^*(PR_2NHR')(CH_3CN)_2]^+$ (R = Ph, *i*-Pr, R' = Ph, C_6F_5), wo die PR_2NHR' Liganden intramolekulare Reaktionen mit dem Butadienfragment und auch dem Metall eingehen (Schema 3, **B**).[6]

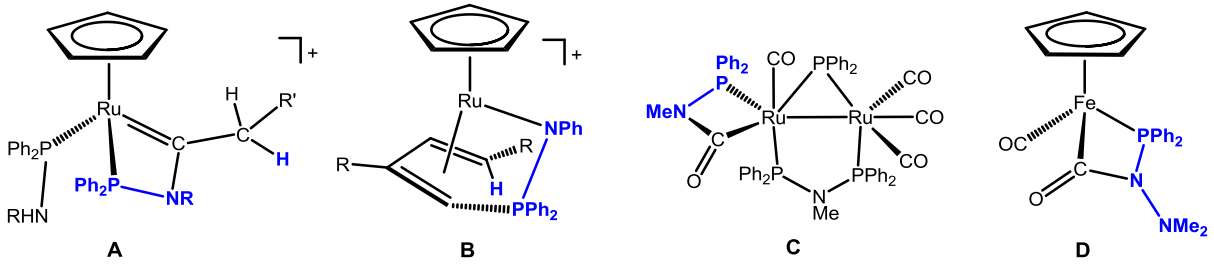

Schema 3: Unterschiedliche Metalle mit einem viergliedrigen Aminophosphinering.

Bunten *et al* haben dinukleare Ruthenium Komplexe $[Ru_2(CO)_3(\mu^2\text{-}PPh_2)(\mu^2\text{-}Ph_2PNMePPh_2)(\kappa^2(C,P)\text{-}C(=O)NMePPh_2)]$ mit Carboxyamido-phospha-rutheniumringen veröffentlicht (Schema 3, **C**).[7] Heberhold und Mitarbeiter berichteten über die Synthese der Halbsandwichkomplexe $[MCp(CO)_2(C(=O)N(S\text{-}NHPtBu_2)]$ (M = Cr, Mo, W).[8]

Für Eisen findet man einen Hydrazinophosphin Komplexe $[FeCp(PPh_2NHNMe_2)(CO)_2]^+$, welcher ähnlich den PR_2NHR'-Liganden reagiert. Die Reaktion dieses Komplexes mit *n*-BuLi liefert einen Carboxamido-phopha-ferrazyklus $[FeCp(CO)(\kappa^2(C,P)\text{-}(C=O)\text{-}NNMe_2\text{-}PPh_2)]$ (Schema 3, **D**).[9]

In der folgenden Arbeit sollten neue Eisenkomplexe mit PR_2NHR'-Liganden dargestellt werden und deren Reaktivität näher untersucht werden.

Einleitung und Problemstellung (Molybdän und Wolfram Komplexe)

Dreizähnige PNP Liganden mit -CH_2PR_2 Substituentenen in den *ortho* Positionen eines Pyridiringes, sogenannte Pincer Liganden, haben große Verwendungen bei den Übergangsmetallen (Fe, Ru, Rh, Ir, Pd, Pt).[12-21] Analoge PNP Liganden mit $NHPR_2$ Substituenten sind wesentlich seltener. Ein erstes Beispiel wurde von Schirmer entwickelt (PNP-Ph).[22] Viele Komplexe mit unterschiedlichen Übergangsmetallen (Ni(II), Pd(II), Pt(II), Fe(II)) und mit unterschiedlichen PNP Pincer-Liganden (-$NR'PR_2$ mit R' = H, alkyl, R = alkyl, aryl), bei denen die sterische, elektronische und stereochemische Eigenschaften einfach und modular geändert werden können, wurden von unserer Gruppe veröffentlicht (Schema 4).[24-27]

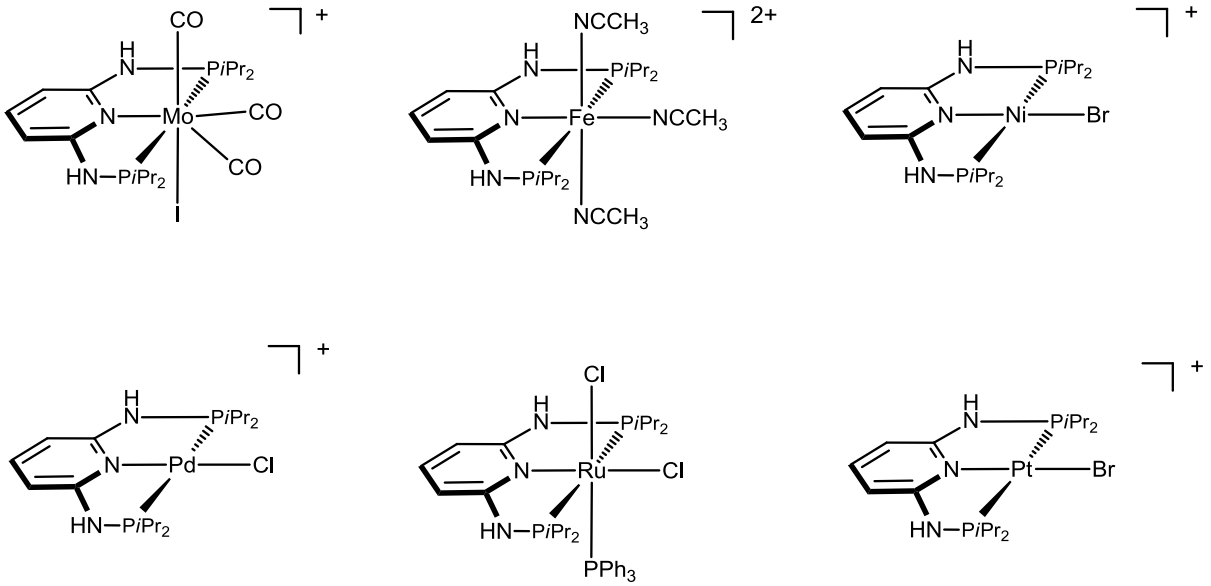

Schema 4: Beispiele von Übergangsmetallkomplexen mit PNP Pincer-Liganden.

In Bezug aud Molybdän und Wolfram findet man überraschenderweise wenige Beispiele von PNP Pincerkomplexen. Walton und Mitarbeiter haben einen dinuclearen Molybdänkomplex (Mo(PNP)ClMo($HPCy_2$)Cl_3) (PNP = 2,6-bis-(dicylohexylphosphinomethyl)pyridin) publiziert (Schema 5).[28]

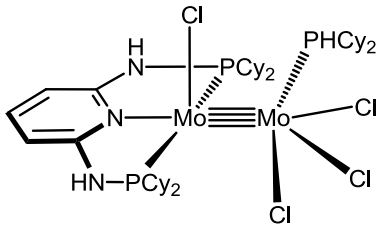

Schema 5: Mo(PNP)(Cl)Mo($HPCy_2$)Cl_3.

Vor einigen Jahren wurde ein Distickstoffmolybdänkomplex von Arashiba in publiziert.[29] Dieser Komplex ist in der Lage Stickstoff zu aktivieren und wurde als Katalysator zur Herstellung von Amoniak verwendet (Schema 6). Bei dieser Reaktion wurde Cobaltocen als Reduktionsmittel und protoniertes 2,6-Dimethylpyridin als Protonenquelle verwendet.

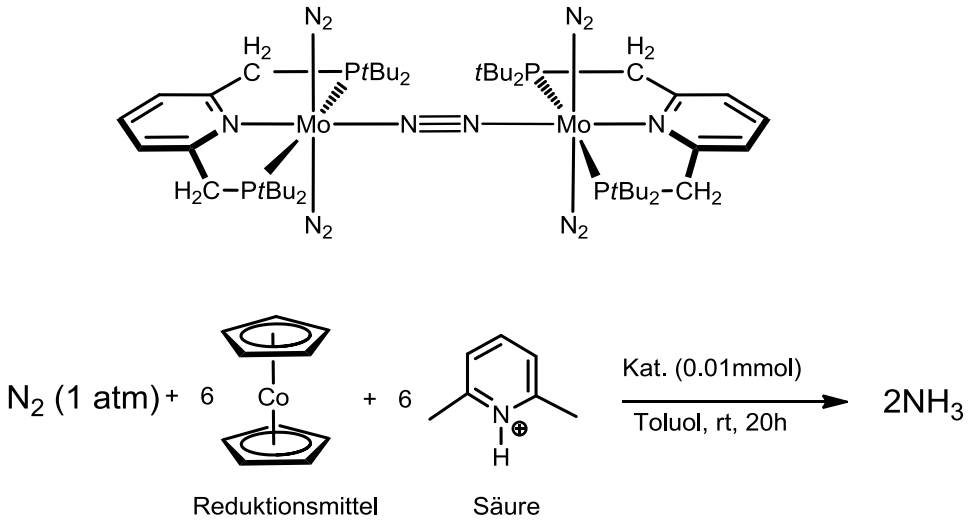

Schema 6: Beispiel eines Distickstoffmolybdänkomplexes und die katalytische Bildung von Ammoniak.

In jüngster Zeit hat Templeton die Synthese von Hydridocarbonyl und Halocarbonyl Wolframkomplexen mit PNP-Pincerliganden vom Typ $HN(SiMe_2CH_2PPh_2)_2$ veröffentlicht (Schema 7).[30]

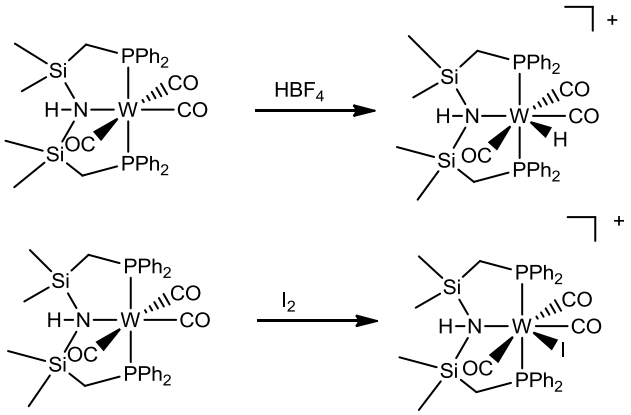

Schema 7: Darstellung von Hydridocarbonyl und Halocarbonyl Wolframkomplexe.

In der folgenden Arbeit sollten neue Molybdän und Wolfram Komplexe mit PNP Pincer Liganden dargestellt werden und deren Reaktivität soll näher untersucht werden.

1. Synthese der Liganden

1.1. Einzähnige PN-Liganden

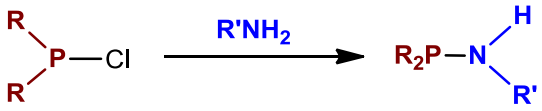

1a R = Ph, R'= *i*Pr
1b R = Ph, R'= *t*Bu
1c R = Ph, R'= *n*Pr
1d R = *i*Pr, R'= *i*Pr
1e R = *i*Pr, R'= Toluidin
1f R = *i*Pr, R'= ^{c}Hex.

Schema 8: Herstellung der PN-Liganden

Die Synthese von Liganden $R_2PN(H)R'$ **(1a-f)** erfolgte durch Umsetzung von R_2PCl mit zwei Äquivalenten von H_2NR' in Et_2O bei 30°C (Schema 8). Die Charakterisierung wurde mittels ^{1}H, $^{13}C\{^{1}H\}$ und $^{31}P\{^{1}H\}$ NMR Spektroskopie gemacht (Tabelle 1).

1.2. Dreizähnige PNP-Liganden

Die Synthese von PNP-Ph **(2a)**, PNP-*i*Pr **(2b)** und PNP-*t*Bu **(2c)** wurde in der Literatur[10,11] beschrieben.

1.2.1. Synthese von PNP^{Me}-*i*Pr

Bei Komplexen spielen die elektronischen und sterischen Eigenschaften von Liganden eine große Rolle. Um die geeignete Kombination von den beiden Effekten zu finden, sollten die Liganden modifiziert werden. Es gibt mehrere Möglichkeiten diese Modifikationen durchzuführen. Eine Möglichkeit ist Substitutenten am Pyridinring einzuführen. Eine weitere Möglichkeit ist Variation der PR_2 Gruppe. Die Möglichkeit die hier gewählt wurde ist die Einführung von Substitutenten an der NH Gruppe (Schema 9).

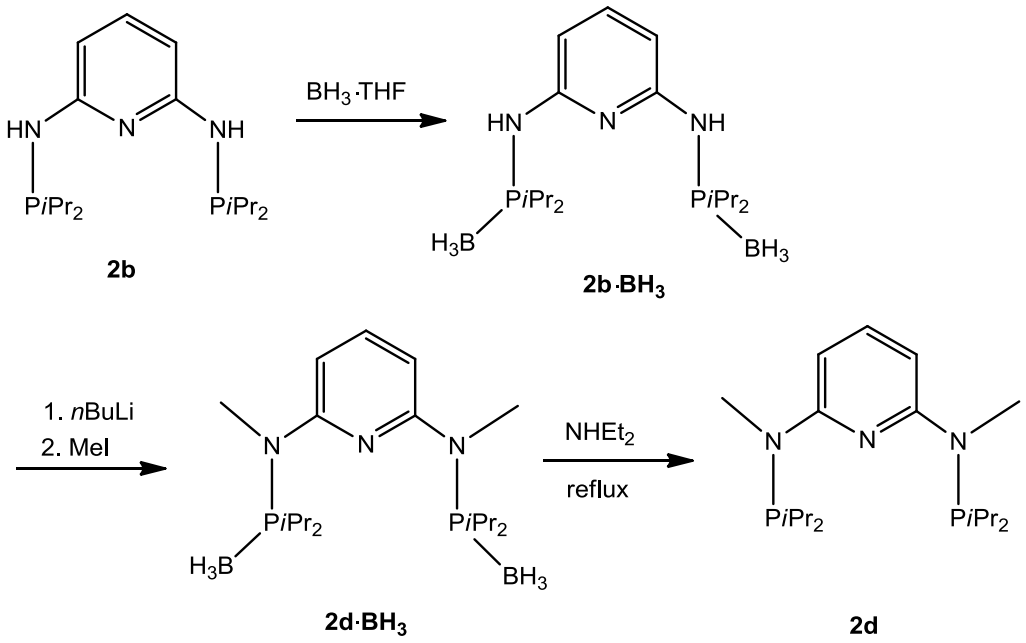

Schema 9: Herstellung des PNP^{Me}-Liganden

Nach dem Schützen des Phosphors von **2b** wurde **2b·BH₃** mit 2 Äquivalenten *n*BuLi deprotoniert und mit Methyliodid umgesetzt. Danach wurde **2d·BH₃** in siedendem Diethylamin entschützt. Das Produkt wurde mittels ^{1}H, $^{13}C\{^{1}H\}$ und $^{31}P\{^{1}H\}$ NMR Spektroskopie charakterisiert (Tabelle 1).

Tabelle 1: $^{31}P\{^{1}H\}$ NMR Signale (ppm) der verschiedenen PN und PNP Liganden (δ, 25 °C, $CDCl_3$, bezogen auf H_3PO_4 (85%))

Ph_2PNiPr **1a**	Ph_2PNtBu **1b**	Ph_2PNnPr **1c**	iPr_2PNiPr **1d**	iPr_2PNtoluidin **1e**
46.4	34.0	52.8	69.6	60.0
iPr_2PN^{c}Hex **1f**	PNP-Ph **2a**	PNP-*i*Pr **2b**	PNP-*t*Bu **2c**	PNP^{Me}-*i*Pr **2d**
69.9	37.7	60.0	70.5	88.5

2-Eisenkomplexe mit einzähnigen PN Liganden

2.1 $Fe(R_2PNHR')_2(CO)_2Br_2$

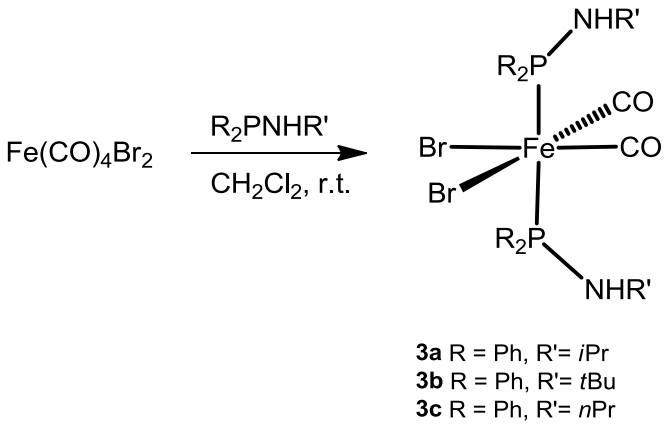

Schema 10: Herstellung der $Fe(R_2PNHR)_2(CO)_2Br_2$-Komplexe

Die Komplexe (Schema 10) wurden durch Umsetzung von $Fe(CO)_4Br_2$ mit 2 Äquivalenten R_2PNHR'hergestellt. Die zwei CO und Br Gruppen stehen *cis* zueinander wogegen die PN-Liganden *trans* zueinander stehen. Die Komplexe wurden mittels ^{1}H, $^{13}C\{^{1}H\}$, $^{31}P\{^{1}H\}$ NMR und IR charakterisiert (Tabelle 2). Im IR Spektrum findet man für die CO Liganden zwei Banden, symmetrische und asymmetrische Streckschwingung, im Bereich von 2040 - 1979 cm^{-1}. Die beiden Phosphoratome sind chemisch äquivalent und man findet deshalb nur ein Singulett im $^{31}P\{^{1}H\}$ NMR Spektrum bei 72.2, 80.6 und 82.3 ppm (*t*Bu, *i*Pr und *n*Pr). Im $^{13}C\{^{1}H\}$ NMR findet man ein Triplett für die beiden Carbonylliganden im Bereich 212.7 und 213.3 ppm.

2.2 [Fe(R_2PNHR')(CO)$_2$(κ^2(*C,P*)-(C=O)-NR'-PR_2)]

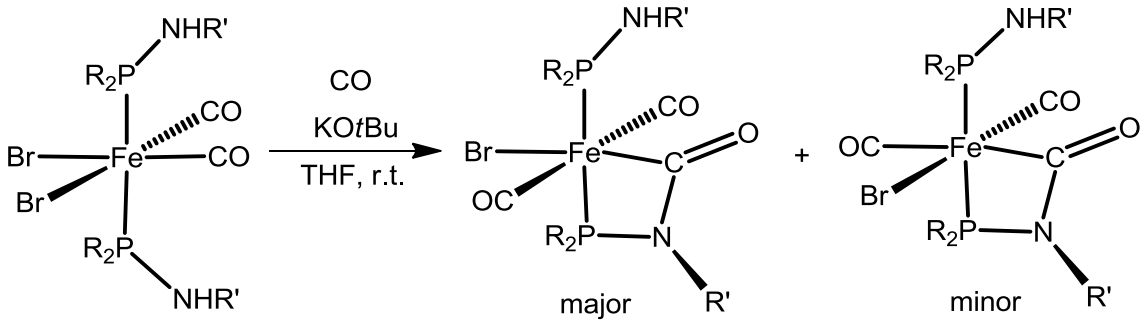

3a R = Ph, R'= *i*Pr
3b R = Ph, R'= *t*Bu

3d R = Ph, R'= *i*Pr
3e R = Ph, R'= *t*Bu

3d' R = Ph, R'= *i*Pr

Schema 11: Herstellung der [Fe(R_2PNHR')(CO)$_2$(κ^2(*C,P*)-(C=O)-NR'-PR_2)] Komplexe

Die Reaktion erfolgte durch Umsetzung von **3a** und **3b** mit KO*t*Bu unter CO Atmosphäre in THF bei Raumtemperatur (Schema 11). Die Ausbeuten liegen zwischen 40 und 50%. Deprotonierung lieferte einen viergliedrigen Carboxyamido-phosphazyklus durch eine intramolekularen nucleophilen Angriff auf einen Carbonyl-Kohlenstoff. Im Fall von **3a** entstehen zwei Isomere im Verhältnis 5:1. Bei Komplex **3d**, welcher laut DFT/B3LYT Berechnungen energetisch günstiger ist, stehen die CO Gruppen zueinander *cis* und bei **3d'** *trans* (Abbildung 1). Die Komplexe wurden mittels ^{1}H-, ^{13}C{^{1}H}-, ^{31}P{^{1}H} NMR und Einkristall Röntgendiffraktion charakterisiert (Abbildung 2, Tabelle 2).

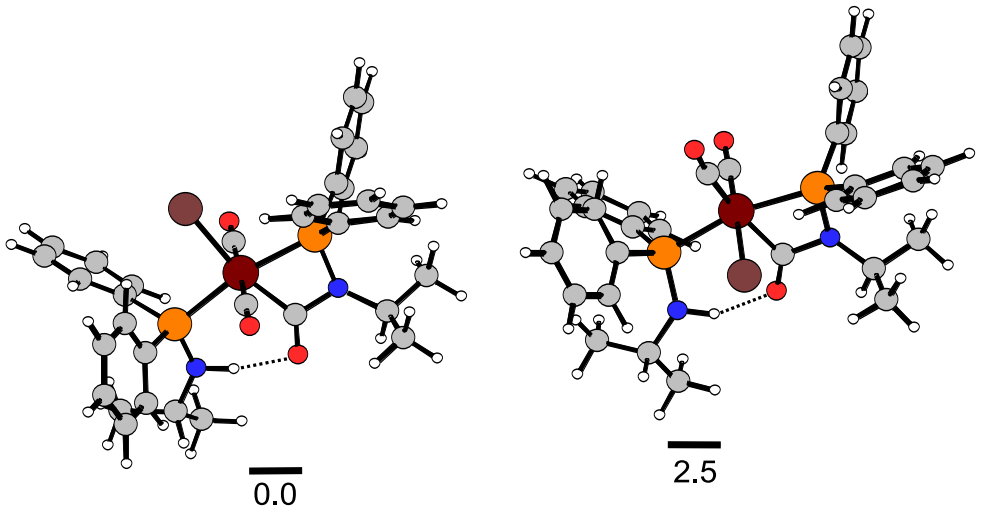

Abbildung 1: Optimierte (DFT/B3LYP) Strukturen von **3d** und **3d'**

Im $^{13}C\{^{1}H\}$ NMR Spektrum gib es ein Triplett für zwei die CO Gruppen bei 212.4 ppm mit einer P-C Kopplungskonstante J_{PC} von 22.7 Hz und für die Carboxyamido Einheit ein dublettisches Dublett bei 206.0 ppm mit Kopplungskonstanten J_{PC} von 9.6 und 13.4 Hz. Im $^{31}P\{^{1}H\}$ NMR gibt es zwei Dubletts bei 95.6 und 85.8 ppm mit einer Kopplungskonstante von 84.7 Hz, welche klar Zeigt, dass die beiden P-Atome in *trans* Position zueinander stehen. Im IR Spektrum findet man die erwarteten zwei Banden für die CO Liganden bei 1955 und 1950 cm^{-1} und für die Carboxyamido Gruppe bei 1619 cm^{-1}. Die Daten von Komplex **3e** sind ähnlich wie die von **3d**.

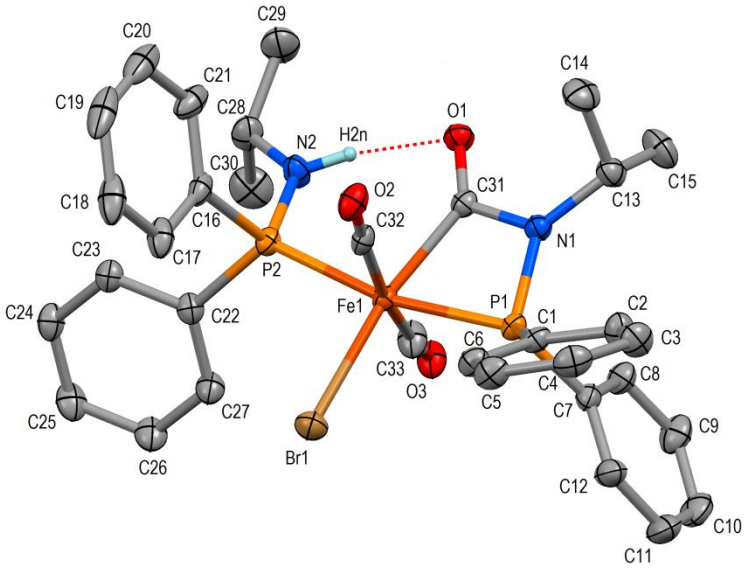

Abbildung 2: ORTEP Diagram von [Fe(R_2PNHR')$(CO)_2$(κ^2(*C,P*)-(C=O)NR'PR_2)] (**3d**) mit Bindungslängen und Winkeln (Å, °): Fe1–Br1 2.4752(6), Fe1–P1 2.2480(9), Fe1–P2 2.2651(9), Fe1–C33 1.799(3), Fe1–C32 1.826(3), Fe1–C31 1.997(3), P2–N2 1.650(3), P1–N1 1.694(3), C31–O1 1.221(4), C31–N1 1.409(4), P1–Fe1–C31 68.9(1), Fe1–P1–N1 85.3(1), Fe1–C31–O1 134.2(2), Fe1–C31–N1 103.6(2), O1–C31–N1 122.2(3), P1–N1–C31 101.5(2), P1–N1–C13 132.4(2), N2···O1 2.839(4).

Die Struktur von **3d** wurde mit kristallographisch bestimmt. Die Geometrie des Komplexes ist ein verzerrter Oktaeder. Die beide Phosphoratome und die beide CO Moleküle sind zueinender *trans* und das Brom steht *trans* zum Kohlenstoffatom der Carboxyamidogruppe. Der Winkel C_{32}-Fe_1-C_{33} ist 170.6(2)° und es gibt eine starke Wasserstoffbrückenbindung zwischen N_2-H_{2n} und O_1.

2.3 [FeCp(R_2PNHR')($CO)_2$]X

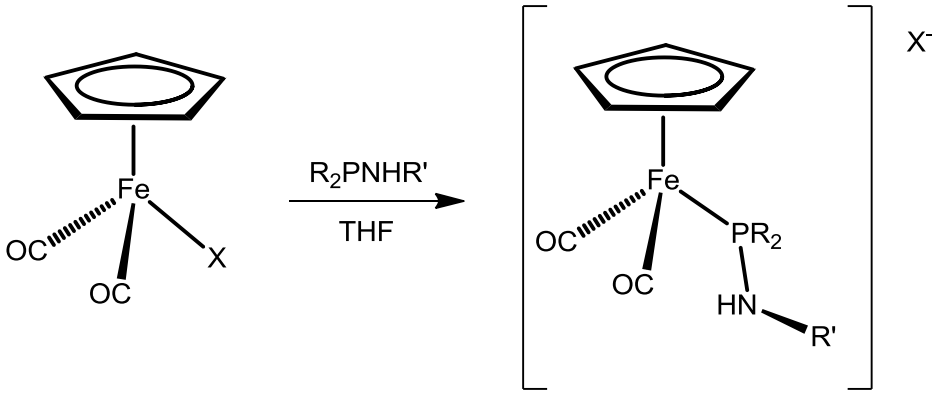

3f R = Ph, R'= *i*Pr, X = Br
3g R = Ph, R'= *t*Bu, X = Br
3h R = Ph, R'= *n*Pr, X = Br
3i R = Ph, R'= *i*Pr, X = Cl
3j R = *i*Pr, R'= ^{c}Hex, X = Cl

Schema 12: Herstellung der [FeCp(R_2PNHR')($CO)_2$]X –Komplexe

Die Komplexe wurden durch Umsetzung von FeCp$(CO)_2$X mit R_2PNHR' in THF hergestellt (Schema 12). Die entstandenen Komplexe sind kationisch und trigonal pyramidal. Die Charakterisierung erfolgte mittels ^{1}H, ^{13}C{^{1}H}, ^{31}P{^{1}H} NMR, IR und Einkristall Röntgendiffraktion (Abbildung 3, Tabelle 2). Im IR Spektrum gibt es zwei Banden für die CO Liganden, die klar zeigen das diese cis zu einander stehen (2043 – 1993 cm^{-1}). Im ^{31}P{^{1}H} NMR Spektrum gibt es ein Singulett zwischen 91.1 und 136.2 ppm und im ^{13}C{^{1}H} NMR gibt es für die zwei CO Liganden ein Dublett zwischen 209.9 und 212.4 ppm mit einer Kopplungskonstante J_{PC} von ca 27 Hz. Es gibt zwischen Br$^-$ und H_{1n}-N_1 eine Wasserstoffbrückenbindung.

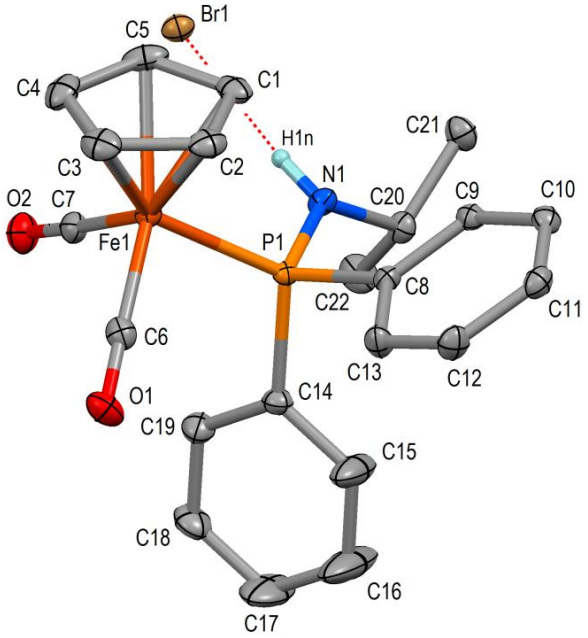

Abbildung 3: ORTEP Diagramm von [FeCp(R_2PNHR')(CO)$_2$]X (**3f**) mit Bindungslängen und Winkeln (Å, °): <Fe1–C_{Cp}> = 2.104(2), Fe1–P1 2.2223(4), Fe1–C6 1.780(2), Fe1–C7 1.785(2), C6–O1 1.141(2), C7–O2 1.139(2), P1–N1 1.6473(13), N1–C20 1.477(2), P1–Fe1–C6 90.73(5), P1–Fe1–C7 93.83(5), C6–Fe1–C7 96.28(7), C20–N1–P1 125.14(10), N1…Br1 3.3854(13).

2.4 FeCp(CO)(κ^2(*C,P*)-(C=O)-NR'-PR_2)

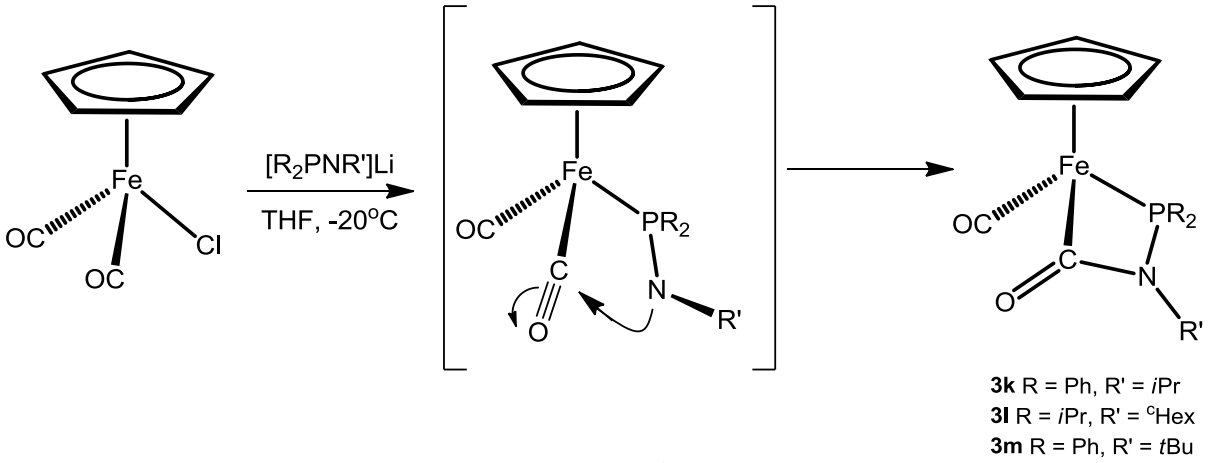

3k R = Ph, R' = *i*Pr
3l R = *i*Pr, R' = ^{c}Hex
3m R = Ph, R' = *t*Bu

Schema 13: Herstellung der FeCp(CO)(κ^2(*C,P*)-(C=O)-NR'-PR_2) Komplexe

Diese Produkte wurden durch Umsetzung von FeCp(CO)$_2$Cl mit deprotonierten PR_2NHR' Liganden hergestellt (Schema 13). Es gibt einen nucleophilen Angriff vom basischen Amidostickstoff an die Carbonylgruppe und entsteht ein viergliedriger

Carboxyamido-phosphazyklus. Die Charakterisierung erfolgte mittels ^{1}H-, ^{13}C{^{1}H}- und ^{31}P{^{1}H} NMR (Abbildung 4, Tabelle 2). Im ^{31}P{^{1}H} NMR Spektrum gibt es ein Singulett 111.6 **(3k)**, 113.0 **(3m)** und 140.0 ppm **(3l)** und es gibt im ^{13}C{^{1}H} NMR für den CO Ligand ein Dublett bei 220.9 **(3k)**, 221.0 **(3l)** und 221.0 ppm **(3m)** mit P-C Kopplungskonstanten zwischen 24.4 und 26.4 Hz. Für die Kohlenstoffe von den Carboxyamidogruppen gibt es auch ein Dublett bei 200.4 ppm (J_{PC} = 39.0 Hz) **(3k)**, 201.1 ppm (J_{PC} = 45.8 Hz) **(3m)** und 199.8 ppm (J_{PC} = 37.8 Hz) **(3m)**. Im IR Spektrum gibt es eine Bande für CO im Bereich von 1937-1914 cm^{-1} und für die Carboxyamidogruppe im Bereich von 1618-1605 cm^{-1}.

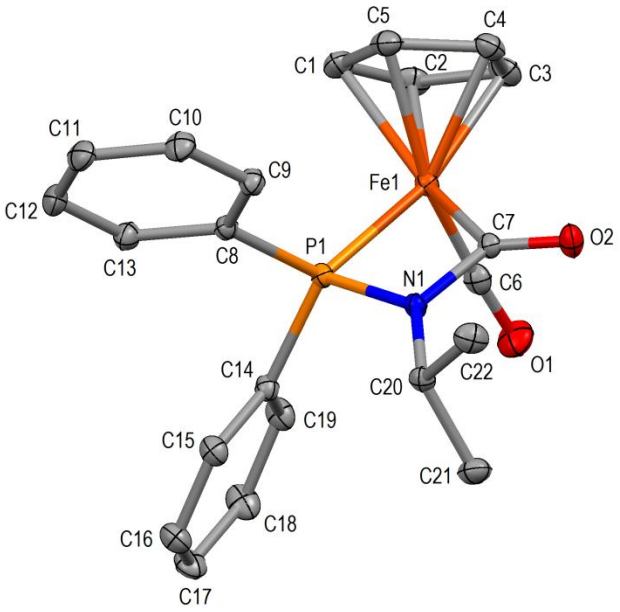

Abbildung 4: ORTEP Diagramm von FeCp(CO)(κ^2(*C,P*)-(C=O)-NR'-PR_2) **(3k)** mit Bindungslängen und Winkeln (Å, °): <Fe1–C_{Cp}> = 2.101(1), Fe1–P1 2.1773(3), Fe1–C6 1.739(1), Fe1–C7 1.981(1), C6–O1 1.158(2), C7–O2 1.219(2), N1–C7 1.404(2), P1–N1 1.6915(10), C6-Fe1-P1 69.01(4), Fe1–C7–O2 133.8(1), Fe1–C7–N7 103.7(1), Fe1–P1–N1 86.95(3), P1–N1–C7 99.7(1).

Anhand der Strukturanalyse zeigen diese Komplexe eine sogenannte „three legged piano stool“ Geometrie. Die Beine entstehen von P, C(CO) und C(=O).

Wenn diese Komplexe mit $[Me_3O]BF_4$ in CH_2Cl_2 umgesetzt werden, entstehen die viergliedrigen aza-phosphin Carbenkomplexe (Schema 13).

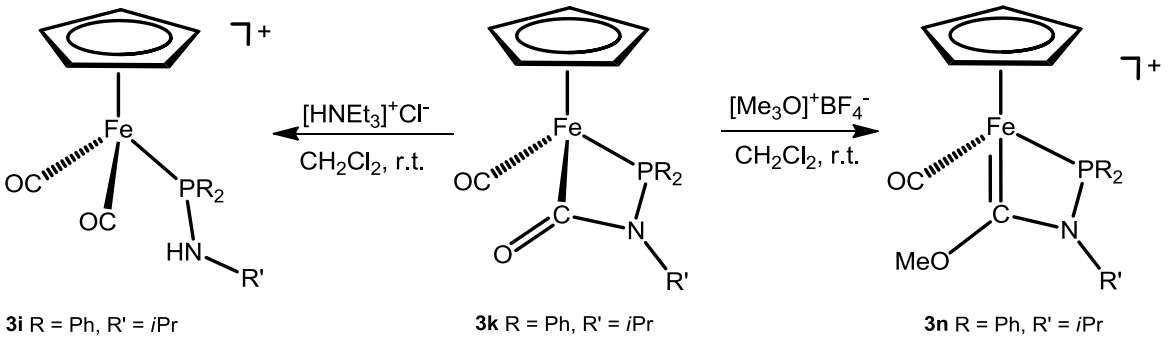

3i R = Ph, R' = *i*Pr **3k** R = Ph, R' = *i*Pr **3n** R = Ph, R' = *i*Pr

Schema 13: Herstellung der Komplexe **3i** und **3n**

Es entsteht **3i** durch eine ringöffnende Reaktion, wenn **3k** statt $[Me_3O]BF_4$ mit NH_4Cl umgesetzt wird. Der Carbenkomplex **(3n)** wurde mittels $^{13}C\{^1H\}$ NMR charakterisiert. Es gibt eine Verschiebung bei 238 ppm, welche mit literaturbekannten Fischer Carbenen übereinstimmen.

Tabelle 2. IR, $^{31}P\{^{1}H\}$ NMR, und $^{13}C\{^{1}H\}$ NMR Daten aller Eisenkomplexe

Komplexe	$\nu_{C\equiv O}$, cm^{-1}	$\nu_{C=O}$, cm^{-1}	δ_P, ppm	$\delta_{C\equiv O}$, ppm	$\delta_{C=O}$, ppm
3a	2040, 1985		80.6	212,7	
3b	2035, 1979		72.2	213.3	
3c	2008, 1987		82.3	212.7	
3d	1966, 1960	1616	95.6, 85.7	212.4	206.0
3e	1955, 1950	1619	90.4, 87.2	213.5, 213.1	206.0
3f	2040, 1993		100.6	210.3	
3g	2038, 1996		91.9	212.4	
3h	2043, 2004		103.1	209.9	
3i	2041, 1993		100.2	210.4	
3j	2026, 1982		136.2	211.0	
3k	1937	1617	111.6	220.9	200.4
3l	1914	1618	140.0	221.0	199.8
3m	1919	1605	113.0	221.0	201.1
3n	2004		115.0	216.3	
3o	2040, 1992		100.1	210.4	

3. Molybdän und Wolfram Komplexe mit PNP Liganden

3.1. Synthese von [M(PNP-R)(CO)$_3$X]X (M = Mo, W, 18e$^-$)

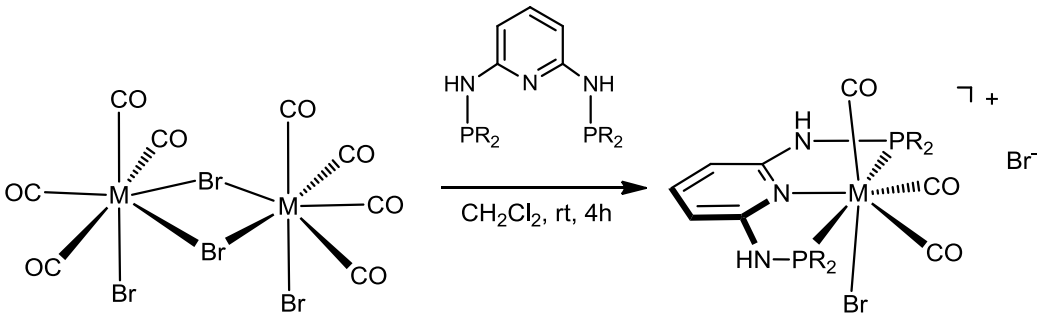

5a M = Mo, R = PNP-Ph
5b M = Mo, R = PNP-*i*Pr
5e M = W, R = PNP-Ph
5f M = W, R = PNP-*i*Pr
5g M = W, R = PNP-*t*Bu

Schema 14: Herstellung der Komplexe **5a, b, e, f** und **g**

Diese Komplexe wurden durch Umsetzung der bekannten Verbindung [M(CO)$_4$(μ-Br)Br]$_2$[23] mit PNP-R Liganden hergestellt (Schema 14). Die Komplexe sind kationisch und siebenfach koordiniert, deshalb zeigen die Komplexe eine verzerrte oktaedrische Struktur. Die Charakterisierung wurde mittels ^{1}H, ^{13}C{^{1}H}, ^{31}P{^{1}H} NMR, IR und ein Kristall Röntgen Diffraktion gemacht (Tabelle 3, Abbildung 5 und 6). Im IR Spektrum gibt es drei CO Banden im Bereich von 2040-1875 cm^{-1}. In den ^{13}C{^{1}H} NMR Spektren gibt es zwei Tripletts für die CO Gruppe mit einer Intensität von 1:2 im Bereich 234.6-191.3 ppm. Vom Komplex **5a** konnte wegen der schlechten Löslichkeit kein ^{13}C{^{1}H} NMR gemessen werden. Es gibt ein Singulett in den ^{31}P{^{1}H} NMR Spektren für jeden Komplex im Bereich von 85.2 – 131.6 ppm.

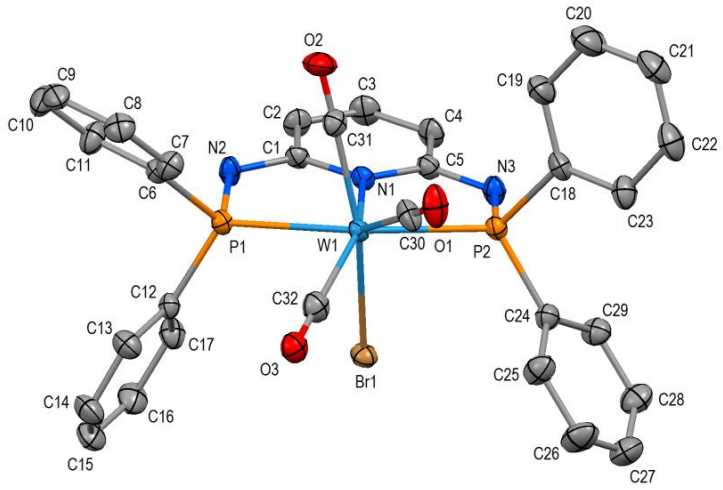

Abbildung 5: ORTEP Diagramm von [W(PNP-Ph)$(CO)_3$Br]Br **(5e)** mit Bindungslängen und Winkeln (Å, °): W-C(31) 2.017(5), W-C(30) 2.020(6), W-C(32) 2.024(8), W-N(1) 2.237(3), W-P(1) 2.4955(10), W-P(2) 2.4895(11), W-Br(1) 2.6015(5); P(1)-W-P(2) 152.34(4), N(1)-W-P(1) 77.44(9), N(1)-W-P(2) 75.92(9), N(1)-W-C(30) 137.76(16), N(1)-W-C(31) 82.35(16), N(1)-W-C(32) 150.87(8), N(1)-W-Br(1) 82.28(9).

Die molekulare Struktur dieser Verbindung wurde mit Hilfe von Einkristall Röntgendifferaktion bestimmt. Zwei CO Gruppe liegen in der PNP Ebene und in *cis* Position zu einander. Die dritte CO Gruppe liegt in axialer Position und *trans* zum Br Atom. Im Wolframkomplex **(5e)** gibt es ein zweites Isomer (14%), bei dem es einen Austausch zwischen Br und C_{32}-O_3 gibt.

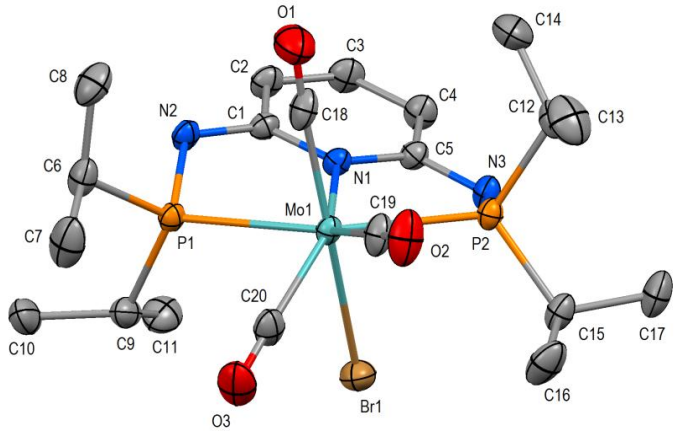

Abbildung 6: ORTEP Diagramm von [Mo(PNP-*i*Pr)(CO)$_3$Br]Br **(5b)** mit Bindungslängen und Winkeln (Å, °): Mo-C(18) 2.037(2), Mo-C(19) 1.979(2), Mo-C(20) 2.006(2), Mo-N(1) 2.236(2), Mo-P(1) 2.5242(5), Mo-P(2) 2.5172(5), Mo-Br(1) 2.6713(3); P(1)-Mo-P(2) 150.80(2), N(1)-Mo-P(1) 75.67(4), N(1)-Mo-P(2) 75.35(4), N(1)-Mo-C(18) 85.95(7), N(1)-Mo-C(19) 77.73(6), N(1)-Mo-C(20) 127.23(6), N(1)-Mo-Br(1) 84.22(4).

3.2. Synthese von Mo(PNP^{Me}-*i*Pr)(CO)X$_2$

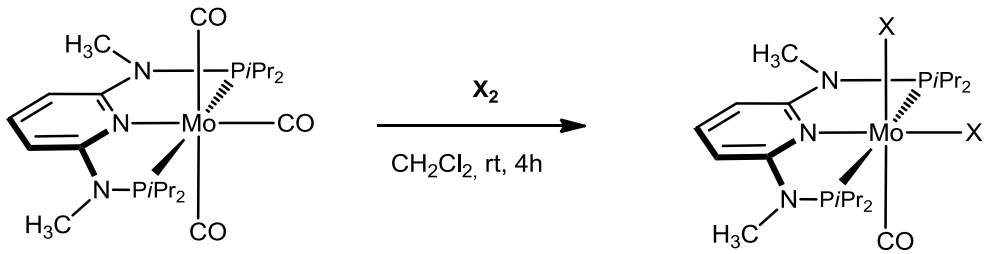

4d

6a X = Br
6b X = I

Schema 15: Herstellung der Komplexe **6a, b**

Die Synthese dieser Komplexe erfolgte durch Umsetzung von **4d** mit elementarem Iod oder Brom. Im Vergleich zu den Komplexen mit PNP-Ph, PNP-*i*Pr und PNP-*t*Bu Liganden entsteht ein oktaedrischer neutraler koordinativ ungesättigter Komplex (Schema 15). Diese Methode funktionierte nicht für Chlor, weil die Stöchiometrie schlecht kontrolliert werden kann und es zu Überoxidationen kam, was zu Bildung von paramagnetischen schwer abzutrennenden Nebenprodukten führte. Deshalb

erfolgte die Darstellung dieses Komplexes durch die Reaktion von $[M(CO)_4(\mu\text{-}Cl)Cl]_2$[23] mit PNP^{Me}-*i*Pr gemäß Schema 16.

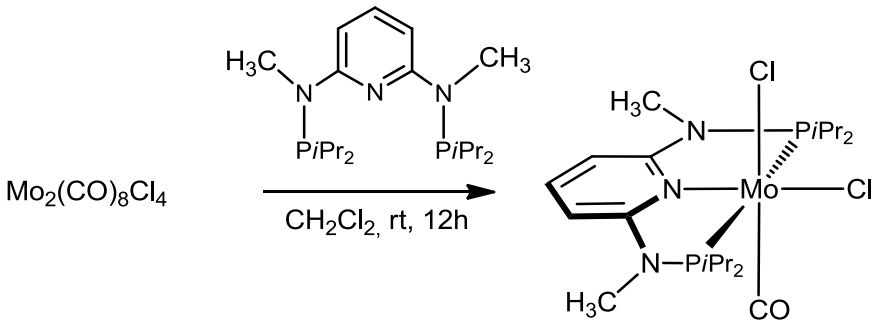

6c

Schema 16: Herstellung von Komplex **6c**

Die Charakterisierung erfolgte mittels ^{1}H, $^{13}C\{^{1}H\}$, $^{31}P\{^{1}H\}$ NMR, IR und Einkristall Röntgendiffraktion (Tabelle 3, Abbildung 8a, 8b, 9, und 10). Das Molekül ist ein verzerrter Oktaeder. Das Molybdänatom liegt signifikannt über der PNP Ebene. Der Winkel zwischen P_1-Mo-P_2 ist ungefähr 128°. Die Liganden X (X= Cl, Br, I) und CO in der axiale Position stehen zu einander *trans* und ein zweites X Atom steht *trans* zum Stickstoff im Pyridinring (Abbildung 8a, 8b, 9, 10). Die Komplexe sind diamagnetisch, weil die $2e_g$ und t_{2g} Orbitale energetisch unterschiedlich sind. Außerdem sind die Komplexe sehr stabil, weil die leere LUMO, LUMO+1 und LUMO+2 Orbitale in der PNP-R Ebene liegen. Metall ist sterisch schlecht für einen Angriff zugänglich (Abbildung 7).

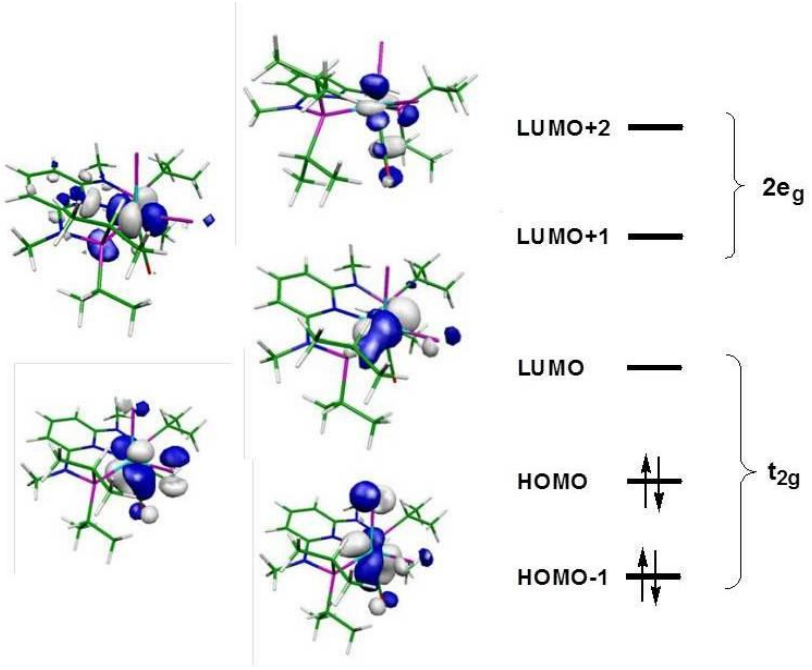

Abbildung 7: HOMO und LUMO Orbitale von **6a, b** und **c**

Der zweite Grund der Stabilität dieser Verbindungsklasse liegt darin, dass Mo Atom von den Liganden sterisch abgeschirmt ist (Abbildung 8a).

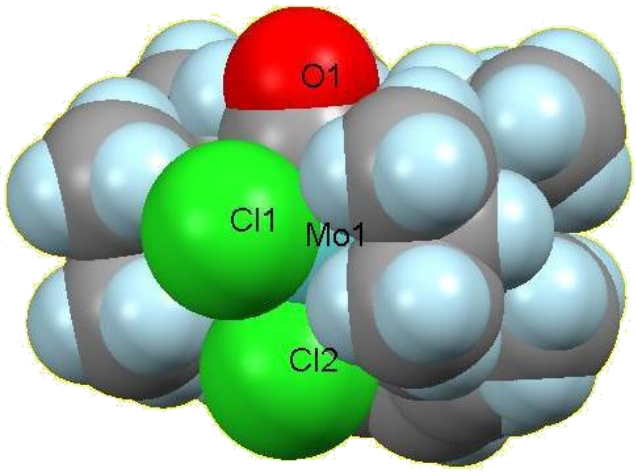

Abbildung 8a: Spacefilling Model von [Mo(PNP^{Me}-*i*Pr)(CO)Cl$_2$] **(6c)**

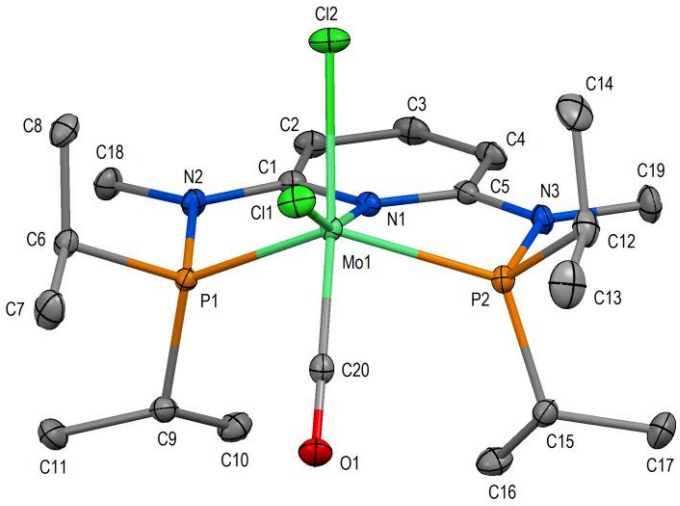

Abbildung 8b: ORTEP Diagramm von [Mo(PNP^{Me}-*i*Pr)(CO)Cl$_2$] **(6c)** mit Bindungslängen und Winkeln (Å, °): Mo-N(1) 2.2691(8), Mo-C(20) 1.9208(10), Mo-P(1) 2.3783(3), Mo-P(2) 2.3579(3), Mo-Cl(1) 2.4052(2), Mo-Cl(2) 2.4792(3); P(1)-Mo-P(2) 128.03(1), N(1)-Mo-P(1) 72.20(2), N(1)-Mo-P(2) 73.65(2), N(1)-Mo-Cl(1) 163.04(2), N(1)-Mo-Cl(2) 79.27(2), N(1)-Mo-C(20) 114.82(4), Cl(1)-Mo-Cl(2) 83.88(1), Cl(1)-Mo-C(20) 82.07(3), Cl(2)-Mo-C(20) 165.87(3).

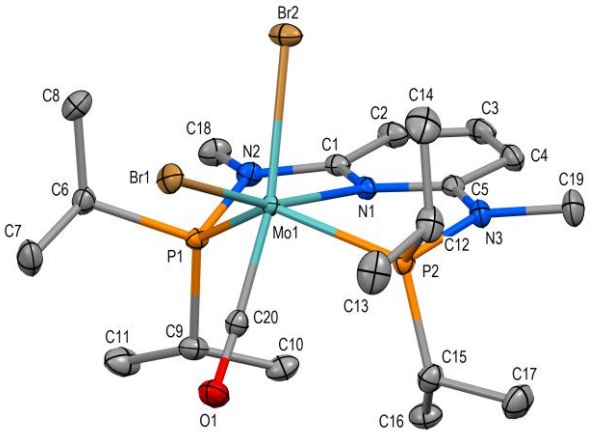

Abbildung 9: ORTEP Diagramm von [Mo(PNP^{Me}-*i*Pr)(CO)Br$_2$] (**6a**) mit Bindungslängen und Winkeln (Å, °): Mo-N(1) 2.2665(12), Mo-C(20) 1.9209(15), Mo-P(1) 2.3847(4), Mo-P(2) 2.3620(4), Mo-Br(1) 2.5494(2), Mo-Br(2) 2.6301(3); P(1)-Mo-P(2) 128.01(2), N(1)-Mo-P(1) 72.13(3), N(1)-Mo-P(2) 73.97(3), N(1)-Mo-Br(1) 163.60(3), N(1)-Mo-Br(2) 78.98(3), N(1)-Mo-C(20) 115.05(5), Br(1)-Mo-Br(2) 84.79(1), Br(1)-Mo-C(20) 81.26(4), Br(2)-Mo-C(20) 165.88(4).

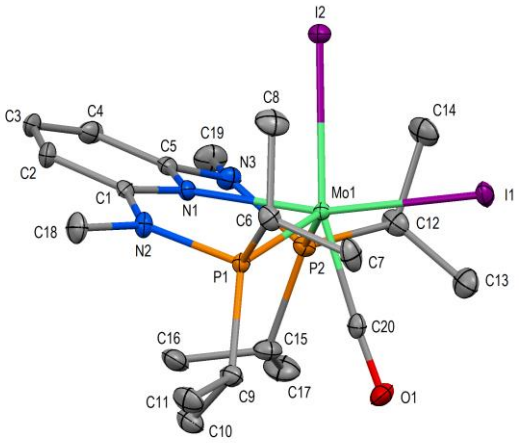

Abbildung 10: ORTEP Diagramm von [Mo(PNP^{Me}-*i*Pr)(CO)I_2] **(6b)** mit Bindungslängen und Winkeln (Å, °): Mo-N(1) 2.275(2), Mo-C(20) 1.915(3), Mo-P(1) 2.3825(7), Mo-P(2) 2.3764(7), Mo-I(1) 2.7657(3), Mo-I(2) 2.8504(3); P(1)-Mo-P(2) 126.11(2), N(1)-Mo-P(1) 74.11(6), N(1)-Mo-P(2) 70.91(6), N(1)-Mo-I(1) 165.50(5), N(1)-Mo-I(2) 79.54(5), N(1)-Mo-C(20) 115.13(9), I(1)-Mo-I(2) 86.36(1), I(1)-Mo-C(20) 79.32(8), I(2)-Mo-C(20) 163.17(7).

Im IR Spektrum gibt es eine Bande bei 1816 **(6a)**, 1824 **(6b)** und 1813 **(6c)**. Zum Vergleich mit den siebenfachkoordinierten kationischen 18e$^-$ Mo(II) Komplexen sind die Phosphorsignale ins Tieffeld verschoben 206.9 **(6a)**, 202.2 **(6b)**, 207.0 **(6c)**.

Wenn **6c** und **6b** in CH_2Cl_2 in Anwesenheit von THF und Acetonitril mit einem Silbersalz umgesetzt werden, entstehten die kationischen oktaedrischen Komplexe [Mo(PNP^{Me}-*i*Pr)(CO)(THF)Cl]SbF_6 **(6d)** und [Mo(PNP^{Me}-*i*Pr)(CO)(NCCH$_3$)I]SbF_6 **(6e)** (Schema 17).

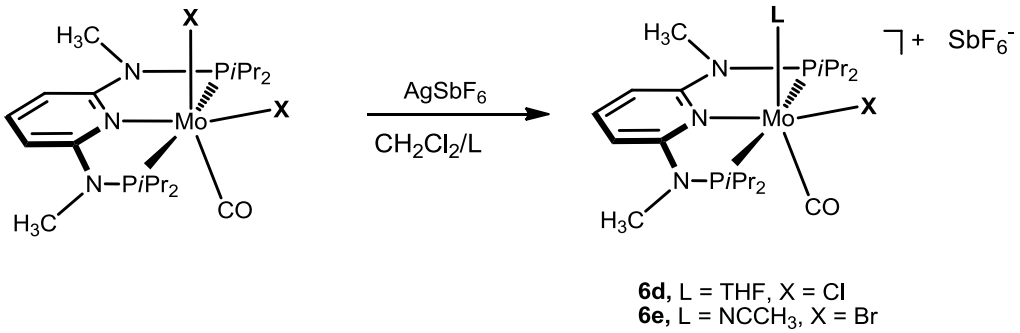

Schema 17: Herstellung von Komplex **6d** und **6e**

Im IR Spektrum haben sich CO Banden zum Vergleich **6c** und **6b** auf 1831cm^{-1} und 1840 cm^{-1}verschoben. Diese Komplexe wurden mittels Einkristall Röntgendiffraktion und ^{1}H-, ^{13}C{^{1}H}-, ^{31}P{^{1}H} NMR, charakterisiert (Tabelle 3, Abbildung 11).

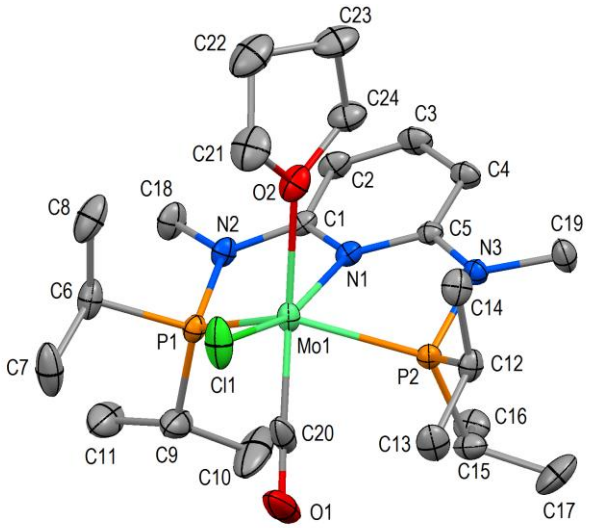

Abbildung 11: ORTEP Diagramm von [Mo(PNP^{Me}-*i*Pr)(CO)(THF)Cl]SbF_6 **(6d)** mit Bindungslängen und Winkeln (Å, °): Mo-N(1) 2.260(2), Mo-C(20) 1.913(4), Mo-P(1) 2.3853(9), Mo-P(2) 2.3717(8), Mo-Cl(1) 2.3966(8), Mo-O(2) 2.312(3); P(1)-Mo-P(2) 125.66(4), N(1)-Mo-P(1) 73.80(6), N(1)-Mo-P(2) 71.82(6), N(1)-Mo-Cl(1) 162.97(9), N(1)-Mo-O(2) 80.18(9), N(1)-Mo-C(20) 113.20(14), Cl(1)-Mo-O(2) 83.09(7), Cl(1)-Mo-C(20) 83.79(13), O(2)-Mo-C(20) 165.21(13).

3.3. Synthese von M(PNP-R)(CO)$_3$ (M = Mo, W)

$Mo(CO)_3$(PNP-R) (R = Ph, *i*Pr und *t*Bu) wurden laut Literatur[10] hergestellt. Weiters wurde [Mo(PNP-R)$(CO)_3$Br]Br durch Reduktion mit Natrium-Amalgam hergestellt (Schema 18).

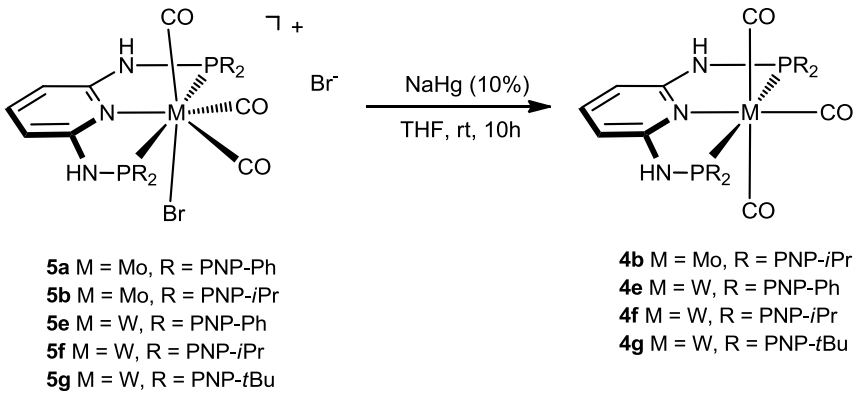

5a M = Mo, R = PNP-Ph
5b M = Mo, R = PNP-*i*Pr
5e M = W, R = PNP-Ph
5f M = W, R = PNP-*i*Pr
5g M = W, R = PNP-*t*Bu

4b M = Mo, R = PNP-*i*Pr
4e M = W, R = PNP-Ph
4f M = W, R = PNP-*i*Pr
4g M = W, R = PNP-*t*Bu

Schema 18: Herstellung der Komplexe M(PNP-R)$(CO)_3$ **(4b, e, f und g)**

Die Umsetzung erfolgte von [M(PNP-R)$(CO)_3$X]X mit 10 % NaHg (3 Äquivalent Na) in THF (Schema 18). Zum Vergleich mit der Literatur hat diese Methode bei den Wolfram-Komplexen große Vorteile. Die Ausbeuten liegen zwischen 70-80 % und die Reaktionszeiten sind wesentlich kürzer. Die Charakterisierung erfolgte mittels ^{1}H-, ^{13}C{^{1}H}-, ^{31}P{^{1}H} NMR und Einkristall Röntgenstrukturanalysen (Tabelle 3, Abbildung 12 und 13). Die Komplexe sind verzerrte Oktaeder mit dem PNP Ligand meridional zum Metall koordiniert. Die Winkel zwischen P_1-W-P_2 und trans-C_{CO}-W-C_{CO} sind 154.43(4) und 165.7(2)° **(4f)** und 151.42(1) und 156.46(9)° **(4g)**. Die Winkel sind äußerst abhängig vom Substituent am Phosphoratom.

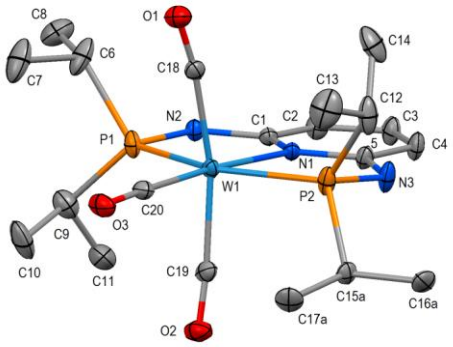

Abbildung 12: ORTEP Diagramm von W(PNP-*i*Pr)$(CO)_3$ (**4f**) mit Bindungslängen und Winkeln (Å, °): W-C(18) 2.015(6), W-C(19) 2.013(6), W-C(20) 1.933(5), W-N(1) 2.255(4), W-P(1) 2.4090(14), W-P(2) 2.4015(14); P(1)-W-P(2) 154.42(5), N(1)-W-P(1) 77.31(11), N(1)-W-P(2) 77.16(11), N(1)-W-C(18) 100.8(2), N(1)-W-C(19) 93.3(2), N(1)-W-C(20) 175.8(2), C(18)-W-C(19) 165.8(2).

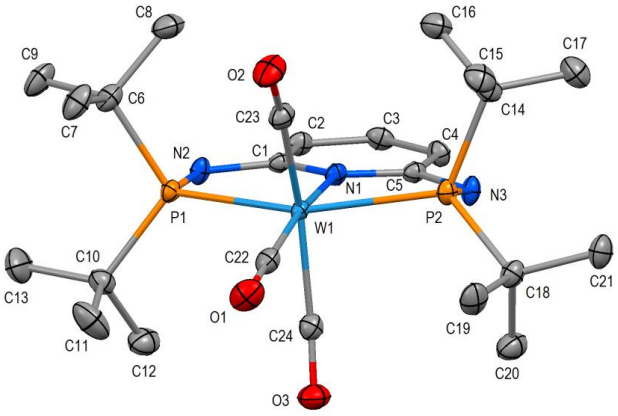

Abbildung 13: ORTEP Diagramm von W(PNP-*t*Bu)$(CO)_3$ (**4g**) mit Bindungslängen und Winkeln (Å, °): W-C(22) 1.941(3), W-C(23) 1.997(2), W-C(24) 2.001(2), W-N(1) 2.277(2), W-P(1) 2.4583(5), W-P(2) 2.4656(5); P(1)-W-P(2) 151.42(2), N(1)-W-P(1) 76.52(4), N(1)-W-P(2) 76.00(4), N(1)-W-C(22) 169.53(8), N(1)-W-C(23) 113.16(8), N(1)-W-C(24) 90.27(7), C(23)-W-C(24) 156.46(9).

Im $^{13}C\{^1H\}$ NMR Spektrum gibt es zwei Tripletts für die CO Gruppen mit der Intensität 1:2 im Bereich von 206-221 ppm und 196-210 ppm. Im $^{31}P\{^1H\}$ NMR Spektrum gibt es ein Singulett mit einer $^1J_{WP}$ Kopplungskonstante im Bereich von 315-329 Hz. Das W-P Signal ist ein Satellit über dem Hauptsgnal wegen dem NMR aktiven ^{183}W (I = ½) Kern. Im IR Spektrum gibt es drei Bande für die CO Gruppen im Bereich von 1966-1759 cm^{-1}.

Der Komplex **4d** wurde durch Umsetzung von $Mo(CO)_3(CH_3CN)_3$[10,11] mit PNP^{Me}-*i*Pr (**2d**) in Acetonitril hergestellt (Schema 19). Die Charakterisierung erfolgte mittels ^1H-, $^{13}C\{^1H\}$-, $^{31}P\{^1H\}$ NMR, IR und Einkristall Röntgendiffraktion gemacht (Tabelle 3, Abbildung 14). Die $^{13}C\{^1H\}$ NMR und IR Spektren sind ähnlich wie **4b** aber die Verschiebung im $^{31}P\{^1H\}$ NMR ist zum Vergleich **4b** ins Tieffeld nach 171.0 ppm verschoben.

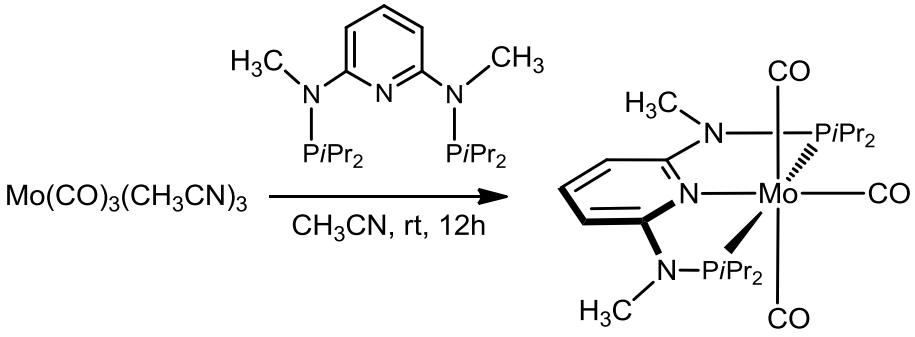

4d

Schema 19: Herstellung der Komplex Mo(PNP^{Me}-*i*Pr)(CO)$_3$ **(4d)**

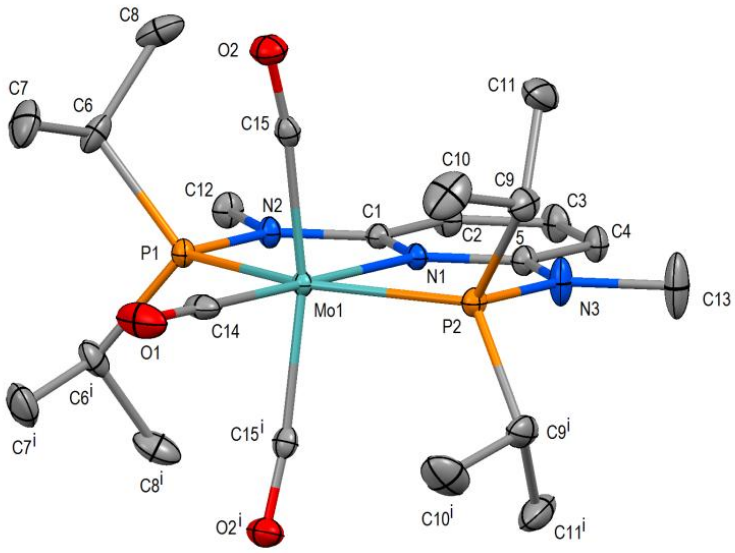

Abbildung 14: ORTEP Diagramm von Mo(PNP^{Me}-*i*Pr)(CO)$_3$ (**4d**) mit Bindungslängen und Winkeln (Å, °): Mo-C(14) 1.956(2), Mo-C(15) 2.0153(13), Mo-N(1) 2.2589(15), Mo-P(1) 2.3977(5), Mo-P(2) 2.4070(5); P(1)-Mo-P(2) 155.25(2), N(1)-Mo-P(1) 77.74(4), N(1)-Mo-P(2) 77.51(4), N(1)-Mo-C(15) 98.52(4).

3.4. Synthese von [M(PNP-R)(CO)$_3$H]BF$_4$ Komplexe

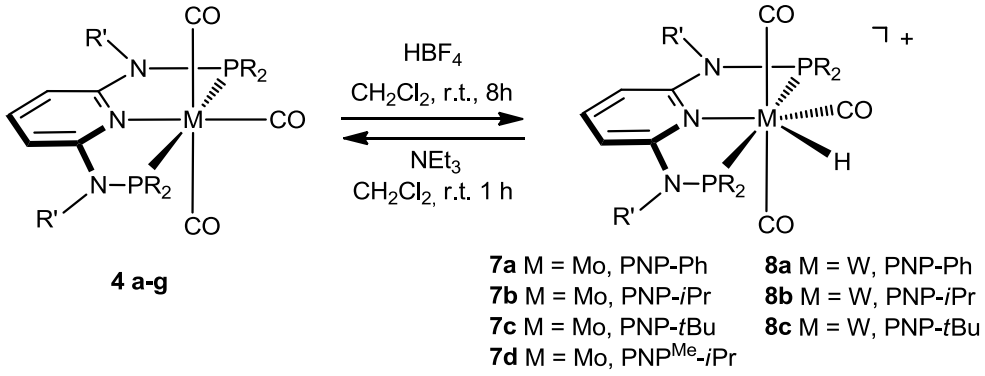

Schema 20: Herstellung der Komplexe [M(PNP-R) (CO)$_3$H]BF$_4$ **(7a-d, 8a-c)**

Diese Komplexe wurden durch Umsetzung von **4a-g** mit HBF$_4$ hergestellt (Schema 20). Die Komplexe sind siebenfach koordiniert und kationisch. Die PNP-R Liganden haben eine meridional Position zum Metallzentrum und sind dynamisch in Lösung. Es erfolgt eine Pseudorotation zwischen H und der Carbonylgruppe in der äquatorialen Position (Abbildung 15, 16, 17).

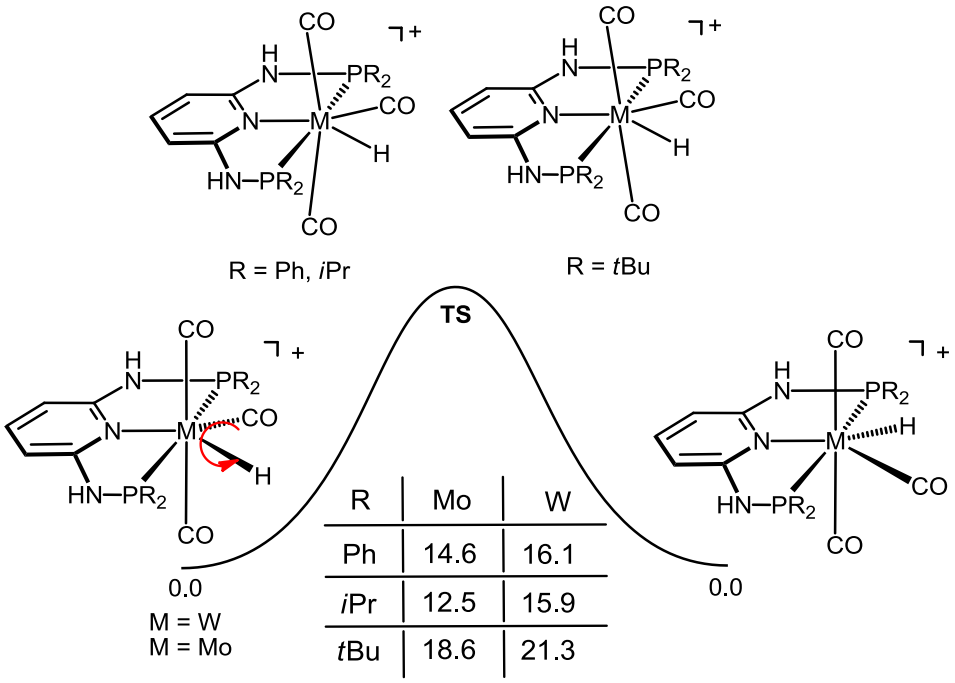

Abbildung 15: Energiediagramm (freie Energie in kcal/mol) für die "Pseudorotation" von CO und Hydrid in den Komplexen [M(PNP)(CO)$_3$H]$^+$ (M = W, Mo).

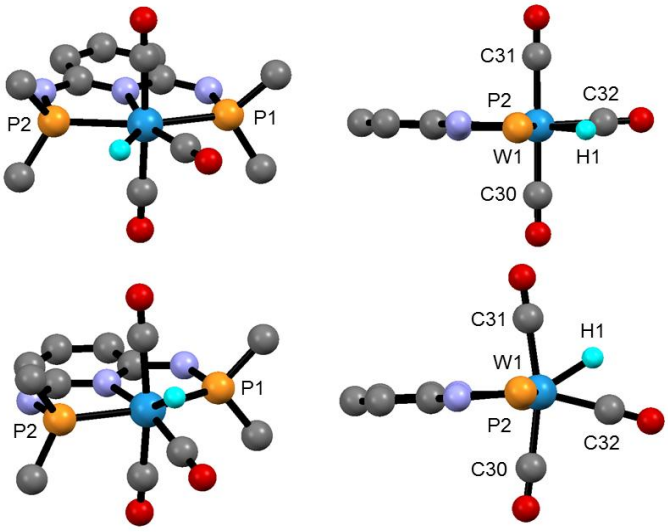

Abbildung 16: Optimierte Struktur (DFT/B3LYP) des Wolfram Komplexes $[W(PNP\text{-}Ph)(CO)_3H]^+$ **(8a)** (oben), Übergangszustand (unten). Phenyl - und Wasserstoffatome wurden der Übersichtlichkeit wegen weggelassen.

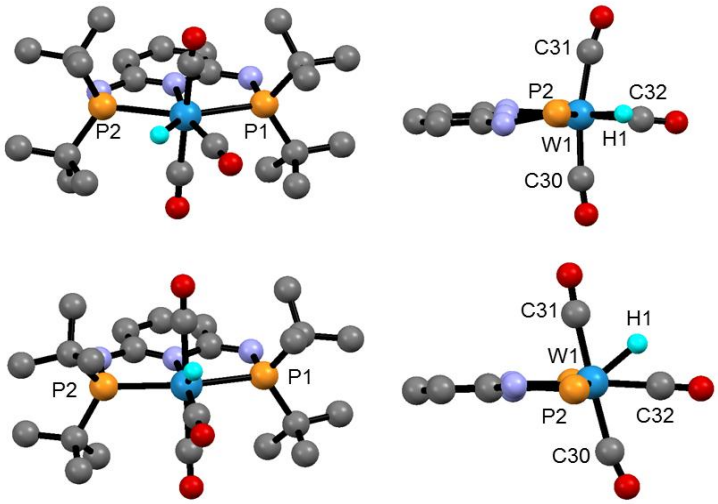

Abbildung 17: Optimierte Struktur (DFT/B3LYP) des Wolfram Komplexes $[W(PNP\text{-}t\text{Bu})(CO)_3H]^+$ **(8c)** (oben), Übergangszustand (unten). *t*Bu- und Wasserstoffatome wurden der Übersichtlichkeit wegen weggelassen.

Diese Rotation ist bei Molybdän Komplexen schneller als bei Wolfram Komplexen und hängt von der Alkylgruppe am Phosphor ab (Abbildung 11). Wegen dieser Rotation findet mankein Signal bei Raumtemperatur im ^{31}P NMR und im ^{1}H NMR sieht man nur ein Triplett für die Hydrid Liganden. Bei der tiefen Temperaturen (-60 °C) gibt es ein dublettisches Dublett sowohl im ^{31}P NMR als auch im ^{1}H NMR (Abbildung 18, Tabelle 3).

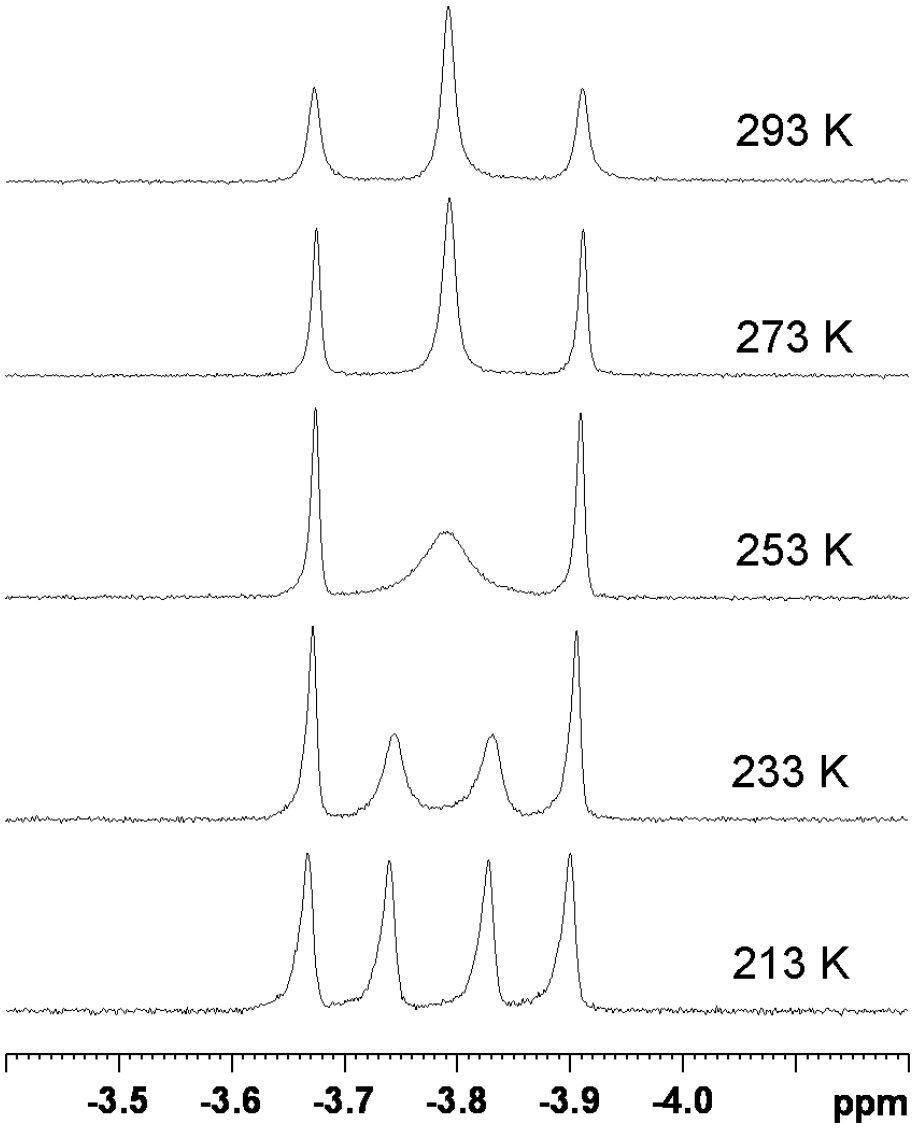

Abbildung 18: Das temperaturabhängige 300 MHz ^{1}H NMR Spektrum von $[Mo(PNP\text{-}Ph)(CO)_3H]BF_4$ (**7a**) in CD_2Cl_2 (Hydridregion)

Außer ^{1}H, $^{13}C\{^{1}H\}$, $^{31}P\{^{1}H\}$ NMR und IR wurden die Komplexe mit Einkristall Röntgendiffraktion charakterisiert (Abbildung 19, 20, 21).

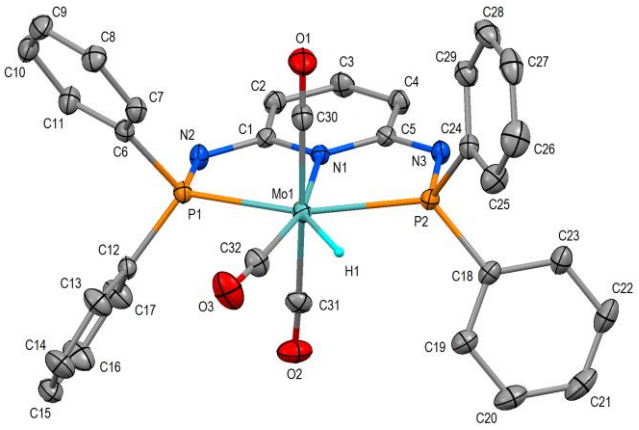

Abbildung 19: ORTEP Diagramm von $[Mo(PNP\text{-}Ph)(CO)_3H]BF_4$ **(7a)** mit Bindungslängen und Winkeln (Å, °): Mo-H(1) 1.67(4), Mo-C(30) 2.0368(15), Mo-C(31) 2.0465(15), Mo-C(32) 2.017(3), Mo-N(1) 2.2357(11), Mo-P(1) 2.4409(4), Mo-P(2) 2.4489(4); P(1)-Mo-P(2) 154.64(1), N(1)-Mo-P(1) 77.39(3), N(1)-Mo-P(2) 77.39(3), N(1)-Mo-C(30) 87.62(5), N(1)-Mo-C(31) 86.97(5), N(1)-Mo-C(32) 163.73(9), N(1)-Mo-H(1) 146.0(15), C(32)-Mo-H(1) 50.2(15).

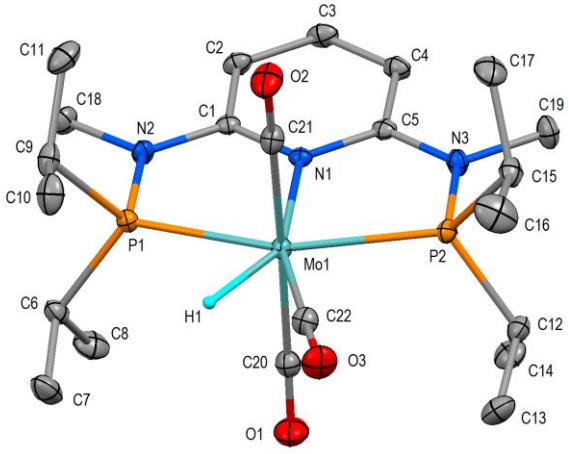

Abbildung 20: ORTEP Diagramm von $[Mo(PNP^{Me}\text{-}i\text{Pr})(CO)_3H]BF_4 \cdot CH_2Cl_2$ **(7d·CH_2Cl_2)** mit Bindungslängen und Winkeln (Å, °): Mo-H(1) 1.63(2), Mo-C(20) 2.0440(13), Mo-C(21) 2.0239(13), Mo-C(22) 1.9856(13), Mo-N(1) 2.2462(10), Mo-P(1) 2.4425(3), Mo-P(2) 2.4776(3); P(1)-Mo-P(2) 154.61(1), N(1)-Mo-P(1) 77.29(3), N(1)-Mo-P(2) 77.31(3), N(1)-Mo-C(20) 94.27(4), N(1)-Mo-C(21) 89.76(4), N(1)-Mo-C(22) 162.26(4), N(1)-Mo-H(1) 145.7(8), C(22)-Mo-H(1) 52.0(8).

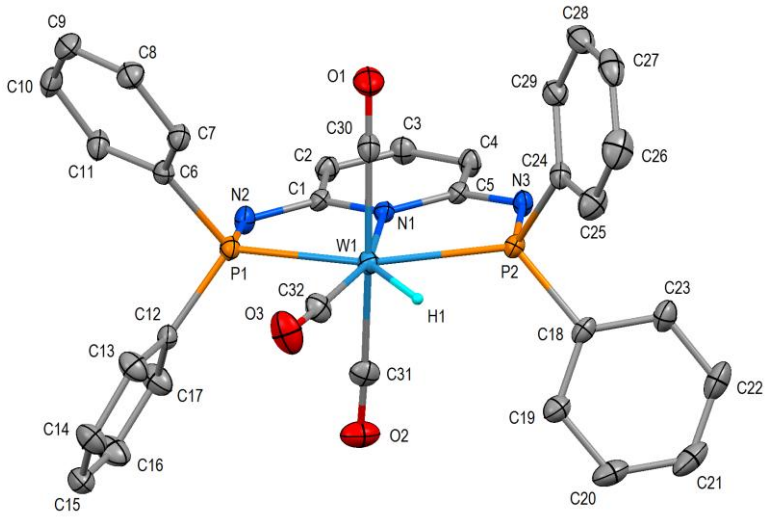

Abbildung 21: ORTEP Diagramm von $[W(PNP\text{-}Ph)(CO)_3H]BF_4$ **(8a)** mit Bindungslängen und Winkeln (Å, °): W-H(1) 1.65(5), W-C(30) 2.033(2), W-C(31) 2.039(2), W-C(32) 2.022(4), W-N(1) 2.2316(15), W-P(1) 2.4444(5), W-P(2) 2.4459(5); P(1)-W-P(2) 154.32(2), N(1)-W-P(1) 77.17(4), N(1)-W-P(2) 77.29(4), N(1)-W-C(30) 87.78(7), N(1)-W-C(31) 86.88(7), N(1)-W-C(32) 162.35(11), N(1)-W-H(1) 143.5(17), C(32)-W-H(1) 53.9(17).

3.5 Synthese von Mo(III) und Mo(IV) PNP-R Halokomplexe

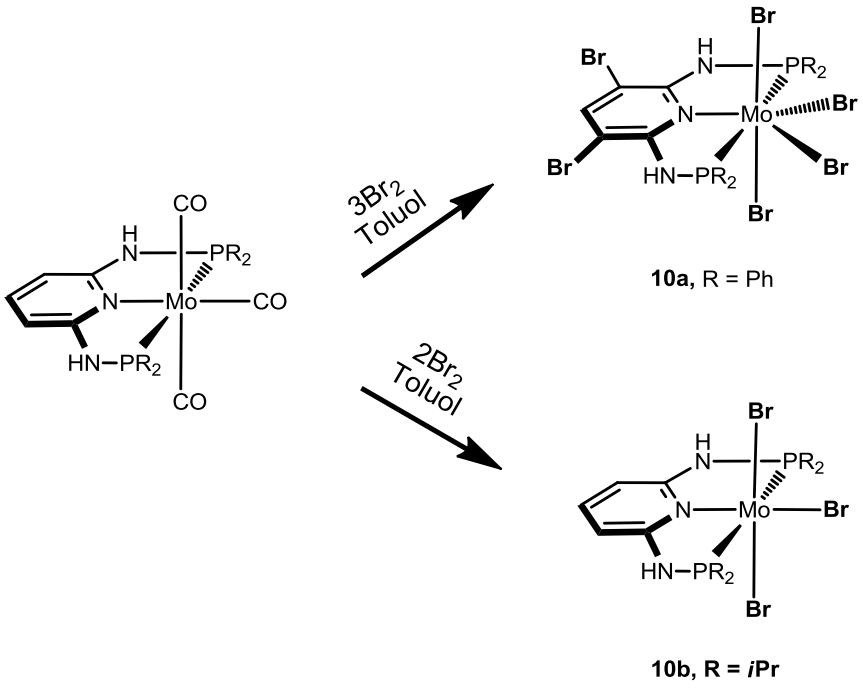

Schema 21: Herstellung der Mo(III) und Mo(IV) Komplexe **(10a, b)**

Die Komplexe wurden durch Umsetzung von Mo(PNP-R)$(CO)_3$ (R = Ph, *i*Pr) mit Br_2 in Toluol hergestellt (Schema 21). Bei der Umsetzung von Mo(PNP-Ph)$(CO)_3$ entstand Mo(PNP^{2Br}-Ph)Br_4 mit Ringsubstitution in den 3 und 5 Positionen (Abbildung 22). Der Komplex ist siebenfach koordiniert und hat eine verzerrte Oktaederstruktur. Zwei Bromatome liegen horizontal zur PNP Ebene, die andere Bromatome liegen in der PNP Ebene.

Mit dem größeren *i*Pr Rest entsteht ein sechsfachkoordinierter oktaedrischer Komplex mit der formalen Oxidationstufe +III. Zwei Bromatome liegen wie bei **10a** horizontal zur PNP-Ebene und drittes Bromatom liegt in der PNP-Ebene trans zum Stickstoffatom (Abbildung 23). Zum Vergleich zu **10a** ist **10b** hat keine verzerrte Struktur sonder ist ein fast perfekter Oktaeder. Die Winkeln zwischen N1-Mo1-Br sind 142.89° **(10a)** und 178.79° **(10b)**.

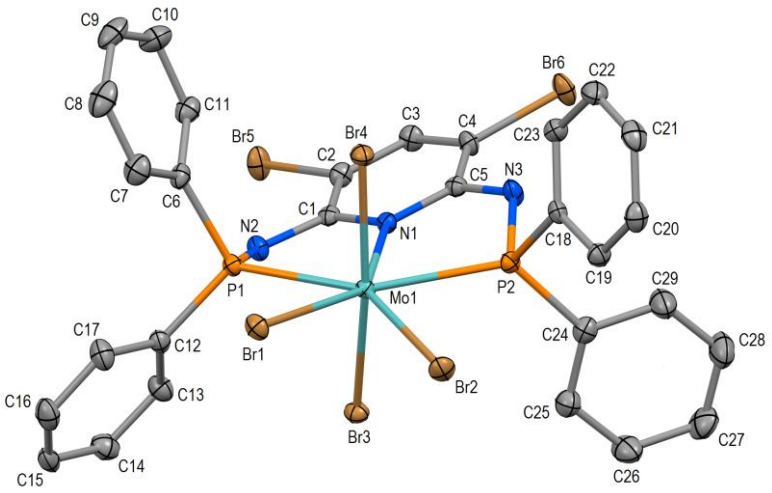

Abbildung 22: ORTEP Diagramm von [Mo(PNP^{2Br}-Ph)Br_4] **(10a)** mit Bindungslängen und Winkeln (Å, °): Mo-N(1) 2.298(2), Mo-P(1) 2.5284(5), Mo-P(2) 2.5248(6), Mo-Br(1) 2.6122(3), Mo-Br(2) 2.5956(3), Mo-Br(3) 2.5438(3), Mo-Br(4) 2.5310(3); P(1)-Mo-P(2) 148.15(2), N(1)-Mo-P(1) 73.99(4), N(1)-Mo-P(2) 74.58(4), N(1)-Mo-Br(1) 142.89(4), N(1)-Mo-Br(2) 139.86(4), N(1)-Mo-Br(3) 86.70(4), N(1)-Mo-Br(4) 85.17(4), P(1)-Mo1-N(1)-C(1) -14.60(12).

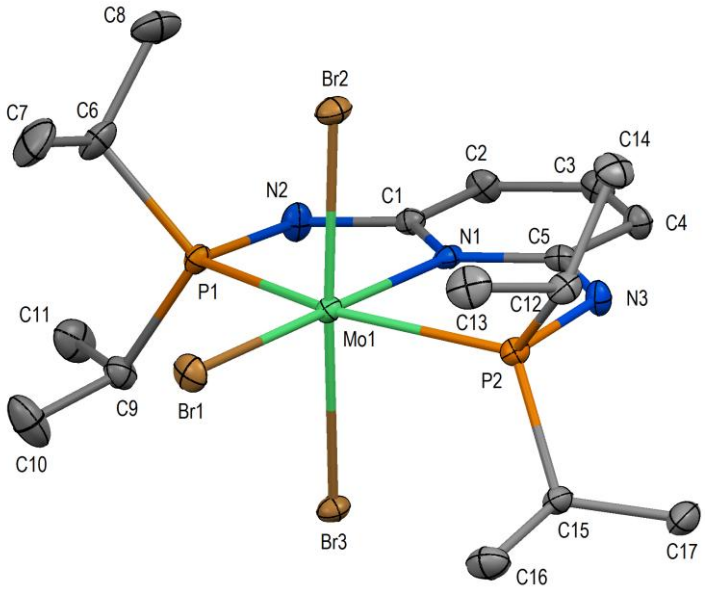

Abbildung 23: ORTEP Diagramm von [Mo(PNP-*i*Pr)Br_3] **(10b)** mit Bindungslängen und Winkeln (Å, °): Mo-N(1) 2.209(2), Mo-P(1) 2.5221(7), Mo-P(2) 2.5170(7), Mo-Br(1) 2.5256(3), Mo-Br(2) 2.5405(3), Mo-Br(3) 2.5806(3); P(1)-Mo-P(2) 156.20(2), N(1)-Mo-P(1) 78.39(6), N(1)-Mo-P(2) 78.26(6), N(1)-Mo-Br(1) 178.79(6), N(1)-Mo-Br(2) 88.71(5), N(1)-Mo-Br(3) 87.95(5), P(1)-Mo1-N(1)-C(1) 179.56(19).

Die Komplexe sind paramagnetisch und konnten nicht mittels NMR Spektroskopie charakterisiert werden. Die Charakterisierung erfolgte mittels Einkristall Röntgendiffraktion und Massenspektroskopie.

3.6 Synthese von [Mo(PNP-R)(O)X]X-Komplexen

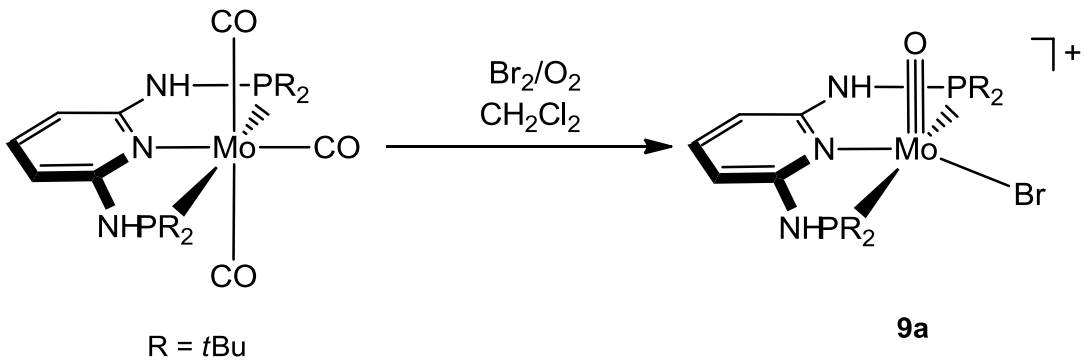

R = *t*Bu

9a

Schema 22: Herstellung des Komplexes [Mo(PNP-*t*Bu)(O)Br]Br **(9a)**

Der Komplex **9a** wurde durch Umsetzung von Mo(PNP-*t*Bu)$(CO)_3$ mit Br_2 in Anwesenheit von Luft hergestellt (Schema 22). Wegen der schwer zu kontrollierenden Stöchiometrie des Sauerstoffes entstanden einige Nebenprodukte, die nicht identifiziert werden konnten.

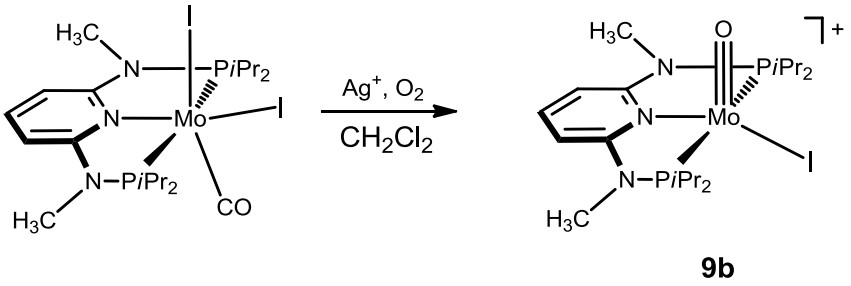

9b

Schema 23: Herstellung des Komplexes [Mo(PNP^{Me}-*i*Pr)(O)I]SbF_6 **(9b)**

Der Komplex **9b** wurde durch Umsetzung von **6b** mit dem Silbersalz $AgSbF_6$ in Anwesenheit von Luft hergestellt (Schema23). Beide Mono-oxo-Komplexe wurden mittels ^{1}H, $^{31}P\{^{1}H\}$ NMR, und ein Einkristall Röntgendiffraktion charakterisiert (Tabella 3). Die Mono-oxo-Komplexe besitzen eine verzrerrte quadratisch-pyramidale Struktur. Der Oxoligand steht senkrecht zur PNP-Ebene und besitzt eine Metall-O dreifache Bindung.

Tabelle 3. IR, ^{1}H, $^{31}P\{^{1}H\}$ NMR, und $^{13}C\{^{1}H\}$ NMR Daten der Molybdän und Wolfram Komplexe mit PNP Liganden.

Komplex	$\nu_{C\equiv O}$, cm^{-1}		δ_P, ppm	$\delta_{C\equiv O}$, ppm	δ_H, ppm
4a	1964, 1765	1858,	116.2	228.4, 211.2	
4b	1936, 1790	1809,	143.6	231.4, 216.9	
4c	1922, 1771	1808,	161.9	233.1, 224.0	
4d	1936, 1795	1810,	171.0	230.8, 217.9	
4e	1955, 1759	1847,	100.2	206.0, 196.6	
4f	1929, 1784	1805,	128.5	221.1, 210.6	
4g	1914, 1759	1799,	147.2	224.7, 219.4	
5a	2040, 1875	1975,	125.3		
5b	2030, 1936	1967,	126.7	234.6, 218.3	
5e	2030, 1933	1958,	85.2	225.4, 210.3	
5f	2023, 1922	1953,	106.6	212.2, 191.3	
5g	2019, 1909	1941,	131.6	229.9, 212.9	
6a	1816		206.9	247.9	
6b	1824		202.2	247.3	
6c	1813		207.0	248.5	
6d	1831		205.9	218.5	
7a	2042, 1937	1940,	111.5, 97.8	212.7, 203.2	-3.78
7b	2035, 1920	1923,	142.3, 121.4	212.3, 205.8	-4.98

7c	2019, 1916	1937,	158.8, 142.8	213.7, 209.5	-4.34
7d	2028, 1910	1928,	166.1, 147.7	210.8, 205.4	-5.49
8a	2038, 1918	1963,	95.5, 84.8	205.9, 196.6	-3.43
8b	2027, 1906	1910,	125.9, 108.6	205.5, 198.0	-4.83
8c	2021, 1897	1934,	141.1, 126.8		-4.16
9a			147.2		
9b			161.0		

Experimenteller Teil

Abkürzungen

BH_3·THF	Boran Tetrahydrofurankomplex
CH_3CN	Acetonitril
CH_2Cl_2	Methylenchlorid
$CHCl_3$	Chloroform
CO	Kohlenmonoxid
Cp	Cyclopentadien
^{c}Hex	Cyclohexyl
Et_2O	Diethylether
HBF_4	Tetrafluoroborsäure
$Me_3O^+.BF_4$	Trimethyloxoniumtetrafluoroborat
MG	Molekulargewicht
$Mo(CO)_6$	Molybdänhexacarbonyl
*n*BuLi	n-Butyllithium
NaHg	Natrium-Quecksilber Amalgam
NEt_3	Triethylamin
Ph	Phenyl
Py	Pyridin
RT	Raumtemperatur
THF	Tetrahydrofuran
$W(CO)_6$	Wolframhexacarbonyl

Allgemeines

Alle Experimente wurden unter Inertgas (Argon) in einer Glovebox und mit Hilfe der Schlenktechnik durchgeführt. Verwendete Reagenzien wurde ohne weiter Reinigung eingesetzt. Die Lösungsmittel wurden nach Standardvorschriften gereinigt und getrocknet.[31] Deuterierte Lösungsmittel wurden bei Aldrich gekauft und über getrocknetes 4 Å Molekularsieb aufbewahrt. Die Komplexe ($FeCp(CO)_2Br$, $FeCp(CO)_2Cl$[32] und $Fe(CO)_4Br_2$[33]) wurden nach Literaturvorschriften hergestellt. Die Liganden (PNP-Ph, PNP-*i*Pr und PNP-*t*Bu) und die Komplexe (Mo(PNP-Ph), Mo(PNP-*i*Pr und Mo(PNP-*t*Bu) wurden nach Literaturvorschriften hergestellt.[24] ^{1}H, ^{13}C und $^{31}P\{^{1}H\}$ NMR Spektren wurde mit einem Bruker AVANCE-250 Spektrometer aufgenommen und gegen $SiMe_4$ und H_3PO_4 (85%) referenziert. FT-IR Spektren wurden an Bruker Tensor 27 Spektrometer aufgenommen.

1. PN- Liganden

Ph_2PNiPr (1a)

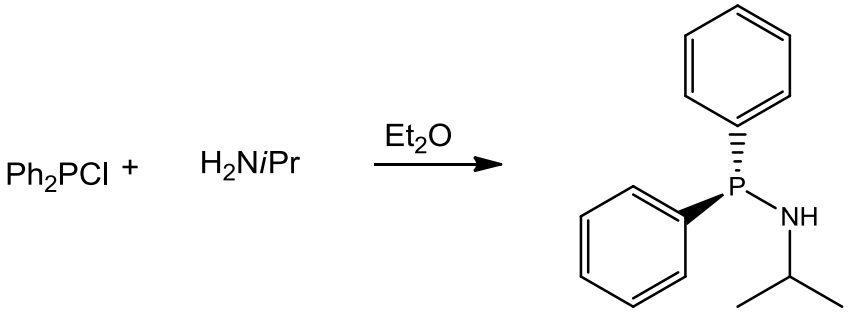

In einem Dreihalskolben mit Rückflußkühler wurde Isopropylamin (3.3 g, 0.055 mol) in Et_2O (150 mL) vorgelegt. Dann wurde Chlorodiphenylphosphin (5.97 g, 0.027 mol) unter Eiskühlung zugetropft. Danach wurde die Eiskühlung entfernt und das Reaktionsgemisch über Nacht gekocht. Anschließend das Reaktionsgemisch wurde unter Argon filtriert und das Lösungsmittel am Hochvakuum abgezogen.

Ausbeute: 6.0 g (91 %) weiß kristallin

Chemical Formula: $C_{15}H_{18}NP$

Elementar Analyse: $C_{15}H_{18}NP$ (M.G: 243.12): C, 7.05; H, 7.46; N,5.76; P, 12.73

^{1}H-NMR (δ, $CDCl_3$, 20 °C): 7.39 (m, 10H, Ph), 3.30 (m, 1H, C*H*$(CH_3)_2$), 1.87 (bs, 1H, N*H*), 1.18 (d, *J* = 6.43 Hz, 6H, CH(C*H*$_3)_2$)

^{13}C{^{1}H}-NMR (δ, $CDCl_3$, 20 °C): 142.9 (d, J_{PC} = 12.39 Hz, Ph), 131.05 (d, J_{PC} = 19.85 Hz, Ph), 128.2 (s, Ph), 128.0 (d, J_{PC} = 6.31 Hz, Ph), 48.5 (d, J_{PC} = 22.72 Hz, *C*H$(CH_3)_2$), 26.05 (d, J_{PC} = 6.31 Hz, CH(*C*H$_3)_2$)

^{31}P{^{1}H}-NMR (δ, $CDCl_3$, 20 °C): 46.4

Ph_2PNtBu (1b)

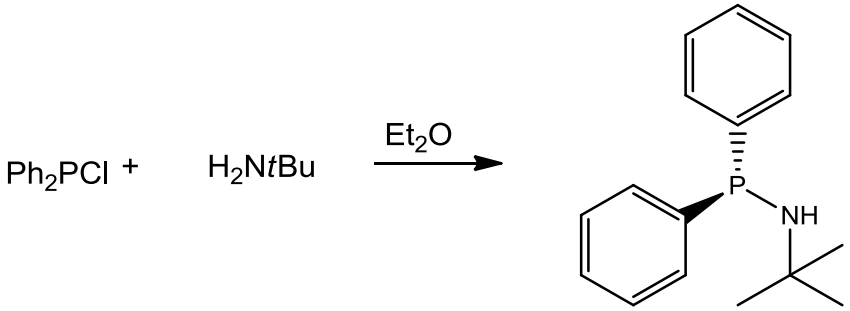

Die Reaktion wurde analog zu **1a** mit tert-Butylamin (4.06 g, 0.05 mmol) durchgeführt.

Ausbeute: 6.6 g (95 %) weiß kristallin

Elementar Analyse: $C_{16}H_{20}NP$ (M.G: 257.31): C, 74.68; H, 7.83; N, 5.44; P, 12.04

^{1}H-NMR (δ, $CDCl_3$, 20 °C): 7.40 (m, 10H, Ph), 2.06 (d, *J* = 11.70 Hz, 1H, N*H*), 1.32 (s, 9H, $C(CH_3)_3$)

$^{13}C\{^1H\}$-NMR (δ, $CDCl_3$, 20 °C): 143.75 (d, J_{PC} = 12.21 Hz, Ph), 130.9 (d, J_{PC} = 20.19 Hz, Ph), 128.2 (s, Ph), 128.1 (s, Ph), 51.35 (d, J_{PC} = 19.21 Hz, $C(CH_3)_3$), 32.2 (d, J_{PC} = 8.21 Hz, $CH(CH_3)_2$)

$^{31}P\{^1H\}$-NMR (δ, $CDCl_3$, 20 °C): 34.0

Ph_2PNnPr (1c)

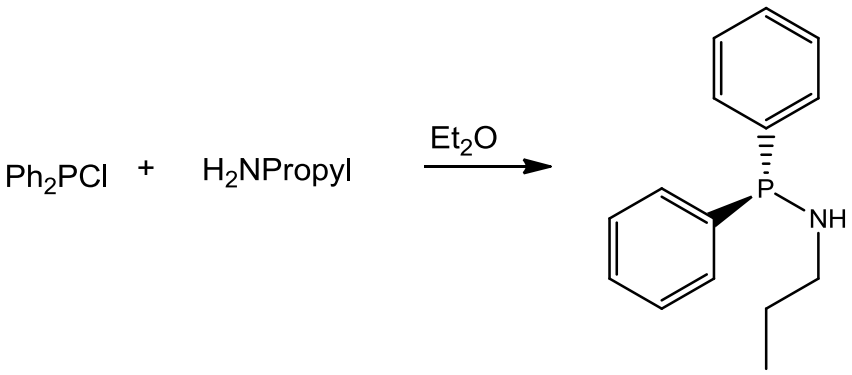

Die Reaktion wurde analog zu **1a** mit Propylamin (3.3 g, 0.055 mmol) durchgeführt.

Ausbeute: 5.8 g (88 %) farblose Flüssigkeit

Elementar Analyse: $C_{15}H_{18}NP$ (M.G: 243.12): C, 74.05; H, 7.46; N, 5.76; P, 12.73

^{1}H-NMR (δ, $CDCl_3$, 20 °C): 7.42 (m, 10H, Ph), 2.93 (m,2H, C*H*$_2$CH$_2$CH$_3$), 1.97 (d, *J* = 6.64 Hz, 1H, N*H*), 1.51 (m, 2H, CH$_2$C*H*$_2$CH$_3$), 0.91 (t, *J* = 7.46 Hz, 3H, CH$_2$CH$_2$C*H*$_3$)

^{13}C{^{1}H}-NMR (δ, $CDCl_3$, 20 °C): 141.85 (d, J_{PC} = 10.88 Hz, Ph), 131.35 (d, J_{PC} = 19.98 Hz, Ph), 128.4 s, Ph), 128.2 (s, Ph), 48.15 (d, J_{PC} = 11.87 Hz, *C*H$_2$CH$_2$CH$_3$), 26.1 (s, CH$_2$*C*H$_2$CH$_3$), 11.4 (s, CH$_2$CH$_2$*C*H$_3$)

^{31}P{^{1}H}-NMR (δ, $CDCl_3$, 20 °C): 52.8

***i*Pr$_2$PN*i*Pr (1d)**

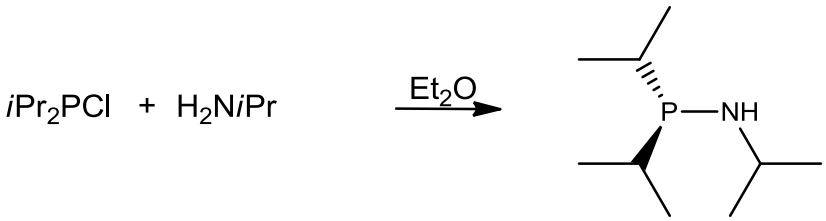

Die Reaktion wurde analog zu **1a** mit Isopropylamin (3.8 g, 0.064 mmo) und Chlorodiisopropylphosphin (4.75 g, 0.031 mmol) durchgeführt.

Ausbeute: 5.6 g (89 %) farblose Flüssigkeit

Elementar Analyse: $C_9H_{22}NP$ (M.G: 175.25): C, 61.68; H, 12.65; N, 7.99; P, 17.67

^{1}H-NMR (δ, $CDCl_3$, 20 °C): 2.97 (m, 1H, N*H*), 1.41 (m, 3H, P(C*H*(CH$_3$)$_2$)$_2$-N(*CH*(CH$_3$)$_2$), 1.45 (d, *J* = 6.47 Hz, 6H, N(CH(C*H*$_3$)$_2$), 0.94 (d, *J* = 2.71 Hz, 3H, P(CH(C*H*$_3$)$_2$)$_2$, 0.92 (d, *J* = 2.59 Hz, 3H, P(CH(C*H*$_3$)$_2$)$_2$, 0.89 (d, *J* = 2.82 Hz, 3H, P(CH(C*H*$_3$)$_2$)$_2$, 0,87 (d, *J* = 2.94 Hz, 3H, P(CH(C*H*$_3$)$_2$)$_2$

^{13}C{^{1}H}-NMR (δ, $CDCl_3$, 20 °C): 48.8 (d, J_{PC} = 25.45 Hz, N(*C*H(CH$_3$)$_2$), 26.2 (d, J_{PC} = 8.33 Hz, N(CH(*C*H$_3$)$_2$), 26.0 (d, J_{PC} = 3.03 Hz, P(*C*H(CH$_3$)$_2$)$_2$), 18.9 (d, J_{PC} = 20.95 Hz, P(CH(*C*H$_3$)$_2$), 16.9 (d, J_{PC} = 7.83 Hz, P(CH(*C*H$_3$)$_2$)

^{31}P{^{1}H}-NMR (δ, $CDCl_3$, 20 °C): 69.6

iPr$_2$PNToluidin (1e)

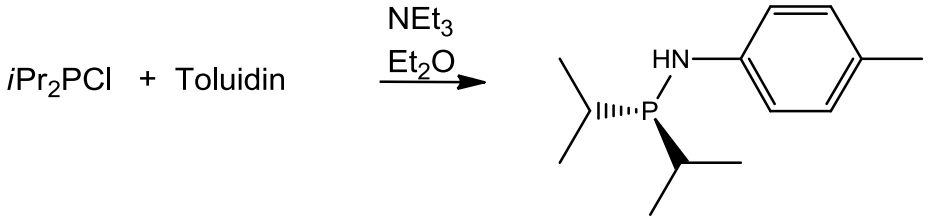

Die Reaktion wurde analog zu **1a** mit 4-Toluidin (3.4 g, 0.032 mmol) und Chlorodiisopropylphosphin (4.75 g, 0.031 mmol) durchgeführt. Der einzige Unterschied ist, 1.1 Äquivalenten Triethylamin wurde als Base verwendet.

Ausbeute: 6.0 g (85 %) starre, gelbliche Flüssigkeit

Elementar Analyse: $C_{13}H_{22}NP$ (M.G: 223.29): C, 69.93; H, 9.93; N, 6.27; P, 13.87

^{1}H-NMR (δ, $CDCl_3$, 20 °C): 7.00 (d, J = 8.62 Hz, 2H, Ph), 6.91 (d, J = 8.92 Hz, 2H, Ph), 3.68 (bs, 1H, *NH), 2*.26 (s, 3H, ArCH_3), 1.74 (m, 2H, P(CH(CH_3)$_2$), 1.14 (d, *J* = 3.75 Hz, 6H, P(CH(CH_3)$_2$), 1.08 (d, *J* = 3.59 Hz, 6H, P(CH(CH_3)$_2$)

^{13}C{^{1}H}-NMR (δ, $CDCl_3$, 20 °C): 146.5 (d, J_{PC} = 16.32 Hz, Ph), 129.5 (s, Ph), 127.4 (s, Ph), 115.7 (d, J_{PC} = 11.36 Hz, Ph), 26.7 (d, J_{PC} = 11.36 Hz, P(*C*H(CH_3)$_2$)), 20.3 (s, Ar*C*H_3), 18.7 d, J_{PC} = 19.87 Hz, P(CH(*C*H_3)$_2$), 17.0 (d, J_{PC} = 8.52 Hz, P(CH(*C*H_3)$_2$)

^{31}P{^{1}H}-NMR (δ, $CDCl_3$, 20 °C): 60.0

iPr$_2$PN^{c}Hex (1f)

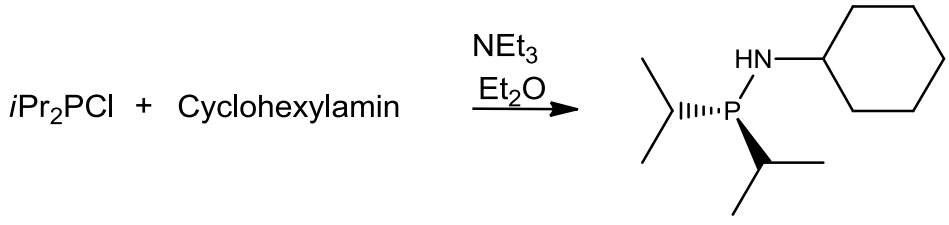

Die Reaktion wurde analog zu **1a** mit Cyclohexylamin (0.60 g, 6 mmol) und Chlorodiisopropylphosphin (0.95 g, 6 mmol) durchgeführt. Der einzige Unterschied ist, 1.1 Äquivalente Triethylamin wurden als Base verwendet.

Ausbeute: 1.1 g (85 %) gelbes Öl.

Elementar Analyse: $C_{12}H_{26}NP$ (M.G: 215.32): C, 66.94; H, 12.17; N, 6.51; P, 14.39

^{1}H-NMR (δ, $CDCl_3$, 20 °C): 2.61 (bs, 1H, NC*H* , 1.90 (d, *J* = 10.79 Hz, 1H, N*H*), 1.56 (m, 1H, P(C*H*$(CH_3)_2$*),* 1.48 (m, 1H, P(C*H*$(CH_3)_2$*),* 1.1 (m, 22H, P(CH(C*H*$_3)_2)_2$- ^{c}Hex)

^{13}C{^{1}H}-NMR (δ, $CDCl_3$, 20 °C): 56.6 (d, J_{PC} = 8.82 Hz, ^{c}Hex), 56.2 (d, J_{PC} = 9.02 Hz, ^{c}Hex), 36.9 (s, ^{c}Hex), 36.7 (s, ^{c}Hex), 36.6 (s, ^{c}Hex), 26.1 (d, J_{PC} = 12.20 Hz, P(*C*H$(CH_3)_2$), 25.7 (s, ^{c}Hex), 25.2 (s, ^{c}Hex , 18.8 (d, J_{PC} = 25.82 Hz, P(CH(*C*$H_3)_2$), 16.7 (d, J_{PC} = 8.06 Hz, P(CH(*C*$H_3)_2$)

^{31}P{^{1}H}-NMR (δ, $CDCl_3$, 20 °C): 69.9

2. PNP- Liganden

N,N'-bis(diisopropylphosphino-boran)-2,6-diaminopyridin (PNP-*i*Pr) (2b·BH_3).

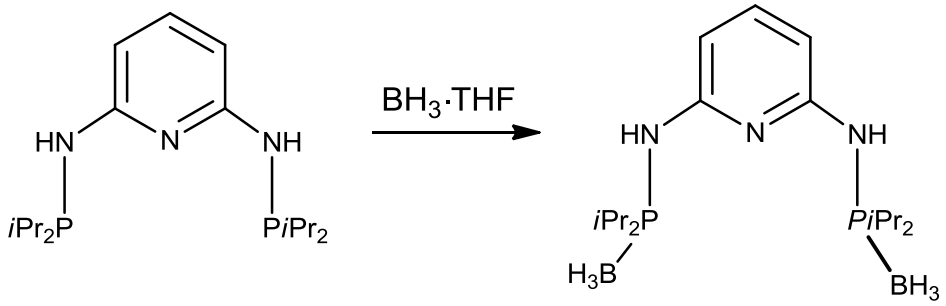

PNP-*i*Pr **2b•BH_3**

PNP-*i*Pr (7.00 g, 20.50 mmol) wurde in THF (100mL) gelöst. Dann wurde BH_3·THF (1.0 M, 43.1 mL, 43.06 mmol) langsam dazugegeben. Das Reaktionsgemisch wurde 30 min bei Raumtemperatur gerührt. Anschließend wurde das Lösungsmittel am Hochvakuum abgezogen und getrocknet.

Ausbeute: 7.57 g (100 %) weißes Pulver.

Elementar Analyse: $C_{17}H_{39}B_2N_3P_2$ (M.G: 369.08): C, 55.32; H, 10.65; B, 5.86; N, 11.39; P, 16.78

^{1}H-NMR (δ, $CDCl_3$, 20 °C): 7.32 (t, *J* = 7.9 Hz, 1H, py^4), 6.26 (d, *J* = 7.9, 2H, $py^{3,5}$), 4.58 (d, *J* = 8.4 Hz, 2H, N*H*), 2.62 (septd, J_1 = 6.9 Hz, J_2 = 13.7 Hz, 4H, C*H*$(CH_3)_2$), 1.16 (m, 24H, CH(C*H*$_3)_2$), 0.60 - -0.15 (bs, 6H, B*H*$_3$).

^{13}C{^{1}H}-NMR (δ, $CDCl_3$, 20 °C): 154.4 (s, $py^{2,6}$), 140.1 (s, py^4), 103.1 (s, $py^{3,5}$), 24.5 (d, *J* = 36.3 Hz, *C*H$(CH_3)_2$), 17.2 (d, *J* = 4.3 Hz, CH(*C*H$_3)_2$), 17.0 (s, CH(*C*H$_3)_2$).

^{31}P{^{1}H}-NMR (δ, $CDCl_3$, 20 °C): 88.5 (br, m).

N,N'-bis(diisopropylphosphino-boran)-N,N'-methyl-2,6-diaminopyridin (PNP^{Me}-*i*Pr) (2d·BH_3).

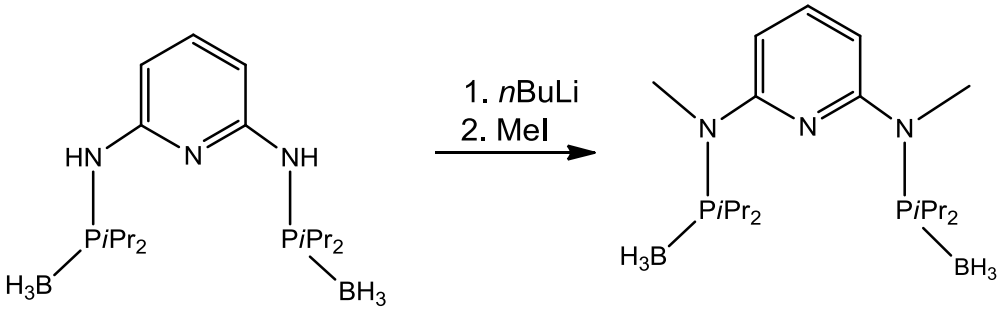

2b·BH_3 **2d·BH_3**

2d·BH_3 (7.45 g, 20.19 mmol) wurde in THF (50 mL) gelöst und auf -20°C gekühlt. Danach wurde *n*-BuLi (17.0 mL, 2.5 M, 41.39 mmol) langsam zugetropft. Das Reaktionsgemisch wurde bei der Raumtemperatur 2 h gerührt. Danach wurde Methyliodid (3.15 mL, 50.46 mmol) langsam mit der Spritze zugetropft. Nach dem Rühren (12 h) bei der Raumtemperatur wurde die Reaktion mit einer gesättigten Ammoniumchloridlösung (100 mL) und konzentriertem Ammoniak gequencht. Die wassrige Phase wurde mit CH_2Cl_2 zweimal extrahiert und die gesammelte organische Phase wurde mit Brain gewaschen und mit Natriumsulfat getrocknet. Nach dem Abziehen des Lösungsmittel am Rotavapor wurde das Produkt durch Kieselgel mit THF gereinigt.

Ausbeute: 5.05 g (63 %) weißes Pulver.

Elementar Analyse: $C_{19}H_{43}B_2N_3P_2$ (M.G: 397.13): C, 57.46; H, 10.91; B, 5.44; N, 10.58; P, 15.60

^{1}H-NMR (δ, $CDCl_3$, 20 °C): 7.48 (t, *J* = 8.0 Hz, 1H, py^4), 6.49 (d, *J* = 8.0, 2H, $py^{3,5}$), 3.17 (d, *J* = 7.9 Hz, 6H, NCH_3), 2.80 (septd, *J* = 7.0 Hz, *J* = 21.2 Hz, 4H, $CH(CH_3)_2$), 1.22 (dd, J_1 = 6.9 Hz, J_2 = 16.5 Hz, 12H, $CH(CH_3)_2$), 1.03 (dd, *J* = 7.0 Hz, *J* = 15.11 Hz, 12H, $CH(CH_3)_2$), 0.70 - -0.30 (bs, 6H, BH_3).

^{13}C{^{1}H}-NMR (δ, $CDCl_3$, 20 °C): 156.9 (s, $py^{2,6}$), 139.1 (s, py^4), 105.8 (s, $py^{3,5}$), 37.6 (s, NCH_3), 25.6 (d, *J* = 36.2 Hz, $CH(CH_3)_2$), 17.8 (s, $CH(CH_3)_2$), 17.2 (s, $CH(CH_3)_2$).

^{31}P{^{1}H}-NMR (δ, $CDCl_3$, 20 °C): 105.9 (br, m).

N,N'-bis(diisopropylphosphino)-N,N'-methyl-2,6-diaminopyridin (PNP^{Me}-*i*Pr) (2d).

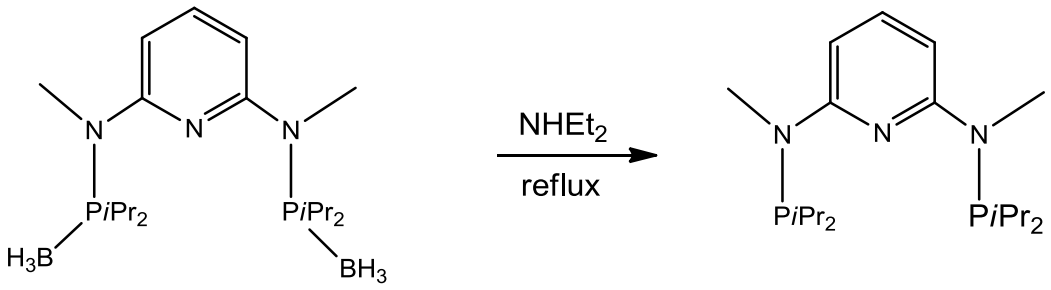

2d·BH_3 **2d**

2d·BH_3 (5.00 g, 12.59 mmol) wurde in 100 mL Et_2NH 72 h refluxiert. Das Lösungsmittel wurde am Rotavapor einrotiert. Der Rückstand wurde in THF gelöst, über Celite filtriert. Die erhaltene gelbliche Flüssigkeit wurde aus Acetonitril umkristallisiert.

Ausbeute: 3.25 g (70 %) weißes Pulver.

Elementar Analyse: $C_{19}H_{37}N_3P_2$ (M.G: 369.46): C, 61.77; H, 10.09; N, 11.37; P, 16.77

^{1}H-NMR (δ, CD_2Cl_2, 20 °C): 7.22 (t, *J* = 8.0 Hz, 1H, py^4), 6.64 (bs, $py^{3,5}$), 3.04 (d, *J* = 2.3 Hz, 6H, NCH_3), 2.22 (bs, 4H, $CH(CH_3)_2$), 1.10 (dd, *J* = 6.9 Hz, *J* = 16.9 Hz, 12H, $CH(CH_3)_2$), 0.98 (dd, *J* = 7.0 Hz, *J* = 12.1 Hz, 12H, $CH(CH_3)_2$).

$^{13}C\{^1H\}$-NMR (δ, CD_2Cl_2, 20 °C): 160.4 (s, $py^{2,6}$), 136.9 (s, py^4), 99.1 (d, *J* = 22.3 Hz, $py^{3,5}$), 33.7 (bs, NCH_3), 26.2 (d, *J* = 15.3 Hz, $CH(CH_3)_2$), 19.4 (s, $CH(CH_3)_2$), 19.2 (s, $CH(CH_3)_2$), 19.0 (s, $CH(CH_3)_2$).

$^{31}P\{^1H\}$-NMR (δ, CD_2Cl_2, 20 °C): 81.3 (bs).

3. Eisen - Komplexe

$Fe(Ph_2PNiPr)_2(CO)_2Br_2$ (3a)

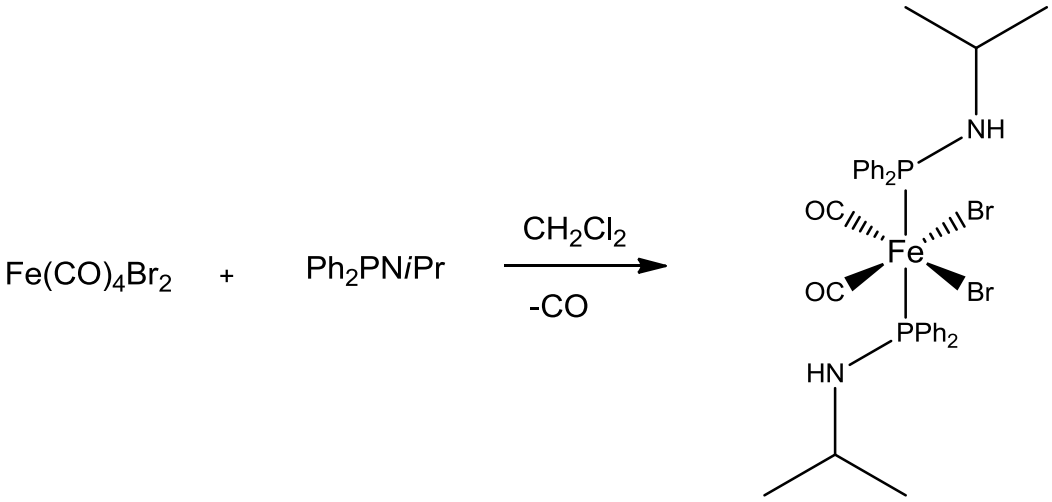

Eisen(II)tetracarbonyldibromid (1 g, 3.05 mmol) wurde im Schlenkrohr in Methylenchlorid (10 mL) gelöst. Danach wurde in Methylenchlorid gelöste Ph_2PNiPr (1.52 g, 6.25 mmol) unter Kühlung zugetropft. Nach dem Rühren Übernacht wurde das Reaktionsgemisch über Celite, Seesand und Glaßwolle filtriert und das Lösungsmittel am Hochvakuum abgezogen. Anschließend wurde das Produkt mit Diethylether gewaschen und getrocknet.

Ausbeute: 1.96 g (85 %) gelbes Pulver

Elementar Analyse: $C_{32}H_{36}Br_2FeN_2O_2P_2$ (M.G: 758.24): C, 50.69; H, 4.79; Br, 21.08; Fe, 7.37; N, 3.69; O, 4.22; P, 8.17

^1H-NMR (δ, $CDCl_3$, 20 °C): 7.99 (bs, 8H, Ph), 7.48 (bs, 12H, Ph), 3.42 (m, 2H, *NH),* 2.29 (m, 2H, $CH(CH_3)_2$), 0.91 (d, *J* = 6.29 Hz, 12H, $CH(CH_3)_2$)

$^{13}C\{^1H\}$-NMR (δ, $CDCl_3$, 20 °C): 212.7 (t, J_{PC} = 22.65 Hz, *C*O), 133.0 (dd, J_{PC} = 5.16 Hz, Ph), 131.7 (dd, J_{PC} = 5.42 Hz, Ph), 130.8 (s, Ph), 127.9 (dd, J_{PC} = 4.64 Hz, Ph), 46.4 (dd, J_{PC} = 4.90 Hz, *C*H(CH_3)$_2$), 24.7 (s, CH(*C*H_3)$_2$)

$^{31}P\{^1H\}$-NMR (δ, $CDCl_3$, 20 °C): 80.6

IR(ATR, 25 °C): 2040.70 (ν_{co}), 1985.93 (ν_{co})

Fe(Ph_2PNtBu)$_2$(CO)$_2Br_2$ (3b)

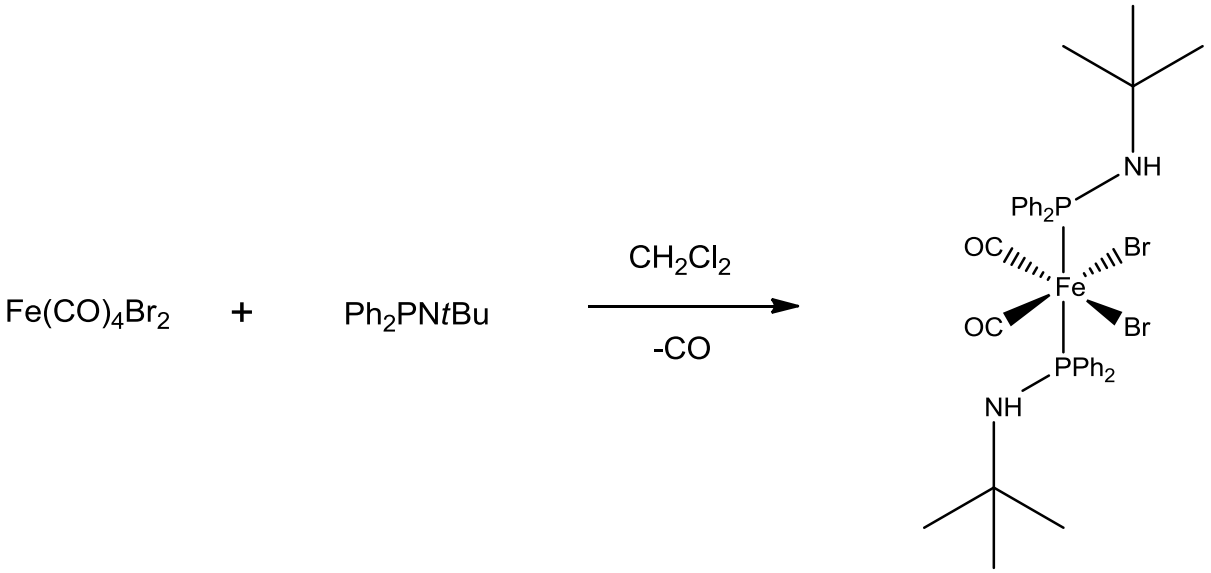

Die Reaktion wurde analog zu **3a** mit Ph_2PN_tBu (1.33 g, 5.16 mmol) durchgeführt.

Ausbeute: 1.7 mg (88 %) gelbes Pulver

Elementar Analyse: $C_{34}H_{40}Br_2FeN_2O_2P_2$ (M.G: 786.29):C, 51.94; H, 5.13; Br, 20.32; Fe, 7.10; N, 3.56; O, 4.07; P, 7.88

^{1}H-NMR (δ, d_6-Aceton, 20 °C): 8.36 (bs, 8H, Ph), 7.48 (bs, 12H, Ph), 3.7 (bs, 2H, *NH),* 0.87 (s, 18H, C(*C*H_3)$_3$)

$^{13}C\{^1H\}$-NMR (δ, $CDCl_3$, 20 °C): 213.3 (t, J_{PC} = 24.01 Hz, *C*O), 134.2 (dd, J_{PC} = 25.74 Hz, Ph), 133.5 (dd, J_{PC} = 5.33 Hz, Ph), 130.7 (s, Ph), 127.7 (dd, J_{PC} = 4.68 Hz, Ph), 55.5 (s, *C*(CH_3)$_3$), 31.7 (s, C(*C*H_3)$_3$)

$^{31}P\{^1H\}$-NMR (δ, d_6-Aceton, 20 °C): 72.2

IR(ATR, 25 °C): 2035.17 (ν_{co}), 1979.53 (ν_{co})

$Fe(Ph_2PN\mathit{n}Pr)_2(CO)_2Br_2$ (3c)

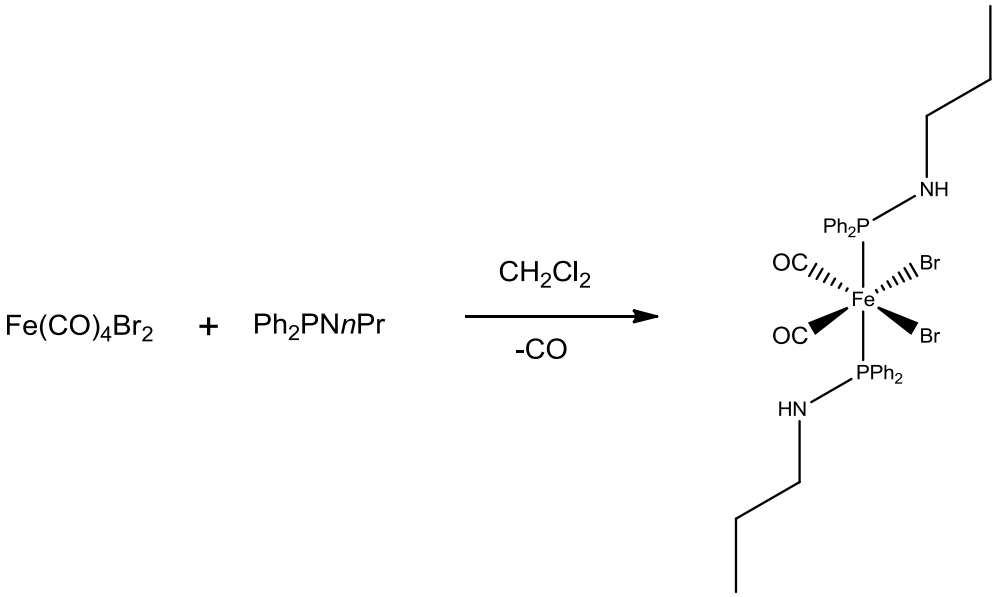

Die Reaktion wurde analog zu **3a** mit Ph_2PNPropyl (1 g, 4.11 mmol) durchgeführt.

Ausbeute: 1.2 mg (80 %) gelbes Pulver

Elementar Analyse: $C_{32}H_{36}Br_2FeN_2O_2P_2$ (M.G: 758.24): C, 51.32; H, 4.96; Br, 20.69; Fe, 7.23; N, 3.63; O, 4.14; P, 8.02

^{1}H-NMR (δ, d_6-Aceton, 20 °C): 7.94 (bs, 8H, Ph), 7.48 (bs, 12H, Ph), 3.61 (bs, 2H, *NH*), 2.52 (bs, 4H, NCH_2), 1.41 (bs, 4H, NCH_2CH_2), 0.84 (bs, 6H, $NCH_2CH_2CH_3$)

^{13}C{^{1}H}-NMR (δ, $CDCl_3$, 20 °C): 212.7 (t, J_{PC} = 24.43 Hz, *C*O), 132.8 (dd, J_{PC} = 4.90 Hz, Ph), 131.7 (dd, J_{PC} = 6.70 Hz, Ph), 130.7 (s, Ph), 127.9 (dd, J_{PC} = 4.90 Hz, Ph), 45.7 (d, J_{PC} = 4.51 Hz, NCH_2), 24.9 (s, NCH_2CH_2), 11.2 (s, $NCH_2CH_2CH_3$)

^{31}P{^{1}H}-NMR (δ, d_6-Aceton, 20 °C): 82.3

IR(ATR, 25 °C): 2008 (ν_{co}), 1987 (ν_{co})

Fe(Ph$_2$PN*i*Pr)(CO)$_2$(κ^2-(*C, P*)-(C=O)-N*i*Pr-PPh$_2$)Br (3d)

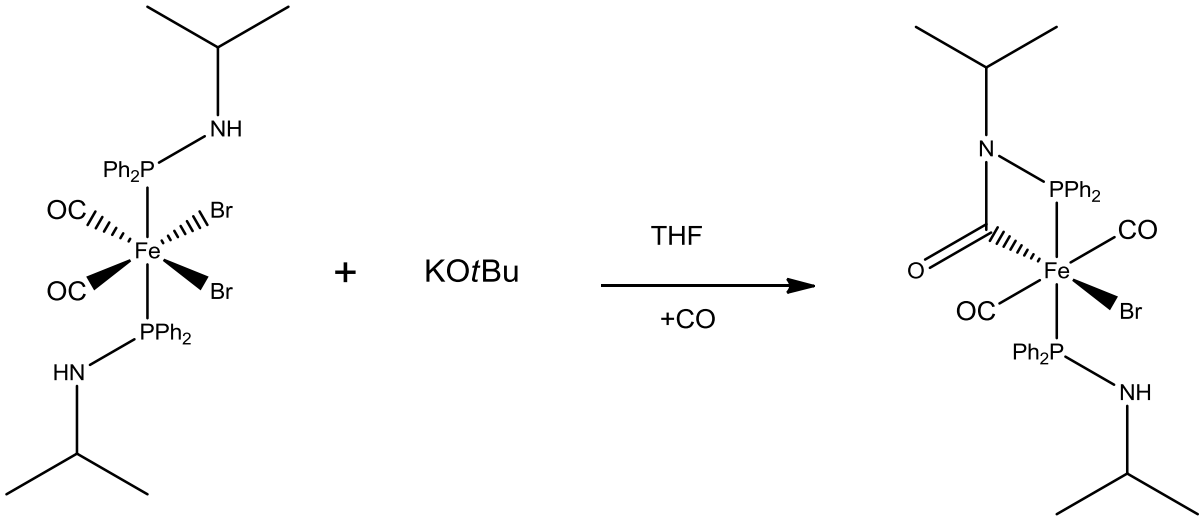

3a (400 mg, 0.53 mmol) und KO^{t}Bu (122 mg,1.06 mmol) wurde in einem Schlenkrohr vorgelegt. Kohlenstoffmonooxid wurde für 5 Min. eingeleitet, THF (10 mL) zugesetzt und Übernacht bei RT gerührt. Die entstandene rote Lösung wurde über Celite und Glaßwolle filtriert. Das Lösungsmittel wurde am Hochvakuum abgezogen, das Produkt in CH_2Cl_2 gelöst und nochmals filtriert. Nach dem Abziehen des Lösungsmittels wurde das Produkt mit n-Hexan gewaschen und getrocknet.

Ausbeute: 185 mg (50 %) rotes Pulver

Elementar Analyse: $C_{33}H_{35}BrFeN_2O_3P_2$ (M.G: 705.34): C, 50.69; H, 4.79; Br, 21.08; Fe, 7.37; N, 3.69; O, 4.22; P, 8.17

^{1}H-NMR (δ, $CDCl_3$, 20 °C): 7.85 (d, *J* = 6.79 Hz, 8H, Ph), 7.50 (d, *J* = 8.38 Hz, 8H, Ph), 7.43 (s, 4H, Ph), 4.70 (d, 1H, *NH*), 3.46 (m, 1H, C*H*(CH_3)$_2$), 3.12 (m, 1H, C*H*(CH_3)$_2$), 1.31 (d, *J* = 6.39 Hz, 6H, CH(C*H*$_3$)$_2$), 0.94 (d, *J* = 6.39 Hz, 6H, CH(C*H*$_3$)$_2$).

^{13}C{^{1}H}-NMR (δ, $CDCl_3$, 20 °C): 212.4 (t, J_{PC} = 22.70 Hz, *C*O), 206.0 (dd, J_{PC} = 9.60 Hz, J_{PC} = 13.44 Hz, NCO), 133.3 (d, J_{PC} = 12.10 Hz, Ph), 130.2 (s, Ph), 128.7 (d, J_{PC} = 11.10 Hz, Ph), 128.0 (d, J_{PC} = 11.10 Hz, Ph), 25.5 (s, *C*H(CH_3)$_2$), 22.0 (s, CH(*C*H$_3$)$_2$).

^{31}P{^{1}H}-NMR (δ, $CDCl_3$, 20 °C): 95.61 (d, J_{PP} = 84.70 Hz), 85.76 (d, J_{PP} = 84.70 Hz)

IR(ATR, 25 °C): 1966 (ν_{co}), 1960 (ν_{co}), 1616 ($\nu_{c=o}$)

Fe(Ph$_2$PN*t*Bu)(CO)$_2$(κ^2(*C*,*P*)-(C=O)-N*t*Bu-PPh$_2$)Br (3e)

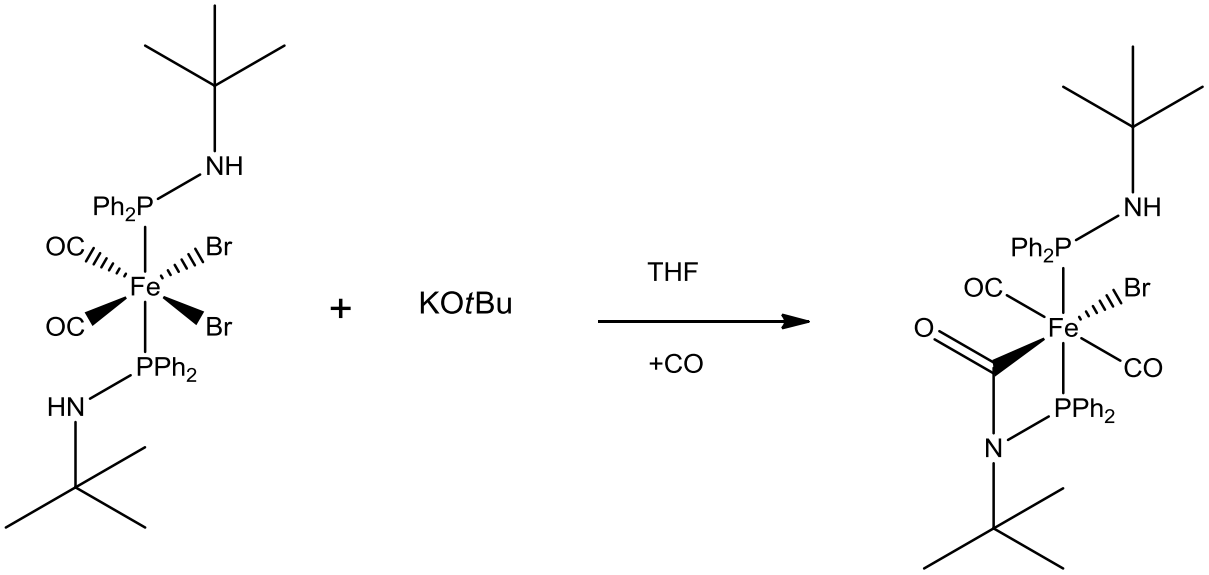

Die Reaktion wurde analog zu **3d** mit **3b** (0.7 g, 0.89 mmol) durchgeführt.

Ausbeute: 260 mg (40 %) rotes Pulver

Elementar Analyse: $C_{35}H_{39}BrFeN_2O_3P_2$ (M.G: 733.39): C, 57.32; H, 5.36; Br, 10.90; Fe, 7.61; N, 3.82; O, 6.54; P, 8.45

^{1}H-NMR (δ, $CDCl_3$, 20 °C): 7.98 (bs, 8H, Ph), 7.42 (bs, 12H, Ph), 4.84 (bs, 1H, *NH*), 3.46 (m, 1H, C*H*(CH_3)$_2$), 1.28 (s, 9H, C(C*H*$_3$)$_3$), 1.05 (s, 9H, C(C*H*$_3$)$_3$.

^{13}C{^{1}H}-NMR (δ, $CDCl_3$, 20 °C): 213.5 (d, J_{PC} = 23.40 Hz, *C*O), 213.1 (d, J_{PC} = 22.94 Hz, *C*O), 206.0 (dd, J_{PC} = 9.60 Hz, J_{PC} = 13.44 Hz, NCO), 135.8 (d, J_{PC} = 2.09 Hz, Ph), 134.5 (d, J_{PC} = 10.75 Hz, Ph), 132.8 (d, J_{PC} = 10.75 Hz, Ph), 132.6 (d, J_{PC} = 11.58 Hz, Ph), 131.4 (d, J_{PC} = 2.32 Hz, Ph), 129.9 (d, J_{PC} = 2.27 Hz, Ph), 128.5 (d, J_{PC} = 10.63 Hz, Ph), 127.6 (d, J_{PC} = 9.99 Hz, Ph), 62.3 (d, J_{PC} = 7.61 Hz, *C*(CH_3)$_3$), 55.9 (d, J_{PC} = 13.88 Hz, *C*(CH_3)$_3$), 32.1 (d, J_{PC} = 3.14 Hz, C(*C*H$_3$)$_3$, 29.5 (d, J_{PC} = 1.46 Hz, C(*C*H$_3$)$_3$).

^{31}P{^{1}H}-NMR (δ, $CDCl_3$, 20 °C): 90.43 (d, J_{PP} = 79.28 Hz), 87.26 (d, J_{PP} = 79.28 Hz).

IR(ATR, 25 °C): 1955 (ν_{co}), 1950 (ν_{co}), 1619 ($\nu_{c=o}$)

[FeCp(Ph$_2$PN*i*Pr)(CO)$_2$]Br (3f)

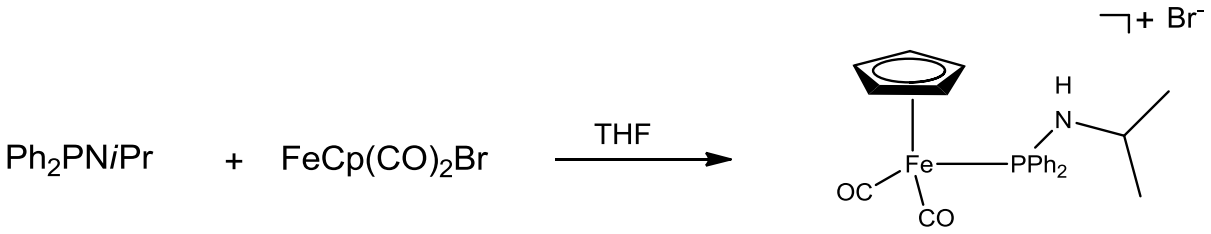

Eisen(II)dicarbonylcylopentadienylbromid (1 g, 3.89 mmol) und Ph$_2$PN*i*Pr (995 mg, 4.01 mmol) wurden in einer Schlenktube in THF Übernacht gerührt. Nach dem Abdekantieren des Lösungsmittels wurde das Produkt mit THF gewaschen und am Hochvakuum getrocknet.

Ausbeute: 1.75 g (90 %) beiges Pulver

Elementar Analyse: $C_{22}H_{23}BrFeNO_2P$ (M.G: 500.14): C, 52.94; H, 4.44; Br, 16.01; Fe, 11.19; N, 2.81; O, 6.41; P, 6.21

^{1}H-NMR (δ, CDCl$_3$, 20 °C): 7.57 (m, 10H, Ph), 5.96 (d, *J* = 10.22 Hz, 1H, N*H*), 5.27 (s, 5H, Cp), 2.99 (bs, 1H, CH(C*H*$_3$)$_2$), 1.16 (d, *J* = 5.38 Hz, 6H, CH(C*H*$_3$)$_2$).

^{13}C{^{1}H}-NMR (δ, CDCl$_3$, 20 °C): 210.3 (d, J_{PC} = 27.10 Hz, *C*O), 135.0 (d, J_{PC} = 59.13 Hz, Ph), 131.7 (s, Ph), 131.6 (s, Ph), 131.3 (d, J_{PC} = 10.72 Hz, Ph), 129.0 (d, J_{PC} = 10.89 Hz, Ph), 88.7 (s, Cp), 48.8 (d, J_{PC} = 9.55 Hz, *C*H(CH$_3$)$_2$), 24.80 (d, J_{PC} = 3.52 Hz, CH(*C*H$_3$)$_2$).

^{31}P{^{1}H}-NMR (δ, CDCl$_3$, 20 °C): 100.6

IR(ATR, 25 °C): 2040 (ν_{co}), 1993 (ν_{co})

[FeCp(Ph$_2$PN*t*Bu)(CO)$_2$]Br (3g)

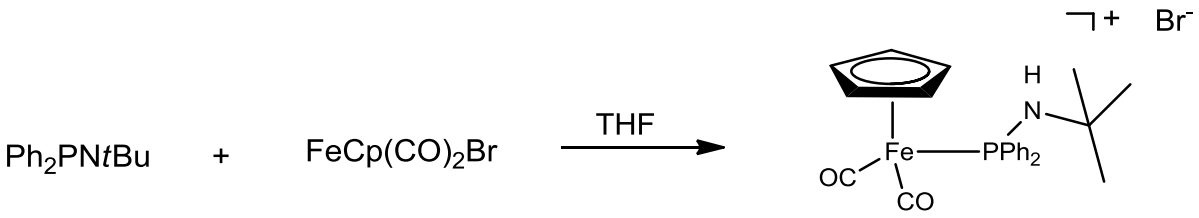

Die Reaktion wurde analog zu **3f** mit FeCp(CO)$_2$Br (1 g, 3.89 mmol) und Ph$_2$PN*t*Bu (1.05 g, 4.01 mmol) durchgeführt.

Ausbeute: 1.84 g (92 %) beiges Pulver

Elementar Analyse: $C_{23}H_{25}BrFeNO_2P$ (M.G: 514.17): C, 53.83; H, 4.71; Br, 15.57; Fe, 10.88; N, 2.73; O, 6.24; P, 6.04

^{1}H-NMR (δ, CDCl$_3$, 20 °C): 7.80 (bs, 4H, Ph), 7.54 (bs, 6H, Ph), 5.38 (d, *J* = 17.94 Hz, 1H, N*H*), 5.17 (s, 5H, Cp), 1.22 (s, 9H, C(C*H*$_3$)$_3$).

^{13}C{^{1}H}-NMR (δ, CDCl$_3$, 20 °C): 212.4 (d, J_{PC} = 26.17 Hz, *C*O), 135.3 (d, J_{PC} = 60.27 Hz, Ph), 131.7 (d, J_{PC} = 3.17 Hz, Ph), 131.3 (d, J_{PC} = 11.10 Hz, Ph), 128.9 (d, J_{PC} = 11.90 Hz, Ph), 89.1 (s, Cp), 58.5 (d, J_{PC} = 13.48 Hz, *C*(CH$_3$)$_3$), 32.0 (s, C(*C*H$_3$)$_3$)

^{31}P{^{1}H}-NMR (δ, CDCl$_3$, 20 °C): 91.9

IR(ATR, 25 °C): 2038 (ν_{co}), 1996 (ν_{co})

[FeCp(Ph$_2$PN*n*Pr)(CO)$_2$]Br (3h)

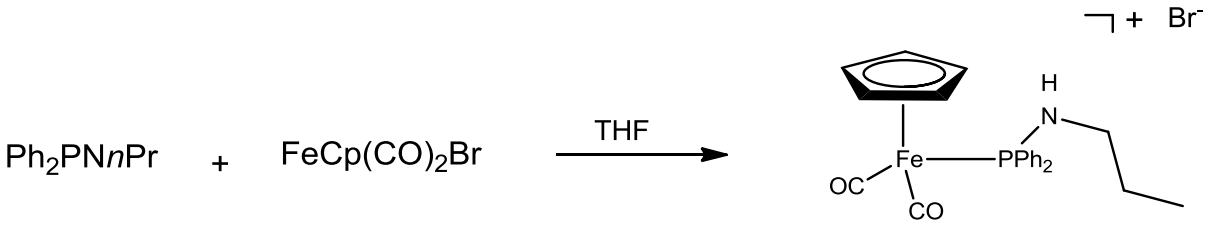

Die Reaktion wurde analog zu **3f** mit $FeCp(CO)_2Br$ (334 mg, 1.30 mmol) und Ph_2PNPropyl (344 mg, 1.43 mmol) durchgeführt.

Ausbeute: 550 mg (85 %) beiges Pulver

Elementar Analyse: $C_{22}H_{23}BrFeNO_2P$ (M.G: 500.14): C, 52.94; H, 4.44; Br, 16.01; Fe, 11.19; N, 2.81; O, 6.41; P, 6.21

^{1}H-NMR (δ, $CDCl_3$, 20 °C): 7.56 (m, 10H, Ph), 6.09 (dt, *J* = 6.83 Hz, *J* = 5.77 Hz, 1H, N*H*), 5.30 (s, 5H, Cp), 2.73 (t, *J* = 7.15 Hz, 2H, NHCH_2), 1.70 (q, *J* = 11.18 Hz, 2H, $NHCH_2CH_2$), 0.65 (t, *J* = 7.15 Hz, 3H, $NHCH_2CH_2CH_3$)

^{13}C{^{1}H}-NMR (δ, $CDCl_3$, 20 °C): 209.9 (d, J_{PC} = 27.33 Hz, *C*O), 134.2 (d, J_{PC} = 58.93 Hz, Ph), 131.7 (d, J_{PC} = 3.06 Hz, Ph), 131.1 (d, J_{PC} = 9.95 Hz, Ph), 129.0 (d, J_{PC} = 13.01 Hz, Ph), 88.7 (s, Cp), 47.7 (d, J_{PC} = 11.48 Hz, NH*C*H_2), 24.6 (d, J_{PC} = 6.12 Hz, $NHCH_2CH_2$), 11.3 (s, $NHCH_2CH_2CH_3$)

^{31}P{^{1}H}-NMR (δ, $CDCl_3$, 20 °C): 103.1

IR(ATR, 25 °C): 2043 (ν_{co}), 2004 (ν_{co})

[FeCp(Ph$_2$PN*i*Pr)(CO)$_2$]Cl (3i)

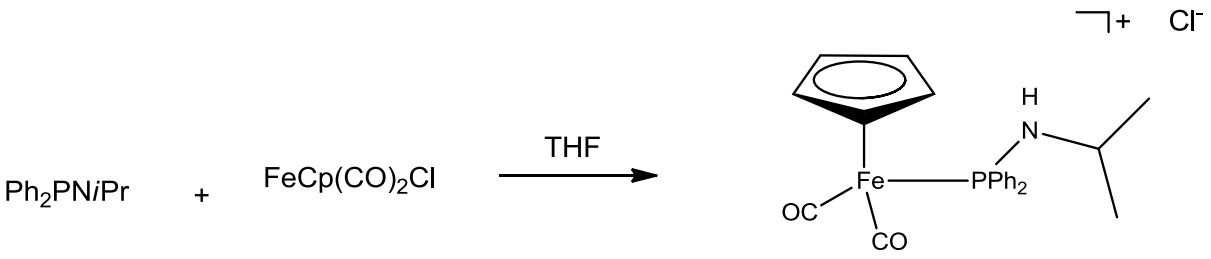

Die Reaktion wurde analog zu **3f** mit $FeCp(CO)_2Cl$ (262 mg, 1.23 mmol) und Ph_2PN_iPr (300 mg, 1.23 mmol) durchgeführt.

Ausbeute: 500 mg (90 %) beiges Pulver

Elementar Analyse: $C_{22}H_{23}ClFeNO_2P$ (M.G: 455.6): C, 58.11; H, 4.88; Cl, 7.80; Fe, 12.28; N, 3.08; O, 7.04; P, 6.81

^{1}H-NMR (δ, $CDCl_3$, 20 °C): 7.55 (bs, 10H, Ph), 6.17 (bs, 1H, N*H*), 5.20 (s, 5H, Cp), 2.95 (bs, 1H, C*H*$(CH_3)_2$*),* 1.08 (bs, 6H, CH(C*H*$_3)_2$*).*

^{13}C{^{1}H}-NMR (δ, $CDCl_3$, 20 °C): 210.4 (d, J_{PC} = 26.49 Hz, *C*O), 135.2 (d, J_{PC} = 60.21 Hz, Ph), 131. (d, J_{PC} = 10.44 Hz, Ph), 129.0 (d, J_{PC} = 11.24 Hz, Ph), 89.3 (s, Cp), 48.6 (s, *C*H$(CH_3)_2$), 25.1 (s, CH(*C*H$_3)_2$)

^{31}P{^{1}H}-NMR (δ, $CDCl_3$, 20 °C): 100.2

IR(ATR, 25 °C): 2041 (ν_{co}), 1993 (ν_{co})

[FeCp(*i*Pr$_2$PN^{c}Hex)(CO)$_2$]Cl (3j)

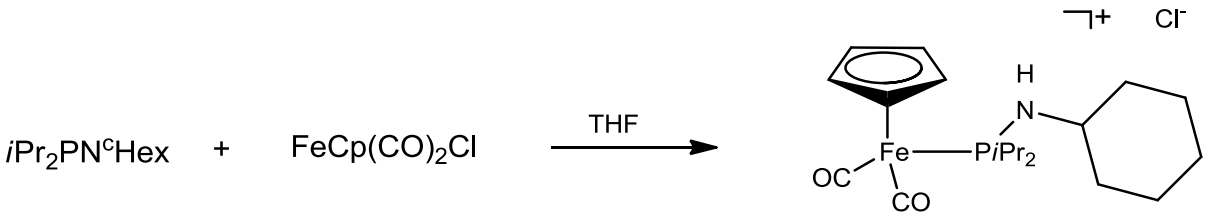

Die Reaktion wurde analog zu **3f** mit FeCp(CO)$_2$Cl (590 mg, 2.8 mmol) und *i*Pr$_2$PNcyclohexyl (600 mg, 2.8 mmol) durchgeführt.

Ausbeute: 850 mg (71 %) beiges Pulver

Elementar Analyse: $C_{19}H_{31}ClFeNO_2P$ (M.G: 392.27): C, 56.24; H, 7.94; Cl, 7.55; Fe, 11.89; N, 2.98; O, 6.81; P, 6.59

^{1}H-NMR (δ, CDCl$_3$, 20 °C): 5.04 (s, 5H, Cp), 3.29 (bs, 1H, N*H*), 2.70 (bs, 1H, ^{c}Hex), 2.27 (bs, 2H, C*H*(CH$_3$)$_2$), 1.70 (bs, 6H, ^{c}Hex), 1.51 (bs, 4H, ^{c}Hex), 1.16 (bs, 12H, CH(C*H*$_3$)$_2$).

^{13}C{^{1}H}-NMR (δ, CDCl$_3$, 20 °C): 211.0 (d, J_{PC} = 25.60 Hz, *C*O), 88.0 (s, Cp), 54.6 (s, N*C*), 36.9 (s, ^{c}Hex), 34.0 (d, J_{PC} = 29.86 Hz, *C*H(CH$_3$)$_2$), 26.0 (s, ^{c}Hex), 25.0 (s, ^{c}Hex), 20.1 (s, CH(*C*H$_3$)$_2$), 19.7 (s, CH(*C*H$_3$)$_2$).

^{31}P{^{1}H}-NMR (δ, CDCl$_3$, 20 °C): 136.2

IR(ATR, 25 °C): 2026 (ν_{co}), 1982 (ν_{co})

FeCp(CO)(κ^2(*C,P*)-(C=O)-N*i*Pr-PPh$_2$) (3k)

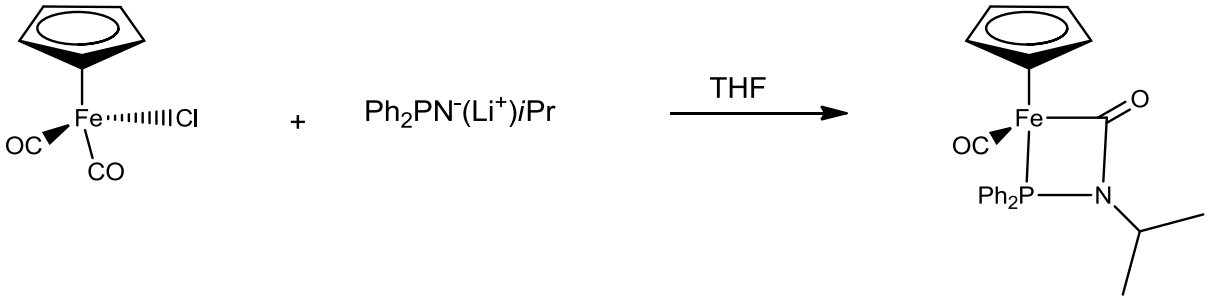

1a (300 mg, 1.23 mmol) in THF (20 mL) wurde in einem Schlenkrohr vorgelegt und auf – 20°C gekühlt. Dann wurde BuLi (500 µL) zugetropft und eine Stunde bei -20°C weitere 1 h bei 0°C gerührt. Danach wurde $FeCp(CO)_2Cl$ (262 mg, 1.23 mmol) dazugegeben und übernacht gerührt. THF wurde am Hochvakuum abgezogen, dann wurde Toluol (10 mL) dazugegeben. Nachdem die Lösung über Glasswolle und Celite filtriert wurde, wurde das Lösungsmittel am Hochvakuum abgezogen. Das Produkt wurde mit n-Pentan gewaschen und getrocknet.

Ausbeute: 207 mg (40 %) rotes Pulver

Elementar Analyse: $C_{22}H_{22}FeNO_2P$ (M.G: 419.23): C, 63.03; H, 5.29; Fe, 13.32; N, 3.34; O, 7.63; P, 7.39

^{1}H-NMR (δ, $CDCl_3$, 20 °C): 7.87 (m, 4H, Ph), 7.51 (m, 6H, Ph), 4.38 (s, 5H, Cp), 3.49 (m, 1H, C*H*$(CH_3)_2$*),* 1.29 (d, 3H, CH(C*H*$_3)_2$), 0.99 (d, 3H, CH(C*H*$_3)_2$*).*

^{13}C{^{1}H}-NMR (δ, $CDCl_3$, 20 °C): 220.9 (d, J_{PC} = 26.01 Hz, *C*O), 200.4 (d, J_{PC} = 39.02 Hz, N*C*O), 137.2 (d, J_{PC} = 40.60 Hz, Ph), 133.8 (d, J_{PC} = 13.53 Hz, Ph), 132.1 (d, J_{PC} = 10.83 Hz, Ph), 130.7 (d, J_{PC} = 13.53 Hz, Ph), 128.6 (d, J_{PC} = 9.47 Hz, Ph), 82.1 (s, Cp), 50.7 (d, J_{PC} = 8.12 Hz, *C*H$(CH_3)_2$), 23.0 (s, CH(*C*H$_3)_2$), 21.4 (s, CH(*C*H$_3)_2$).

^{31}P{^{1}H}-NMR (δ, $CDCl_3$, 20 °C): 111.6

IR(ATR, 25 °C): 1937 (ν_{co}), 1617 ($\nu_{c=o}$)

FeCp(CO)(κ^2(*C,P*)-(C=O)-N^{c}Hex-P*i*Pr$_2$) (3l)

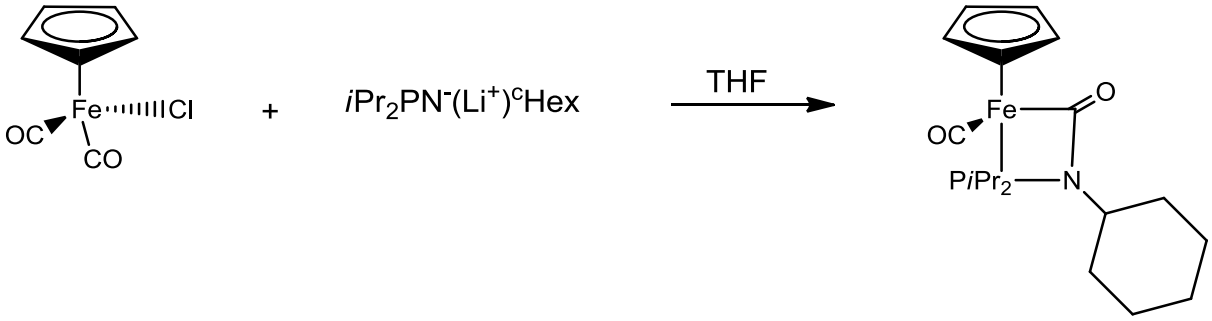

Die Reaktion wurde analog zu **3k** mit *i*Pr$_2$PN^{c}Hex (376 mg, 1,75 mmol), BuLi (0,7 mL, 2,5 M Lösung in Hexan) und FeCp(CO)$_2$Cl (370 mg, 1,75 mmol) durchgeführt.

Ausbeute: 307 mg (45 %) oranges Pulver

Elementar Analyse: $C_{19}H_{30}FeNO_2P$ (M.G: 380.26): C, 58.48; H, 7.49; Fe, 14.31; N, 3.59; O, 8.20; P, 7.94

^{1}H-NMR (δ, CDCl$_3$, 20 °C): 4.61 (s, 5H, Cp), 2,93 (m, 1H, NC*H*), 2.54 (m, 1H, C*H*(CH$_3$)$_2$), 2.18 (m, 1H, C*H*(CH$_3$)$_2$), 1,69 (bs, 4H, ^{c}Hex), 1,53 (bs, 6H, ^{c}Hex), 1.32 (d, *J* = 10.97 Hz, 3H, CH(C*H*$_3$)$_2$), 1,30 (s, 1H, ^{c}Hex), 1.25 (d, *J* = 7.31 Hz, 3H, CH(C*H*$_3$)$_2$).

^{13}C{^{1}H}-NMR (δ, CDCl$_3$, 20 °C): 221.0 (d, J_{PC} = 26.35 Hz, *C*O), 199.8 (d, J_{PC} = 37.77 Hz, N*C*O), 80.8 (s, Cp), 58.5 (d, J_{PC} = 8.12 Hz, N*C* ^{c}$_{Hex}$), 32.7 (d, J_{PC} = 71.94 Hz, *C*H(CH$_3$)$_2$), 30.6 (d, J_{PC} = 19.25 Hz, ^{c}Hex), 27.9 (d, J_{PC} = 15.87 Hz, ^{c}Hex), 26.8 (s ^{c}Hex), 25.3 (s ^{c}Hex), 20.4 (d, J_{PC} = 5.74 Hz, CH(*C*H$_3$)$_2$), 18.7 (s, ^{c}Hex), 18.0 (d, J_{PC} = 5.74 Hz, CH(*C*H$_3$)$_2$).

^{31}P{^{1}H}-NMR (δ, CDCl$_3$, 20 °C): 140,0

IR(ATR, 25 °C): 1914 (ν_{co}), 1618 ($\nu_{c=o}$)

FeCp(CO)(κ^2(*C,P*)-(C=O)-N*t*Bu-PPh$_2$) (3m)

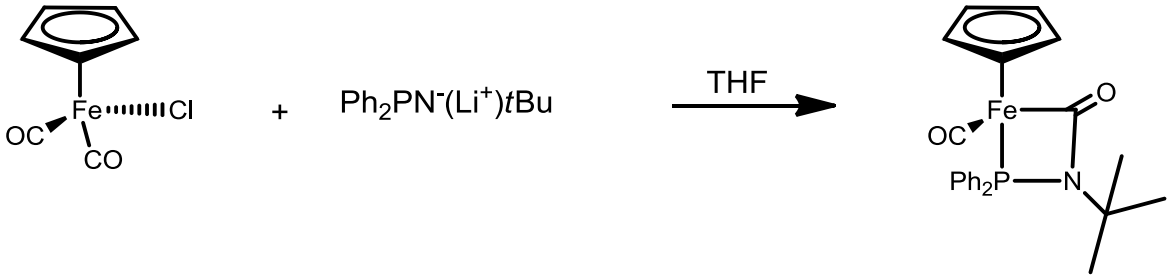

Die Reaktion wurde analog zu **3k** mit Ph_2PN_tBu (400 mg, 1,55 mmol), BuLi (0,6 mL, 2,5 M Lösung in Hexan) und $FeCp(CO)_2Cl$ (165 mg, 1,55 mmol) durchgeführt.

Ausbeute: 335 mg (50 %) rotes Pulver

Elementar Analyse: $C_{23}H_{24}FeNO_2P$ (M.G: 43.25): C, 63.76; H, 5.58; Fe, 12.89; N, 3.23; O, 7.39; P, 7.15

^{1}H-NMR (δ, $CDCl_3$, 20 °C): 7.90 (m, 4H, Ph), 7.48 (m, 6H, Ph), 4.39 (s, 5H, Cp), 1.20 (s, 9H, C(C*H*$_3$)$_3$).

^{13}C{^{1}H}-NMR (δ, $CDCl_3$, 20 °C): 221.0 (d, J_{PC} = 24.37 Hz, *C*O), 201.1 (s, N*C*O), 133. (d, J_{PC} = 41.32 Hz, Ph), 132.7 (d, J_{PC} = 12.50 Hz, Ph), 130.7 (d, J_{PC} = 11.65 Hz, Ph), 128.6 (d, J_{PC} = 7.42 Hz, Ph), 82.8 (s, Cp), 65.8 (s, *C*H(CH$_3$)$_2$), 29.5 (s, CH(*C*H$_3$)$_2$)

^{31}P{^{1}H}-NMR (δ, $CDCl_3$, 20 °C): 113.0

IR(ATR, 25 °C): 1919 (ν_{co}), 1605 ($\nu_{c=o}$)

FeCp(CO)(κ^2(*P, C*)=C(OMe)-N*i*Pr-PPh$_2$) (3n)

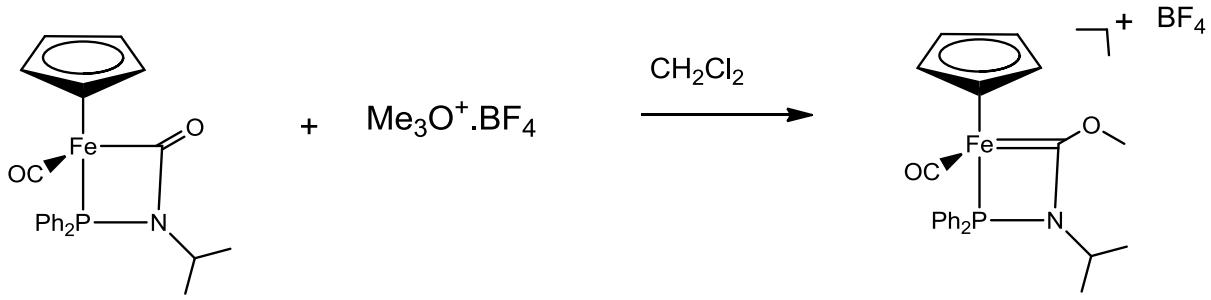

3k (500 mg, 1.19 mmol) und $Me_3O^+.BF_4$ (177 mg, 1.19 mmol) wurden in Methylenchlorid 4 h gerührt. Nach der Filtration über Glasswolle und Celite wurde Lösungsmittel am Hochvakuum abgezogen. Das Produkt wurde mit n-Hexan gewaschen und getrocknet.

Ausbeute: 360 mg (58 %) rotes Pulver

Elementar Analyse: $C_{23}H_{25}BF_4FeNO_2P$ (M.G: 521.04): C, 53.01; H, 4.84; B, 2.07; F, 14.58; Fe, 10.72; N, 2.69; O, 6.14; P, 5.94

^{1}H-NMR (δ, CDCl$_3$, 20 °C): 7.58 (m, 10H, Ph), 4.80 (s, 5H, Cp), 4.33 (s, 3H, *OCH*$_3$), *3*.93 (m, 1H, C*H*(CH$_3$)$_2$*),* 1.40 (d, 3H, CH(C*H*$_3$)$_2$), 0.92 (d, 3H, CH(C*H*$_3$)$_2$.

^{13}C{^{1}H}-NMR (δ, CDCl$_3$, 20 °C): 238.0 (d, J_{PC} = 34.75 Hz, Fe=*C*), 216.3 (d, J_{PC} = 22.20 Hz, *C*O), 134.4 (d, J_{PC} = 14.27 Hz, Ph), 132.8 (d, J_{PC} = 2.59 Hz, Ph), 133.3 (d, J_{PC} = 11.10 Hz, Ph), 129.9 (d, J_{PC} = 11.28 Hz, Ph), 83.1 (s, Cp), 55.8 (d, J_{PC} = 5.5 Hz, *C*H(CH$_3$)$_2$), 21.8 (s, CH(*C*H$_3$)$_2$), 20.8 (s, CH(*C*H$_3$)$_2$)

^{31}P{^{1}H}-NMR (δ, CDCl$_3$, 20 °C): 115.0

IR(ATR, 25 °C): 2004 (ν_{co})

[FeCp(Ph$_2$PN*i*Pr(CO)$_2$]Cl (3o)

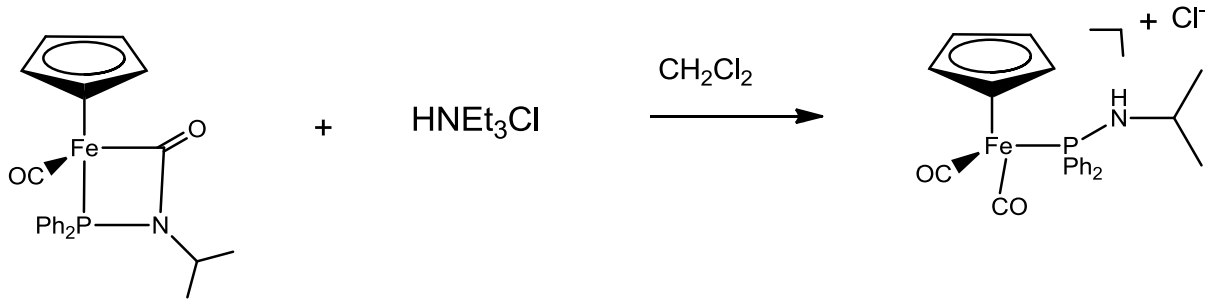

Die Reaktion wurde analog zu **3n** mit **3k** (500 mg, 1.19 mmol) und Triethylammoniumhydrochlorid (165 mg, 1.19 mmol) durchgeführt.

Ausbeute: 514 mg (95 %) beiges Pulver

Elementar Analyse: $C_{22}H_{23}ClFeNO_2P$ (M.G: 455.69): C, 58.11; H, 4.88; Cl, 7.80; Fe, 12.28; N, 3.08; O, 7.04; P, 6.81

^{1}H-NMR (δ, CDCl$_3$, 20 °C): 7.51 (bs, 10H, Ph), 6.2 (bs, 1H, N*H*), 5.19 (s, 5H, Cp), 2.95 (bs, 1H, C*H*(CH$_3$)$_2$*),* 1.09 (bs, 6H, CH(C*H*$_3$)$_2$*).*

^{13}C{^{1}H}-NMR (δ, CDCl$_3$, 20 °C): 210.4 (d, J_{PC} = 26.49 Hz, *C*O), 135.2 (d, J_{PC} = 60.21 Hz, Ph), 131. (d, J_{PC} = 10.44 Hz, Ph), 129.0 (d, J_{PC} = 11.24 Hz, Ph), 89.3 (s, Cp), 48.6 (s, *C*H(CH$_3$)$_2$), 25.1 (s, CH(*C*H$_3$)$_2$).

^{31}P{^{1}H}-NMR (δ, CDCl$_3$, 20 °C): 100.1

IR(ATR, 25 °C): 2040 (ν_{co}), 1992 (ν_{co})

4-Mo(0)-Komplexe

Mo(PNP^{Me}-*i*Pr)(CO)$_3$ (4a)

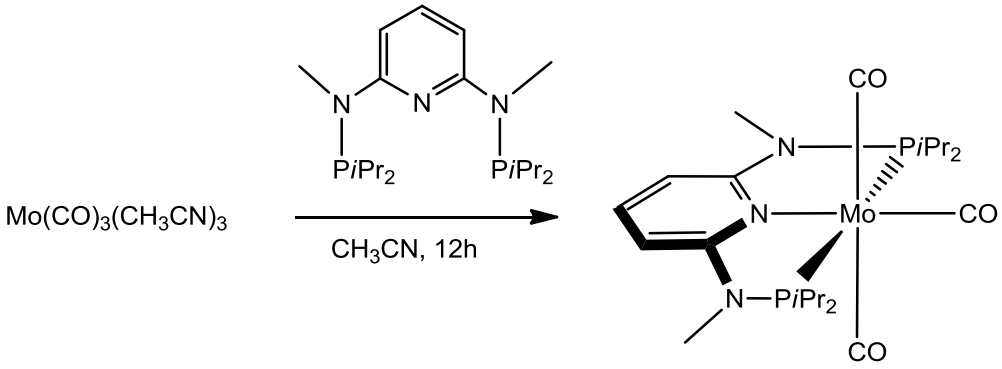

$Mo(CO)_6$ (714 mg, 2.7 mmol) wurde in Acetonitril (10 mL) 4 h unter Rückflux gekocht danach wurde PNP^{Me}-*i*Pr (1.00 g, 2.7 mmol) dazugegeben und weiter 12 h unter Rückfluss gekocht. Nachdem Abziehen des Lösungsmittel wurde das Produkt zweimal mit Diethylether gewaschen und am Hochvakuum getrocknet.

Ausbeute: 1.19 g (80%) gelbes Pulver

Elementar Analyse: $C_{22}H_{37}MoN_3O_3P_2$ (M.G: 549,46): C, 48.09; H, 6.79; Mo, 17.46; N, 7.65; O, 8.74; P, 11.27

^{1}H-NMR (δ, CD_2Cl_2, 20 °C): 7.40 (t, *J* = 7.6 Hz, 1H, py), 6.30 (d, *J* = 7.6 Hz, 2H, py), 3.01 (s, 6H, NC*H*$_3$), 2.47 (m, 4H, C*H*(CH_3)$_2$), 1.30 (m, 12H, CH(C*H*$_3$)$_2$), 1.09 (m, 12H, CH(C*H*$_3$)$_2$).

^{13}C{^{1}H} NMR (δ, CD_2Cl_2, 20 °C): 230.8 (t, *J* = 6.0 Hz, *C*O), 217.9 (t, *J* = 10.8 Hz, *C*O), 174.9 (t, *J* = 2.6 Hz, py), 137.8 (s, py), 96.7 (t, *J* = 2.2 Hz, py), 33.9 (t, *J* = 1.8 Hz, N(*C*H$_3$)$_2$), 32.9 (t, *J* = 9.0 Hz, *C*H(CH$_3$)$_2$), 29.6 (s, N(*C*H$_3$)$_2$), 19.2 (t, *J* = 7.5 Hz, CH(*C*H$_3$)$_2$),18.1 (s, CH(*C*H$_3$)$_2$).

^{31}P{^{1}H} NMR (δ, CD_2Cl_2, 20 °C): 171.0 (s).

IR(ATR, 25 °C): 1936 (ν_{co}), 1810 (ν_{co}), 1795 (ν_{co}).

5-W(II)-Komplexe

[W(PNP-Ph)(CO)$_3$Br]Br (5a)

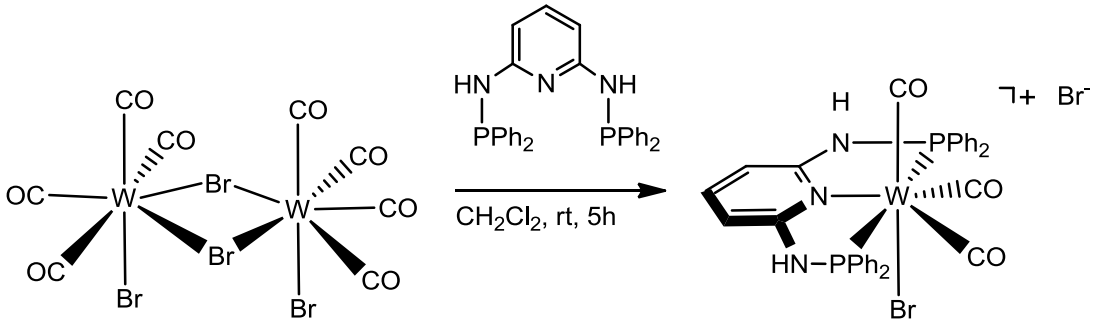

$W(CO)_6$ (2.0 g, 5.68 mmol) wurde in CH_2Cl_2 (30mL) suspendiert und auf -70°C gekühlt. Nach der Zugabe von Brom (292 μL, 5.68 mmol) wurde das Gemisch 1 h bei -70°C und eine weitere Stunde bei der Raumtemperatur gerührt. Danach wurde PNP-Ph (2.72 g, 5.68 mmol) dazugegeben und 5 h bei Raumtemperatur gerührt. Nach dem Abziehen des Lösungsmittel am Hochvakuum wurde das Produkt mit einem Lösungsmittelgemisch aus Methanol-Et_2O (1/9) zweimal gewaschen und getrocknet.

Ausbeute: 4.11 g (80%) gelbes Pulver

Elementar Analyse: $C_{32}H_{25}Br_2N_3O_3P_2W$ (M.G: 905,16): C, 42.46; H, 2.78; Br, 17.66; N, 4.64; O, 5.30; P, 6.84; W, 20.31

^{1}H NMR (δ, Aceton-d$_6$, 20 °C): 10.85 (bs, 2H, N*H*), 7.78 (bs, 11H, py, Ph), 7.60 (bs, 10H, Ph), 7.43 (d, *J* = 7.6 Hz, 2H, py).

^{13}C{^{1}H} NMR (δ, CDCl$_3$, 20 °C): 225.4 (t, *J* = 10.3 Hz, *C*O), 210.3 (t, *J* = 8.6 Hz, *C*O), 159.7 (d, *J* = 7.5 Hz, py), 159.6 (d, *J* = 7.5 Hz, py), 133.1 (s, py), 131.9 (s, Ph), 131.9 (s, Ph), 129.0 (d, *J* = 5.0 Hz, Ph), 128.2 (d, *J* = 5.4 Hz, Ph), 103.1 (s, py).

^{31}P{^{1}H} NMR (δ, Aceton-d$_6$, 20 °C): 85.2.

IR(ATR, 25 °C): 2030 (ν_{co}), 1958 (ν_{co}), 1933 (ν_{co}).

[W(PNP-*i*Pr)(CO)$_3$Br]Br (5b)

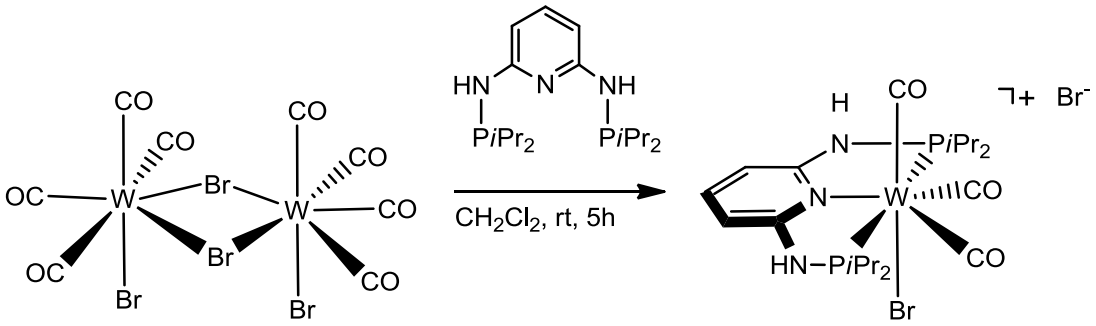

Diese Reaktion wurde analog zu **5a** mit $W(CO)_6$ (2.0 g, 5.68 mmol), Brom (292 μL, 5.68 mmol) und PNP-*i*Pr (1.95 g, 5.69 mmol) durchgeführt.

Ausbeute: 3.06 g (70%) gelbes Pulver

Elementar Analyse: $C_{20}H_{33}Br_2N_3O_3P_2W$ (M.G: 769,09): C, 31.23; H, 4.32; Br, 20.78; N, 5.46; O, 6.24; P, 8.05; W, 23.90

^{1}H NMR (δ, CD_2Cl_2, 20 °C): 9.32 (bs,2H, N*H*), 7.66 (t, *J* = 7.2 Hz, 1H, py), 6.67 (d, *J* = 8.1 Hz, 2H, py), 3.54 (m, 2H, C*H*(CH_3)$_2$), 2.88 (m, 2H, C*H*(CH_3)$_2$) 1.43 (m, 24H, CH(C*H*$_3$)$_2$).

^{13}C{^{1}H} NMR (δ, CD_2Cl_2, 20 °C): 212.2 (t, *J* = 10.1 Hz, *C*O), 191.3 (t, *J* = 7.6 Hz, *C*O), 161.0 (s,py), 142.2 (s, py), 101.9 (s, py), 30.6 (t, *J* = 15.0 Hz, *C*H(CH_3)$_2$), 29.3 (t, *J* = 15.3 Hz, *C*H(CH_3)$_2$), 19.2 (s, CH(*C*H_3)$_2$, 19.1 (s, CH(*C*H_3)$_2$, 18.9 (s, CH(*C*H_3)$_2$, 17.7 (s, CH(*C*H_3)$_2$.

^{31}P{^{1}H} NMR (δ, CD_2Cl_2, 20 °C): 106.6.

IR(ATR, 25 °C): 2023 (ν_{co}), 1953 (ν_{co}), 1922 (ν_{co}).

[W(PNP-*t*Bu)(CO)$_3$Br]Br (5c)

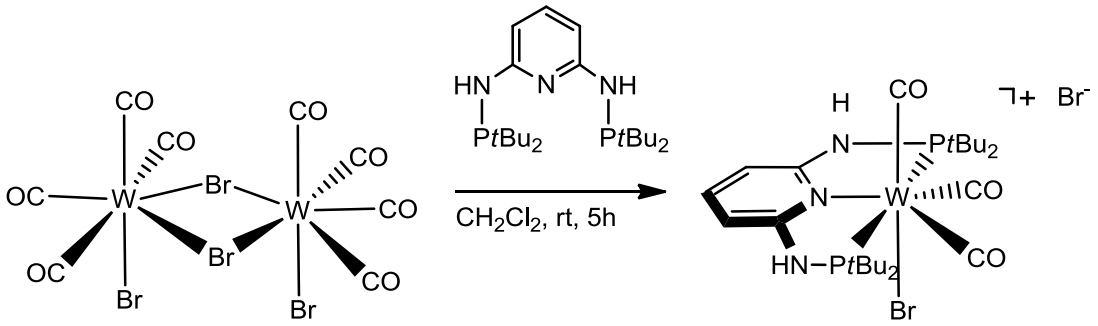

Diese Reaktion wurde analog zu **5a** mit W(CO)$_6$ (2.0 g, 5.68 mmol), Brom (292 μL, 5.68 mmol) und PNP-*t*Bu (2.26 g, 5.69 mmol) durchgeführt.

Ausbeute: 2.51 g (60%) gelbes Pulver

Elementar Analyse: $C_{24}H_{41}Br_2N_3O_3P_2W$ (M.G: 825.20): C, 34.93; H, 5.01; Br, 19.37; N, 5.09; O, 5.82; P, 7.51; W, 22.28

^{1}H NMR (δ, CD_2Cl_2, 20 °C): 9.11 (s,2H, N*H*), 7.74 (d, *J* = 7.8 Hz, 2H, py), 7.23 (t, *J* = 8.7 Hz, 1H, py), 1.70 (d, *J* = 8.2 Hz, 9H, C(C*H*$_3$)$_3$), 1.68 (d, *J* = 7.3 Hz, 9H, C(C*H*$_3$)$_3$), 1.54 (d, *J* = 7.5 Hz, 9H, C(C*H*$_3$)$_3$), 1.48 (d, *J* = 7.1 Hz, 9H, C(C*H*$_3$)$_3$).

^{13}C{^{1}H} NMR (δ, $CDCl_3$, 20 °C): 229.9 (t, *J* = 14.8 Hz, *C*O), 212.9 (t, *J* = 7.6 Hz, *C*O), 162.6 (t, *J* = 4.2 Hz, py), 153.3 (d, *J* = 5.8 Hz, py), 149.9 (s, py), 103.8 (s, py), 46.0 (t, *J* = 7.2 Hz, *C*(CH$_3$)$_3$), 44.6 (t, *J* = 7.2 Hz ,*C*(CH$_3$)$_3$), 31.9 (s, C(*C*H$_3$)$_3$, 30.4 (s, C(*C*H$_3$)$_3$, 26.9 (s, C(*C*H$_3$)$_3$.

^{31}P{^{1}H} NMR (δ, CD_2Cl_2, 20 °C): 131.6

IR(ATR, 25 °C): 2019 (ν_{co}), 1941 (ν_{co}), 1909 (ν_{co}).

6-Mo(II)-Komplexe

[Mo(PNP-Ph)(CO)$_3$Br]Br (5a)

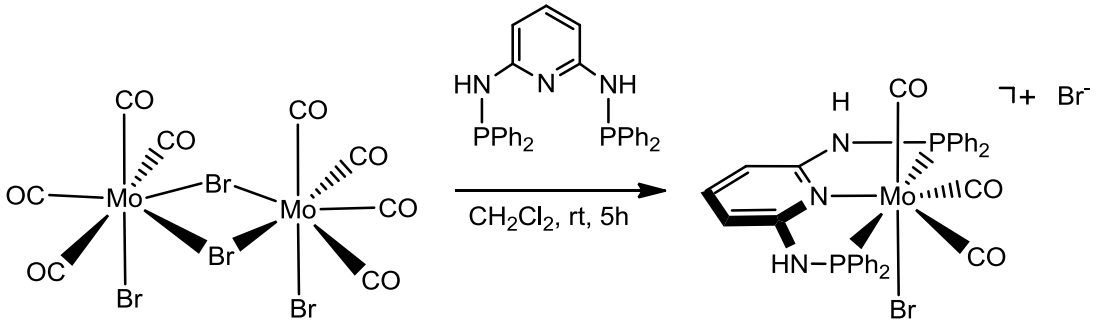

Diese Reaktion wurde analog zu 5a mit $Mo(CO)_6$ (300 mg, 1.14 mmol), Br_2 (59 µL, 1.14 mmol) und PNP-Ph (570 mg, 1.20 mmol) durchgeführt.

Ausbeute: 775 mg (83%) gelbes Pulver

Elementar Analyse: $C_{32}H_{25}Br_2MoN_3O_3P_2$ (M.G: 817,28): C, 47.03; H, 3.08; Br, 19.55; Mo, 11.74; N, 5.14; O, 5.87; P, 7.58

^{1}H NMR (δ, Aceton-d$_6$, 20 °C): 8.70 (s, 2H, N*H*), 7.59 (m, 5H, Ph), 7.47 (m, 5H, Ph), 7.16 (t, *J* = 7.2 Hz, 1H, py), 7.01 (m, 5H, Ph), 6.85 (m, 5H, Ph), 6.56 (d, *J* = 7.8 Hz, 2H, py).

^{31}P{^{1}H} NMR (δ, Aceton-d$_6$, 20 °C): 125.3

IR(ATR, 25 °C): 2040 (ν_{co}), 1975 (ν_{co}), 1875 (ν_{co}).

[Mo(PNP-*i*Pr)(CO)$_3$Br]Br (5b)

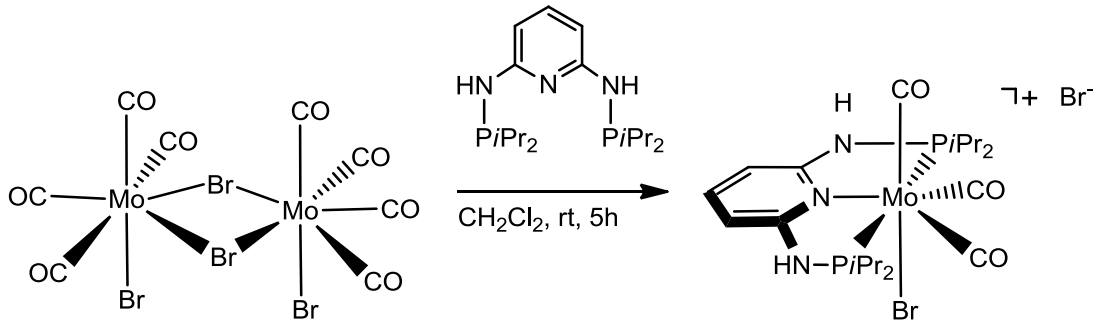

Diese Reaktion wurde analog zu **5a** mit $Mo(CO)_6$ (500 mg, 1.89 mmol), Br_2 (98 µL, 1.89 mmol) und PNP-*i*Pr (678 mg, 1.98 mmol) durchgeführt.

Ausbeute: 965 mg (75%) gelbes Pulver

Elementar Analyse: $C_{20}H_{33}Br_2MoN_3O_3P_2$ (M.G: 681,21): C, 35.26; H, 4.88; Br, 23.46; Mo, 14.09; N, 6.17; O, 7.05; P, 9.09

^{1}H NMR (δ, $CDCl_3$, 20 °C): 9.08 (s, 2H, N*H*), 7.24 (d, *J* = 9.9 Hz, 2H, py), 7.10 (t, *J* = 7.4 Hz, 1H, py), 3.55 (m, 2H, C*H*$(CH_3)_2$), 2.96 (m, 2H, C*H*$(CH_3)_2$). 1.44 (m, 24H, CH(C*H*$_3)_2$).

^{13}C{^{1}H} NMR (δ, $CDCl_3$, 20 °C): 234.6 (t, *J* = 7.2 Hz, *C*O), 218.3 (t, *J* = 11.5 Hz, *C*O), 175.1 (s, py), 175.0 (s, py), 160.0 (t, *J* = 4.9 Hz, py), 142.1 (s, py), 102.7 (s, py), 30.8 (d, *J* = 12.8 Hz, *C*H$(CH_3)_2$), 30.6 (d, *J* = 14.9 Hz, *C*H$(CH_3)_2$), 30.3 (d, *J* = 12.4 Hz, *C*H$(CH_3)_2$), 30.1 (d, *J* = 11.6 Hz, *C*H$(CH_3)_2$), 19.4 (s, CH(*C*H$_3)_2$, 19.3 (s, CH(*C*H$_3)_2$, 19.1 (s, CH(*C*H$_3)_2$, 18.1 (s, CH(*C*H$_3)_2$.

^{31}P{^{1}H} NMR (δ, $CDCl_3$, 20 °C): 126.7

IR(ATR, 25 °C): 2030 (ν_{co}), 1967 (ν_{co}), 1936 (ν_{co}).

Mo(PNP^{Me}-*i*Pr)(CO)Br$_2$ (6a)

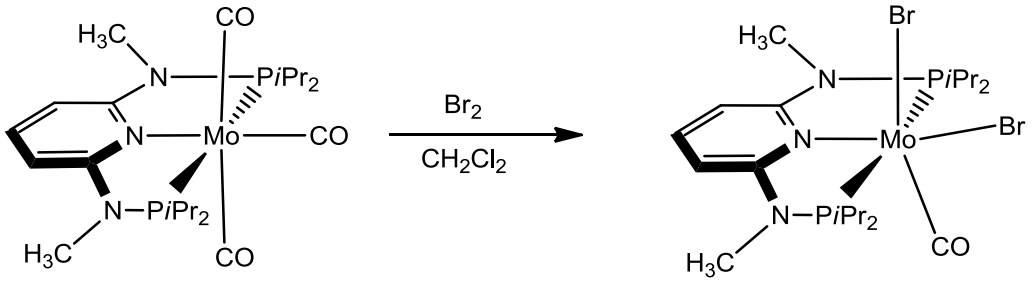

Nachdem Mo(PNP^{Me}-*i*Pr)(CO)$_3$ (100 mg, 0.18 mmol) in CH_2Cl_2 in einem Schlenktube vorgelegt wurde, wurde Br_2 (0.10 µL, 0.19 mmol) dazugegeben und 4 h bei der Raumtemperatur gerührt. Nach dem Filtrieren über Celite wurde das Lösungsmittel am Hochvakuum abgezogen. Anschließend wurde das Produkt mit Et_2O gewaschen und getrocknet.

Ausbeute: 113 mg (95%) blaues Pulver

Elementar Analyse: $C_{20}H_{37}Br_2MoN_3OP_2$ (M.W: 653,24): C, 36.77; H, 5.71; Br, 24.46; Mo, 14.69; N, 6.43; O, 2.45; P, 9.48

^{1}H NMR (δ, $CDCl_3$, 20 °C): 7.58 (t, *J* = 8.32 Hz, 1H, py), 6.21 (d, *J* = 8.04 Hz, 2H, py), 3.14 (s, 6H, NC*H*$_3$), 2.81 (m, 2H, C*H*(CH$_3$)$_2$), 2.56 (m, 2H, C*H*(CH$_3$)$_2$), 1.52 (d, *J* = 6.87 Hz, 3H, CH(C*H*$_3$)$_2$), 1.45 (d, *J* = 6.82 Hz, 3H, CH(C*H*$_3$)$_2$), 1.29 (m, 12H, CH(C*H*$_3$)$_2$), 0.71 (d, *J* = 6.95 Hz, 3H, CH(C*H*$_3$)$_2$), 0.64 (d, *J* = 6.95 Hz, 3H, CH(C*H*$_3$)$_2$).

^{13}C{^{1}H} NMR (δ, $CDCl_3$, 20 °C): 247.9 (t, *J* = 32.01 Hz, *C*O), 161.5 (t, *J* = 8.09 Hz, py), 141.0 (s, py), 98.2 (s, py), 34.6 (s, N(*C*H$_3$)$_2$), 30.2 (d, *J* = 29.09 Hz, *C*H(CH$_3$)$_2$), 20.3 (d, *J* = 24.48 Hz, *C*H(CH$_3$)$_2$), 18.2 (s, CH(*C*H$_3$)$_2$), 17.9 (s, CH(*C*H$_3$)$_2$), 17.5 (s, CH(*C*H$_3$)$_2$), 16.3 (s, CH(*C*H$_3$)$_2$).

^{31}P{^{1}H} NMR (δ, $CDCl_3$, 20 °C): 206.9

IR(ATR, 25 °C): 1816 (ν_{co}).

Mo(PNP^{Me}-*i*Pr)(CO)I_2 (6b)

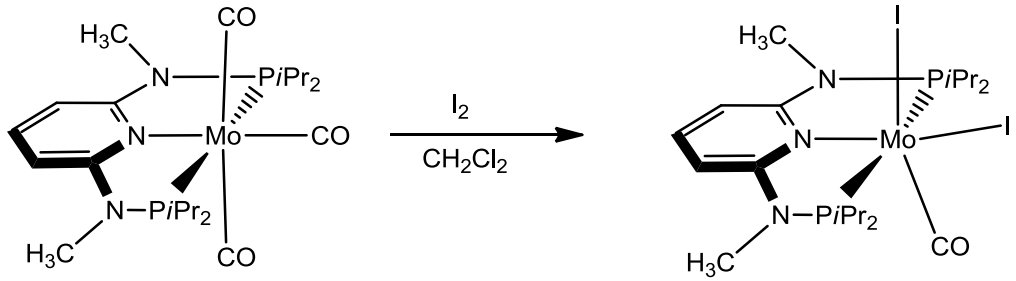

Die Reaktion wurde analog zu 6d mit I_2 (49 mg, 0.19 mmol) durchgeführt.

Ausbeute: 121 mg (90%) blaues Pulver

Elementar Analyse: $C_{20}H_{37}I_2MoN_3OP_2$ (M.W: 747.24): C, 32.15; H, 4.99; I, 33.97; Mo, 12.84; N, 5.62; O, 2.14; P, 8.29

^{1}H NMR (δ, $CDCl_3$, 20 °C): 7.66 (t, *J* = 8.30 Hz, 1H, py), 6.22 (d, *J* = 8.32 Hz, 2H, py), 3.13 (s, 6H, NC*H*$_3$), 2.78 (m, 2H, C*H*$(CH_3)_2$), 2.37 (m, 2H, C*H*$(CH_3)_2$), 1.39 (m, 18H, CH(C*H*$_3)_2$), 0.72 (d, *J* = 6.92 Hz, 3H, CH(C*H*$_3)_2$), 0.66 (d, *J* = 6.90 Hz, 3H, CH(C*H*$_3)_2$).

^{13}C{^{1}H} NMR (δ, CD_2Cl_2, 20 °C): 247.3 (t, *J* = 26.52 Hz, *C*O), 162.0 (t, *J* = 7.57 Hz, py), 142.3 (s, py), 99.1 (s, py), 34.4 (t, *J* = 2.72 Hz, N(*C*$H_3)_2$), 30.2 (d, *J* = 28.75 Hz, *C*H$(CH_3)_2$), 20.0 (d, *J* = 18.29 Hz, *C*H$(CH_3)_2$), 19.2 (s, CH(*C*$H_3)_2$), 17.8 (s, CH(*C*$H_3)_2$), 17.7 (s, CH(*C*$H_3)_2$), 16.9 (s, CH(*C*$H_3)_2$).

^{31}P{^{1}H} NMR (δ, $CDCl_3$, 20 °C): 202.2

IR(ATR, 25 °C): 1824 (ν_{co}).

Mo(PNP^{Me}-*i*Pr)(CO)Cl$_2$ (6c)

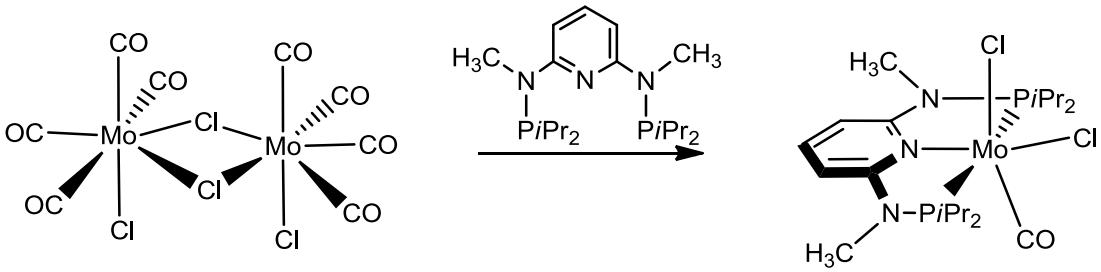

$Mo_2(CO)_8Cl_4$ (150 mg, 0.27 mmol) wurde in CH_2Cl_2 gelöst. Dann wurde PNP^{Me}-*i*Pr (209 mg, 0.56 mmol) dazugegeben und bei der Raumtemperatur 4 h gerührt. Nach der Filtration über Celite wurde das Lösungsmittel am Hochvakuum abgezogen und das Produkt mit Diethylether gewaschen. Anschließend wurde das Produkt am Hochvakuum getrocknet.

Ausbeute: 140 mg (92%) blaues Pulver

Elementar Analyse: $C_{20}H_{37}Cl_2MoN_3OP_2$ (M.W: 564.34): C, 42.57; H, 6.61; Cl, 12.56; Mo, 17.00; N, 7.45; O, 2.84; P, 10.98

^{1}H NMR (δ, $CDCl_3$, 20 °C): 7.58 (t, *J* = 8.82 Hz, 1H, py), 6.19 (d, *J* = 7.79 Hz, 2H, py), 3.14 (s, 6H, NC*H*$_3$), 2.82 (m, 2H, C*H*(CH$_3$)$_2$), 2.69 (m, 2H, C*H*(CH$_3$)$_2$), 1.51 (d, *J* = 6.32 Hz, 3H, CH(C*H*$_3$)$_2$), 1.44 (d, *J* = 6.32 Hz, 3H, CH(C*H*$_3$)$_2$), 1.30 (m, 12H, CH(C*H*$_3$)$_2$), 0.71 (d, *J* = 6.67 Hz, 3H, CH(C*H*$_3$)$_2$), 0.65 (d, *J* = 6.65 Hz, 3H, CH(C*H*$_3$)$_2$).

^{13}C{^{1}H} NMR (δ, CD_2Cl_2, 20 °C): 248.5 (t, *J* = 35.21 Hz, *C*O), 161.3 (t, *J* = 7.09 Hz, py), 140.8 (s, py), 97.9 (s, py), 34.4 (s, N(*C*H$_3$)$_2$), 30.2 (d, *J* = 29.93 Hz, *C*H(CH$_3$)$_2$), 21.3 (d, *J* = 26.27 Hz, *C*H(CH$_3$)$_2$), 17.8 (s, CH(*C*H$_3$)$_2$), 17.6 (s, CH(*C*H$_3$)$_2$), 17.4 (s, CH(*C*H$_3$)$_2$), 16.0 (s, CH(*C*H$_3$)$_2$).

^{31}P{^{1}H} NMR (δ, $CDCl_3$, 20 °C): 207.0.

IR(ATR, 25 °C): 1813 (ν_{co}).

[Mo(PNP^{Me}-*i*Pr)(CO)(THF)Cl]SbF_6 (6d)

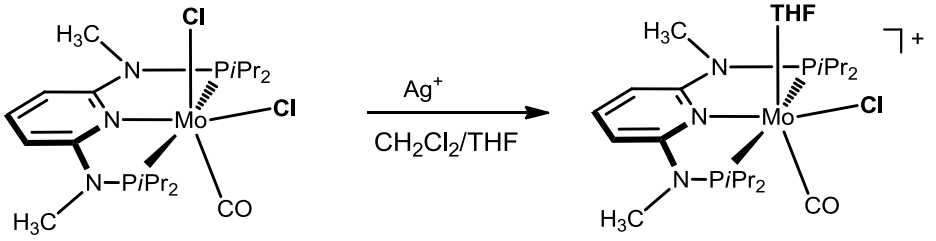

6c **6d**

Mo(PNP^{Me}-*i*Pr)(CO)$(Cl)_2$ (150 mg, 0.26 mmol) wurde mit $AgSbF_6$ (95 mg, 0.28 mmol) in CH_2Cl_2:THF (9:1) umgesetzt. Die Reaktion wurde Übernacht gerührt danach wurde über Glaßwolle und Celite filtriert. Das Lösungsmittel wurde am Hochvakuum abgezogen und das Produkt wurde getrocknet.

Ausbeute: 195 mg (90%) grünes Pulver

Elementar Analyse: $C_{24}H_{45}ClF_6MoN_3O_2P_2Sb$ (M.G: 836,74): C, 34.45; H, 5.42; Cl, 4.24; F, 13.62; Mo, 11.47; N, 5.02; O, 3.82; P, 7.40; Sb, 14.55

^{1}H NMR (δ, CD_2Cl_2, 20 °C): 7.83 (t, *J* = 7.43 Hz, 1H, py), 6.43 (d, *J* = 7.10 Hz, 2H, py), 3.71 (s, 4H, thf), 3.23 (s, 6H, NCH_3), 2.85 (m, 4H, C$H(CH_3)_2$), 1.85 (s, 4H, thf), 1.38 (m, 18H, CH(CH_3)$_2$), 1,14 (m, 6H, CH(CH_3)$_2$)

^{13}C{^{1}H} NMR (δ, CD_2Cl_2, 20 °C): 218.5 (t, *J* = 6.35 Hz, *C*O), 162.3 (t, *J* = 6.79 Hz, py), 146.0 (s, py), 128.9 (s, py), 74.4 (s, thf), 36.3 (s, N(*C*H_3)$_2$), 31.0 (t, *J* = 12.45 Hz, *C*H$(CH_3)_2$), 25.5 (s, thf), 19.5 (s, CH(*C*H_3)$_2$), 19.2 (s, CH(*C*H_3)$_2$), 19.0 (s, CH(*C*H_3)$_2$), 18.8 (s, CH(*C*H_3)$_2$).

^{31}P{^{1}H} NMR (δ, CD_2Cl_2, 20 °C): 193.9

IR(ATR, 25 °C): 1831 (ν_{co}).

[Mo(PNP^{Me}-*i*Pr)(CO)(NCCH$_3$)Br]SbF$_6$ (6e)

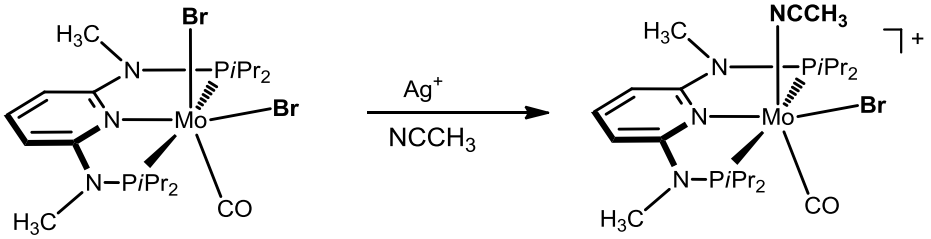

6a **6e**

Mo(PNP^{Me}-*i*Pr)(CO)(Br)$_2$ (300 mg, 0.46 mmol) wurde mit $AgSbF_6$ (165 mg, 0.48 mmol) in Acetonitril umgesetzt. Die Reaktion wurde Übernacht gerührt danach wurde über Glaßwolle und Celite filtriert. Das Lösungsmittel wurde am Hochvakuum abgezogen und das Produkt wurde getrocknet.

Ausbeute: 390 mg (90%) blaues Pulver

Elementar Analyse: $C_{22}H_{40}ClF_6MoN_4OP_2Sb$ (M.G: 850,14): C, 31.08; H, 4.74; Br, 9.40; F, 13.41; Mo, 11.29; N, 6.59; O, 1.88; P, 7.29; Sb, 14.32

^{1}H NMR (δ, CD_2Cl_2, 20 °C): 7.65 (t, *J* = 8.04 Hz, 1H, py), 6.40 (d, *J* = 7.52 Hz, 2H, py), 3.12 (s, 6H, NC*H*$_3$), 2.80 (m, 2H, C*H*(CH$_3$)$_2$), 2.67 (m, 2H, C*H*(CH$_3$)$_2$), 2.20 (s, 3H, NCC*H*$_3$), 1.28 (m, 12H, CH(C*H*$_3$)$_2$), 1,07 (m, 12H, CH(C*H*$_3$)$_2$).

^{13}C{^{1}H} NMR (δ, CD_2Cl_2, 20 °C): 162.1 (t, *J* = 6.35 Hz, py), 143.6 (s, py), 132.4 (s, N*C*CH$_3$), 99.0 (s, py), 34.6 (s, N(*C*H$_3$)$_2$), 30.7 (d, *J* = 27.00 Hz, *C*H(CH$_3$)$_2$), 22.1 (d, *J* = 20.07 Hz, *C*H(CH$_3$)$_2$), 17.5 (s, CH(*C*H$_3$)$_2$), 17.2 (s, CH(*C*H$_3$)$_2$), 17.3 (s, CH(*C*H$_3$)$_2$), 15.7 (s, NC*C*H$_3$).

^{31}P{^{1}H} NMR (δ, CD_2Cl_2, 20 °C): 178.6

IR(ATR, 25 °C): 1840 (ν_{co}).

7-W(0)-Komplexe

W(PNP-Ph)(CO)$_3$ (7a)

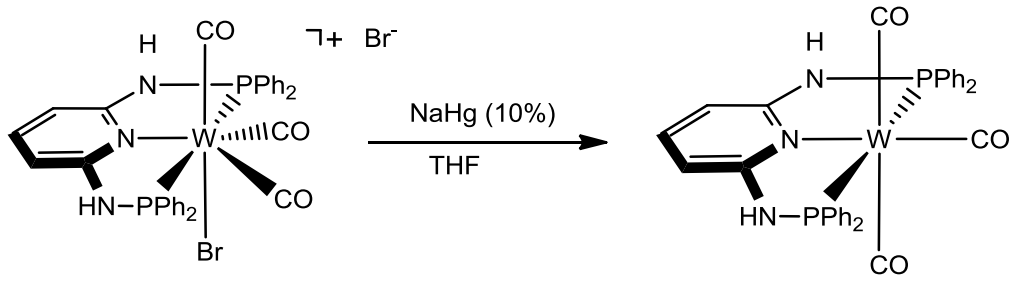

NaHg 10% (16 mg, 0.66 mmol) wurde in THF (10 mL) vorgelegt. Anschließend wurde **5a** (200 mg, 0.22 mmol) in THF (5 mL) dazugegeben und 8 h gerührt. Das Lösungsmittel wurde am Hochvakuum abgezogen und der Rückstand in Aceton gelöst und über Celite durch Kanüle filtriert. Nach dem Abziehen des Lösungsmittels am Hochvakuum wurde das Produkt zweimal mit Diethylether (10 mL) gewaschen und getrocknet.

Ausbeute: 140 mg (85%) gelbes Pulver

Elementar Analyse: $C_{32}H_{25}N_3O_3P_2W$ (M.G: 745,35): C, 51.57; H, 3.38; N, 5.64; O, 6.44; P, 8.31; W, 24.67

^{1}H NMR (δ, Aceton-d$_6$, 20 ^{o}C): 7.64 (t, *J* = 8.6 Hz, 1H, py), 7.44 (bs, 8H, Ph), 7.30 (m, 12H, Ph), 6.43 (d, *J* = 7.6 Hz, 2H, py), 5.93 (d, *J* = 8.9 Hz, 2H, N*H*).

^{13}C{^{1}H} NMR (δ, Aceton-d$_6$, 20 ^{o}C): 206.0 (t, *J* = 4.6 Hz, *C*O), 196.6 (t, *J* = 9.1 Hz, *C*O), 159.6 (d, *J* = 4.7 Hz, py), 159.3 (d, *J* = 5.5 Hz, py), 142.1 (s, py), 132.0 (s, Ph), 131.0 (d, *J* = 12.4 Hz, Ph), 129.1 (d, *J* = 11.5 Hz, Ph), 127.9 (d, *J* = 6.6 Hz, Ph), 102.0 (d, *J* = 10.7 Hz, py).

^{31}P{^{1}H} NMR (δ, Aceton-d$_6$, 20 ^{o}C): 100.2 (s, $J_{W\text{-}P}$ = 327 Hz).

IR(ATR, 25 °C): 1955 (ν_{co}), 1847 (ν_{co}), 1759 (ν_{co}).

W(PNP-*i*Pr)(CO)$_3$ (7b)

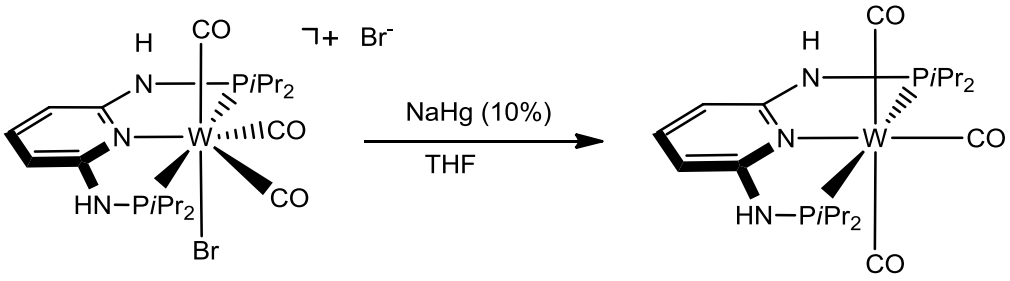

Die Reaktion wurde analog zu **7a** mit **5b** (500 mg, 0.65 mmol) und NaHg (45 mg, 1.95 mmol) durchgeführt.

Ausbeute: 315 mg (85%) gelbes Pulver

Elementar Analyse: $C_{20}H_{33}N_3O_3P_2W$ (M.G: 609,28): C, 39.43; H, 5.46; N, 6.90; O, 7.88; P, 10.17; W, 30.17

^{1}H NMR (δ, CD_2Cl_2, 20 °C): 7.15 (t, *J* = 8.2 Hz, 1H, py), 6.15 (d, *J* = 7.9 Hz, 2H, py), 5.50 (bs, 2H, N*H*), 2.40 (m, 4H, C*H*(CH_3)$_2$), 1.24 (m, 24H, CH(C*H*$_3$)$_2$).

^{13}C{^{1}H} NMR (δ, CD_2Cl_2, 20 °C): 221.1 (t, *J* = 2.0 Hz, *C*O), 210.6 (t, *J* = 7.1 Hz, *C*O), 162.5 (t, *J* = 8.5 Hz, py), 137.1 (s, py), 96.6 (t, *J* = 3.1 Hz, py), 32.60 (t, *J* = 12.8 Hz, *C*H(CH_3)$_2$), 18.5 (t, *J* = 1.7 Hz, CH(*C*H$_3$)$_2$), 18.1 (t, *J* = 2.9 Hz, CH(*C*H$_3$)$_2$).

^{31}P{^{1}H} NMR (δ, CD_2Cl_2, 20 °C): 128.5 (s, $J_{W\text{-}P}$ = 315 Hz).

IR(ATR, 25 °C): 1929 (ν_{co}), 1805 (ν_{co}), 1784 (ν_{co}).

W(PNP-*t*Bu)(CO)$_3$ (7c)

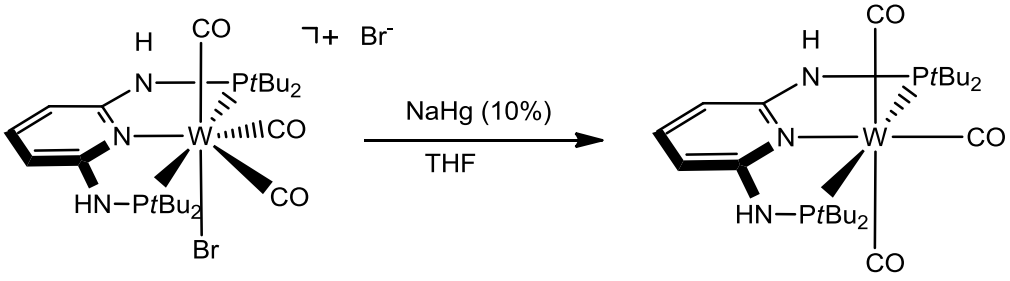

Die Reaktion wurde analog zu **7a** mit **5c** (350 mg, 0.42 mmol) und NaHg (30 mg, 1.27 mmol) durchgeführt.

Ausbeute: 215 mg (77%) gelbes Pulver

Elementar Analyse: $C_{24}H_{41}N_3O_3P_2W$ (M.G: 993,61): C, 29.01; H, 4.16; N, 4.23; O, 4.83; Pt, 39.27; W, 18.50

^{1}H NMR (δ, CD_2Cl_2, 20 °C): 7.37 (bs, 2H, N*H*), 7.18 (t, *J* = 8.0 Hz, 1H, py), 6.29 (d, *J* = 7.5 Hz, 2H, py), 1.41 (t, *J* = 5.6 Hz, 36H, C(CH_3)$_3$).

^{13}C{^{1}H} NMR (δ, Aceton-d_6, 20 °C): 224.7 (t, *J* = 6.4 Hz,*C*O), 219.4 (t, *J* = 7.0 Hz, *C*O), 162.6 (d, *J* = 6.7 Hz, py), 137.8 (s, py), 97.1 (s, py), 40.7 (t, *J* = 7.5 Hz, *C*(CH$_3$)$_3$), 25.8 (d, *J* = 7.3 Hz, C(*C*H$_3$)$_3$).

^{31}P{^{1}H} NMR (δ, CD_2Cl_2, 20 °C): 147.2 (s, $J_{W\text{-}P}$ = 329 Hz).

IR(ATR, 25 °C): 1914 (ν_{co}), 1799 (ν_{co}), 1759 (ν_{co}).

Alternative Herstellung von Mo(PNP-*i*Pr)(CO)$_3$ (4b)

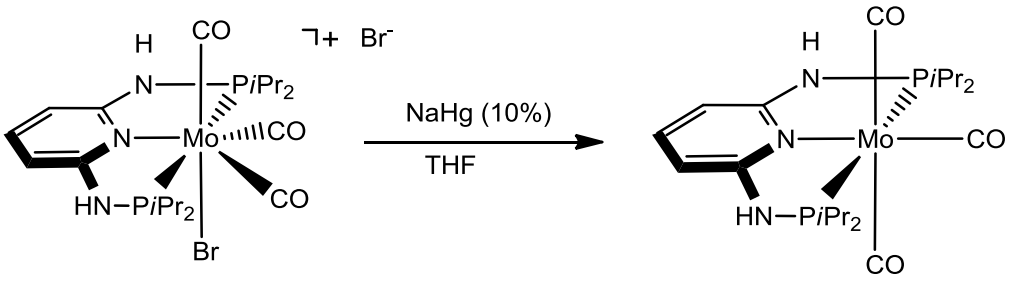

Die Reaktion wurde analog zu **7a** mit **6b** (88 mg, 0.13 mmol) und NaHg (9 mg, 0.39 mmol) durchgeführt.

Ausbeute: 61 mg (90%) gelbes Pulver

Alle Spektren sind gleich wie in der Literatur.[13]

8-Mo(II) und W(II) Hydridocarbonylkomplexe

$[Mo(PNP\text{-}Ph)(CO)_3H]BF_4$ (8a).

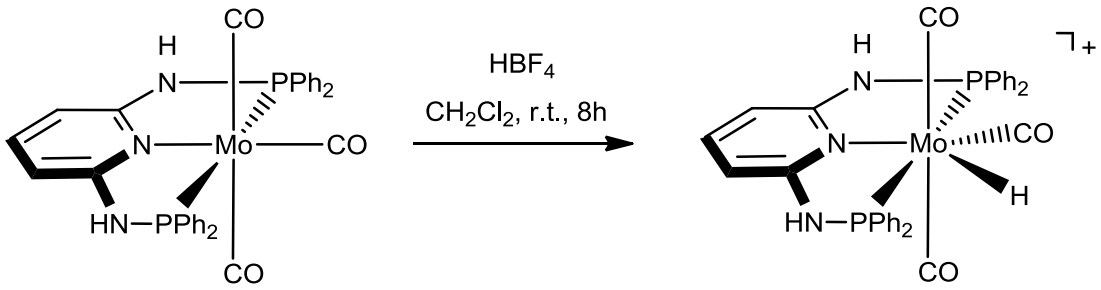

Nachdem $Mo(PNP\text{-}Ph)(CO)_3$ (200 mg, 0.30 mmol) in CH_2Cl_2 gelöst wurde, wurde HBF_4 (46 μL, 0.45 mmol, 54% Lösung in Et_2O) dazugegeben und 8 h bei der Raumtemperatur gerührt. Der entstandene helle gelbe Niederschlag wurde durch einen Glastrichter filtriert und mit Et_2O gewaschen. Anschließend wurde das Produkt am Hochvakuum getrocknet.

Ausbeute: 193 mg (85%) hell gelbes Pulver

Elementar Analyse: $C_{32}H_{26}BF_4MoN_3O_3P_2$ (M.G: 745,28): C, 51.57; H, 3.52; B, 1.45; F, 10.20; Mo, 12.88; N, 5.64; O, 6.44; P, 8.31

^{1}H NMR (δ,Aceton-d_6, -60 °C): 9.25 (s, 2H, N*H*), 8.23 (m, 13H, Ph, py), 7.93 (m, 8H, Ph,), 6.99 (d, *J* = 8.0 Hz, 2H, py), -3.78 (dd, $^2J_{HP}$ = 21.6 Hz, $^2J_{HP}$ = 48.5 Hz, 1H, Mo*H*).

^{13}C{^{1}H} NMR (δ, CD_2Cl_2, 20 °C): 212.7 (t, *J* = 11.2 Hz, *C*O), 203.2 (t, *J* = 8.4 Hz, *C*O), 158.4 (d, *J* = 6.1 Hz, py), 158.1 (d, *J* = 8.3 Hz, py), 141.6 (s, py), 135.3 (s, py), 134.5 (d, *J* = 55.6 Hz, Ph), 131.8 (s, Ph), 130.7 (d, *J* = 13.7 Hz, Ph), 129.0 (d, *J* = 11.1 Hz, Ph), 102.2 (d, *J* = 8.3 Hz, py).

^{31}P{^{1}H} NMR (δ, Aceton-d_6, -60 °C): 111.5 (d, $^2J_{PP}$ = 88.4 Hz), 97.8 (d, $^2J_{PP}$ = 88.4 Hz).

IR(ATR, 25 °C): 2042 (ν_{co}), 1940 (ν_{co}), 1937 (ν_{co}).

[Mo(PNP-*i*Pr)(CO)$_3$H]BF$_4$ (8b).

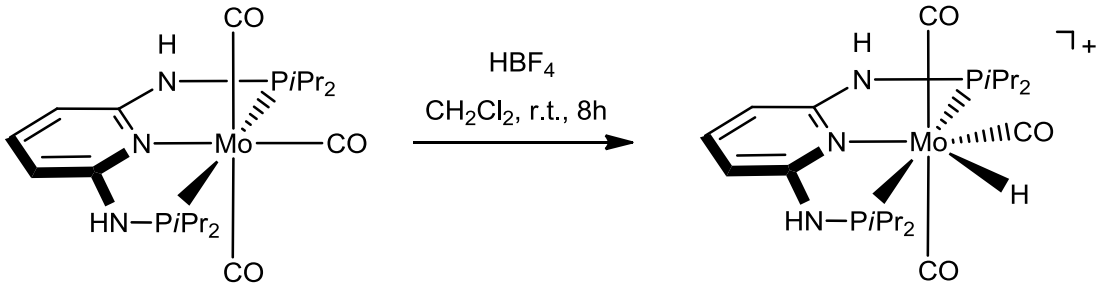

Die Reaktion wurde analog zu **8a** mit Mo(PNP-*i*Pr)(CO)$_3$ (200 mg, 0.38 mmol) und HBF$_4$ (78 μL, 0.45 mmol, 54% Lösung in Et$_2$O) durchgeführt.

Ausbeute: 200 mg (87%) hell gelbes Pulver

Elementar Analyse: $C_{20}H_{34}BF_4MoN_3O_3P_2$ (M.G: 609.21): C, 39.43; H, 5.63; B, 1.77; F, 12.47; Mo, 15.75; N, 6.90; O, 7.88; P, 10.17

^{1}H NMR (δ,Aceton-d$_6$, -60 ^{o}C): 8.86 (d, *J* = 41.2 Hz, 2H, N*H*), 8.00 (t, *J* = 8.2 Hz, 1H, py), 6.95 (d, *J* = 2.91 Hz, 1H, py), 6.92 (d, *J* = 2.91 Hz, 1H, py), 3.27 (m, 4H, C*H*(CH$_3$)$_2$), 1.83 (m, 24H, CH(C*H*$_3$)$_2$), -4.98 (dd, $^2J_{HP}$ = 36.7 Hz, $^2J_{HP}$ = 51.0 Hz, 1H, Mo*H*).

^{13}C{^{1}H} NMR (δ, CD$_2$Cl$_2$, 20 ^{o}C): 212.3 (t, *J* = 11.3 Hz, *C*O), 205.8 (t, *J* = 9.0 Hz, *C*O), 159.8 (d, *J* = 3.9 Hz, py), 159.7 (d, *J* = 3.9 Hz, py), 141.5 (s, py), 100.5 (d, *J* = 7.5 Hz, py), 31.5 (d, *J* = 29.5 Hz, *C*H(CH$_3$)$_2$), 17.8 (d, *J* = 2.3 Hz, CH(*C*H$_3$)$_2$).

^{31}P{^{1}H} NMR (δ, Aceton-d$_6$, -60 ^{o}C): 142.3 (d, $^2J_{PP}$ = 90.4 Hz), 121.4 (d, $^2J_{PP}$ = 90.4 Hz).

IR(ATR, 25 °C): 2035 (ν_{co}), 1923 (ν_{co}), 1920 (ν_{co}).

[Mo(PNP-*t*Bu)(CO)$_3$H]BF$_4$ (8c).

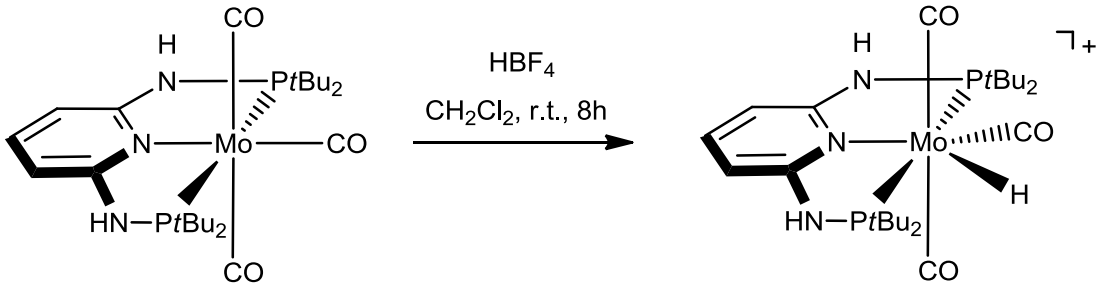

Die Reaktion wurde analog zu **8a** mit Mo(PNP-*t*Bu)(CO)$_3$ (240 mg, 0.42 mmol) und HBF_4 (85 μL, 0.62 mmol, 54% Lösung in Et_2O) durchgeführt.

Ausbeute: 243 mg (87%) hell gelbes Pulver

Elementar Analyse: $C_{24}H_{42}BF_4MoN_3O_3P_2$ (M.G: 665,32): C, 43.33; H, 6.36; B, 1.62; F, 11.42; Mo, 14.42; N, 6.32; O, 7.21; P, 9.31

^{1}H NMR (δ,Aceton-d$_6$, -60 ^{o}C):): 8.06 (bs, 2H, N*H*), 7.62 (t, *J* = 8.3 Hz, 1H, py), 6.62 (d, *J* = 7.9 Hz, 2H, py), 1.82 (d, *J* = 5.8 Hz, 18H, C(C*H*$_3$)$_3$),1.80 (d, *J* = 6.5 Hz, 18H, C(C*H*$_3$)$_3$), -4.34 (dd, $^2J_{HP}$ = 20.7 Hz, $^2J_{HP}$ = 47.8 Hz, 1H, Mo*H*).

^{13}C{^{1}H} NMR (δ, Aceton-d$_6$, 20 ^{o}C): 213.7 (t, *J* = 12.1 Hz, *C*O), 209.5 (t, *J* = 9.4 Hz, *C*O), 160 (d, *J* = 7.0 Hz, py), 141.8 (s, py), 137.9 (s, py), 101.5 (d, *J* = 6.5 Hz, py), 97.3 (s, py), 41.2 (d, *J* = 15.8 Hz, *C*(CH$_3$)$_3$), 24.8 (d, *J* = 7.1 Hz, C(*C*H$_3$)$_3$).

^{31}P{^{1}H} NMR (δ, Aceton-d$_6$, -60 ^{o}C): 158.8 (d, $^2J_{PP}$ = 81.5 Hz), 142.8 (d, $^2J_{PP}$ = 81.5 Hz).

IR(ATR, 25 °C): 2019 (ν_{co}), 1937 (ν_{co}), 1916 (ν_{co}).

[Mo(PNP^{Me}-*i*Pr)(CO)$_3$H]BF$_4$ (8d).

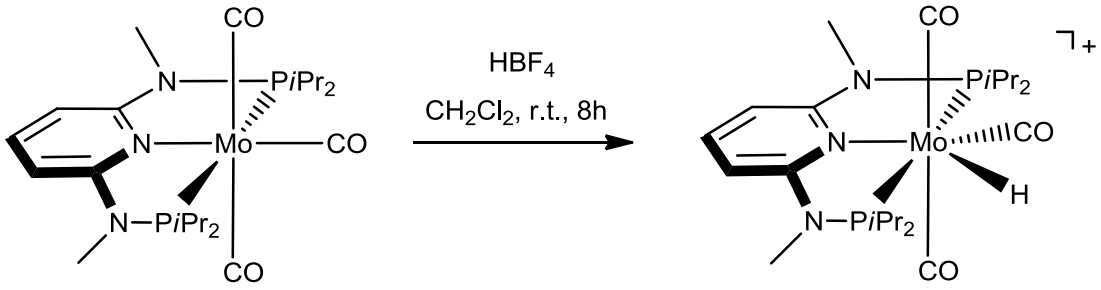

Die Reaktion wurde analog zu **8a** mit Mo(PNP^{Me}-*i*Pr)(CO)$_3$ (67 mg, 0.11 mmol) und HBF$_4$ (23 μL, 0.17 mmol, 54% Lösung in Et$_2$O) durchgeführt.

Ausbeute: 63 mg (90%) hell gelbes Pulver

Elementar Analyse: $C_{22}H_{38}BF_4MoN_3O_3P_2$ (M.G: 637,27): C, 41.46; H, 6.01; B, 1.70; F, 11.92; Mo, 15.06; N, 6.59; O, 7.53; P, 9.72

^{1}H NMR (δ,acetone-d$_6$, -60 °C): 7.93 (t, *J* = 8.2 Hz, 1H, py), 6.65 (d, *J* = 8.2 Hz, 2H, py), 3.41 (s, 6H, N(C*H*$_3$)), 3.25 (m, 4H, C*H*(CH$_3$)$_2$), 1.24 (d, *J* = 7.00 Hz, 6H, CH(C*H*$_3$)$_2$), 1.22 (d, *J* = 7.80 Hz, 12H, CH(C*H*$_3$)$_2$), 1.16 (d, *J* = 7.00 Hz, 6H, CH(C*H*$_3$)$_2$), -5.49 (dd, $^2J_{HP}$ = 20.9 Hz, $^2J_{HP}$ = 49.3 Hz, 1H, Mo*H*).

^{13}C{^{1}H} NMR (δ, CD$_2$Cl$_2$, 20 °C): 210.8 (t, *J* = 10.8 Hz, *C*O), 205.4 (t, *J* = 9.5 Hz, *C*O), 161 (t, *J* = 5.2 Hz, py), 141.9 (s, py), 100.7 (s, py), 35.3 (s, N*C*H$_3$), 32.3 (d, *J* = 24.9 Hz, *C*H(CH$_3$)$_2$), 19.3 (d, *J* = 7.6 Hz, CH(*C*H$_3$)$_2$), 17.9 (s, CH(*C*H$_3$)$_2$).

^{31}P{^{1}H} NMR (δ, Aceton-d$_6$, -60 °C): 166.1 (d, $^2J_{PP}$ = 85.4 Hz), 147.7 (d, $^2J_{PP}$ = 85.4 Hz).

IR (ATR, cm^{-1}): 2028 (ν_{co}), 1928 (ν_{co}), 1910 (ν_{co}).

[W(PNP-Ph)(CO)$_3$H]BF$_4$ (8e).

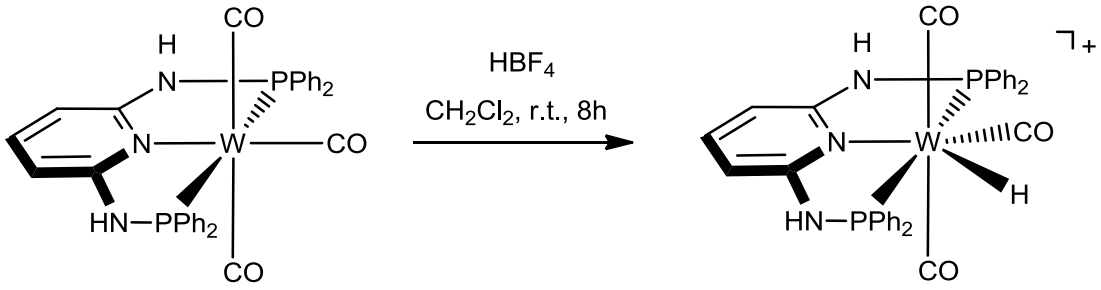

Die Reaktion wurde analog zu **8a** mit W(PNP-Ph)(CO)$_3$ (210 mg, 0.28 mmol) und HBF$_4$ (58 μL, 0.42 mmol, 54% Lösung in Et$_2$O) durchgeführt.

Ausbeute: 186 mg (80%) hell gelbes Pulver

Elementar Analyse: $C_{32}H_{26}BF_4N_3O_3P_2W$ (M.G: 833,16): C, 46.13; H, 3.15; B, 1.30; F, 9.12; N, 5.04; O, 5.76; P, 7.44; W, 22.07

^{1}H NMR (δ,Aceton-d$_6$, -60 °C): 9.74 (bs, 2H, N*H*), 8.15 (s, 8H, Ph), 8.25 (t, *J* = 8.4 Hz, 1H, py), 8.15 (m, 8H, Ph), 7.94 (m, 12H, Ph), 7.04 (d, *J* = 8.0 Hz, 2H, py), -3.43 (dd, $^2J_{HP}$ = 22.4 Hz, $^2J_{HP}$ = 53.8 Hz 1H, W*H*).

^{13}C{^{1}H} NMR (δ, Aceton-d$_6$, 20 °C): 205.9 (t, *J* = 9.7 Hz, *C*O), 196.6 (t, *J* = 8.7 Hz, *C*O), 159.5 (d, *J* = 5.9 Hz, py), 159.3 (d, *J* = 5.9 Hz, py), 142.1 (s, py), 132.0 (s, py), 130.9 (d, *J* = 13.0 Hz, Ph), 129.5 (d, *J* = 13.7 Hz, Ph), 129.1 (d, *J* = 12.1 Hz, Ph), 127.9 (d, *J* =4.6 Hz, Ph), 102.0 (d, *J* = 9.4 Hz, py).

^{31}P{^{1}H} NMR (δ, Aceton-d$_6$, -60 °C): 95.5 (d, $^2J_{PP}$ = 85.9 Hz), 84.8 (d, $^2J_{PP}$ = 85.9 Hz).

IR(ATR, 25 °C): 2038 (ν_{co}), 1963 (ν_{co}), 1918 (ν_{co}).

[W(PNP-*i*Pr)(CO)$_3$H]BF$_4$ (8f).

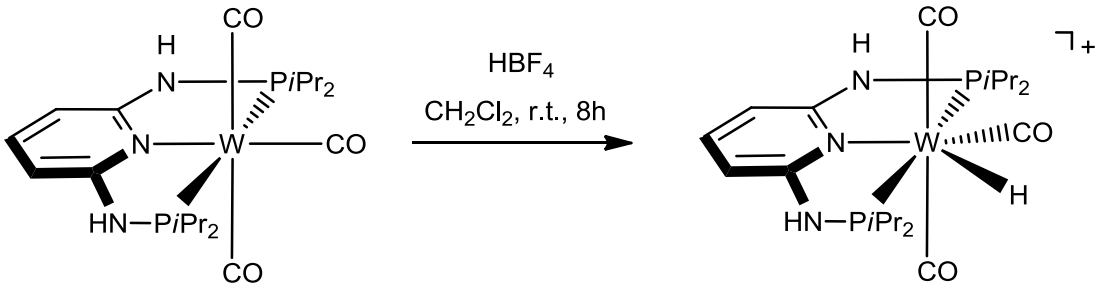

Die Reaktion wurde analog zu **8a** mit W(PNP-*i*Pr)(CO)$_3$ (200 mg, 0.33 mmol) und HBF$_4$ (20 μL, 0.49 mmol, 54% Lösung in Et$_2$O) durchgeführt.

Ausbeute: 207 mg (90%) hell gelbes Pulver

Elementar Analyse: $C_{20}H_{34}BF_4N_3O_3P_2W$ (M.G: 697,09): C, 34.46; H, 4.92; B, 1.55; F, 10.90; N, 6.03; O, 6.89; P, 8.89; W, 26.37

^{1}H NMR (δ, CD_2Cl_2, 20 °C): 8.47 (bs, 2H, N*H*), 7.50 (t, *J* = 8.5 Hz, 1H, py), 6.67 (d, *J* = 7.7 Hz, 2H, py), 2.41 (m, 4H, C*H*(CH$_3$)$_2$), 1.30 (m, 28H, CH(C*H*$_3$)$_2$), -4.83 (dd, $^2J_{HP}$ = 23.3 Hz, $^2J_{HP}$ = 54.7 Hz, 1H, W*H*).

^{13}C{^{1}H} NMR (δ, CD_2Cl_2, 20 °C): 205.5 (t, *J* = 8.5 Hz, *C*O), 198.0 (t, *J* = 8.1 Hz, *C*O), 160.1 (d, *J* = 3.9 Hz, py), 141.6 (s, py), 100.4 (d, *J* = 6.4 Hz, py), 31.9 (d, *J* = 25.5 Hz, *C*H(CH$_3$)$_2$), 18.0 (d, *J* = 4.2 Hz, CH(*C*H$_3$)$_2$).

^{31}P{^{1}H} NMR (δ, CD_2Cl_2, 20 °C): 125.9 (d, $^2J_{PP}$ = 80.0 Hz), 108.6 (d, $^2J_{PP}$ = 80.0 Hz).

IR(ATR, 25 °C): 2027 (ν_{co}), 1910 (ν_{co}), 1906 (ν_{co}).

[W(PNP-*t*Bu)(CO)$_3$H]BF$_4$ (8g).

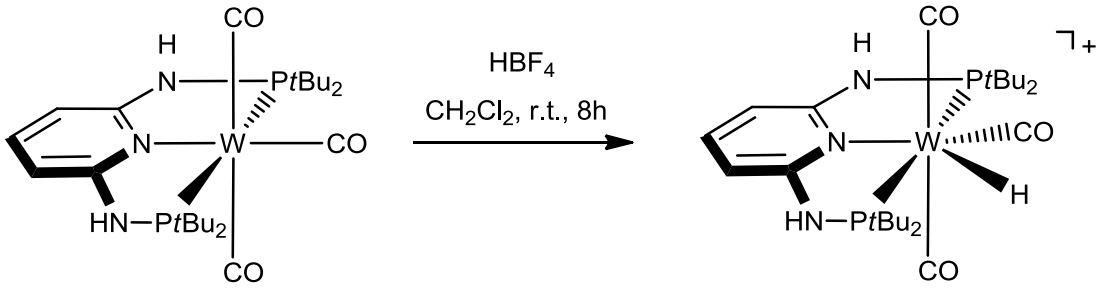

Die Reaktion wurde analog zu **8a** mit W(PNP-*t*Bu)(CO)$_3$ (200 mg, 0.30 mmol) und HBF$_4$ (18 μL, 0.45 mmol, 54% Lösung in Et$_2$O) durchgeführt.

Ausbeute: 207 mg (90%) hell gelbes Pulver

Elementar Analyse: $C_{24}H_{42}BF_4N_3O_3P_2W$ (M.G: 753,20): C, 38.27; H, 5.62; B, 1.44; F, 10.09; N, 5.58; O, 6.37; P, 8.22; W, 24.41

^{1}H NMR (δ, Aceton-d$_6$, 20 °C): 8.00 (bs, 2H, N*H*), 7.60 (t, *J* = 6.7 Hz, 1H, py), 6.75 (d, *J* = 8.3 Hz, 2H, py), 1.59 (s, 18H, C(C*H*$_3$)$_3$), 1.53 (s, 18H, C(C*H*$_3$)$_3$). -4.16 (dd, $^2J_{HP}$ = 37.8 Hz, $^2J_{HP}$ = 50.8 Hz, 1H, W*H*).

^{31}P{^{1}H} NMR (δ, CD$_2$Cl$_2$, 20 °C): 141.1 (d, $^2J_{PP}$ = 83.6 Hz), 126.8 (d, $^2J_{PP}$ = 83.6 Hz).

IR(ATR, 25 °C): 2021 (ν_{co}), 1934 (ν_{co}), 1897 (ν_{co}).

9-Mo(III) und Mo(IV) Komplexe

Mo(PNP^{2Br}-Ph)Br$_4$ (10a)

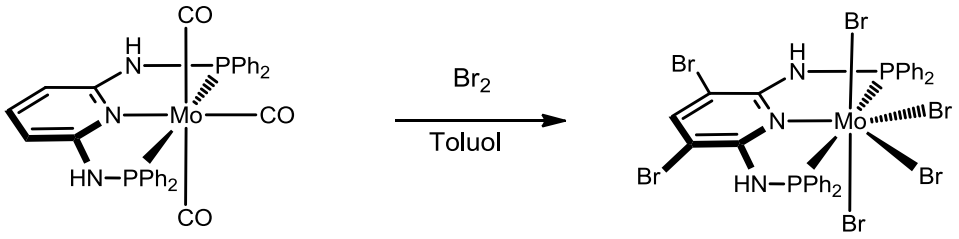

Mo(PNP-Ph)(CO)$_3$ (2.9 g, 4.41 mmol) wurde mit Br_2 (0.700 mL, 13.5 mmol) in Toluol (20 mL) bei 0°C umgesetzt. Nach 4 h wurde das Lösungsmittel abdekantiert und das Produkt mit Et_2O gewaschen danach unter Hochvakuum getrocknet.

Ausbeute: 4.17 g (90%) oranges Pulver

Elementar Analyse: $C_{29}H_{23}Br_6MoN_3P_2$ (M.G: 1050,84): C, 33.15; H, 2.21; Br, 45.62; Mo, 9.13; N, 4.00; P, 5.90

Mo(PNP-*i*Pr)Br$_3$ (10b)

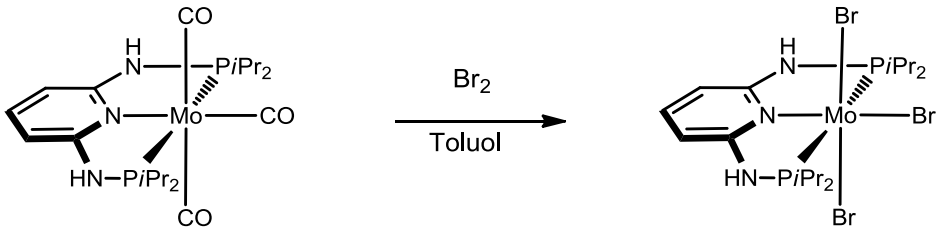

Die Reaktion wurde analog zu 9a mit Mo(PNP-*i*Pr)(CO)$_3$ (720 mg, 1.38 mmol) und Br_2 (217 µL, 4.14 mmol) durchgeführt.

Ausbeute: 880 mg (94%) oranges Pulver

Elementar Analyse: $C_{17}H_{33}Br_3MoN_3P_2$ (M.G: 677,08): C, 30.16; H, 4.91; Br, 35.40; Mo, 14.17; N, 6.21; P, 9.15

10-Molybdänoxokomplexe

[Mo(PNP-*t*Bu)(O)Br]Br (9a)

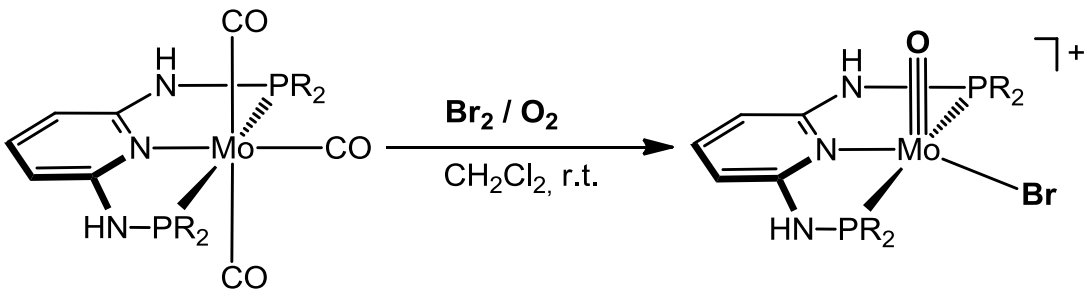

R = *t*Bu

$Mo(PNP\text{-}tBu)(CO)_3$ (200 mg, 0.35 mmol) wurde mit Br_2 (19 µL, 0.37 mmol) in CH_2Cl_2 umgesetzt. Nach dem Rühren Übernacht wurde das Gemisch über Glaßwolle und Celite filtriert danach wurde das Lösungsmittel am Hochvakuum abgezogen. Nachdem das Produkt mit Et_2O gewaschen hat wurde es getrocknet.

Ausbeute: 117 mg (50%) hell grünes Pulver

Elementar Analyse: $C_{21}H_{41}Br_2MoN_3OP_2$ (M.G: 669,29): C, 37.69; H, 6.17; Br, 23.88; Mo, 14.34; N, 6.28; O, 2.39; P, 9.26

^{1}H NMR (δ, CD_2Cl_2, 20 °C): 9.58 (bs, 2H, N*H*), 7.63 (d, *J* = 8.8 Hz, 2H, py), 6.37 (t, *J* = 7.5 Hz, 1H, py), 1.66 (m, 18H, $C(CH_3)_3$), 1.34 (m, 18H, $C(CH_3)_3$).

^{31}P{^{1}H} NMR (δ, CD_2Cl_2, 20 °C): 147.2

[Mo(PNP^{Me}-*i*Pr)(O)I]SbF_6 (9b)

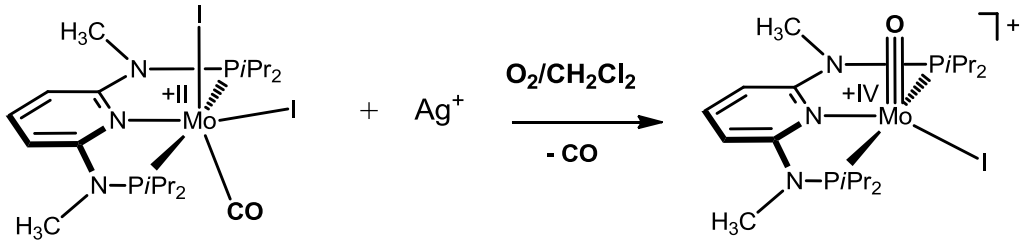

$Mo(PNP^{Me}\text{-}iPr)(CO)(I)_2$ (200 mg, 0.27 mmol) wurde mit $AgSbF_6$ (97 mg, 0.28 mmol) in CH_2Cl_2:in Anwesenheit von Luft umgesetzt. Die Reaktion wurde Übernacht gerührt danach wurde über Glaßwolle und Celite filtriert. Das Lösungsmittel wurde am Hochvakuum abgezogen und das Produkt wurde getrocknet.

Ausbeute: 210 mg (92%) grünes Pulver

Elementar Analyse: $C_{19}H_{37}F_6IMoN_3OP_2Sb$ (M.G: 844,08): C, 27.04; H, 4.42; F, 13.50; I, 15.03; Mo, 11.37; N, 4.98; O, 1.90; P, 7.34; Sb, 14.43

^{1}H NMR (δ, CD_2Cl_2, 20 °C): 8.05 (t, *J* = 8.38 Hz, 1H, py), 6.64 (d, *J* = 8.49 Hz, 2H, py), 3.33 (s, 6H, NC*H*$_3$), 3.06 (m, 2H, C*H*(C*H*$_3$)$_2$), 2.98 (m, 2H, C*H*(C*H*$_3$)$_2$), 1.30 (m, 18H, CH(C*H*$_3$)$_2$), 0.76 (m, 6H, CH(C*H*$_3$)$_2$).

^{13}C{^{1}H} NMR (δ, CD_2Cl_2, 20 °C): 218.5 (t, *J* = 6.35 Hz, *C*O), 162.3 (t, *J* = 6.79 Hz, py), 146.0 (s, py), 128.9 (s, py), 74.4 (s, thf), 36.3 (s, N(*C*H$_3$)$_2$), 31.0 (t, *J* = 12.45 Hz, *C*H(CH$_3$)$_2$), 25.5 (s, thf), 19.5 (s, CH(*C*H$_3$)$_2$), 19.2 (s, CH(*C*H$_3$)$_2$), 19.0 (s, CH(*C*H$_3$)$_2$), 18.8 (s, CH(*C*H$_3$)$_2$).

^{31}P{^{1}H} NMR (δ, CD_2Cl_2, 20 °C): 161.0

DFT-Rechnungen und Strukturbestimmung

Theoretische Berechnungen

Alle Berechnungen wurde mit dem Gaussian 09 Software Paket auf Phoenix Linux Cluster der TU Wien durchgeführt.[34] Die Geometrien und Energien der Modelkomplexe und deren Übergangszustände wurden mit dem B3LYP Funktional optimiert.[35] Für die Beschreibung der Elektronen der Eisen, Molybdän und Wolframatome wurde das Stuttgart/Dresden ECP (SDD) verwendet,[36] für alle anderen Atome wurde der 6-31g** Basissatz verwendet.[37]

Kristallographische Strukturbestimmung

Kristallographische Daten und experimentelle Details finden sich in den Tabellen 4-5. Alle röntgenographischen Daten wurden bei T = 100 K auf einem Bruker Kappa Apex-2 CCD Flächendetektor-Diffraktometer (Mo-Kα Strahlung, Graphitmonochromator (λ = 0.71073 Å), φ- und ω- Scan Frames im Ausmaß von Vollkugeln des reziproken Raums) gesammelt. Korrekturen wurden für Absorption und $\lambda/2$-Effekt wurden mit dem Programm SADABS vorgenommen.[38] Die Kristallstrukturen wurden unter Verwendung des Programms SHELXS97[39] gelöst. Strukturverfeinerungen erfolgten auf Basis von F^2-Werten mit dem Programm SHELXL97. Nicht-Wasserstoffatome wurden anisotrop verfeinert, Wasserstoffatome wurden in kritischen Fällen unrestringiert verfeinert. In allen anderen Fällen wurden sie in idealisierte Positionen eingesetzt und reitend verfeinert.

Table 4. Ausführliche Kristallstrukturinformationen der Komplexe **3k, 3f, und 3d**.

	3k	**3f**	**3d**
Formula	$C_{22}H_{22}FeNO_2P$	$C_{22}H_{23}BrFeNO_2P$	$C_{33}H_{35}BrFeN_2O_3P_2$
Fw	419.23	500.14	705.33
cryst.size, mm	0.45 x 0.26 x 0.14	0.59 x 0.20 x 0.18	0.25 x 0.20 x 0.18
color, shape	red plate	yellow prism	red prism
crystal system	monoclinic	monoclinic	monoclinic
space group	$P2_1/n$ (no. 14)	$P2_1/c$ (no. 14)	$P2_1/c$ (no. 14)
a, Å	10.0648(3)	13.2697(2)	10.1667(4)
b, Å	14.5893(5)	17.5534(2)	17.7127(7)
c, Å	13.4024(4)	9.2565(2)	18.9313(8)
α, deg	90	90	90
β, deg	92.871(2)	92.768(2)	105.453(2)
γ, deg	90	90	90
V, $Å^3$	1965.52(11)	2153.59(6)	3285.9(2)
T, K	100(2)	100(2)	100(2)
Z	4	4	4
ρ_{calc}, g cm^{-3}	1.417	1.543	1.426
μ, mm^{-1} (MoKα)	0.865	2.647	1.807
F(000)	872	1016	1448
absorption	multi-scan, 0.89-0.76	multi-scan, 0.65-0.43	multi-scan, 0.74-0.58
θ range, deg	2.06–30.11	1.93-30.00	2.08-27.50
no. of rflns measd	65996	39753	50035
R_{int}	0.034	0.023	0.076
no. of rflns unique	5771	6253	7526
no. of rflns I>2σ(I)	4787	5578	5356
no. of params /	246 / 0	258 / 0	387 / 136
R_1 (I > 2σ(I)) [a]	0.0253	0.0269	0.0406
R_1 (all data)	0.0366	0.0320	0.0742
wR_2 (I > 2σ(I))	0.0593	0.0682	0.0891
wR_2 (all data)	0.0642	0.0713	0.1081
Diff.Four.peaks	-0.32 / 0.40	-0.45 / 0.82	-0.60 / 0.77

Table 5. Ausführliche Kristallstrukturinformationen der Komplexe **5e·CH_3OH, 5b, 4d, 4f·THF·½C_6H_{14}, 4g·THF, 7a, 7d·CH_2Cl_2, 8a, 6a, 6b, 6c, 10a, 10b.**

	5e·CH_3OH	**5b**	**4d**	**4f·THF·½C_6H_{14}**
formula	$C_{33}H_{29}Br_2N_3O_4P_2W$	$C_{20}H_{33}Br_2MoN_3O_3P_2$	$C_{22}H_{37}MoN_3O_3P_2$	$C_{27}H_{48}N_3O_4P_2W$
Fw	937.20	681.19	549.43	724.47
cryst.size, mm	0.16 x 0.06 x	0.59 x 0.20 x	0.24 x 0.14 x	0.50 x 0.40 x
color, shape	orange prism	yellow plate	yellow prism	yellow plate
crystal system	triclinic	monoclinic	orthorhombic	Monoclinic
space group	*P*-1 (no. 2)	*C*2/c (no. 15)	*P*nma (no.	$P2_1/c$ (no. 14)
a, Å	10.1741(6)	29.6913(15)	18.6552(5)	10.1399(10)
b, Å	13.1580(7)	10.7919(5)	12.1772(3)	15.5053(18)
c, Å	14.1040(8)	16.7764(8)	10.9035(2)	20.036(2)
α, deg	99.456(3)	90	90	90
β, deg	95.412(3)	97.954(1)	90	94.485(5)
γ, deg	104.306(3)	90	90	90
V, $Å^3$	1786.63(17)	5323.9(4)	2476.93(10)	3140.5(6)
T, K	296(2)	173(2)	100(2)	100(2)
Z	2	8	4	4
ρ_{calc}, g cm^{-3}	1.742	1.700	1.473	1.532
μ, mm^{-1} (MoKα)	5.598	3.640	0.687	3.815
F(000)	908	2720	1144	1468
absorption	multi-scan, 0.77-	multi-scan, 0.50-	multi-scan,	multi-scan,
θ range, deg	1.96–30.00	2.30-30.00	2.18–30.07	1.66–30.00
no. of rflns measd	46633	36362	20758	77629
R_{int}	0.060	0.022	0.033	0.042
no. of rflns unique	10399	7732	3770	9124
no. of rflns $I>2\sigma(I)$	7880	6562	3328	6686
no. of params /	393 / 6	294 / 96	167 / 0	366 / 55
R_1 ($I > 2\sigma(I)$) [a]	0.0385	0.0273	0.0217	0.0421
R_1 (all data)	0.0625	0.0351	0.0276	0.0767
wR_2 ($I > 2\sigma(I)$)	0.0822	0.0693	0.0507	0.0785
wR_2 (all data)	0.0884	0.0734	0.0534	0.0998
Diff.Four.peaks	-1.39 / 1.56	-1.01 / 0.97	-0.32 / 0.43	-1.52 / 2.63

Table 5: Ausführliche Kristallstrukturinformationen der Komplexe **3a·CH_3OH, 4b, 2d, 5b·THF·½C_6H_{14}, 4g·THF, 7a, 7d·CH_2Cl_2, 8a, 6a, 6b, 6c, 10a, 10b.**

	4g·THF	**7a**	**7d·CH_2Cl_2**	**8a**	6d
formula	$C_{28}H_{49}N_3O_4P_2W$	$C_{32}H_{26}BF_4MoN_3O_3P_2$	$C_{23}H_{40}BCl_2F_4MoN_3O_3P_2$	$C_{32}H_{26}BF_4N_3O_3P_2W$	$C_{24}H_{45}ClF_6MoN_3O_2P_2Sb$
fw	737.48	745.25	722.17	833.16	836.71
cryst.size, mm	0.30 x 0.17 x	0.42 x 0.35 x	0.32 x 0.30 x	0.24 x 0.08 x	0.28 x 0.22 x
color, shape	yellow block	yellow block	yellow plate	yellow	green block
crystal system	monoclinic	orthorhombic	monoclinic	orthorhombic	monoclinic
space group	$P2_1/n$ (no.	*P*bca (no.	$P2_1/n$ (no.	*P*bca (no.	$P2_1/c$ (no.
a, Å	8.9480(2)	17.4696(5)	8.4324(3)	17.5150(4)	11.4932(4)
b, Å	16.2069(4)	15.5290(4)	23.4895(7)	15.5022(3)	9.6174(3)
c, Å	21.6874(5)	23.3940(6)	16.2384(5)	23.3387(5)	29.2482(10)
α, deg	90	90	90	90	90
β, deg	95.539(1)	90	104.815(2)	90	92.387(2)
γ, deg	90	90	90	90	90
V, $Å^3$	3130.41(13)	6346.5(3)	3109.46(17)	6336.9(2)	3230.14(19)
T, K	100(2)	100(2)	100(2)	100(2)	100(2)
Z	4	8	4	8	4
ρ_{calc}, g cm^{-3}	1.565	1.560	1.543	1.747	1.721
μ, mm^{-1} (MoKα)	3.828	0.576	0.751	3.809	1.468
F(000)	1496	3008	1480	3264	1680
absorption	multi-scan,	multi-scan,	multi-scan,	multi-scan,	multi-scan,
θ range, deg	1.89-30.00	1.96–30.00	2.17–30.00	1.96–30.00	2.21–30.00
no. of rflns	59364	147535	52608	103531	80030
R_{int}	0.023	0.030	0.030	0.032	0.026
no. of rflns	9120	9239	9052	9225	9421
no. of rflns	8540	8380	8280	8120	8736
no. of params /	355 / 0	440 / 0	366 / 0	440 / 0	383 / 0
R_1 ($I > 2\sigma(I)$) [a]	0.0202	0.0252	0.0216	0.0200	0.0437
R_1 (all data)	0.0226	0.0302	0.0253	0.0260	0.0476
wR_2 ($I > 2\sigma(I)$)	0.0470	0.0595	0.0504	0.0385	0.0998
wR_2 (all data)	0.0479	0.0636	0.0525	0.0406	0.1027
Diff.Four.peaks	-1.03 / 1.40	-0.71 / 0.50	-0.43 / 0.45	-0.87 / 0.74	-1.52 / 1.48
					$Å^{-3}$

Table 5: Ausführliche Kristallstrukturinformationen der Komplexe **3a·CH_3OH, 4b, 2d, 5b·THF·½C_6H_{14}, 4g·THF, 7a, 7d·CH_2Cl_2, 8a, 6a, 6b, 6c, 10a, 10b.**

	6c	**6a**	**6b**	**10a**	**10b**
Formula	$C_{20}H_{37}Cl_2MoN_3OP_2$	$C_{20}H_{37}Br_2MoN_3OP_2$	$C_{20}H_{37}I_2MoN_3OP_2$	$C_{25}H_{51}Br_3MoN_3O_2P_2$	$C_{29}H_{23}Br_6MoN_3P_2$
Fw	564.31	653.23	747.21	823.30	1050.84
cryst.size,	0.48 x 0.44	0.28 x 0.25	0.30 x 0.20	0.50 x 0.40	0.32 x 0.28
color, shape	green block	green block	green	yellow	brown
crystal	monoclinic	monoclinic	orthorhom	monoclinic	monoclinic
space group	$P2_1/n$ (no.	$P2_1/n$ (no.	$P2_1/c$ (no.	$P2_12_12_1$	$P2_1/n$ (no.
a, Å	15.2750(3)	15.3996(8)	20.8211(7)	10.0540(3)	12.0003(1
b, Å	11.3110(2)	11.2076(5)	15.7605(5)	15.6381(5)	20.2671(1
c, Å	15.3045(3)	15.6189(7)	17.6677(6)	21.3696(7)	13.0528(1
α, deg	90	90	90	90	90
β, deg	106.401(1)	105.005(2)	114.312(2)	90	93.856(5)
γ, deg	90	90	90	90	90
V, $Å^3$	2536.65(8)	2603.8(2)	5283.5(3)	3359.84(1	3167.4(5)
T, K	100(2)	100(2)	100(2)	100(2)	100(2)
Z	4	4	8, (*Z*' = 2)	4	4
ρ_{calc}, g cm^{-3}	1.478	1.666	1.879	1.628	2.204
μ, mm^{-1}	0.871	3.712	2.971	4.079	8.111
F(000)	1168	1312	2912	1660	2000
absorption	multi-scan,	multi-scan,	multi-scan,	multi-scan,	multi-scan,
θ range, deg	2.22–30.00	2.16–30.00	2.15–	1.91–	1.86-30.00
no. of rflns	39490	54727	86452	138014	75436
R_{int}	0.018	0.023	0.050	0.057	0.034
no. of rflns	7384	7581	15409	13163	9221
no. of rflns	7091	7003	12721	11385	8401
no. of	272 / 0	272 / 0	564 / 0	335 / 0	370 / 0
R_1 ($I > 2\sigma(I)$)	0.0169	0.0195	0.0265	0.0327	0.0202
R_1 (all data)	0.0178	0.0229	0.0392	0.0485	0.0249
wR_2 ($I >$	0.0447	0.0483	0.0510	0.0636	0.0430
wR_2 (all data)	0.0453	0.0498	0.0553	0.0683	0.0443
Diff.Four.peaks	-0.36 / 0.84	-0.38 / 1.15	-0.82 /	-0.76 /	-0.59 /

[a] $R1 = \Sigma||F_o|-|F_c|| / \Sigma|F_o|$, $wR2 = \{\Sigma[w(F_o^2 - F_c^2)^2] / \Sigma[w(F_o^2)^2]\}^{½}$, GooF = $\{\Sigma[w(F_o^2 - F_c^2)^2] / (n-p)\}^{½}$

Literaturverzeichnis

[1] (a) J. Gopalakrishnan, Appl. Organomet. Chem. **2009**, 23, 291. (b) J. Ansell, M. Wills, Chem. Soc. Rev. **2002**, 31, 259. (c) Z. Fei, P. J. Dyson, Coord. Chem. Rev. **2005**, 249, 2056. (c) T. Appleby, J. D. Woollins, Coord. Chem. Rev. **2002**, 235, 121. (e) M. S. Balakrishna, V. Sreenivasa Reddy, S. S. Krishnamurthy, J. F. Nixon, J. C. T. R. Burckett St. Laurent, Coord. Chem. Rev. **1994**, 1291.

[2] (a) S. Priya, M. S. Balakrishna, J. T. Mague, J. Organomet. Chem. **2003**, 679, 116. (b) S. Priya, M. S. Balakrishna, S. M. Mobin, R. McDonald, J. Organomet. Chem. **2003**, 688, 227. (c) K. G. Gaw, A. M. Z. Slawin, M. B. Smith, Organometallics **1999**, 18, 3255. (d) D. Fenske, B. Maczek, K. Maczek, Z. Anorg. Allg. Chem. **1997**, 623, 1113. (e) O. Kühl, P. C. Junk, E. Hey-Hawkins, Z. Anorg. Allg. Chem. **2000**, 626, 1591. (f) O. Kühl, S. Blaurock, J. Sieler, E. Hey-Hawkins, Polyhedron **2001**, 20, 111. (g) O. Kühl, T. Koch, F. B. Somoza Jr., P. C. Junk, E. Hey-Hawkins, D. Plat, M. S. Eisen, J. Organomet. Chem. **2000**, 604, 116. (h) G. Suss-Fink, M. A. Pellingeelli, A. Tiripicchhio, J. Organomet. Chem. **1987**, 320, 101. (i) E. W. Ainscough, A. M. Brodie, S. T. Wong, J. Chem. Soc., Dalton Trans. **1977**, 915.

[3] For recent examples see: (a) S. Kuppuswawamy, M. W. Bezpalko, T. M. Powers, M. M. Turnbull, B. M. Foxman, C. M. Thomas, Inorg. Chem. **2012**, 51, 8225. (b) D. A. Evers, A. H. Bluestein, B. M. Foxman, C. M. Thomas, Dalton Trans. **2012**, 41, 8111. (c) B. G. Cooper, C. M. Fafard, B. M. Foxman, C. M. Thomas, Organometallics **2010**, 29, 5179.

[4] (a) H. Nagashima, T. Sue, T. Oda, A. Kanemitsu, T. Matsumoto, Y. Motoyama, Y. Sunada, Organometallics **2006**, 25, 1987. (b) Y. Sunada, T. Sue, T. Matsumoto, H. Nagashima, J. Organomet. Chem. **2006**, 691, 3176. (c) T. Sue, Y. Sunada, H. Nagashima, Eur. J. Inorg. Chem. **2007**, 2897. (d) H. Tsutsumi, Y. Sunada, Y. Shiota, K. Yoshizawa, H. Nagashima, Organometallics **2009**, 28, 1988.

[5] S. Pavlik, K. Mereiter, R. Schmid, K. Kirchner, Organometallics **2003**, 22, 1771.

[6] M. Jimenez-Tenorio, M. C. Puerta, P. Valerga, Eur. J. Inorg. Chem. **2005**, 2631.

[7] K. A. Bunten, D. H. Farrar, A. J. Poë, A. J. Lough, Organometallics 2000, 19, 3674.

[8] M. Herberhold, W. Ehrenreich, K. Guldner, W. Jellen, U. Thewalt, H. Klein, Zeitschrift für Naturforschung, Teil B: Anorganische Chemie, Organische Chemie (1983), 38B(11), 1383-7.

[9] C. J. Harlan, T. C. Wright, J. L. Atwood, S. G. Bott, Inorg. Chem. **1991**, 30, 1955.

[10] (a) Schirmer, W.; Flörke, U.; Haupt, H.-J. Z. Anorg. Allg. Chem. **1987**, 545, 83. (b) Schirmer, W.; Flörke, U.; Haupt, H.-J. Z. Anorg. Allg. Chem. **1989**, 574, 239.

[11] Benito-Garagorri, D., Becker, E.; Wiedermann, J.; Lackner, W.; Pollak, M.; Mereiter, K.; Kisala, J.; Kirchner, K. Organometallics **2006**, 25, 1900.

[12] Dahloff, W. V.; Nelson, S. M. J. Chem. Soc. A **1971**, 2184.

[13] (a) Vasapollo, G.; Giannoccaro, P.; Nobile, C. F.; Sacco, A. Inorg. Chim. Acta **1981**, 48, 125. (b) Steffey, B. D.; Miedaner, A.; Maciejewski-Farmer, M. L.; Bernatis, P. R.; Herring, A. M.; Allured, V. S.; Carperos, V.; DuBois, D. L. Organometallics **1994**, 13, 4844. (c) Hahn, C.; Sieler, J.; Taube, R. Chem. Ber. **1997**, 130, 939. (d) Hahn, C.; Vitagliano, A.; Giordano, F.; Taube, R. Organometallics **1998**, 17, 2060. (e) Hahn, C.; Spiegler, M.; Herdtweck, E., Taube, R. Eur. J. Inorg. Chem. **1999**, 435.

[14] Jiang, Q.; Van Plew, D.; Murtuza, S.; Zhang, X. Tetrahedron Lett. **1996**, 37, 797.

[15] (a) Andreocci, M. V.; Mattogno, G.; Zanoni, R.; Giannoccaro, P.; Vasapollo, G. Inorg. Chim. Acta **1982**, 63, 225. (b) Sacco, A.; Vasapollo, G.; Nobile, C.; Piergiovanni, A.; Pellinghelli, M. A.; Lanfranchi, M. J. Organomet. Chem. **1988**, 356, 397. (c) Abbenhuis, R. A. T. M.; del Rio, I.; Bergshoef, M. M.; Boersma, J.; Veldman, N.; Spek, A. L.; van Koten, G. Inorg. Chem. **1998**, 37, 1749.

[16] (a) Rahmouni, N.; Osborn, J. A.; De Cian, A.; Fisher, J.; Ezzamarty, A. Organometallics **1998**, 17, 2470. (b) Sablong, R.; Newton, C.; Dierkes, P.; Osborn, J. A. Tetrahedron Lett. **1996**, 37, 4933. (c) Sablong, R.; Osborn, J. A.

Tetrahedron Lett. **1996**, 37, 4937. (d) Barloy, L.; Ku, S. Y.; Osborn, J. A.; De Cian, A.; Fischer, J. Polyhedron **1997**, 16, 291.

[17] (a) Zhang, J.; Leitus, G.; Ben-David, Y.; Milstein, D. J. Am. Chem. Soc. **2005**, 127, 10840. (b) Zhang, J.; Gandelman, M.; Shimon, L. J. W.; Rozenberg, H.; Milstein, D. Organometallics **2004**, 23, 4026. (c) Hermann, D.; Gandelman, M.; Rozenberg, H.; Shimon, L. J. W.; Milstein, D. Organometallics **2002**, 21, 812.

[18] Gibson, D. H.; Pariya, C.; Mashuta, M. S. Organometallics **2004**, 23, 2510.

[19] Katayama, H.; Wada, C.; Taniguchi, K.; Ozawa, F. Organometallics **2002**, 21, 3285.

[20] Jia, G.; Lee, H. M.; Williams, I. D.; Lau, C. P.; Chen, Y. Organometallics **1997**, 16, 3941.

[21] Müller, G.; Klinga, M.; Leskelä, M.; Rieger, B. Z. Anorg. Allg. Chem. **2002**, 628, 2839.

[22] (a) Schirmer, W.; Flörke, U.; Haupt, H.-J. Z. Anorg. Allg. Chem. **1987**, 545, 83. (b) Schirmer, W.; Flörke, U.; Haupt, H.-J. Z. Anorg. Allg. Chem. **1989**, 574, 239.

[23] Cotton, A, F.; Falvello, R. L.; Meadows, H. J.; Amer. Chem. Soc. **1984**, 23, 4688.

[24] Benito-Garagorri, D., Becker, E.; Wiedermann, J.; Lackner, W.; Pollak, M.; Mereiter, K.; Kisala, J.; Kirchner, K. Organometallics **2006**, 25, 1900.

[25] (a) Benito-Garagorri, D., Puchberger, M.; Mereiter, K.; Kirchner, K. Angew. Chem., Int. Ed., **2008**, 47, 9142; Angew. Chem. **2008**, 120, 9282. (b) Benito-Garagorri, D., Alves, L. G.; Puchberger, M.; Mereiter, K.; Veiros, L. F.; Calhorda, M. J.; Carvalho, M. D.; Ferreira, L. P.; Godinho, M.; Kirchner, K.; Organometallics **2009**, 28, 6902. (c) Benito-Garagorri, D.; Alves, L. G.; Veiros, L. F.; Standfest-Hauser, C. M.; Tanaka, S.; Mereiter, K.; Kirchner, K. Organometallics **2010**, 29, 4923.

[26] (a) Alves, L. G.; Dazinger, G.; Veiros, L. F.; Kirchner, K. Eur. J. Inorg. Chem. **2010**, 3160. (b) Benito-Garagorri, D., Wiedermann, J.; Pollak, M.; Mereiter, K.; Kirchner, K. Organometallics **2007**, 26, 217.

[27] Benito-Garagorri, D., Mereiter, K.; Kirchner, K. Eur. J. Inorg. Chem. **2006**, 4374.

[28] (a) Lang, H.-F.; Fanwick, P. E.; Walton, R. A. Inorg. Chim. Acta **2002**, 392, 1.

[29] (a) Kinoshita, E.; Arashiba, K.; Kuriyama, S.; Miyake, Y. Shimazaki, R.; Nakanishi, H.; Nishibayashi, Y. Organometallics **2012**, 31, 8437. (b) Arashiba, A.; Sasaki, K.; Kuriyama, S.; Miyake, Y.; Nakanishi, H.; Nishibayashi, Y. Organometallics **2012**, 31, 2035. (c) Arashiba, K.; Miyake, Y.; Nishibayashi, Y. Nat.Chemistry, **2011**, 3, 120.

[30] Leah A. Wingard, Peter S. White and Joseph L. Templeton. Dalton Trans., **2012**, 41, 11438.

[31] Perrin, D. D.; Armarego, W. L. F. Purification of Laboratory Chemicals, 3rd ed.; Pergamon: New York, **1988**.

[32] T. S. Piper, F. A. Cotton, G. J. Wilkinson, Inorg. Nucl. Chem. **1955**, 1, 165.

[33] W. Hieber, A. Z. Wirsching, Anorg. Allg. Chem. **1940**, 245, 305.

[34] Frisch, M. J. et.al. Gaussian 09, Revision A.02; Gaussian, Inc., Wallingford, CT, **2009**.

[35] (a) Becke, A. D. J. Chem. Phys. **1993**, 98, 5648. (b) Miehlich, B.; Savin, A.; Stoll, H.; Preuss, H. Chem. Phys. Lett **1989**, 157, 200. (c) Lee, C.; Yang, W.; Parr, G. Phys. Rev. B **1988**, 37, 785.

[36] (a) Haeusermann, U.; Dolg, M.; Stoll, H.; Preuss, H. Mol. Phys. **1993**, 78, 1211. (b) Kuechle, W.; Dolg, M.; Stoll, H.; Preuss, H. J. Chem. Phys. **1994**, 100, 7535. (c) Leininger, T.; Nicklass, A.; Stoll, H.; Dolg, M.; Schwerdtfeger, P. J. Chem. Phys. **1996**, 105, 1052.

[37] (a) McLean, A. D.; Chandler, G. S. J. Chem. Phys. **1980**, 72, 5639. (b) Krishnan, R.; Binkley, J. S.; Seeger, R.; Pople, J. A. J. Chem. Phys. **1980**, 72, 650. (c) Wachters, A. J. H. Chem. Phys. **1970**, 52, 1033. (d) Hay, P. J. J. Chem. Phys. **1977**, 66, 4377. (e) Raghavachari, K.; Trucks, G. W. J. Chem. Phys. **1989**, 91, 1062. (f) Binning Jr., R. C.; Curtiss, L. A. J. Comp. Chem., **1990**, 11, 1206. (g) McGrath, M. P.; Radom, L. J. Chem. Phys. **1991**, 94, 511.

[38] Bruker programs: APEX2, version 2009.9–0; SAINT, version 7.68 A; SADABS, version 2008/1; SHELXTL, version 2008/4, Bruker AXS Inc., Madison, WI, **2009**.

[39] Sheldrick, G. M. Acta Cryst. **2008**, A64, 112-122.

DI Özgür Öztopcu

Aloisgasse 1/3

1020 Wien, Österreich

Persönliche Daten

Geburtsdatum:	01.Feb.1975
Staatsangehörigkeit:	Türkei
Familienstand:	Ledig

Ausbildung

04/2010 bis 10/2013	Dissertation, Institut für Angewandte Synthesechemie, TU Wien
10/2006 bis 04/2010	Master Studium, Institut für Angewandte Synthesechemie, TU Wien
10/1998 bis 06/1999	Master Studium, Verfahrenstechnik, TU Istanbul
10/1994 bis 06/1998	Bachelor Studium, Verfahrenstechnik, TU Istanbul
09/1989 bis 06/1992:	Kartal Gymnasium, Istanbul (Türkei)
09/1986 bis 06/1989:	Kazimkarabekir Hauptschule, Erzincan (Türkei)
09/1981 bis 06/1986:	Keklikkayasi Köyü Grundschule, Erzincan (Türkei)

Berufserfahrung

10/2010 bis 10/2014	Technische Universität Wien, Universitätsassistent
11/2003 bis 03/2004	Belginoil/Gebze-Türkei , Technische Vertriebsleitung
08/2000 bis 07/2003	Flokser/Istanbul-Türkei, Produktionsingenieur

Sprachen

Türkisch	Muttersprache
Kurdisch	Muttersprache
Deutsch	Fließend in Wort und Schrift
Englisch	Gut in Wort und Schrift

Publikationen

Synthesis and Characterization of Hydrido Carbonyl Molybdenum and Tungsten PNP Pincer Complexes

Author(s): Özgür Öztopcu, Christian Holzhacker, Michael Puchberger, Matthias Weil, Kurt Mereiter, Luis F. Veiros, and Karl Kirchner

Source: Organometallics, 2013, *32* (10)

Reactivity of iron complexes containing monodentate aminophosphine ligands - Formation of four-membered carboxamido-phospha-metallacycles

Author(s): Oeztopcu, Oezguer; Stoeger, Berthold; Kurt, Mereiter B.; Kirchner, Karl.

Source: Journal of organometallic chemistry, 2013, 735 (80)

Synthesis, Structure, Ligand Dynamics, and Catalytic Activity of Cationic [Pd(eta(3)-allyl)(kappa(2)(E,N)-EN-chelate)(+) (E = P, O, S, Se) Complexes

Author(s): Bichler, Bernhard; Veiros, Luis F.; Oeztopcu, Oezguer; Kirchner, Karl.

Source: Organometallics, 2011, 30 (5928)

Tri- and tetracoordinate copper(I) complexes bearing bidentate soft/hard SN and SeN ligands based on 2-aminopyridine

Author(s): Oeztopcu, Oezguer; Mereiter, Kurt; Puchberger, Michael; Kirchner, Karl.

Source: Dalton transactions, 2011, 40 (7008)

Synthesis and characterization of ruthenium p-cymene complexes bearing bidentate P-N and E-N ligands (E = S, Se) based on 2-aminopyridine

Author(s): Lackner-Warton, Wolfgang; Tanaka, Shinji; Standfest-Hauser, Christina M.; Kirchner, Karl.

Source: Polyhedron, 2010, 29 (3097)

Bis{2-[(diisopropylphosphanyl)amino]pyridine-kappa N-2(1),P}copper(I) hexafluoridophosphate

Author(s): Oeztopcu, Oezguer; Kirchner, Karl; Mereiter, Kurt

Source: ACTA crystallographica section e-structure reports online, 2010, 66 (M729)

Poster Presentation

Özgür Öztopcu, Christian Holzhacker, Michael Puchberger, Mathias Weil, Kurt Mereiter, Luis F. Veiros, and Karl Kirchner, Synthesis and Characterization of Molybdenum and Tungsten PNP Pincer Complexes, Österreichische Chemietage, 23. - 26. September 2013, Graz

Özgür Öztopcu, Berthold Stöger, Kurt Mereiter, and Karl A. Kirchner, Reactivity of Iron Complexes containing Aminophosphine Ligands - Formation of Four-membered Aza-Phospha-Metallacycles, XXV International conference on organometallic chemistry, 2-7 September 2012, Lisbon, Portugal

Özgür Öztopcu, Michael Puchberger, Kurt Mereiter, and Karl A. Kirchner, Tri- and Tetracoordinate Copper(I) Complexes bearing Bidentate Soft/Hard SN and SeN Ligands based on 2-Aminopyridine, Österreichische Chemietage, 26. - 29. September 2011, Linz

Journal of Organometallic Chemistry 735 (2013) 80–87

Contents lists available at SciVerse ScienceDirect

Journal of Organometallic Chemistry

journal homepage: www.elsevier.com/locate/jorganchem

Reactivity of iron complexes containing monodentate aminophosphine ligands – Formation of four-membered carboxamido-phospha-metallacycles

Özgür Öztopcu [a], Berthold Stöger [b], Kurt Mereiter [b], Karl Kirchner [a,*]

[a] Institute of Applied Synthetic Chemistry, Vienna University of Technology, Getreidemarkt 9, A-1060 Vienna, Austria
[b] Institute of Chemical Technologies and Analytics, Vienna University of Technology, Getreidemarkt 9, A-1060 Vienna, Austria

ARTICLE INFO

Article history:
Received 12 February 2013
Received in revised form
13 March 2013
Accepted 14 March 2013

Keywords:
Iron
Cyclopentadienyl
Carbon monoxide
Aminophosphines
Nucleophilic attack
Ferracycles

ABSTRACT

Treatment of $[FeCp(CO)_2Cl]$ with 1 equiv of the amidophosphine ligands $Li[R_2PNR']$ (R = Ph, *i*Pr, R′ = *i*Pr, *t*Bu, Cy) afforded complexes of the type $[FeCp(CO)(\kappa^2(C,P)\text{-}(C{=}O){-}NiPr\text{-}PPh_2)]$ (**1a**), $[FeCp(CO)(\kappa^2(C,P)\text{-}(C{=}O)\text{-}NtBu\text{-}PPh_2)]$ (**1b**), and $[FeCp(CO)(\kappa^2(C,P)\text{-}(C{=}O)\text{-}NCy\text{-}PiPr_2)]$ (**1c**) in 40–50% yields. Complex **1a** was also formed when $[FeCp(CO)_2(PPh_2NHiPr)]^+$ (**2**) was reacted with 1 equiv of KO*t*Bu. These complexes feature a four-membered carboxamido-phospha-ferracycle as a result of an intramolecular nucleophilic attack of the amidophosphine ligand on coordinated CO. Upon treatment of **1a** with the electrophile $[Me_3O]BF_4$ the aminocarbene complex $[FeCp(CO)(\kappa^2(C,P){=}C(OMe)\text{-}NiPr\text{-}PPh_2)]^+$ (**3**) was obtained bearing an aza-phospha-carbene moiety. Upon treatment of *cis*,*trans*,*cis*-$[Fe(CO)_2(Ph_2PNHiPr)_2(Br)_2]$ (**4a**) and *cis*,*trans*,*cis*-$[Fe(CO)_2(Ph_2PNHtBu)_2(Br)_2]$ (**4b**) with KO*t*Bu the carboxamido-phospha-ferracycles *trans*-$[Fe(CO)_2(\kappa^2(C,P)\text{-}(C{=}O)\text{-}NiPr\text{-}PPh_2)(Ph_2PNHiPr)Br]$ (**5a**) and *trans*-$[Fe(CO)_2(\kappa^2(C,P)\text{-}(C{=}O)\text{-}NtBu\text{-}PPh_2)(Ph_2PNHtBu)Br]$ (**5b**) were formed in moderate yield. Finally, representative structures were determined by X-ray crystallography.

1. Introduction

Aminophosphines of the type PR_2NHR' containing a direct polar P(III)–N bonds have received considerable attention in recent years as versatile ligands for transition metals [1]. They are accessible in large quantities through the use of relatively simple condensation processes from inexpensive starting materials, i.e., primary amines and PR_2Cl compounds which contain dialkyl or diaryl substituents as well as achiral and chiral P–O and P–N containing phosphine units. Thus, variations of electronic, steric, and stereochemical parameters may be achieved in a very facile fashion. Due to their soft/hard donor atoms as well their acidic NH hydrogen, these polyfunctional ligands exhibit numerous coordination modes as illustrated in Scheme 1. As middle and late transition metals **M** are concerned PR_2NHR' ligands typically coordinate in $\kappa^1(P)$-fashion **I** [2], while $\kappa^1(N)$-coordination is unknown. Upon deprotonation of the PR_2NHR' ligands, anionic amidophosphines $[PR_2NR']^-$ are readily obtained which exhibit a higher affinity toward electropositive metals due to their increased nucleophilicity at the N-site. Thus, in conjunction with early transition metals **M'**, amidophosphine ligands were shown to display $\kappa^2(P,N)$ coordination **II**, and, albeit less common, also $\kappa^1(N)$-coordination **III**, while in the presence of both early and middle/late transition metals, amidophosphine ligands were shown to act as μ^2 bridging ligand thereby forming heterobimetallic complexes of the type **IV** [3,4].

Besides interesting structural features, PR_2NHR' ligands display various reactivities opening up a range of synthetically useful transformations [5]. For instance, we have recently shown [6] that in vinylidene and allenylidene complexes $[RuCp(PPh_2NHR)_2(=C{=}(C)_n{=}CHR')]^+$ and $[RuTp(PPh_2NHR)_2(=C{=}(C)_n{=}CHR')]^+$ ($n = 0$, 1; R = Ph, *n*-Pr; R′ = alkyl, aryl; Tp = trispyrazoloylborate) an intramolecular addition of the NHR' moiety to the α-carbon of the cumulene moiety takes place (Scheme 2) resulting in the formation of novel four-membered aza-phospha-carbenes (Scheme 3, **A**). Complexes of the types $[RuCp(PPh_2NHPh)(CH_3CN)_2]^+$ and $[RuCp^*(PR_2NHR')(CH_3CN)_2]^+$ (R = Ph, *i*-Pr, R′ = Ph, C_6F_5) have been found to react with terminal alkynes and diynes to give amido butadiene complexes involving PR_2NHR' ligand migration (Scheme 3, **B**) [7,8]. Bunten et al. reported [9] the synthesis of the dinuclear ruthenium complex $[Ru_2(CO)_3(\mu^2\text{-}PPh_2)(\mu^2\text{-}Ph_2PNMePPh_2)(\kappa^2(C,P)\text{–}C(=O)NMePPh_2)]$ containing a carboxamido-phospha-ruthenacyclic moiety (Scheme 3, **C**). Herberhold et al. reported on the preparation of half sandwich complexes of the type $[MCp(CO)_2(C(=O)N(S\text{-}NHPtBu_2)PtBu_2)]$ (M = Cr, Mo, W) by reacting $[MCp(CO)_3H]$ with $PtBu_2PN = S{=}NPtBu_2$

* Corresponding author. Tel.: +43 1 58801 163611; fax: +43 1 58801 16399.
E-mail address: kkirch@mail.tuwien.ac.at (K. Kirchner).

0022-328X/$ – see front matter © 2013 Elsevier B.V. All rights reserved.
http://dx.doi.org/10.1016/j.jorganchem.2013.03.027

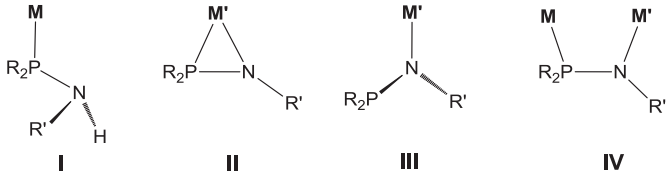

Scheme 1. Most common bonding modes of aminophosphine and amidophosphine ligands.

(Scheme 3, **D**) [10]. As iron complexes are concerned, $[FeCp(CO)_2(PPh_2NHNMe_2]^+$ bearing a hydrazinophosphine ligand, which is closely related to PR_2NHR' ligands, was shown to react with *n*BuLi to give the carboxamido-phospha-ferracycle [FeCp(-CO)(κ^2(*C*,*P*)-(C=O)-NNMe$_2$-PPh$_2$)] (Scheme 3, **E**) [11].

In the present paper we report on the synthesis of iron(II) complexes containing aminophosphine ligands of the type PR_2NHR' with R = Ph, *i*Pr, R′ = *i*Pr, *t*Bu, Cy. We describe the reactivity of these complexes yielding, upon treatment with strong bases, novel cyclic four-membered carboxamido-phospha-ferracycle formed via intramolecular addition of the amine moiety of the bifunctional aminophosphine ligand according to Scheme 4.

2. Results and discussion

Treatment of $[FeCp(CO)_2Cl]$ with 1 equiv of the amidophosphine ligands $[R_2PNR']^-$ (R = Ph, *i*Pr, R′ = *i*Pr, *t*Bu, Cy), prepared *in situ* by the reaction of R_2PNHR' with *n*BuLi in THF at −20 °C, afforded complexes of the type [FeCp(CO)(κ [2](*C*,*P*)-(C=O)−N*i*Pr-PPh$_2$)] (**1a**), [FeCp(CO)(κ^2(*C*,*P*)-(C=O)-N*t*Bu-PPh$_2$)] (**1b**), and [FeCp(-CO)(κ^2(*C*,*P*)-(C=O)-NCy-P*i*Pr$_2$)] (**1c**) in reasonable isolated yields (40−50%) (Scheme 5). Although no intermediate could be detected spectroscopically, it is most likely that the deprotonated R_2PNHR' ligand first forms a complex with a κ^1(*P*)-bound rather than a κ^1(*N*)-bound amidophosphine. It has to be noted that κ^1(*N*) coordinated $[PR_2NR']^-$ ligands to late transition metals are, according to our knowledge, unknown.

Subsequently, intramolecular, chelate assisted, nucleophilic attack of the amido moiety of the PR_2NR' ligand at one of the two CO ligands took place resulting in the formation of novel four-membered carboxamido-phospha-ferracycle. This is also supported by the fact that **1a** is readily formed if the cationic dicarbonyl complex $[FeCp(CO)_2(PPh_2NHiPr)]^+$ with either Br^- (**2**) or BF_4^- (**2'**) as counterions was treated with KO*t*Bu as base according to Scheme 6. In the absence of base, even at elevated temperatures, no reaction took place. Complexes **2** and **2'** were readily obtained by the treatment of $[FeCp(CO)_2Br]$ with 1 equiv of the PPh_2NHiPr ligand in the absence or presence of $NaBF_4$, respectively, in THF at room temperature (Scheme 6).

All complexes are thermally robust orange solids that are air stable both in the solid state and in solution for several days. Their identity was unequivocally established by ^{1}H, ^{13}C{^{1}H} and ^{31}P{^{1}H} NMR, IR spectroscopy, and elemental analysis. In addition, the molecular structures of complexes **1a** and **2** were determined by X-ray crystallography. Structural views are depicted in Figs. 1 and 2 with selected bond distances and angles reported in the captions.

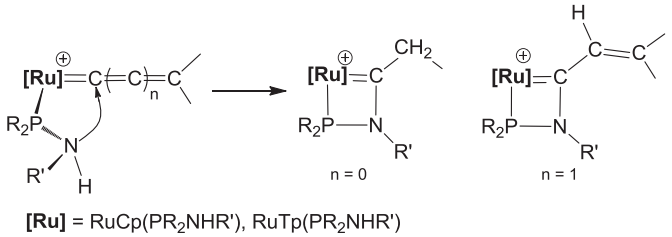

Scheme 2. Intramolecular addition of the NHR' moiety of an aminophosphine to the α-carbon of a cumulene moiety.

Complexes **1a**−**c** display a single resonance in the ^{31}P{^{1}H} NMR at 111.6, 113.0, and 140.0 ppm, respectively. In the ^{13}C{^{1}H} NMR spectra, the Cp ring gives rise to a singlet in the range of about 80−82 ppm. The CO ligands exhibit a low-field doublet at 220.9, 221.0, and 221.0 ppm with coupling constants J_{PC} of 24.4−26.4 Hz, while the resonance of the carboxamido carbon atoms give rise to a doublet centered at 200.4 (J_{PC} = 39.0 Hz), 201.1 (J_{PC} = 45.8 Hz), and 199.8 ppm (J_{PC} = 37.8 Hz), respectively. In the IR spectrum, the characteristic CO stretching frequency of the CO ligand and the carboxamido unit was observed at 1937, 1919, and 1914 cm^{-1} and 1617, 1605, and 1618 cm^{-1}, respectively. For comparison, the IR stretching frequency of the carboxamido unit in [FeCp(CO)(κ^2(*C*,*P*)-(C=O)-NNMe$_2$-PPh$_2$)] was found at 1642 cm^{-1} [11].

Complex **1a** adopts a typical three legged piano stool conformation with the C and P atoms of the C(=O)N*i*Pr-PPh$_2$ moiety and the C atom of the CO ligand as the legs (Fig. 1). The Fe1−C(Cp) distance on average is 2.101(1) Å. The iron carbon bond distances Fe1−C6 and Fe1−C7 are 1.739(1) and 1.981(1) Å, respectively, the latter being typical for an iron carbon single bond. Thus, also in agreement with the NMR and IR spectroscopic data, **1a** is best described as a carboxamido complex (**A**) rather than an aminocarbene complex (**B**) (Scheme 7). The Fe1-P1 bond distance of 2.1773(3) Å is typical for iron phosphine complexes but slightly shorter than Fe1−P1 = 2.2223(4) Å in the parent complex **2** (Fig. 2). The C7−Fe1−P1 bite angle of the chelating C(=O)N*i*Pr-PPh$_2$ ligand is 69.43(4)°. For comparison, in the related complex [FeCp(-CO)(κ^2(*C*,*P*)-(C=O)-NNMe$_2$-PPh$_2$)] the bite angle is 70.5(1)°.

Since acyl and carbamoyl ligands are typically nucleophilic at the carbonyl oxygen, *i.e.*, resonance structure **B** may play a role, the reaction with carbon-based electrophiles may lead to amino-carbene complexes. It has to be kept in mind however that an electrophilic attack may occur also at the N atom of the carboxamido moiety resulting in P−N bond cleavage with concomitant N-alkylation.

Treatment of **1a** with $[Me_3O]BF_4$ (1 equiv) at room temperature for 4 h in CH_2Cl_2 as the solvent results in the formation of the aza-phospha-carbene complex [FeCp(CO)(κ^2(*C*,*P*) = C(OMe)-N*i*Pr-PPh$_2$)]$^+$ (**3**) in 58% isolated yield (Scheme 8). This class of complexes belongs to a rare series of transition metal complexes in which the carbene moiety is part of a four-membered chelate ligand coordinated in a κ^2 [2](*C*,*P*) mode [6,7,12]. Complex **3** was characterized by elemental analysis and by ^{1}H, ^{13}C{^{1}H}, and ^{31}P{^{1}H} NMR spectroscopy. Characteristic features comprise, in the ^{13}C{^{1}H} NMR spectrum, a marked low-field doublet resonance at 238.0 ppm (d, J_{CP} = 34.8 Hz) assignable to the carbene carbon atom of the four-membered aza-phospha-carbene moiety. The carbonyl resonance gives rise to a doublet centered at 216.3 ppm (d, J_{CP} = 22.2 Hz). The ^{31}P{^{1}H} NMR spectrum of **3** reveals a singlet at 115.0 ppm (*cf.* 111.6 ppm in **1a**).

On the other hand, protonation of **1a** with the Brønsted acid $[HNEt_3]^+$ led to clean formation of complex **2a** in 95% isolated yield (Scheme 8). Selective N-protonation took place which was associated with C−N bond cleavage and reformation of the CO and $Ph_2PNHiPr$ ligands.

In search of related iron systems where carboxamido-phosphacycles may also be formed via nucleophilic attack of a κ^1(*P*)-coordinated PR_2NHR' ligand, we prepared complexes of the type *cis*,-*trans*,*cis*-[Fe(CO)$_2$(Ph$_2$PNH*i*Pr)$_2$(Br)$_2$] (**4a**) and *cis*,*trans*,*cis*-[Fe(CO)$_2$(Ph$_2$PNH*t*Bu)$_2$(Br)$_2$] (**4b**). These compounds were readily obtained as red, air stable solids by reacting *cis*-[Fe(CO)$_4$(Br)$_2$] with 2 equivs of the respective PR_2NHR' ligands in 85 and 88% yield (Scheme 9) in CH_2Cl_2 at room temperature. In these complexes the CO and bromide ligands are in a mutual *cis* position, whereas the phosphine ligands are *trans* to one another.

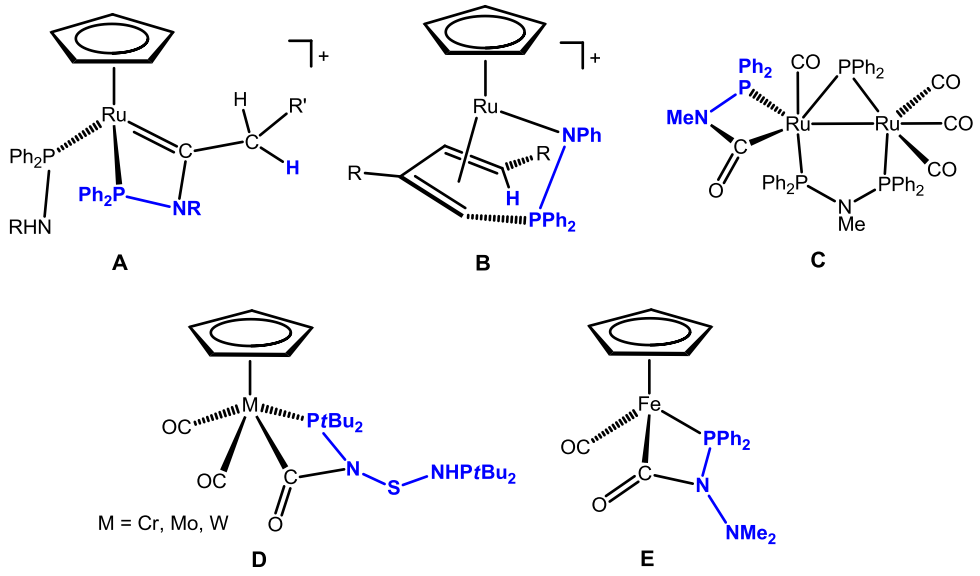

Scheme 3. Aminophosphine ligands displaying various transformations to give unusual transition metal complexes.

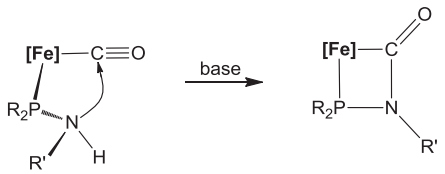

Scheme 4. Intramolecular addition of the NHR' moiety of a aminophosphine ligand to coordinated CO.

Treatment of **4a** with 2 equivs of KO*t*Bu in the presence of CO in THF at room temperature afforded the isomeric complexes *trans*-[$Fe(CO)_2(\kappa^2(C,P)$-(C=O)–N*i*Pr-$PPh_2)(Ph_2PNHiPr)Br$] (**5a**) and *cis*-[$Fe(CO)_2(\kappa^2(C,P)$-(C=O)–N*i*Pr-$PPh_2)(Ph_2PNHiPr)Br$] (**5a'**) in a roughly 5:1 ratio in 50% overall yield. In agreement with experimental data DFT/B3LYP calculations confirm that the isomer with a *trans* CO arrangement is slightly more stable by 2.5 kcal/mol (free energy) than the corresponding *cis* isomer. In the case of **4b** only one isomer, *viz trans*-[$Fe(CO)_2(\kappa^2(C,P)$-(C=O)-N*t*Bu-$PPh_2)(Ph_2PNHtBu)Br$] (**5b**), was formed in 40% yield (Scheme 9). These reactions again involve attack of the amido moiety of a deprotonated PR_2NHR' ligand on coordinated CO. It has to be mentioned that the yields of **5a** and **5b** were independent of whether 1 or 2 equivs of KO*t*Bu were used, i.e., complexes such as [$Fe(CO)_2(\kappa^2(C,P)$-(C=O)–N*i*Pr-$PPh_2)_2$], were not observed. Complexes **5a** and **5b** are thermally robust red solids that are air stable in the solid state but slowly decompose in solution. Their identity was unequivocally established by ^1H, $^{13}C\{^1H\}$ and $^{31}P\{^1H\}$ NMR, IR spectroscopy, and elemental analysis.

In the $^{13}C\{^1H\}$ NMR spectrum of the major isomer **5a** the most noticeable resonances are a low-field signal of the two *trans* CO ligands observed as triplet centered at 212.4 ppm with a P–C coupling constants of 22.7 Hz. The resonance of the carboxamido moiety give rise to a doublet of doublets centered at 206.0 ppm with P–C couplings constant of 9.6 and 13.4 Hz. The $^{31}P\{^1H\}$ NMR spectrum of **5a** reveals two doublets centered at 95.6 and 85.8 ppm with a large coupling constant of 84.7 Hz which is indicative for the phosphorus atoms being in a mutual *trans* position. Most ^1H and $^{13}C\{^1H\}$ NMR of resonances of the minor isomer **5a'** could not be reliably assigned since they were superimposed by the signals of the major isomer **5a**. In the $^{31}P\{^1H\}$ NMR spectrum, however, **5a'** also exhibits two doublets centered at 94.8 (d, J_{PP} = 115.9 Hz) and 90.0 ppm (d, J_{PP} = 115.9 Hz). The large coupling constant again is consistent with a *trans*-P,P configuration. Similar NMR spectra were observed for **5b**, and are thus not discussed here. In the IR spectrum of **5a** and **5b** the two CO ligands give rise to two bands at 1966 and 1960 cm^{-1} (**5a**) and 1955 and 1950 cm^{-1} (**5b**) which can be assigned to the asymmetric CO stretching frequency (*cf* 2143 cm^{-1} in free CO). As expected the symmetric CO stretching frequency is IR

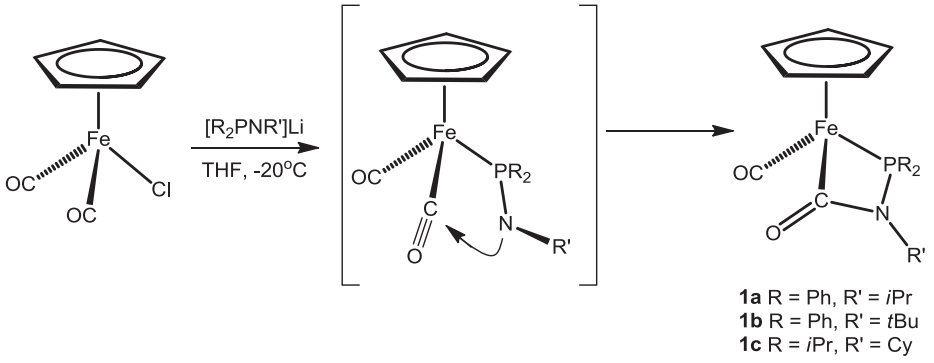

Scheme 5. Synthesis of complexes **1a**–**c**.

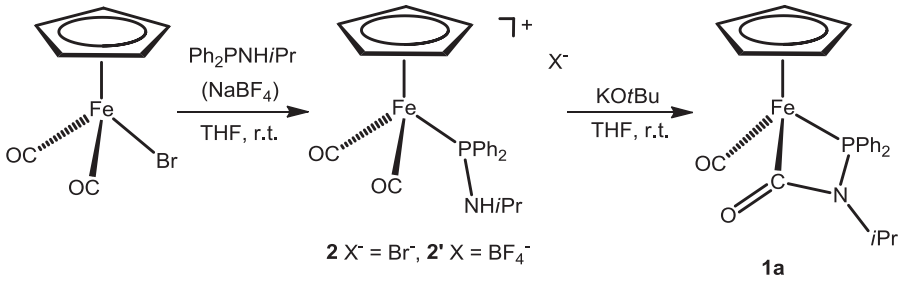

Scheme 6. Synthesis of complex **1a** via intermediate **2**.

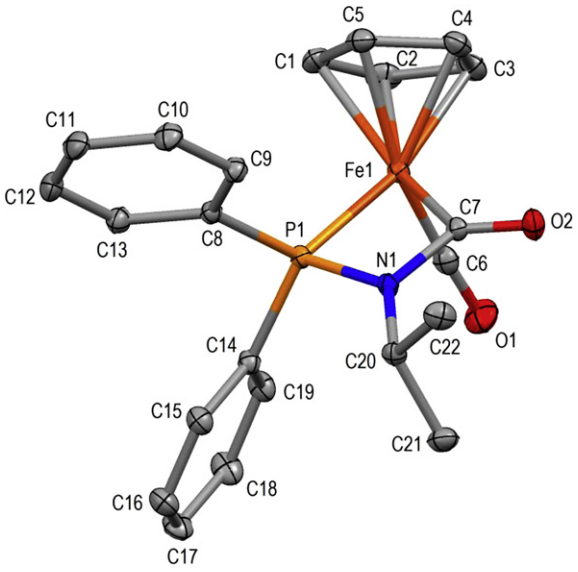

Fig. 1. Molecular structure of [FeCp(CO)(κ^2(*C*,*P*)-(C=O)-N*i*Pr-PPh$_2$)] (**1a**) showing 50% displacement ellipsoids. Selected distances and angles (Å, °): <Fe1–C$_{Cp}$> = 2.101(1), Fe1–P1 2.1773(3), Fe1–C6 1.739(1), Fe1–C7 1.981(1), C6–O1 1.158(2), C7–O2 1.219(2), N1–C7 1.404(2), P1–N1 1.6915(10), C7–Fe1–P1 69.43(4), Fe1–C7–O2 133.8(1), Fe1–C7–N7 103.7(1), Fe1–P1–N1 86.95(3), P1–N1–C7 99.7(1).

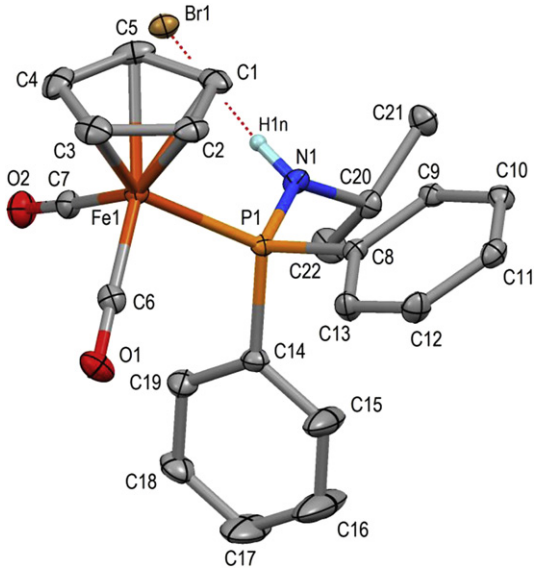

Fig. 2. Molecular structure of **2** showing 50% displacement ellipsoids. Selected distances and angles (Å, °): <Fe1–C$_{Cp}$> = 2.104(2), Fe1–P1 2.2223(4), Fe1–C6 1.780(2), Fe1–C7 1.785(2), C6–O1 1.141(2), C7–O2 1.139(2), P1–N1 1.6473(13), N1–C20 1.477(2), P1–Fe1–C6 90.73(5), P1–Fe1–C7 93.83(5), C6–Fe1–C7 96.28(7), C20–N1–P1 125.14(10), N1 Br1 3.3854(13).

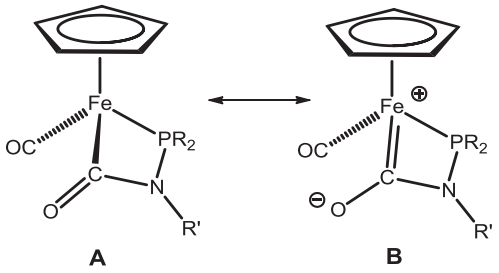

Scheme 7. Resonance structures of complexes **1a**–**c**.

inactive which is also confirmed by DFT/B3LYP calculations. The appearance of two the resonances, which are only 5–6 cm^{-1} apart, may be due to intermolecular interactions, e.g. C=O···HN bonds, in the solid state [13]. The CO vibration of the carboxamido phospha cycle is shifted to lower wavenumbers observed at 1619 and 1616 and cm^{-1}, respectively. The scaled calculated frequencies ν_{CO} together with the experimentally observed values are given in Table 1 and show a reasonably good agreement.

The molecular structure of complex **5a** was determined by X-ray crystallography. A structural view is depicted in Fig. 3 with selected bond distances and angles reported in the caption. The geometry about the metal center is distorted octahedral with the two phosphorus and carbon atoms in *trans* position and the bromide and carbon atom of carboxamido moiety atoms in *cis* position (Fig. 3). The C32–Fe1–C33 bond angle is 170.6(2)°. The chelate system Fe1–P1–N1–(C31=O1)–Fe1 resembles closely in bond lengths and bond angles the corresponding system in complex **1a**, except for the bond Fe1-P1, which is 2.1773(3) Å in **1a** while it is 2.2480(9) Å in **5a** due to the *trans*-influence of phosphorus P2 (Fe1–P2 = 2.2651(9) Å). The short intramolecular hydrogen bond N2–H2n···O1 in **5a** (N2···O1 = 2.839(4) Å) has no effect on the bond angle Fe1-C31–O1 = 134.2(2)° as evident from the corresponding angle 133.8(1)° in complex **1a** which lacks this interaction.

3. Conclusion

In the present study iron(II) complexes featuring one or two aminophosphine ligands of the type PR$_2$NHR' with R = Ph, *i*Pr and R = *i*Pr, *t*Bu, Cy were synthesized. We demonstrated that upon treatment of [FeCp(CO)$_2$X] (*X* = Cl, Br) with the anionic amidophosphine ligands [R$_2$PNR']–, or upon deprotonation of the PR$_2$NHR' ligand in complexes [FeCp(CO)$_2$(PR$_2$NHR'$_2$)]$^+$ and *cis*,*trans*,*cis*-[Fe(CO)$_2$(Ph$_2$PNHR')$_2$(Br)$_2$] complexes featuring four-membered carboxamido-phospha-ferracycles were obtained. In the course of these reactions the highly nucleophilic amido nitrogen atom reacted readily in an intramolecular fashion with the electrophilic carbon atom of a CO ligand. We have further demonstrated that the carboxamido-phospha-ferracycles react with the carbon-based electrophile [Me$_3$O]$^+$ to afford an aza-phospha-carbene. This is a

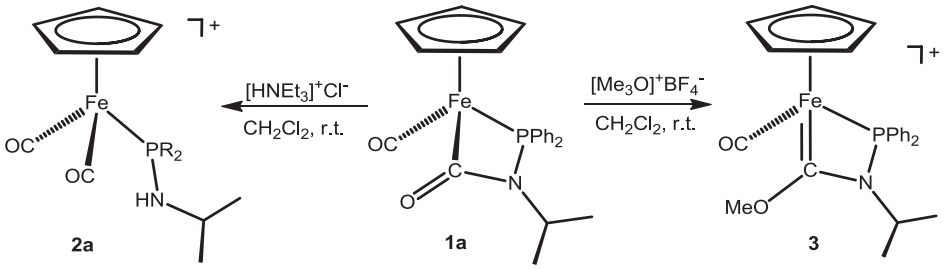

Scheme 8. Reactivity of complex **1a** toward the electrophile $[Me_3O]BF_4$ and the base NEt_3.

relatively rare type of transition metal complexes in which the carbene moiety is part of a four-membered chelate ligand coordinated in a $\kappa^2(C,P)$ mode. In the presence of protons, the carboxamidophospha-ferracycle underwent clean C–N bond cleavage thereby reforming the starting complex $[FeCp(CO)_2(PR_2NHR'_2)]^+$.

4. Experimental

4.1. General

All manipulations were performed under an inert atmosphere of argon by using Schlenk techniques. The solvents were purified according to standard procedures [14]. The ligands PPh_2NHiPr, PPh_2NHtBu, and PPh_2NHCy [15] and the complexes $[FeCp(CO)_2Cl]$, of $[FeCp(CO)_2Br]$ [16], and *cis*-$[Fe(CO)_4Br_2]$ [17] were prepared according to the literature. The deuterated solvents were purchased from Aldrich and dried over 4 Å molecular sieves [1]. H, $^{13}C\{^1H\}$, and $^{31}P\{^1H\}$ NMR spectra were recorded on Bruker AVANCE-250 and AVANCE-300 DPX spectrometers and were referenced to $SiMe_4$ and H_3PO_4 (85%), respectively.

4.2. Syntheses

4.2.1. *[FeCp(CO)(κ^2(C,P)-(C=O)–NiPr-PPh$_2$)]* (**1a**)

A solution of PPh_2NHiPr (300 mg, 1.23 mmol) in THF (20 mL) was cooled to −20 °C and *n*BuLi (500 μL, 1.23 mmol, 2.5 M solution in *n*-hexane) was slowly added. The solution was stirred for 2 h at −20 °C and an additional hour at room temperature. After that, $[FeCp(CO)_2Cl]$ (262 mg, 1.23 mmol) was added and the mixture was stirred for 8 h at room temperature. The solvent was then removed under reduced pressure. The residue was redissolved in toluene (10 mL) and the solution was filtered through Celite. After removal of the solvent under reduced pressure, an orange solid was obtained which was washed with *n*-pentane (10 mL) and dried under vacuum. Yield: 207 mg (40%). Anal. calcd. for $C_{22}H_{22}FeNO_2P$: C, 63.03; H, 5.29; N, 3.34. Found: C, 63.09; H, 5.12; N, 3.28. ^1H NMR (δ, $CDCl_3$, 20 °C): 7.87 (m, 4H, Ph), 7.51 (m, 6H, Ph), 4.38 (s, 5H, Cp), 3.49 (m, 1H, C*H*$(CH_3)_2$), 1.29 (d, J = 5.8 Hz, 3H, CH(C*H*$_3)_2$), 0.99 (d, J = 6.7 Hz, 3H, CH(C*H*$_3)_2$). $^{13}C\{^1H\}$ NMR (δ, $CDCl_3$, 20 °C): 220.9 (d, J_{PC} = 26.0 Hz, *C*O), 200.4 (d, J_{PC} = 39.0 Hz, NC*O*), 137.2 (d, J_{PC} = 40.6 Hz, Ph), 133.8 (d, J_{PC} = 13.5 Hz, Ph), 131.8 (d, J_{PC} = 2.7 Hz, Ph), 130.7 (d, J_{PC} = 13.5 Hz, Ph), 130.4 (d, J_{PC} = 2.7 Hz, Ph), 128.6 (d, J_{PC} = 9.5 Hz, Ph), 128.4 (d, J_{PC} = 7.5 Hz, Ph), 82.1 (s, Cp), 50.7 (d, J_{PC} = 8.1 Hz, *C*H$(CH_3)_2$), 23.0 (s, CH(*C*H$_3)_2$), 21.4 (s, CH(*C*H$_3)_2$). $^{31}P\{^1H\}$ NMR (δ, $CDCl_3$, 20 °C): 111.6. IR (ATR, 25 °C): 1937 ($\nu_{C=O}$), 1617 ($\nu_{C=O}$).

4.2.2. *[FeCp(CO)(κ^2(C,P)-(C=O)-NtBu-PPh$_2$)]* (**1b**)

This complex was prepared analogously to **1a** with $[FeCp(CO)_2Cl]$ (400 mg, 1.55 mmol) and $Ph_2PNHtBu$ (400 mg, 1.55 mmol), and *n*BuLi (630 μL, 1.48 mmol, 2.5 M solution in *n*-hexane) as starting materials. Yield: 335 mg (50%). Anal. calcd for $C_{23}H_{24}FeNO_2P$: C, 63.76; H, 5.58; N, 3.23. Found: C, 63.66; H, 5.63; N, 3.19. ^1H NMR (δ, $CDCl_3$, 20 °C): 7.90 (m, 4H, Ph), 7.48 (m, 6H, Ph), 4.39 (s, 5H, Cp), 1.20 (s, 9H, C(C*H*$_3)_3$). $^{13}C\{^1H\}$ NMR (δ, $CDCl_3$, 20 °C): 221.0 (d, J_{PC} = 24.4 Hz, *C*O), 201.1 (d, J_{PC} = 45.8 Hz, NC*O*), 136.4 (d, J_{PC} = 39.3 Hz, Ph), 133.8 (d, J_{PC} = 41.3 Hz, Ph), 132.7 (d, J_{PC} = 12.5 Hz, Ph), 131.2 (d, J_{PC} = 3.2 Hz, Ph), 130.7 (d, J_{PC} = 11.7 Hz, Ph), 130.3 (d, J_{PC} = 3.2 Hz, Ph), 128.6 (d, J_{PC} = 7.4 Hz, Ph), 128.4 (d, J_{PC} = 5.8 Hz, Ph), 82.8 (s, Cp), 65.8 (s, *C*H$(CH_3)_2$), 29.5 (s, CH(*C*H$_3)_2$). $^{31}P\{^1H\}$ NMR (δ, $CDCl_3$, 20 °C): 113.0. IR (ATR, 25 °C): 1919 ($\nu_{C=O}$), 1605 ($\nu_{C=O}$).

4.2.3. *[FeCp(CO)(κ^2(C,P)-(C=O)-NCy-PiPR$_2$)]* (**1c**)

This complex was prepared analogously to **1a** with $[FeCp(CO)_2Cl]$ (370 mg, 1.75 mmol), Ph_2PNHCy (376 mg, 1.75 mmol), and *n*BuLi (700 μL, 1.75 mmol, 2.5 M solution in *n*-hexane) as starting materials. Yield: 307 mg (45%). Anal. calcd for $C_{19}H_{30}FeNO_2P$: C, 58.48; H, 7.49; N, 3.59. Found: C, 58.53; H, 7.40; N, 3.62. ^1H NMR (δ, $CDCl_3$, 20 °C): 4.61 (s, 5H, Cp), 2,93 (m, 1H, NC*H*), 2.54 (m, 1H, C*H*$(CH_3)_2$), 2.18 (m, 1H, C*H*$(CH_3)_2$), 1,69 (bs, 4H, Cy), 1,53 (bs, 6H, Cy), 1.32 (d, J = 11.0 Hz, 3H, CH(C*H*$_3)_2$), 1.30 (s, 1H, Cy), 1.25 (d, J = 7.3 Hz, 3H, CH(C*H*$_3)_2$). $^{13}C\{^1H\}$ NMR (δ, $CDCl_3$, 20 °C): 221.0 (d, J_{PC} = 26.4 Hz, *C*O), 199.8 (d, J_{PC} = 37.8 Hz, NC*O*), 80.8 (s, Cp), 58.5 (d, J_{PC} = 8.1 Hz, NC), 32.7 (d, J_{PC} = 71.9 Hz, C*H*$(CH_3)_2$), 30.6 (d, J_{PC} = 19.3 Hz, Cy), 27.9 (d, J_{PC} = 15.9 Hz, Cy), 26.8 (s, Cy), 25.3 (s, Cy), 20.4 (d, J_{PC} = 5.7 Hz, CH(*C*H$_3)_2$), 18.7 (s, Cy), 18.0 (d, J_{PC} = 5.74 Hz, CH(*C*H$_3)_2$). $^{31}P\{^1H\}$

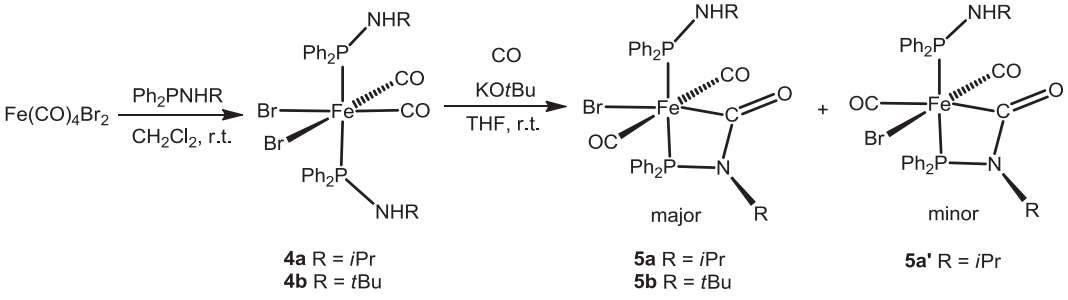

Scheme 9. Synthesis of complexes **5a** and **5b** via intermediates **4a** and **4b**.

Table 1
Comparison of the DFT/B3LYP calculated and experimental ν_{CO} absorptions of **5a**.

	$\nu_{CO\ sym}/cm^{-1}$	$\nu_{CO\ asym}/cm^{-1}$	$\nu_{NC=O}/cm^{-1}$
Calcd.	2022	1980	1615
Exptl.	Not observed	1966/1960	1616

NMR (δ, $CDCl_3$, 20 °C): 140.0. IR (ATR, 25 °C): 1914 ($\nu_{C=O}$), 1618 ($\nu_{C=O}$).

*4.2.4. [FeCp(CO)$_2$(Ph$_2$PNHiPr)]Br (**2**)*

To a solution of [FeCp(CO)$_2$Br] (1.00 g, 3.89 mmol) in THF (10 mL) Ph$_2$PNH*i*Pr (995 mg, 4.01 mmol) was added and the reaction mixture was stirred overnight at room temperature. Removal of the solvent afforded **2** as a yellow solid. Yield: 1.75 g (90%). Anal. calcd for $C_{22}H_{23}BrFeNO_2P$: C, 52.94; H, 4.44; N, 2.81. Found: C, 53.04; H, 4.39; N, 2.85. ^{1}H NMR (δ, $CDCl_3$, 20 °C): 7.61-7.53 (m, 10H, Ph), 5.96 (d, J = 10.2 Hz, 1H, N*H*), 5.27 (s, 5H, Cp), 2.99 (bs, 1H, CH(C*H*$_3$)$_2$), 1.16 (d, J = 5.4 Hz, 6H, CH(C*H*$_3$)$_2$).). ^{13}C{^{1}H} NMR (δ, $CDCl_3$, 20 °C): 210.3 (d, J_{PC} = 27.1 Hz, *C*O), 135.0 (d, J_{PC} = 59.1 Hz, Ph), 131.7 (d, J_{PC} = 10.4 Hz, Ph), 131.3 (d, J_{PC} = 10.7 Hz, Ph), 129.0 (d, J_{PC} = 10. 9 Hz, Ph), 88.7 (s, Cp), 48.8 (d, J_{PC} = 9.6 Hz, *C*H(CH$_3$)$_2$), 24.8 (d, J_{PC} = 3.52 Hz, CH(*C*H$_3$)$_2$). ^{31}P{^{1}H} NMR (δ, $CDCl_3$, 20 °C): 100.6. IR (ATR, 25 °C): 2040 ($\nu_{C=O}$), 1993 ($\nu_{C=O}$).

*4.2.5. [FeCp(CO)$_2$(Ph$_2$PNHiPr)]BF$_4$ (**2'**)*

This complex was prepared analogously to **2** with [FeCp(CO)$_2$Br] (350 mg, 1.65 mmol) and Ph$_2$PNH*i*Pr (400 mg, 1.65 mmol) as starting materials but in the presence of $NaBF_4$ (182 mg, 1.65 mmol). Yield: 600 mg (72%). Anal. calcd for $C_{22}H_{23}BF_4FeNO_2P$: C, 52.11; H, 4.17; N, 2.76. Found: C, 52.14; H, 4.08; N, 2.80. NMR and IR spectra were identical to those of **2**.

*4.2.6. Reaction of [FeCp(CO)$_2$(Ph$_2$PNHiPr)]BF$_4$ with KOtBu. Formation of [FeCp(CO)(κ^2(C,P)-(C=O)–NiPr-PPh$_2$)] (**1a**)*

A solution of [FeCp(CO)$_2$(Ph$_2$PNH*i*Pr)]BF$_4$ (**2a'**) (220 mg, 0.44 mmol) in THF (10 mL) was treated with KO*t*Bu (55 mg, 0.48 mmol) and was stirred for 8 h. The solvent was removed under vacuum and the crude product was redissolved in toluene and filtered through Celite. After removal of the solvent under reduced pressure, **1a** was obtained which was washed with *n*-pentane (10 mL) and dried under vacuum. Yield: 87 mg (48%).

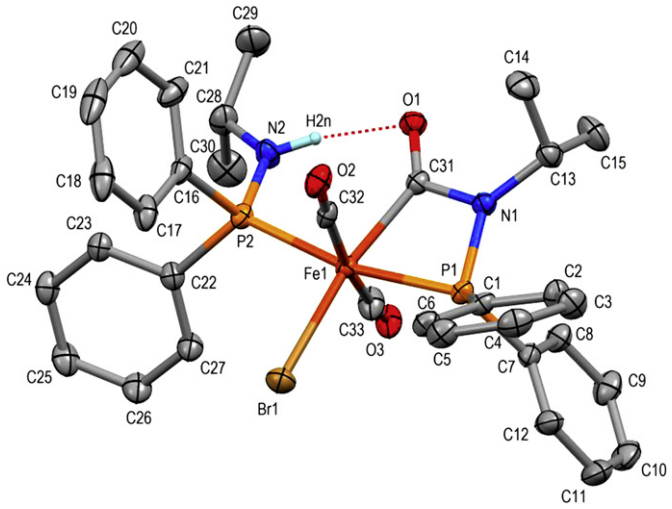

Fig. 3. Molecular structure of *trans*-[Fe(CO)$_2$(κ^2(C,P)-(C=O)-NiPr-PPh$_2$)(Ph$_2$PNHiPr)Br] (**5a**) (major isomer) showing 40% displacement ellipsoids. Selected distances and angles (Å, °): Fe1–Br1 2.4752(6), Fe1–P1 2.2480(9), Fe1–P2 2.2651(9), Fe1–C33 1.799(3), Fe1–C32 1.826(3), Fe1–C31 1.997(3), P2–N2 1.650(3), P1–N1 1.694(3), C31–O1 1.221(4), C31–N1 1.409(4), C32–Fe1–C33 170.6(2), P1–Fe1–P2 167.1(1), P1–Fe1–C31 68.9(1), Fe1–P1–N1 85.3(1), Fe1–C31–O1 134.2(2), Fe1–C31–N1 103.6(2), O1–C31–N1 122.2(3), P1–N1–C31 101.5(2), P1–N1–C13 132.4(2), N2 O1 2.839(4).

*4.2.7. [FeCp(CO)(κ^2(C,P)=C(OMe)-NiPr-PPh$_2$)]BF$_4$ (**3**)*

A solution of **1a** (500 mg, 1.19 mmol) in CH_2Cl_2 (10 mL) was treated with [Me$_3$O]BF$_4$ (177 mg, 1.19 mmol). After stirring for 4 h, insoluble materials were removed by filtration through Celite. On removal of the solvent, **5** was obtained as an orange solid which was washed with *n*-hexane, and dried under vacuum. Yield: 360 mg (58%). Anal. calcd for $C_{35}H_{39}BBrF_4FeN_2O_3P$: C, 53.27; H, 4.98; N, 3.55. Found: C, 53.19; H, 4.89; N, 3.64. ^{1}H NMR (δ, $CDCl_3$, 20 °C): 7.58 (m, 10H, Ph), 4.80 (s, 5H, Cp), 4.33 (s, 3H, *OCH*$_3$), 3.93 (m, 1H, *CH*(CH$_3$)$_2$), 1.40 (d, J = 6.4 Hz, 3H, CH(*CH*$_3$)$_2$), 0.92 (d, J = 6.4 Hz, 3H, CH(*CH*$_3$)$_2$). ^{13}C{^{1}H} NMR (δ, $CDCl_3$, 20 °C): 238.0 (d, J_{PC} = 34.8 Hz, Fe=*C*), 216.3 (d, J_{PC} = 22.2 Hz, *C*O), 134.7 (d, J_{PC} = 22.3 Hz, Ph), 134.4 (d, J_{PC} = 14.2 Hz, Ph), 134.2 (d, J_{PC} = 22.2 Hz, Ph), 132.8 (d, J_{PC} = 2.59 Hz, Ph), 131.9 (d, J_{PC} = 2.5 Hz, Ph), 131.3 (d, J_{PC} = 11.1 Hz, Ph), 129.9 (d, J_{PC} = 11.3 Hz, Ph), 83.1 (s, Cp), 64.9 (s, OCH$_3$), 55.8 (d, J_{PC} = 5.5 Hz, *C*H(CH$_3$)$_2$), 21.8 (s, CH(*C*H$_3$)$_2$), 20.8 (s, CH(*C*H$_3$)$_2$). ^{31}P{^{1}H} NMR (δ, $CDCl_3$, 20 °C): 115.0. IR (ATR, 25 °C): 2004 ($\nu_{C=O}$).

*4.2.8. Protonation of **1a** with [HNEt$_3$]Cl. Formation of **2***

A solution of **1a** (500 mg, 1.19 mmol) in CH_2Cl_2 (10 mL) was treated with [HNEt$_3$]Cl (165 mg, 1.19 mmol). After stirring for 4h, insoluble materials were removed by filtration through Celite. On removal of the solvent, **2** was obtained as a yellow solid which was collected on a glass frit, washed with *n*-hexane, and dried under vacuum. Yield: 514 mg (95%).

*4.2.9. cis,trans,cis-[Fe(CO)$_2$(Ph$_2$PNHiPr)$_2$(Br)$_2$] (**4a**)*

To a solution of *cis*-[Fe(CO)$_4$Br$_2$] (1.00 g, 3.05 mmol) in CH_2Cl_2 (10 mL) Ph$_2$PNH*i*Pr (1.52 g, 6.25 mmol) was added at 0 °C and the mixture was stirred overnight at room temperature. The solution was then filtered through Celite. After removal of the solvent under reduced pressure, an orange solid was obtained which was washed with diethyl ether (10 mL) and dried under vacuum. Yield: 1.96 g (85%). Anal. calcd for $C_{32}H_{36}Br_2FeN_2O_2P_2$: C, 50.69; H, 4.79; N, 3.69. Found: C, 50.72; H, 4.86; N, 3.60. ^{1}H NMR (δ, $CDCl_3$, 20 °C): 7.99 (bs, 8H, Ph), 7.48 (bs, 12H, Ph), 3.42 (bs, 2H, *NH*), 2.29 (m, 2H, *CH*(CH$_3$)$_2$), 0.91 (d, J_{PC} = 6.3 Hz, 12H, CH(*CH*$_3$)$_2$). ^{13}C{^{1}H} NMR (δ, $CDCl_3$, 20 °C): 212.7 (t, J_{PC} = 22.7 Hz, *C*O), 133.6 (d, J_{PC} = 25. Hz, Ph), 133.0 (dd, J_{PC} = 5.1 Hz, Ph), 131.7 (dd, J_{PC} = 5.4 Hz, Ph), 130.8 (s, Ph, 127.9 (dd, J_{PC} = 4.6 Hz, Ph), 46.4 (dd, J_{PC} = 4.9 Hz, *C*H(CH$_3$)$_2$), 24.7 (s, CH(*C*H$_3$)$_2$). ^{31}P{^{1}H} NMR (δ, $CDCl_3$, 20 °C): 80.6. IR (ATR, 25 °C): 2041 ($\nu_{C=O}$), 1986 ($\nu_{C=O}$).

*4.2.10. cis,trans,cis-[Fe(CO)$_2$(Ph$_2$PNHtBu)$_2$(Br)$_2$] (**4b**)*

This complex was prepared analogously to **4a** with *cis*-[Fe(CO)$_4$Br$_2$] (845 mg, 2.58 mmol) and Ph$_2$PNH*t*Bu (1.33 g, 5.16 mmol) as starting materials. Yield: 1.7 mg (88%). Anal. calcd for $C_{34}H_{40}Br_2FeN_2O_2P_2$: C, 51.94; H, 5.13; N, 3.56. Found: C, 52.04; H, 5.20; N, 3.46. ^{1}H NMR (δ, acetone-d$_6$, 20 °C): 8.36 (bs, 8H, Ph), 7.48 (bs, 12H, Ph), 3.7 (bs, 2H, *NH*), 0.87 (s, 18H, C(*CH*$_3$)$_3$). ^{13}C{^{1}H} NMR (δ, $CDCl_3$, 20 °C): 213.3 (t, J_{PC} = 24.0 Hz, *C*O), 134.2 (dd, J_{PC} = 25.7 Hz, Ph), 133.5 (dd, J_{PC} = 5.3 Hz, Ph), 130.7 (s, Ph), 127.7 (dd, J_{PC} = 4.7 Hz, Ph), 55.5 (s, *C*(CH$_3$)$_3$), 31.7 (s, C(*CH*$_3$)$_3$). ^{31}P{^{1}H} NMR (δ, acetone-d$_6$, 20 °C): 72.2. IR (ATR, 25 °C): 2035 ($\nu_{C=O}$), 1980 ($\nu_{C=O}$).

*4.2.11. trans-[Fe(CO)$_2$(κ^2(C,P)-(C=O)–NiPr-PPh$_2$)(Ph$_2$PNHiPr)Br] (**5a**) and cis-[Fe(CO)$_2$(κ^2(C,P)-(C=O)–NiPr-PPh$_2$)(Ph$_2$PNHiPr)Br] (**5a'**)*

A Schlenk tube was charged with **4a** (400 mg, 0.53 mmol) and KO*t*Bu (122 mg, 1.06 mmol). Under a CO atmosphere THF (10 mL) was added and the mixture was stirred overnight at room

Table 2
Details for the crystal structure determinations of compounds **1a**, **2**, and **5a**.

	1a	**2**	**5a**
Formula	$C_{22}H_{22}FeNO_2P$	$C_{22}H_{23}BrFeNO_2P$	$C_{33}H_{35}BrFeN_2O_3P_2$
fw	419.23	500.14	705.33
Cryst.size, mm	0.45 × 0.26 x 0.14	0.59 × 0.20 × 0.18	0.25 × 0.20 × 0.18
Color, shape	Red plate	Yellow prism	Red prism
Crystal system	Monoclinic	Monoclinic	Monoclinic
Space group	$P2_1/n$ (no. 14)	$P2_1/c$ (no. 14)	$P2_1/c$ (no. 14)
a, Å	10.0648(3)	13.2697(2)	10.1667(4)
b, Å	14.5893(5)	17.5534(2)	17.7127(7)
c, Å	13.4024(4)	9.2565(2)	18.9313(8)
α, deg	90	90	90
β, deg	92.871(2)	92.768(2)	105.453(2)
γ, deg	90	90	90
V, Å^3	1965.52(11)	2153.59(6)	3285.9(2)
T, K	100(2)	100(2)	100(2)
Z	4	4	4
ρ_{calc}, g cm^{-3}	1.417	1.543	1.426
μ, mm^{-1} (MoKα)	0.865	2.647	1.807
F(000)	872	1016	1448
Absorption corrections	Multi-scan, 0.89–0.76	Multi-scan, 0.65–0.43	Multi-scan, 0.74–0.58
θ range, deg	2.06–30.11	1.93-30.00	2.08-27.50
No. of rflns measd	65996	39753	50035
R_{int}	0.034	0.023	0.076
No. of rflns unique	5771	6253	7526
No. of rflns I > 2σ(I)	4787	5578	5356
No. of params/restraints	246/0	258/0	387/136
R_1 (I > 2σ(I)) [a]	0.0253	0.0269	0.0406
R_1 (all data)	0.0366	0.0320	0.0742
wR_2 (I > 2σ(I))	0.0593	0.0682	0.0891
wR_2 (all data)	0.0642	0.0713	0.1081
Diff.Four.peaks min/max, eÅ^{-3}	−0.32/0.40	−0.45/0.82	−0.60/0.77

[a] $R1 = \Sigma||F_o|-|F_c||/\Sigma|F_o|$, $wR2 = \{\Sigma[w(F_o^2 - F_c^2)^2]/\Sigma[w(F_o^2)^2]\}^{1/2}$, GooF = $\{\Sigma[w(F_o^2 - F_c^2)^2]/(n-p)\}^{1/2}$

temperature. The red solution was then filtered through Celite and the solvent was removed under reduced pressure. The residue was redissolved in CH_2Cl_2. Insoluble materials were removed by filtration. After evaporation of the solvent *in vacuo*, a red solid was obtained which was washed with *n*-pentane (10 mL) and dried under vacuum. Yield: 185 mg (50%). Anal. calcd for $C_{33}H_{35}BrFeN_2O_3P_2$: C, 56.19; H, 5.00; N, 3.97. Found: C, 56.00; H, 5.12, N, 4.01. Major isomer: ^{1}H NMR (δ, $CDCl_3$, 20 °C): 7.85 (d, *J* = 6.79 Hz, 8H, Ph), 7.50 (d, *J* = 8.38 Hz, 8H, Ph), 7.43 (s, 4H, Ph), 4.70 (bs, 1H, *NH)*, 3.46 (m, 1H, C*H*(CH_3)$_2$), 3.12 (m, 1H, C*H*(CH_3)$_2$), 1.31 (d, *J* = 6.4 Hz, 6H, CH(C*H*$_3$)$_2$), 0.94 (d, *J* = 6.4 Hz, 6H, CH(C*H*$_3$)$_2$). ^{13}C{^{1}H} NMR (δ, $CDCl_3$, 20 °C): 212.4 (t, J_{PC} = 22.7 Hz, *C*O), 206.0 (dd, J_{PC} = 9.6 Hz, J_{PC} = 13.4 Hz, N*C*O), 135.1 (d, J_{PC} = 37.5 Hz, Ph), 133.3 (d, J_{PC} = 12.1 Hz, Ph), 133.1 (d, J_{PC} = 13.5 Hz, Ph), 131.8 (s, Ph), 130.2 (s, Ph), 128.7 (d, J_{PC} = 11.1 Hz, Ph), 128.0 (d, J_{PC} = 11.1 Hz, Ph), 45.7 (t, J_{PC} = 12.7 Hz, Ph), 25.5 (s, *C*H(CH_3)$_2$), 22.0 (s, CH(*C*H$_3$)$_2$). ^{31}P{^{1}H} NMR (δ, $CDCl_3$, 20 °C): 95.6 (d, J_{PP} = 84.7 Hz), 85.8 (d, J_{PP} = 84.7 Hz). IR (ATR, 25 °C): 1966 ($\nu_{C=O}$), 1960 ($\nu_{C=O}$), 1616 ($\nu_{C=O}$). Minor isomer *cis*-[Fe(CO)$_2$(κ^2(*C*,*P*)-(C=O)–N*i*Pr-PPh$_2$)(Ph$_2$PNH*i*Pr)Br] (**5a'**): Most ^{1}H and ^{13}C NMR resonances are superimposed by the signals of the major isomer and could not reliably assigned. ^{31}P{^{1}H} NMR (δ, $CDCl_3$, 20 °C): 94.8 (d, J_{PP} = 115.9 Hz), 90.0 (d, J_{PP} = 115.9 Hz).

4.2.12. *trans*-[Fe(CO)$_2$(κ^2(C,P)-(C=O)-NtBu-PPh$_2$)(Ph$_2$PNHtBu)Br] (**5b**)

This complex was prepared analogously to **5a** with **4b** (0.70 g, 0.89 mmol) as starting material. Yield: 260 mg (40%). Anal. calcd for $C_{35}H_{39}BrFeN_2O_3P_2$: C, 57.32; H, 5.36; N, 3.82. Found: C, 57.40; H, 5.29; N, 3.79. ^{1}H NMR (δ, $CDCl_3$, 20 °C): 7.98 (bs, 8H, Ph), 7.42 (bs, 12H, Ph), 4.84 (bs, 1H, *NH)*, 3.46 (m, 1H, C*H*(CH_3)$_2$), 1.28 (s, 9H, C(C*H*$_3$)$_3$), 1.05 (s, 9H, C(C*H*$_3$)$_3$). ^{13}C{^{1}H} NMR (δ, $CDCl_3$, 20 °C): 213.3 (dd, J_{PC} = 23.4 Hz, J_{PC} = 22.9 Hz *C*O), 206.0 (dd, J_{PC} = 9.6 Hz, J_{PC} = 13.4 Hz, N*C*O), 136.2 (d, J_{PC} = 47.7 Hz, Ph), 136.1 (d, J_{PC} = 47.7 Hz, Ph), 134.5 (d, J_{PC} = 10.8 Hz, Ph), 132.8 (d, J_{PC} = 10.8 Hz, Ph), 132.6 (d, J_{PC} = 11.6 Hz, Ph), 131.4 (d, J_{PC} = 2.3 Hz, Ph), 129.9 (d, J_{PC} = 2.3 Hz, Ph), 128.5 (d, J_{PC} = 10.6 Hz, Ph), 127.6 (d, J_{PC} = 10.0 Hz, Ph), 62.3 (d, J_{PC} = 7.6 Hz, *C*(CH_3)$_3$), 55.9 (d, J_{PC} = 13.9 Hz, *C*(CH_3)$_3$), 32.1 (d, J_{PC} = 3.1 Hz, C(*C*H$_3$)$_3$), 29.5 (d, J_{PC} = 1.5 Hz, C(*C*H$_3$)$_3$). ^{31}P{^{1}H} NMR (δ, $CDCl_3$, 20 °C): 90.4 (d, J_{PP} = 79.3 Hz), 87.3 (d, J_{PP} = 79.3 Hz. IR (ATR, 25 °C): 1955 ($\nu_{C=O}$), 1950 ($\nu_{C=O}$),1619 ($\nu_{C=O}$).

4.3. X-ray structure determinations

Single crystals for X-ray diffraction were obtained as follows: [FeCp(CO)(κ^2(*C*,*P*)-(C=O)–N*i*Pr-PPh$_2$)] (**1a**), by vapor diffusion of *n*-pentane into a THF solution, [FeCp(CO)$_2$(Ph$_2$PNH*i*Pr)]Br (**2**) by vapor diffusion of Et_2O into a CH_2Cl_2 solution; *trans/cis*-[Fe(CO)$_2$(κ^2(*C*,*P*)-(C=O)–N*i*Pr-PPh$_2$)(Ph$_2$PNH*i*Pr)Br] (**5a**/**5a'**) by vapor diffusion of Et_2O into a CH_2Cl_2 solution. The color of the crystals varied from orange to red brown. X-ray diffraction data were collected at *T* = 100 K on a Bruker Kappa APEX-2 CCD diffractometer with an Oxford Cryosystems cooler using graphite-monochromatised Mo-Kα radiation (λ = 0.71073 Å) and fine sliced φ- and ω-scans covering complete spheres of the reciprocal space. After data integration with program SAINT corrections for absorption and detector effects were applied with the program SADABS [18] The structures were solved by direct methods (SHELXS97) and refined on *F* [2] with the program SHELXL97 [19] Non-hydrogen atoms were refined anisotropically. Most H atoms were placed in calculated positions and thereafter refined as riding. In (**5a**) Br was partly substituted by CO and vice versa (84% *trans*- and 16% in *cis*-dicarbonyl configuration), and the subordinately occupied sites were refined with distance and displacement parameter restraints. All crystal structures were checked with the program PLATON [20] Molecular graphics was generated with program MERCURY [21] Crystal data and experimental details are given in Table 2.

4.4. Computational details

Calculations were performed using the Gaussian 09 software package [22], and the B3LYP functional [23] without symmetry constraints. The optimized geometries were obtained with the Stuttgart/Dresden ECP (SDD) basis set [24] to describe the electrons of the iron atom. For all other atoms the 6–31g** basis set was employed [25]. Frequency calculations were performed to confirm the nature of the stationary points. A scaling factor of 0.9521 was applied for the CO frequencies [26].

Acknowledgments

Financial support by the Austrian Science Fund (FWF) is gratefully acknowledged (Project No. P24202-N17).

References

[1] (a) J. Gopalakrishnan, Appl. Organomet. Chem. 23 (2009) 291;
(b) J. Ansell, M. Wills, Chem. Soc. Rev. 31 (2002) 259;
(c) Z. Fei, P.J. Dyson, Coord. Chem. Rev. 249 (2005) 2056;
(d) T. Appleby, J.D. Woollins, Coord. Chem. Rev. 235 (2002) 121;
(e) M.S. Balakrishna, V. Sreenivasa Reddy, S.S. Krishnamurthy, J.F. Nixon, J.C.T.R. Burckett, St. Laurent, Coord. Chem. Rev. 129 (1994) 1.
[2] (a) S. Priya, M.S. Balakrishna, J.T. Mague, J. Organomet. Chem. 679 (2003) 116;
(b) S. Priya, M.S. Balakrishna, S.M. Mobin, R. McDonald, J. Organomet. Chem. 688 (2003) 227;
(c) K.G. Gaw, A.M.Z. Slawin, M.B. Smith, Organometallics 18 (1999) 3255;
(d) D. Fenske, B. Maczek, K. Maczek, Z. Anorg. Allg. Chem. 623 (1997) 1113;
(e) O. Kühl, P.C. Junk, E. Hey-Hawkins, Z. Anorg. Allg. Chem. 626 (2000) 1591;
(f) O. Kühl, S. Blaurock, J. Sieler, E. Hey-Hawkins, Polyhedron 20 (2001) 111;
(g) O. Kühl, T. Koch, F.B. Somoza Jr., P.C. Junk, E. Hey-Hawkins, D. Plat, M.S. Eisen, J. Organomet. Chem. 604 (2000) 116;
(h) G. Suss-Fink, M.A. Pellingeelli, A. Tiripicchhio, J. Organomet. Chem. 320 (1987) 101;
(i) E.W. Ainscough, A.M. Brodie, S.T. Wong, J. Chem. Soc. Dalton Trans. (1977) 915.
[3] For recent examples see: (a) S. Kuppuswawamy, M.W. Bezpalko, T.M. Powers, M.M. Turnbull, B.M. Foxman, C.M. Thomas, Inorg. Chem. 51 (2012) 8225;
(b) D.A. Evers, A.H. Bluestein, B.M. Foxman, C.M. Thomas, Dalton Trans. 41 (2012) 8111;
(c) B.G. Cooper, C.M. Fafard, B.M. Foxman, C.M. Thomas, Organometallics 29 (2010) 5179.
[4] (a) H. Nagashima, T. Sue, T. Oda, A. Kanemitsu, T. Matsumoto, Y. Motoyama, Y. Sunada, Organometallics 25 (2006) 1987;
(b) Y. Sunada, T. Sue, T. Matsumoto, H. Nagashima, J. Organomet. Chem. 691 (2006) 3176;
(c) T. Sue, Y. Sunada, H. Nagashima, Eur. J. Inorg. Chem. (2007) 2897;
(d) H. Tsutsumi, Y. Sunada, Y. Shiota, K. Yoshizawa, H. Nagashima, Organometallics 28 (2009) 1988.
[5] For a review of the chemistry of N-phosphinoamides see O. Kühl, Coord. Chem. Rev. 250 (2006) 2867.
[6] S. Pavlik, K. Mereiter, M. Puchberger, K. Kirchner, Organometallics 24 (2005) 3561.
[7] S. Pavlik, K. Mereiter, R. Schmid, K. Kirchner, Organometallics 22 (2003) 1771.
[8] M. Jimenez-Tenorio, M.C. Puerta, P. Valerga, Eur. J. Inorg. Chem. (2005) 2631.
[9] K.A. Bunten, D.H. Farrar, A.J. Poë, A.J. Lough, Organometallics 19 (2000) 3674.
[10] M. Herberhold, W. Ehrenreich, K. Guldner, W. Jellen, U. Thewalt, H.P. Klein, Z. Naturforsch. 38B (1983) 1383.
[11] C.J. Harlan, T.C. Wright, J.L. Atwood, S.G. Bott, Inorg. Chem. 30 (1991) 1955.
[12] For related cyclic aminocarbenes, see (a) J. Ruiz, L. García, B.F. Perandones, M. Vivanco, Angew. Chem. Int. Ed. 50 (2011) 3010;
(b) S. Zhang, Q. Xu, J. Sun, J. Chen, Organometallics 20 (2001) 2387;
(c) J. Yin, J. Chen, W. Xu, Z. Zhang, Y. Tang, Organometallics 7 (1988) 21.
[13] (a) P. Braunstein, J.-P. Taquet, O. Siri, R. Welter, Angew. Chem. Int. Ed. 43 (2004) 5922;
(b) S. Camiolo, S.J. Coles, P.A. Gale, M.B. Hursthouse, T.A. Mayer, M.A. Paver, Chem. Commun. (2000) 275.
[14] D.D. Perrin, W.L.F. Armarego, Purification of Laboratory Chemicals, third ed., Pergamon, New York, 1988.
[15] (a) H.H. Sisler, N.L. Smith, J. Org. Chem. 26 (1961) 611;
(b) N. Poetschke, M. Nieger, M.A. Khan, E. Niecke, M.T. Ashby, Inorg. Chem. 36 (1997) 4087.
[16] T.S. Piper, F.A. Cotton, G.J. Wilkinson, Inorg. Nucl. Chem. 1 (1955) 165.
[17] W. Hieber, A.Z. Wirsching, Anorg. Allg. Chem. 245 (1940) 305.
[18] Bruker Computer Programs: APEX2, SAINT, SADABS, and SHELXTL, Bruker AXS Inc, Madison, WI, 2012.
[19] G.M. Sheldrick, Acta Crystallogr. A64 (2008) 112.
[20] A.L. Spek, J. Appl. Crystallogr. 36 (2003) 7.
[21] C.F. Macrae, P.R. Edgington, P. McCabe, E. Pidcock, G.P. Shields, R. Taylor, M. Towler, J. van de Streek, J. Appl. Crystallogr. 39 (2006) 453.
[22] M.J. Frisch, et al., Gaussian 09, Revision A.02, Gaussian, Inc., Wallingford, CT, 2009.
[23] (a) A.D. Becke, J. Chem. Phys. 98 (1993) 5648;
(b) B. Miehlich, A. Savin, H. Stoll, H. Preuss, Chem. Phys. Lett. 157 (1989) 200;
(c) C. Lee, W. Yang, G. Parr, Phys. Rev. B 37 (1988) 785.
[24] a) U. Haeusermann, M. Dolg, H. Stoll, H. Preuss, Mol. Phys. 78 (1993) 1211;
b) W. Kuechle, M. Dolg, H. Stoll, H. Preuss, J. Chem. Phys. 100 (1994) 7535;
c) T. Leininger, A. Nicklass, H. Stoll, M. Dolg, P. Schwerdtfeger, J. Chem. Phys. 105 (1996) 1052.
[25] (a) A.D. McLean, G.S. Chandler, J. Chem. Phys. 72 (1980) 5639;
(b) R. Krishnan, J.S. Binkley, R. Seeger, J.A. Pople, J. Chem. Phys. 72 (1980) 650;
(c) A.J.H. Wachters, Chem. Phys. 52 (1970) 1033;
(d) P.J. Hay, J. Chem. Phys. 66 (1977) 4377;
(e) K. Raghavachari, G.W. Trucks, J. Chem. Phys. 91 (1989) 2457;
(f) L.A. Curtiss, M.P. McGrath, J.-P. Blaudeau, N.E. Davis, R.C. Binning Jr., L. Radom, J. Chem. Phys. 103 (1995) 6104;
(g) M.P. McGrath, L. Radom, J. Chem. Phys. 94 (1991) 511.
[26] L. Yu, G.N. Srinivas, M. Schwartz, J. Mol. Struct. (Theochem) 625 (2003) 215.

ORGANOMETALLICS

Article

pubs.acs.org/Organometallics

Synthesis and Characterization of Hydrido Carbonyl Molybdenum and Tungsten PNP Pincer Complexes

Özgür Öztopcu,[†] Christian Holzhacker,[†] Michael Puchberger,[‡] Matthias Weil,[§] Kurt Mereiter,[§] Luis F. Veiros,[∥] and Karl Kirchner*[,†]

[†]Institute of Applied Synthetic Chemistry, [‡]Institute of Materials Chemistry, and [§]Institute of Chemical Technologies and Analytics, Vienna University of Technology, Getreidemarkt 9, A-1060 Vienna, Austria

[∥]Centro de Química Estrutural, Instituto Superior Técnico, Universidade Técnica de Lisboa, Av. Rovisco Pais No. 1, 1049-001 Lisboa, Portugal

Supporting Information

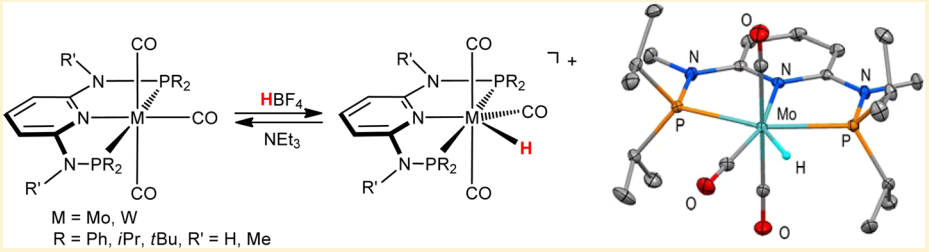

ABSTRACT: In the present study the Mo(0) and W(0) complexes $[M(PNP)(CO)_3]$ as well as seven-coordinate cationic hydridocarbonyl Mo(II) and W(II) complexes of the type $[M(PNP)(CO)_3H]^+$, featuring PNP pincer ligands based on 2,6-diaminopyridine, have been prepared and fully characterized. The synthesis of Mo(0) complexes $[Mo(PNP)(CO)_3]$ was accomplished by treatment of $[Mo(CO)_3(CH_3CN)_3]$ with the respective PNP ligands. The analogous W(0) complexes were prepared by reduction of the bromocarbonyl complexes $[W(PNP)(CO)_3Br]^+$ with NaHg. These intermediates were obtained from the known dinuclear complex $[W(CO)_4(\mu\text{-Br})Br]_2$, prepared in situ from $W(CO)_6$ and stoichiometric amounts of Br_2. Addition of HBF_4 to $[M(PNP)(CO)_3]$ resulted in clean protonation at the molybdenum and tungsten centers to generate the Mo(II) and W(II) hydride complexes $[M(PNP)(CO)_3H]^+$. The protonation is fully reversible, and upon addition of NEt_3 as base the Mo(0) and W(0) complexes $[M(PNP)(CO)_3]$ are regenerated quantitatively. All heptacoordinate complexes exhibit fluxional behavior in solution. The mechanism of the dynamic process of the hydrido carbonyl complexes was investigated by means of DFT calculations, revealing that it occurs in a single step. The structures of representative complexes were determined by X-ray single-crystal analyses.

INTRODUCTION

Tridentate PNP ligands in which the central pyridine-based ring donor contains $-CH_2PR_2$ substituents in the two ortho positions are widely utilized ligands in transition-metal chemistry (e.g., Fe, Ru, Rh, Ir, Pd, Pt).[1−10] As part of our effort to create tridentate PNP pincer-type ligands in which the steric, electronic, and stereochemical properties can be easily varied, we have recently described the synthesis of a series of modularly designed PNP ligands based on N-heterocyclic diamines and R_2PCl which contain both bulky and electron-rich dialkylphosphines as well as various P−O bond containing achiral and chiral phosphine units.[11] In these PNP ligands the central pyridine ring contains $-NR'PR_2$ (R′ = H, alkyl, R = alkyl, aryl) substituents in the two ortho positions. This methodology was first developed for the synthesis of *N*,*N*′-bis(diphenylphosphino)-2,6-diaminopyridine (PNP-Ph).[12]

With these types of PNP ligands, we have thus far studied their reactivity toward different transition-metal fragments, which resulted in the preparation of a range of new pincer transition-metal complexes, including several new square-planar Ni(II), Pd(II), and Pt(II) PNP complexes,[13] various iron complexes acting as CO sensors[14] and catalysts for the coupling of aromatic aldehydes with ethyldiazoacetate,[15] and several pentacoordinated nickel complexes.[16] Surprisingly, as far as group 6 PNP complexes are concerned, only a few examples have been described in the literature. A few years ago Haupt and co-workers reported the synthesis of $[M(PNP\text{-}Ph)(CO)_3]$ (M = Cr, Mo, W),[12] while Walton and co-workers described the synthesis of the dinuclear molybdenum complex $[Mo(PNP)Mo(HPCy_2)Cl_3]$ (PNP = 2,6-bis-(dicyclohexylphosphinomethyl)pyridine).[17] Most recently, dinuclear molybdenum and tungsten dinitrogen complexes bearing bulky PNP pincer ligands were found to work as effective catalysts for the formation of ammonia from dinitrogen.[18] Finally, Templeton and co-workers described the synthesis of a series of hydrido carbonyl and halo carbonyl tungsten pincer complexes featuring the silazane-based PNP

Received: March 25, 2013
Published: May 7, 2013

   dx.doi.org/10.1021/om400254k | *Organometallics* 2013, 32, 3042−3052

pincer-type ligand $HN(SiMe_2CH_2PPh_2)_2$.[19] In a preliminary study we have prepared cationic seven-coordinate halo carbonyl molybdenum pincer complexes of the types $[Mo(PNP\text{-}iPr)(CO)_3I]^+$ and $[Mo(PNP\text{-}iPr)(CO)_2(CH_3CN)I]^+$.[13] Here we report on the synthesis, characterization, and reactivity of a series of new hydrido carbonyl molybdenum(II) and tungsten(II) PNP pincer complexes.[20]

RESULTS AND DISCUSSION

Molybdenum(0) and Tungsten(0) Complexes. We have recently reported the synthesis of molybdenum tricarbonyl complexes of the type $[Mo(PNP)(CO)_3]$ (**2a–c**) by reacting $[Mo(CO)_3(CH_3CN)_3]$, prepared in situ by refluxing a solution of $[Mo(CO)_6]$ in CH_3CN for 4 h, with the PNP ligands PNP-Ph (**1a**), PNP-*i*Pr (**1b**), and PNP-*t*Bu (**1c**) in 74–90% isolated yields.[13] The same procedure was followed with the N-methylated PNP ligand PNP^{Me}-*i*Pr (**1d**), affording $[Mo(PNP^{Me}\text{-}iPr)(CO)_3]$ (**2d**) in 80% yield (Scheme 1). The new

Scheme 1

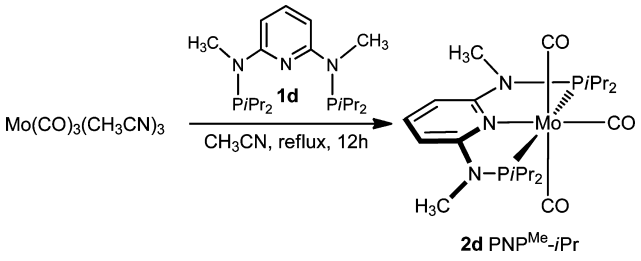

PNP ligand **1d** was prepared in a three-step procedure involving borane protection of the phosphine, a deprotonation/alkylation step, and deprotection of the phosphine, as shown in Scheme 2. The analogous tungsten complexes

Scheme 2

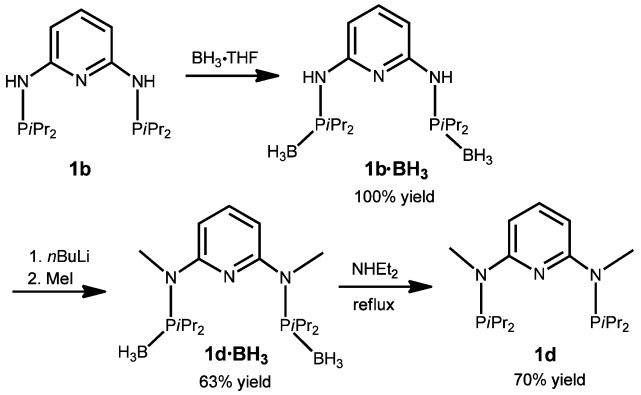

$[W(PNP)(CO)_3]$ can be prepared in a similar fashion but require much longer reaction times (several days to prepare the intermediate $[W(CO)_3(CH_3CN)_3]$); moreover, the yields turned out to be significantly lower (10–25%). It has to be noted that already a few years ago Haupt and co-workers reported the synthesis of $[M(PNP\text{-}Ph)(CO_3)]$ (M = Mo, W) in 34 and 22% yields.[12] We thus developed an alternative method to obtain tungsten(0) complexes $[W(PNP)(CO)_3]$ via the intermediacy of the known dinuclear complex $[W(CO)_4(\mu\text{-}Br)Br]_2$,[21] prepared in situ from $W(CO)_6$ and stoichiometric amounts of Br_2 in CH_2Cl_2 at −70 °C. Treatment of a solution of $[W(CO)_4(\mu\text{-}Br)Br]_2$ in CH_2Cl_2 at room temperature with the PNP ligands **1a–c** afforded on workup the seven-coordinate tungsten(II) complexes $[W(PNP)(CO)_3Br]Br$ (**3a–c**) in 60–80% yields (Scheme 3).

It has to be noted that the reaction of PNP ligands with $[Mo(CO)_4(\mu\text{-}Br)Br]_2$,[21] prepared in situ from $Mo(CO)_6$ and Br_2 in CH_2Cl_2 at −70 °C, affords the analogous seven-coordinate molybdenum complexes $[Mo(PNP)(CO)_3Br]Br$. This has been demonstrated for the synthesis of $[Mo(PNP\text{-}Ph)(CO)_3Br]Br$ (**4a**) and $[Mo(PNP\text{-}iPr)(CO)_3Br]Br$ (**4b**), as illustrated in Scheme 3.

The solid-state structures of **3a** and **4b** were determined by single-crystal X-ray diffraction. Molecular views of **3a** and **4b** are depicted in Figures 1 and 2, respectively, with selected bond distances and angles reported in the captions. While the Mo-bonded bromide in **4b** was clearly in an axial position, the bromide in the tungsten complex **3a** adopted an axial position at about 86% occupancy (Br1 in Figure 1), while the remaining 14% exchanged places with the carbonyl group C32–O3.

Stirring complexes **3a–c** with an excess of 10% sodium amalgam in THF gave the desired W(0) complexes $[W(PNP\text{-}Ph)(CO)_3]$ (**5a**), $[W(PNP\text{-}iPr)(CO)_3]$ (**5b**), and $[W(PNP\text{-}tBu)(CO)_3]$ (**5c**) as yellow solids in 70–80% isolated yields (Scheme 3). This methodology also yields the analogous Mo(0) complexesl thus being an alternative method to that described previously.[13] The use of Zn as reducing reagent turned out to be problematic, due to the formation of highly soluble and, thus, difficult to remove bromozincate anions, e.g., $[ZnBr_3\cdot solvent]^-$ (solvent = acetone, THF) and $ZnBr_4^{2-}$. Complexes **5a–c** were fully characterized by a combination of ^1H, $^{13}C\{^1H\}$, and $^{31}P\{^1H\}$ NMR spectroscopy, IR spectroscopy, and elemental analysis. Characteristic features of **5a–c** comprise, in the $^{13}C\{^1H\}$ NMR spectrum, two low-field triplet resonances (1/2 ratio) in the ranges of 206–221 and 196–210 ppm assignable to the carbonyl carbon atoms *trans* and *cis* to the pyridine nitrogen, respectively. The $^{31}P\{^1H\}$ NMR spectra exhibit singlet resonances at 85.2, 106.6.1, and 131.6 ppm with $^1J_{WP}$ coupling constants of 315–329 Hz. The tungsten–phosphorus coupling was observed as a doublet satellite due to ^{183}W, 14% abundance with $I = {}^1/_2$, superimposed over the dominant singlet. The IR spectra show the typical three strong to medium absorption bands of a *mer* CO arrangement in the range of 2017–1760 cm^{-1} assignable to one weaker symmetric and two strong asymmetric ν_{CO} stretching modes. The ν_{CO} frequencies, in particular the symmetric CO stretch, is indicative of the increasing electron donor strengths of the PNP ligands and follow the order PNP-Ph < PNP-*i*Pr ≈ PNP^{Me}-*i*Pr < PNP-*t*Bu (Table 1). The CO stretching frequencies are 1964 (**2a**, PNP-Ph), 1936 (**2b**, PNP-*i*Pr), 1936 (**2d**, PNP^{Me}-*i*Pr), and 1922 cm^{-1} (**2c**, PNP-*t*Bu). The same order is found for the respective tungsten complexes. In all complexes the PNP pincer ligand adopts the typical *mer* coordination mode with no evidence for any *fac* isomers.[22]

In addition to the spectroscopic characterization, the solid-state structures of **2d** and **5b,c** were determined by single-crystal X-ray diffraction. Structural views are depicted in Figures 3–5, respectively, with selected bond distances and angles given in the captions. The coordination geometry around the tungsten center of **5b,c** corresponds to a distorted octahedron with P1–W–P2 and *trans*-C_{CO}–W–C_{CO} bond angles 154.43(4) and 165.7(2)° (**5b**), and 151.42(1) and 156.46(9)° (**5c**), respectively. For comparison, in the analogous

dx.doi.org/10.1021/om400254k | Organometallics 2013, 32, 3042–3052

Scheme 3

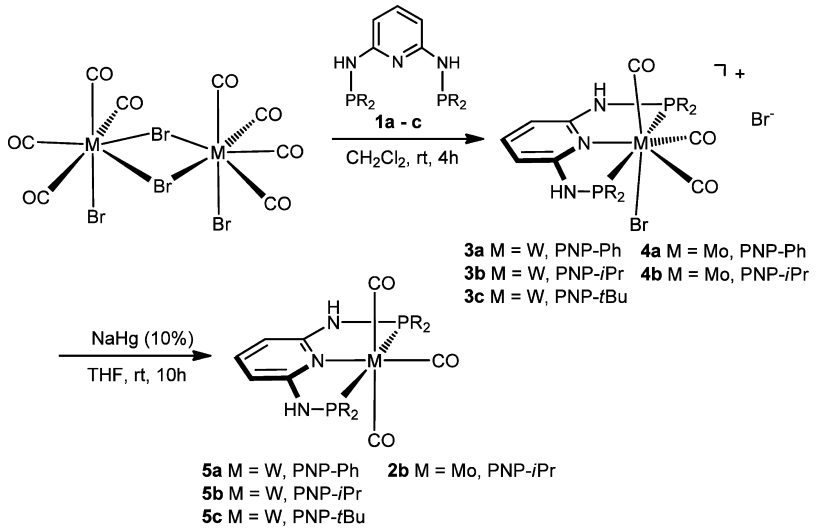

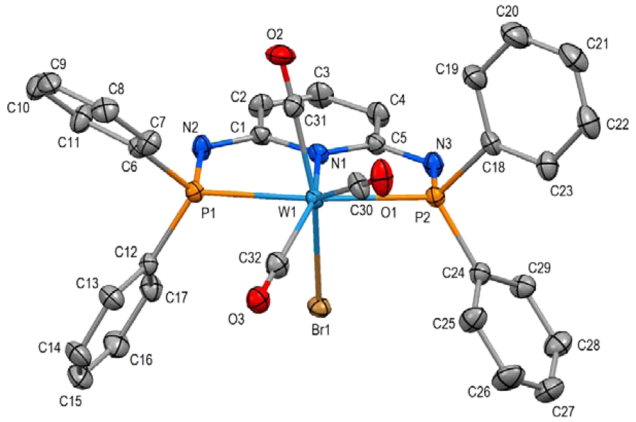

Figure 1. Structural view of $[W(PNP\text{-}Ph)(CO)_3Br]Br{\cdot}CH_3OH$ (**3a**·CH_3OH) showing 20% thermal ellipsoids (H atoms, Br^- counterion, solvent molecule and subordinate Br/CO positions omitted for clarity). Selected bond lengths (Å) and bond angles (deg): W–C(31) = 2.017(5), W–C(30) = 2.020(6), W–C(32) = 2.024(8), W–N(1) = 2.237(3), W–P(1) = 2.4955(10), W–P(2) = 2.4895(11), W–Br(1) = 2.6015(5); P(1)–W–P(2) = 152.34(4), N(1)–W–P(1) = 77.44(9), N(1)–W–P(2) = 75.92(9), N(1)–W–C(30) = 137.76(16), N(1)–W–C(31) = 82.35(16), N(1)–W–C(32) = 150.87(8), N(1)–W–Br(1) = 82.28(9).

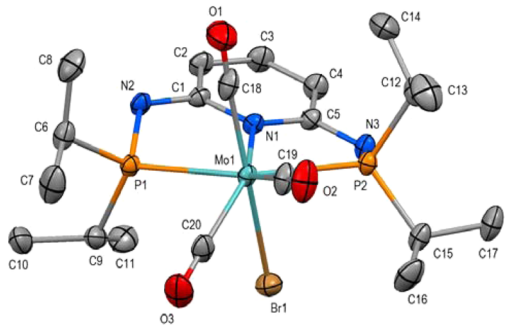

Figure 2. Structural view of $[Mo(PNP\text{-}iPr)(CO)_3Br]Br$ (**4b**) showing 50% thermal ellipsoids (Br^- counterion omitted for clarity). Selected bond lengths (Å) and bond angles (deg): Mo–C(18) = 2.037(2), Mo–C(19) = 1.979(2), Mo–C(20) = 2.006(2), Mo–N(1) = 2.236(2), Mo–P(1) = 2.5242(5), Mo–P(2) = 2.5172(5), Mo–Br(1) = 2.6713(3); P(1)–Mo–P(2) = 150.80(2), N(1)–Mo–P(1) = 75.67(4), N(1)–Mo–P(2) = 75.35(4), N(1)–Mo–C(18) = 85.95(7), N(1)–Mo–C(19) = 77.73(6), N(1)–Mo–C(20) = 127.23(6), N(1)–Mo–Br(1) = 84.22(4).

$[Mo(PNP)(CO)_3]$ complexes **2a–d** the P1–Mo–P2 angles are hardly affected by the size of the substituents of the phosphorus atoms, being 155.0(2), 155.62(1), 155.3(1), and 151.73(1)°, respectively.[12,13] The carbonyl–Mo–carbonyl angles of the CO ligands *trans* to one another, on the other hand, vary strongly with the bulkiness of the PR_2 moiety (PNP-Ph_2 < PNP-iPr_2 < PNP^{Me}-*i*Pr < PNP-*t*Bu_2) and decrease from 171.1(8)° in $[Mo(PNP\text{-}Ph)(CO)_3]$, to 166.03(5)° in $[Mo(PNP\text{-}iPr)(CO)_3]$, to 162.93(7)° in $[Mo(PNP^{Me}\text{-}iPr)(CO)_3]$, and finally to 156.53(4)° in $[Mo(PNP\text{-}tBu)(CO)_3]$.

Molybdenum(II) and Tungsten(II) Hydride Complexes. Addition of HBF_4 to a CH_2Cl_2 solution of $[Mo(PNP)(CO)_3]$ (**2a–d**) and $[W(PNP)(CO)_3]$ (**5a–c**) resulted in an immediate color change from yellow to pale yellow consistent with protonation at the tungsten and molybdenum centers to generate tungsten(II) and molybdenum(II) hydride complexes $[Mo(PNP)(CO)_3H]BF_4$ (**7a–d**) and $[W(PNP)(CO)_3H]BF_4$ (**8a–c**), respectively (Scheme 4). The protonation is fully reversible, and upon addition of NEt_3 as base the Mo(0) and W(0) complexes $[M(PNP)(CO)_3]$ are re-formed

Table 1. Selected IR, $^{31}P\{^1H\}$ NMR, and $^{13}C\{^1H\}$ NMR Data for $[M(PNP)(CO)_3]$ and $[M(PNP)(CO)_3H]^+$ (M = Mo, W)

complex	ν_{CO}, cm^{-1}	δ_P, ppm	δ_{CO}, ppm	δ_H, ppm
2a	1964, 1858, 1765	116.2	228.4, 211.2	
2b	1936, 1809, 1790	143.6	231.4, 216.9	
2c	1922, 1808, 1771	161.9	233.1, 224.0	
2d	1936, 1810, 1795	171.0	230.8, 217.9	
5a	1955, 1847, 1759	100.2	206.0, 196.6	
5b	1929, 1805, 1784	128.5	221.1, 210.6	
5c	1914, 1799, 1759	147.2	224.7, 219.4	
7a	2042, 1940, 1937	111.5, 97.8	212.7, 203.2	−3.78
7b	2035, 1923, 1920	142.3, 121.4	212.3, 205.8	−4.98
7c	2019, 1937, 1916	158.8, 142.8	213.7, 209.5	−4.34
7d	2028, 1928, 1910	166.1, 147.7	210.8, 205.4	−5.49
8a	2038, 1963, 1918	95.5, 84.8	205.9, 196.6	−3.43
8b	2027, 1910, 1906	125.9, 108.6	205.5, 198.0	−4.83
8c	2021, 1934, 1897	141.1, 126.8		−4.16

dx.doi.org/10.1021/om400254k | *Organometallics* 2013, 32, 3042–3052

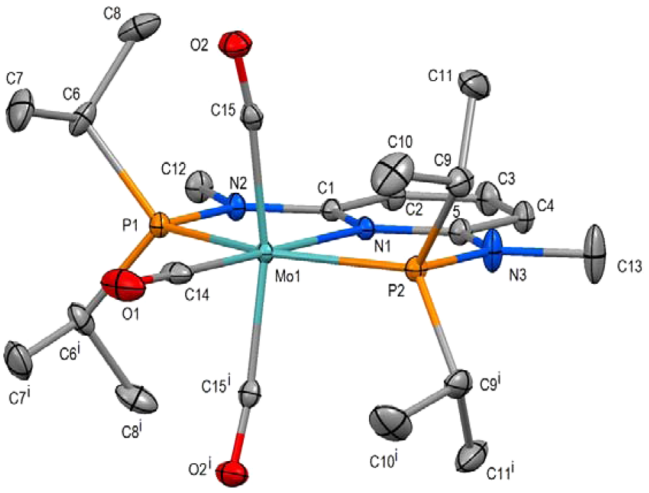

Figure 3. Structural view of $[Mo(PNP^{Me}\text{-}iPr)(CO)_3]$ (**2d**) showing 50% thermal ellipsoids (H atoms are omitted for clarity; the complex is mirror symmetric; symmetry code i for x, $^1/_2 - y$, z). Selected bond lengths (Å) and bond angles (deg): Mo−C(14) = 1.956(2), Mo−C(15) = 2.0153(13), Mo−N(1) = 2.2589(15), Mo−P(1) = 2.3977(5), Mo−P(2) = 2.4070(5); P(1)−Mo−P(2) = 155.25(2), N(1)−Mo−P(1) = 77.74(4), N(1)−Mo−P(2) = 77.51(4), N(1)−Mo−C(15) = 98.52(4), C(15)−Mo−C(15^i) = 162.93(7).

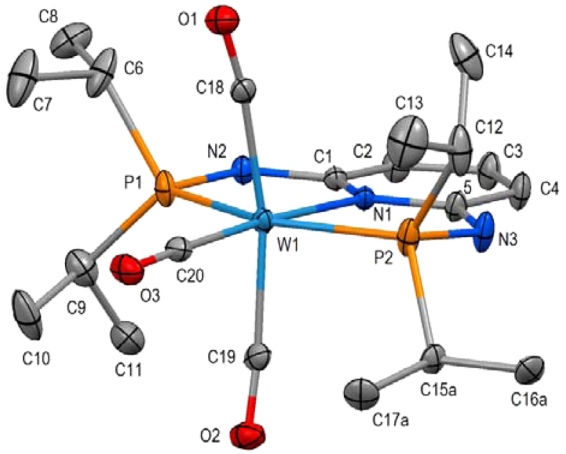

Figure 4. Structural view of $[W(PNP\text{-}iPr)(CO)_3]\cdot THF\cdot {}^1/_2C_6H_{14}$ (**5b**·THF·$^1/_2C_6H_{14}$) showing 30% thermal ellipsoids (H atoms, solvent molecules, and alternative orientation of *i*Pr group C(16a)−C(15a)−C(17a) omitted for clarity). Selected bond lengths (Å) and bond angles (deg): W−C(18) = 2.014(5), W−C(19) = 2.015(5), W−C(20) = 1.934(4), W−N(1) = 2.257(3), W−P(1) = 2.4080(12), W−P(2) = 2.4013(12); P(1)−W−P(2) = 154.43(4), N(1)−W−P(1) = 77.30(9), N(1)−W−P(2) = 77.18(9), N(1)−W−C(18) = 100.8(2), N(1)−W−C(19) = 93.3(2), N(1)−W−C(20) = 175.8(2), C(18)−W−C(19) = 165.7(2).

quantitatively (Scheme 4). All hydride complexes are thermally robust pale yellow solids that are air stable in the solid state but slowly decompose in solution. Characterization was accomplished by elemental analysis and by ^{1}H, ^{13}C{^{1}H}, and ^{31}P{^{1}H} NMR and IR spectroscopy (Table 1). The recording of a ^{13}C{^{1}H} NMR spectrum of **8c** was precluded due to the poor solubility of this complex in most common solvents.

Seven-coordinate complexes are well-known for their fluxional behavior in solution,[23,24] since typically none of the idealized geometries such as capped prism, capped octahedron, and pentagonal bipyramid or any of the less symmetrical

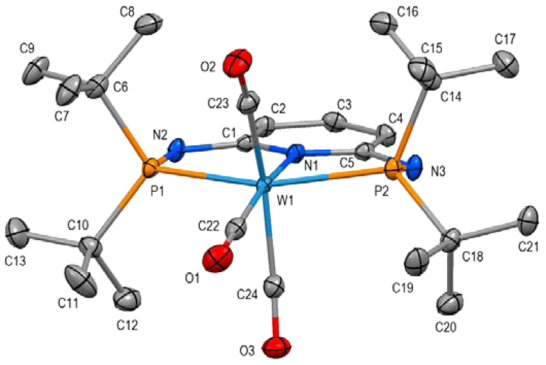

Figure 5. Structural view of $[W(PNP\text{-}tBu)(CO)_3]\cdot THF$ (**5c**·THF) showing 50% thermal ellipsoids (H atoms and solvent molecule omitted for clarity). Selected bond lengths (Å) and bond angles (deg): W−C(22) = 1.941(3), W−C(23) = 1.997(2), W−C(24) = 2.001(2), W−N(1) = 2.277(2), W−P(1) = 2.4583(5), W−P(2) = 2.4656(5); P(1)−W−P(2) = 151.42(2), N(1)−W−P(1) = 76.52(4), N(1)−W−P(2) = 76.00(4), N(1)−W−C(22) = 169.53(8), N(1)−W−C(23) = 113.16(8), N(1)−W−C(24) = 90.27(7), C(23)−W−C(24) = 156.46(9).

Scheme 4

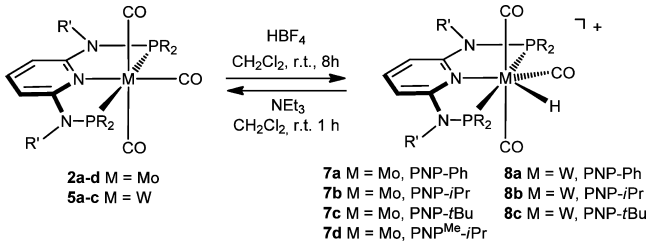

arrangements are typically characterized by a markedly lower total energy.[25] Hence, interconversions between these various structures are quite facile. The fluxional behavior of complexes **7a−d** and **8a−c** was evident in variable-temperature ^{1}H and ^{31}P{^{1}H} NMR spectra. At room temperature, the ^{1}H NMR spectrum of complexes **7** and **8** confirmed the presence of one hydride ligand, which appeared in the range of −3.89 to −5.36 ppm either as a well-resolved doublet of doublets (**8b,c**) or as triplets (**7a−d**, **8a**).

At −60 °C, all hydride resonances appear as a well-resolved doublet of doublets with one large and one small coupling constant of about 21−36 and 47−53 Hz, respectively. As an example, the variable-temperature 300 MHz ^{1}H NMR spectra of the hydride region of $[Mo(PNP\text{-}Ph)(CO)_3H]BF_4$ (**7a**) are shown in Figure 6. At low temperatures the hydride signal constitutes the X part of an AMX spin system, giving rise to a doublet of doublets which, at elevated temperatures in the fast exchange regime, becomes a simple A_2X spin system where the X part exhibits a triplet resonance.

In the ^{13}C{^{1}H} NMR spectrum of complexes **7a−d** and **8a−d** the most noticeable resonances are two low-field resonances of the carbonyl carbon atoms *trans* and *cis* to the pyridine nitrogen observed as two triplets in a 1:2 ratio. At room temperature, no ^{31}P{^{1}H} NMR signals could be detected for molybdenum complexes **7a−d** and the tungsten complex **8a** due to their fluxional behavior. At −60 °C, however, the ^{31}P{^{1}H} NMR spectra of all complexes **8** give rise to two doublets with a large geminal coupling constant of about 80 Hz, which is indicative of the phosphorus atoms being in mutually *trans* positions. The IR spectra of **7** and **8** show three strong to

dx.doi.org/10.1021/om400254k | *Organometallics* 2013, 32, 3042−3052

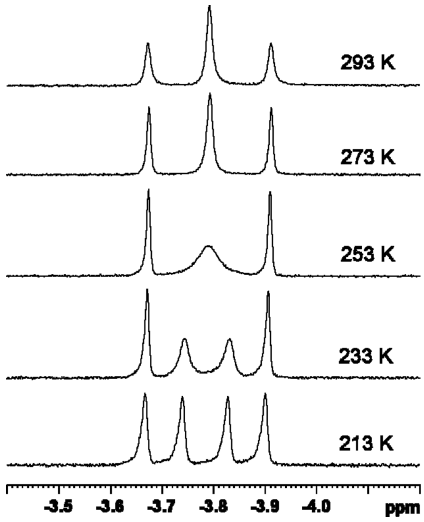

Figure 6. Variable-temperature 300 MHz ^{1}H NMR spectra of the hydride region of [Mo(PNP-Ph)(CO)$_3$H]BF$_4$ (**7a**) in CD_2Cl_2.

medium absorption ν_{CO} bands of the one symmetric and the two asymmetric vibration modes (Table 1), which again are typical for a *mer* CO arrangement.

In addition to the spectroscopic characterization, the solid-state structures of **7a**,**d** and **8a** were determined by single-crystal X-ray diffraction. Structural diagrams are depicted in Figures 7−9, respectively, with selected bond distances given in the captions. The coordination geometry around the molybdenum center corresponds to a distorted capped octahedron, in which a hydride ligand occupies the capping position of an octahedral face. The crystal structure showed the tridentate PNP ligand to be bound meridionally with three carbonyl ligands filling the remaining three sites. The carbonyl *trans* to nitrogen was pushed toward one of the phosphine ligands to accommodate the hydride ligand. The metal−hydride bond length in the three complexes averages 1.65 Å (1.64−1.70 Å), the mean bond angle H−M−P to the nearest P atom is 67° (65−69°), and the mean bond angle H−M−C between hydride and the equatorial carbonyl group is 53° (50−55°). The hydride to carbonyl C atom distance (1.62 Å in **7d**) and the almost linear attachment of the equatorial carbonyl group (Mo1−C22−O3 = 179° in **7d**) do not indicate a significant bonding interaction between hydride and the adjacent carbonyl C atom in the three structurally characterized hydrido carbonyl complexes.

The mechanism of the dynamic process of the hydrido carbonyl complexes was investigated by means of DFT

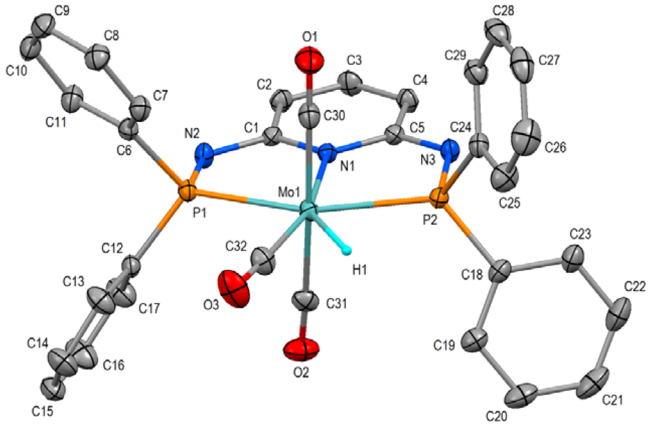

Figure 7. Structural view of [Mo(PNP-Ph)(CO)$_3$H]BF$_4$ (**7a**) showing 50% thermal ellipsoids (BF$_4^-$ counterion and alternative orientation of C(32)−O(3) and H(1) omitted for clarity). Selected bond lengths (Å) and bond angles (deg): Mo−H(1) = 1.67(4), Mo−C(30) = 2.0368(15), Mo−C(31) = 2.0465(15), Mo−C(32) = 2.017(3), Mo−N(1) = 2.2357(11), Mo−P(1) = 2.4409(4), Mo−P(2) = 2.4489(4); P(1)−Mo−P(2) = 154.64(1), N(1)−Mo−P(1) = 77.39(3), N(1)−Mo−P(2) = 77.39(3), N(1)−Mo−C(30) = 87.62(5), N(1)−Mo−C(31) = 86.97(5), N(1)−Mo−C(32) = 163.73(9), N(1)−Mo−H(1) = 146.0(15), C(32)−Mo−H(1) = 50.2(15).

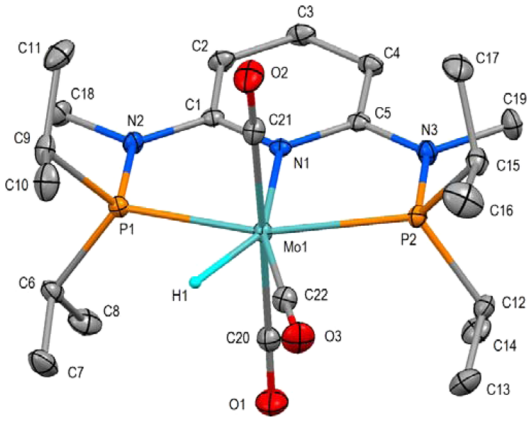

Figure 8. Structural view of [Mo(PNP^{Me}-*i*Pr)(CO)$_3$H]BF$_4$·CH_2Cl_2 (**7d**·CH_2Cl_2) showing 50% thermal ellipsoids (BF$_4^-$ counterion and CH_2Cl_2 omitted for clarity). Selected bond lengths (Å) and bond angles (deg): Mo−H(1) = 1.63(2), Mo−C(20) = 2.0440(13), Mo−C(21) = 2.0239(13), Mo−C(22) = 1.9856(13), Mo−N(1) = 2.2462(10), Mo−P(1) = 2.4425(3), Mo−P(2) = 2.4776(3); P(1)−Mo−P(2) = 154.61(1), N(1)−Mo−P(1) = 77.29(3), N(1)−Mo−P(2) = 77.31(3), N(1)−Mo−C(20) = 94.27(4), N(1)−Mo−C(21) = 89.76(4), N(1)−Mo−C(22) = 162.26(4), N(1)−Mo−H(1) = 145.7(8), C(22)−Mo−H(1) = 52.0(8).

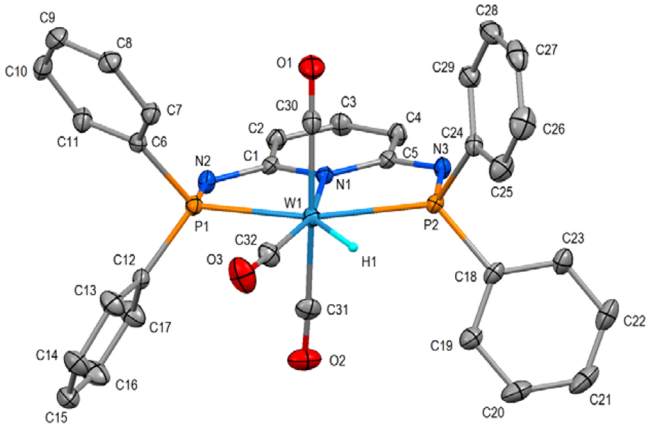

Figure 9. Structural view of [W(PNP-Ph)(CO)$_3$H]BF$_4$ (**8a**) showing 50% thermal ellipsoids (BF$_4^-$ counterion and alternative orientation of C(32)−O(3) and H(1) omitted for clarity). Selected bond lengths (Å) and bond angles (deg): W−H(1) = 1.65(5), W−C(30) = 2.033(2), W−C(31) = 2.039(2), W−C(32) = 2.022(4), W−N(1) = 2.2316(15), W−P(1) = 2.4444(5), W−P(2) = 2.4459(5); P(1)−W−P(2) = 154.32(2), N(1)−W−P(1) = 77.17(4), N(1)−W−P(2) = 77.29(4), N(1)−W−C(30) = 87.78(7), N(1)−W−C(31) = 86.88(7), N(1)−W−C(32) = 162.35(11), N(1)−W−H(1) = 143.5(17), C(32)−W−H(1) = 53.9(17).

dx.doi.org/10.1021/om400254k | *Organometallics* 2013, 32, 3042−3052

calculations[26] for the molybdenum and tungsten complexes $[Mo(PNP)(CO)_3H]^+$ (**7a–c**) and $[W(PNP)(CO)_3H]^+$ (**8a–c**). The free energy profile for the "pseudorotation" is depicted in Figure 10. The optimized structures of **8a,c** and the

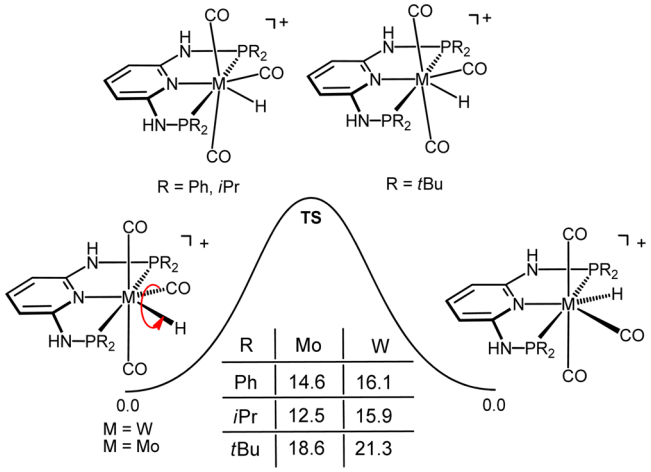

Figure 10. Free energy profile (in kcal/mol) for the "pseudorotation" of CO and hydride ligands in the complexes $[M(PNP)(CO)_3H]^+$ (M = W, Mo).

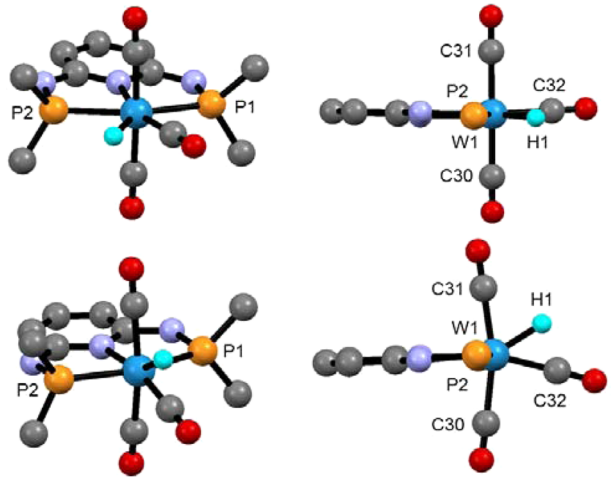

Figure 11. Front (left) and side views (right) of the optimized structures (DFT/B3LYP) of the tungsten complex $[W(PNP\text{-}Ph)(CO)_3H]^+$ (**8a**; top) and the transition state **TS** (bottom) with most phenyl carbon atoms and hydrogen atoms omitted for clarity.

corresponding transition states **TS** are shown in Figures 11 and 12. In the fluxional process, the CO and the hydride ligands in the PNP plane exchange positions in a single-step path. During that process the rest of the molecule has to change in order to accommodate the overall transformations associated with the pseudorotation. The main geometry change that happens along the path is the hydride ligand moving from the PNP plane to the perpendicular plane, i.e., the plane of the three CO ligands, in the transition state (**TS**) and then back to the PNP plane again but on the other side of the CO ligand. Thus, in **TS**, the two *trans* CO ligands have to create enough space to allow the presence of an extra ligand in the NCCC plane, opening the corresponding OC–M–CO angle and bending away from the

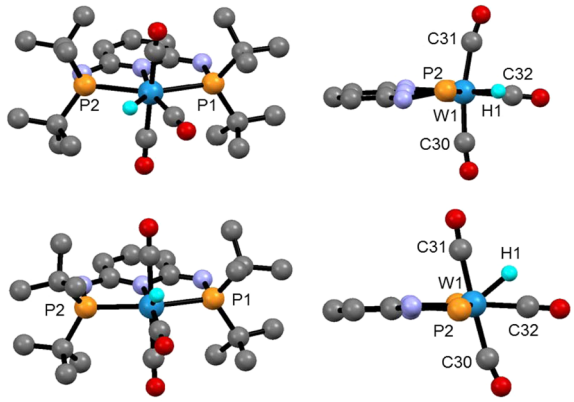

Figure 12. Front (left) and side views (right) of the optimized structures (DFT/B3LYP) of the tungsten complex $[W(PNP\text{-}tBu)(CO)_3H]^+$ (**8c**; top) and the transition state **TS** (bottom) with most *t*Bu carbon atoms and hydrogen atoms omitted for clarity.

hydride ligand. Accordingly, In the case of the molybdenum and tungsten PNP complexes bearing the less bulky Ph and iPr substituents (**7a,b** and **8a,b**), the C30–W1–C31 angle changes from about 177° in the ground-state structure to 166° in **TS**, where both *trans* CO ligands are bent toward the PNP ligand (Figure 11). On the other hand, in the case of the molybdenum and tungsten PNP complexes bearing the bulky *t*Bu substituents (**7c** and **8c**) the situation is somewhat different. The C30–W1–C31 angle increases from 169° in the minima to 178° in **TS**, while one of the two *trans* CO ligands is severely bent away from the PNP ligand and the other one is bent toward the PNP ligand (Figure 12). In the course of all these transformations also the H1–W1–C32 angles change from about 55° in **7a–c** and **8a–c** to roughly 43° in the **TS**, respectively. Bond distances are hardly affected by the interconversion. It is interesting to note that, in agreement with the X-ray structures of **7a**, **7d**, and **8a** (Figures 6–8), the distance between H1 and C32 is rather short, being in the range of 1.80–1.66 Å. A Wiberg index[27] of 0.20, in **8c**, seems to indicate an attractive interaction between the hydride and the neighboring C_{CO} atom (C32). Most importantly, the free energy barriers $\Delta G^{\ddagger}$ are 18.6 and 21.3 kcal/mol for **7c** and **8c**, respectively, containing the bulky *t*Bu substituents. In the case of all other complexes the free energy barrier is lower, being in the range of 12.5–16.1 kcal/mol, as shown in Figure 9. These results corroborate a process that can be stopped in the temperature range employed in the NMR studies and a more facile process in the case of the Mo species, as observed.

CONCLUSION

In the present study the Mo(0) and W(0) complexes $[M(PNP)CO)_3]$ as well as seven-coordinate cationic hydrido carbonyl and halo carbonyl Mo(II) and W(II) complexes of the type $[M(PNP)(CO)_3Br]^+$ and $[M(PNP)(CO)_3H]^+$ featuring PNP pincer ligands based on 2,6-diaminopyridine were prepared and fully characterized. The synthesis of the Mo(0) complexes $[Mo(PNP)CO)_3]$ was accomplished by treatment of $[Mo(CO)_3(CH_3CN)_3]$ with the respective PNP ligands. The analogous W(0) complexes were prepared by reduction of the bromo carbonyl complexes $[W(PNP)(CO)_3Br]^+$ with NaHg. These intermediates were obtained from the known dinuclear complex $[W(CO)_4(\mu\text{-}Br)Br]_2$, prepared in situ from $W(CO)_6$ and stoichiometric amounts of Br_2. Addition of HBF_4 to $[M(PNP)(CO)_3]$ resulted in protonation at the tungsten and

dx.doi.org/10.1021/om400254k | *Organometallics* 2013, 32, 3042–3052

molybdenum centers to formally generate the Mo(II) and W(II) hydride complexes $[M(PNP)(CO)_3H]^+$. The protonation is fully reversible, and upon addition of NEt_3 as base the Mo(0) and W(0) complexes $[M(PNP)(CO)_3]$ are re-formed quantitatively. All seven-coordinate complexes exhibit fluxional behavior in solution, since none of the idealized geometries (capped prism, capped octahedron, and pentagonal bipyramid) or any of the less symmetrical arrangements are typically characterized by a markedly lower total energy. The mechanism of the dynamic process of the hydrido carbonyl complexes was investigated by means of DFT calculations, revealing that it occurs in a single step. Thereby the CO and the hydride ligands which are situated in the PNP plane are interconverted. The structures of representative complexes were determined by X-ray single-crystal analyses.

EXPERIMENTAL SECTION

General Considerations. All manipulations were performed under an inert atmosphere of argon by using Schlenk techniques. The solvents were purified according to standard procedures.[28] The ligands and complexes *N,N′*-bis(diphenylphosphino)-2,6-diaminopyridine (PNP-Ph; **1a**), N,N′-bis(diisopropylphosphino)-2,6-diaminopyridine (PNP-*i*Pr; **1b**), *N,N′*-bis(di-*tert*-butylphosphino)-2,6-diaminopyridine (PNP-*t*Bu; **1c**), [Mo(PNP-Ph)(CO)$_3$] (**2a**), [Mo(PNP-*i*Pr)(CO)$_3$] (**2b**), and [Mo(PNP-*t*Bu)(CO)$_3$] (**2c**) were prepared according to the literature.[13] The deuterated solvents were purchased from Aldrich and dried over 4 Å molecular sieves. ^{1}H, ^{13}C{^{1}H}, and ^{31}P{^{1}H} NMR spectra were recorded on Bruker AVANCE-250 and AVANCE-300 DPX spectrometers and were referenced to $SiMe_4$ and H_3PO_4 (85%), respectively.

***N,N′*-Bis(diisopropylphosphino-borane)-2,6-diaminopyridine (PNP-*i*Pr; 1b·BH$_3$).** BH_3·THF (43.1 mL, 1.0 M, 43.06 mmol) was added slowly to a solution of **1b** (7.00 g, 20.50 mmol) in 100 mL of dry THF. After the mixture was stirred for 30 min at room temperature, the solvent was evaporated under reduced pressure. The white solid was further dried under vacuum for 2 h to give the product in quantitative yield. Anal. Calcd for $C_{17}H_{39}B_2N_3P_2$: C, 55.32; H, 10.65; N, 11.39. Found: C, 55.28; H, 10.70; N, 11.43. ^{1}H NMR (δ, $CDCl_3$, 20 °C): 7.32 (t, J = 7.9 Hz, 1H, py^4), 6.26 (d, J = 7.9, 2H, py^{3,5}), 4.58 (d, J = 8.4 Hz, 2H, N*H*), 2.62 (septd, J = 6.9 Hz, J = 13.7 Hz, 4H, C*H*(CH$_3$)$_2$), 1.16 (m, 24H, CH(C*H*$_3$)$_2$), 0.60 to −0.15 (bs, 6H, B*H*$_3$). ^{13}C{^{1}H} NMR (δ, $CDCl_3$, 20 °C): 154.4 (s, py^{2,6}), 140.1 (s, py^4), 103.1 (s, py^{3,5}), 24.5 (d, J = 36.3 Hz, *C*H(CH$_3$)$_2$), 17.2 (d, J = 4.3 Hz, CH(*C*H$_3$)$_2$), 17.0 (s, CH(*C*H$_3$)$_2$). ^{31}P{^{1}H} NMR (δ, $CDCl_3$, 20 °C): 88.5 (br, m).

***N,N′*-Bis(diisopropylphosphino-borane)-*N,N′*-methyl-2,6-diaminopyridine (PNP^{Me}-*i*Pr; 1d·BH$_3$).** To a solution of **1b·BH$_3$** (7.45 g, 20.19 mmol) in THF (50 mL) at −20 °C was slowly added *n*-BuLi (17.0 mL, 2.5 M, 41.39 mmol). The reaction mixture was allowed to reach room temperature and was stirred for 2 h. Methyl iodide (3.15 mL, 50.46 mmol) was then added slowly via syringe. After the mixture was stirred for 12 h at room temperature, the reaction was quenched with a saturated NH_4Cl solution (100 mL) and 5 mL of concentrated NH_3. The aqueous phase was extracted twice with CH_2Cl_2, and the combined organic phases were washed with 25 mL of brine and dried over Na_2SO_4. The solvent was removed under reduced pressure to afford **1d·BH$_3$** as a yellow oil. The crude product was purified via flash chromatography using silica gel and THF to give the product as a white solid. Anal. Calcd for $C_{19}H_{43}B_2N_3P_2$: C, 57.56; H, 10.91; N, 10.58. Found: C, 57.62; H, 10.89; N, 10.61. Yield: 5.05 g (63%). ^{1}H NMR (δ, $CDCl_3$, 20 °C): 7.48 (t, J = 8.0 Hz, 1H, py^4), 6.49 (d, J = 8.0, 2H, py^{3,5}), 3.17 (d, J = 7.9 Hz, 6H, NC*H*$_3$), 2.80 (septd, J = 7.0 Hz, J = 21.2 Hz, 4H, C*H*(CH$_3$)$_2$), 1.22 (dd, J_1 = 6.9 Hz, J_2 = 16.5 Hz, 12H, CH(C*H*$_3$)$_2$), 1.03 (dd, J = 7.0 Hz, J = 15.11 Hz, 12H, CH(C*H*$_3$)$_2$), 0.70 to −0.30 (bs, 6H, B*H*$_3$). ^{13}C{^{1}H} NMR (δ, $CDCl_3$, 20 °C): 156.9 (s, py^{2,6}), 139.1 (s, py^4), 105.8 (s, py^{3,5}), 37.6 (s, NCH$_3$), 25.6 (d, J = 36.2 Hz, *C*H(CH$_3$)$_2$), 17.8 (s, CH(*C*H$_3$)$_2$), 17.2 (s, CH(*C*H$_3$)$_2$). ^{31}P{^{1}H} NMR (δ, $CDCl_3$, 20 °C): 105.9 (br, m).

***N,N′*-Bis(diisopropylphosphino)-*N,N′*-methyl-2,6-diaminopyridine (PNP^{Me}-*i*Pr; 1d).** **1d·BH$_3$** (5.00 g, 12.59 mmol) was refluxed for 72 h in 100 mL of Et_2NH. After removal of the solvent under reduced pressure the remaining oil was dissolved in THF, filtered through Celite, and obtained as a yellow oil after evaportaion of the solvent under reduced pressure. The crude product was purified by recrystallization from acetonitrile to afford **2d** as a white solid. Anal. Calcd for $C_{19}H_{37}N_3P_2$: C, 61.77; H, 10.09; N, 11.37. Found: C, 61.69; H, 10.16; N, 11.44. Yield: 3.25 g (70%). ^{1}H NMR (δ, CD_2Cl_2, 20 °C): 7.22 (t, J = 8.0 Hz, 1H, py^4), 6.64 (bs, py^{3,5}), 3.04 (d, J = 2.3 Hz, 6H, NC*H*$_3$), 2.22 (bs, 4H, C*H*(CH$_3$)$_2$), 1.10 (dd, J = 6.9 Hz, J = 16.9 Hz, 12H, CH(C*H*$_3$)$_2$), 0.98 (dd, J = 7.0 Hz, J = 12.1 Hz, 12H, CH(C*H*$_3$)$_2$). ^{13}C{^{1}H} NMR (δ, CD_2Cl_2, 20 °C): 160.4 (s, py^{2,6}), 136.9 (s, py^4), 99.1 (d, J = 22.3 Hz, py^{3,5}), 33.7 (bs, NCH$_3$), 26.2 (d, J = 15.3 Hz, *C*H(CH$_3$)$_2$), 19.4 (s, CH(*C*H$_3$)$_2$), 19.2 (s, CH(*C*H$_3$)$_2$), 19.0 (s, CH(*C*H$_3$)$_2$). ^{31}P{^{1}H} NMR (δ, CD_2Cl_2, 20 °C): 81.3 (bs).

[Mo(PNP^{Me}-*i*Pr)(CO)$_3$] (2d). A suspension of $Mo(CO)_6$ (714 mg 2.7 mmol) in acetonitrile (10 mL) was refluxed for 4 h. After that PNP^{Me}-*i*Pr (**1d**; 1.00 g, 2.7 mmol) was added and the mixture was refluxed for an additional 12 h. The solvent was then removed under reduced pressure, and the product was washed twice with diethyl ether and dried under vacuum. Yield: 1.19 g (80%). Anal. Calcd for $C_{22}H_{37}MoN_3O_3P_2$: C, 48.09; H, 6.79; N, 7.65. Found: C, 48.15; H, 6.82; N, 7.61. ^{1}H NMR (δ, CD_2Cl_2, 20 °C): 7.40 (t, J = 7.6 Hz, 1H, py), 6.30 (d, J = 7.6 Hz, 2H, py), 3.01 (s, 6H, NC*H*$_3$), 2.47 (m, 4H, C*H*(CH$_3$)$_2$), 1.30 (m, 12H, CH(C*H*$_3$)$_2$), 1.09 (m, 12H, CH(C*H*$_3$)$_2$). ^{13}C{^{1}H} NMR (δ, CD_2Cl_2, 20 °C): 230.8 (t, J = 6.0 Hz, *C*O), 217.9 (t, J = 10.8 Hz, *C*O), 174.9 (t, J = 2.6 Hz, py), 137.8 (s, py), 96.7 (t, J = 2.2 Hz, py), 33.9 (t, J = 1.8 Hz, N(*C*H$_3$)$_2$), 32.9 (t, J = 9.0 Hz, *C*H(CH$_3$)$_2$), 29.6 (s, N(*C*H$_3$)$_2$), 19.2 (t, J = 7.5 Hz, CH(*C*H$_3$)$_2$), 18.1 (s, CH(*C*H$_3$)$_2$). ^{31}P{^{1}H} NMR (δ, CD_2Cl_2, 20 °C): 171.0 (s). IR (ATR, cm^{-1}): 1936 (ν_{CO}), 1810 (ν_{CO}), 1795 (ν_{CO}).

[W(PNP-Ph)(CO)$_3$Br]Br (3a). To a suspension of $W(CO)_6$ (2.0 g, 5.68 mmol) in CH_2Cl_2 (30 mL) was added Br_2 (292 μL, 5.68 mmol) at −70 °C, and the mixture was stirred for 1 h at that temperature and for an additional 1 h at room temperature. After that, PNP-Ph (**1a**; 2.72 g, 5.68 mmol) was added and the mixture was stirred for 5 h at room temperature. After removal of the solvent under reduced pressure, a yellow solid was obtained, which was washed with a 1/9 methanol/diethyl ether mixture and dried under vacuum. Yield: 4.11 g (80%). Anal. Calcd for $C_{32}H_{25}Br_2N_3O_3P_2W$: C, 42.46; H, 2.78; N, 4.64. Found: C, 42.29; H, 2.79; N, 4.55. ^{1}H NMR (δ, acetone-d_6, 20 °C): 10.85 (bs, 2H, N*H*), 7.78 (bs, 11H, py, Ph), 7.60 (bs, 10H, Ph), 7.43 (d, J = 7.6 Hz, 2H, py). ^{13}C{^{1}H} NMR (δ, $CDCl_3$, 20 °C): 225.4 (t, J = 10.3 Hz, *C*O), 210.3 (t, J = 8.6 Hz, *C*O), 159.7 (d, J = 7.5 Hz, py), 159.6 (d, J = 7.5 Hz, py), 133.1 (s, py), 131.9 (s, Ph), 131.9 (s, Ph), 129.0 (d, J = 5.0 Hz, Ph), 128.2 (d, J = 5.4 Hz, Ph), 103.1 (s, py). ^{31}P{^{1}H} NMR (δ, acetone-d_6, 20 °C): 85.2. IR (ATR, cm^{-1}): 2030 (ν_{CO}), 1958 (ν_{CO}), 1933 (ν_{CO}).

[W(PNP-*i*Pr)(CO)$_3$Br]Br (3b). This complex was prepared analogously to **3a** with $W(CO)_6$ (2.0 g, 5.68 mmol) and PNP-*i*Pr (**1b**; 1.95 g, 5.69 mmol) as starting materials. Yield: 3.06 g (70%). Anal. Calcd for $C_{20}H_{33}Br_2N_3O_3P_2W$: C, 31.23; H, 4.32; N, 5.46. Found: C, 31.13; H, 4.42; N, 5.50. ^{1}H NMR (δ, CD_2Cl_2, 20 °C): 9.32 (bs, 2H, N*H*), 7.66 (t, J = 7.2 Hz, 1H, py), 6.67 (d, J = 8.1 Hz, 2H, py), 3.54 (m, 2H, C*H*(CH$_3$)$_2$), 2.88 (m, 2H, C*H*(CH$_3$)$_2$), 1.43 (m, 24H, CH(C*H*$_3$)$_2$). ^{13}C{^{1}H} NMR (δ, CD_2Cl_2, 20 °C): 212.2 (t, J = 10.1 Hz, *C*O), 191.3 (t, J = 7.6 Hz, *C*O), 161.0 (s, py), 142.2 (s, py), 101.9 (s, py), 30.6 (t, J = 15.0 Hz, *C*H(CH$_3$)$_2$), 29.3 (t, J = 15.3 Hz, *C*H(CH$_3$)$_2$), 19.2 (s, CH(*C*H$_3$)$_2$), 19.1 (s, CH(*C*H$_3$)$_2$), 18.9 (s, CH(*C*H$_3$)$_2$), 17.7 (s, CH(*C*H$_3$)$_2$). ^{31}P{^{1}H} NMR (δ, CD_2Cl_2, 20 °C): 106.6. IR (ATR, cm^{-1}): 2023 (ν_{CO}), 1953 (ν_{CO}), 1922 (ν_{CO}).

[W(PNP-*t*Bu)(CO)$_3$Br]Br (3c). This complex was prepared analogously to **3a** with $W(CO)_6$ (2.0 g, 5.68 mmol) and PNP-*t*Bu (**1c**) (2.26 g, 5.69 mmol) as starting materials. Yield: 2.51 g (60%). Anal. Calcd for $C_{24}H_{41}Br_2N_3O_3P_2W$: C, 34.93; H, 5.01; N, 5.09. Found: C, 34.81; H, 5.02; N, 5.20. ^{1}H NMR (δ, CD_2Cl_2, 20 °C): 9.11 (s, 2H, N*H*), 7.74 (d, J = 7.8 Hz, 2H, py), 7.23 (t, J = 8.7 Hz, 1H, py), 1.70 (d, J = 8.2 Hz, 9H, C(C*H*$_3$)$_3$), 1.68 (d, J = 7.3 Hz, 9H, C(C*H*$_3$)$_3$), 1.54 (d, J = 7.5 Hz, 9H, C(C*H*$_3$)$_3$), 1.48 (d, J = 7.1 Hz, 9H, C(C*H*$_3$)$_3$).

dx.doi.org/10.1021/om400254k | *Organometallics* 2013, 32, 3042−3052

$^{13}C\{^1H\}$ NMR (δ, $CDCl_3$, 20 °C): 229.9 (t, J = 14.8 Hz, *C*O), 212.9 (t, J = 7.6 Hz, *C*O), 162.6 (t, J = 4.2 Hz, py), 153.3 (d, J = 5.8 Hz, py), 149.9 (s, py), 103.8 (s, py), 46.0 (t, J = 7.2 Hz, $C(CH_3)_3$), 44.6 (t, J = 7.2 Hz, $C(CH_3)_3$), 31.9 (s, $C(CH_3)_3$), 30.4 (s, $C(CH_3)_3$), 26.9 (s, $C(CH_3)_3$). $^{31}P\{^1H\}$ NMR (δ, CD_2Cl_2, 20 °C): 131.6. IR (ATR, cm^{-1}): 2019 (ν_{CO}), 1941 (ν_{CO}), 1909 (ν_{CO}).

[Mo(PNP-Ph)(CO)$_3$Br]Br (4a). This complex was prepared analogously to **3a** with $Mo(CO)_6$ (300 mg, 1.14 mmol) and PNP-Ph (**1a**; 570 mg, 1.20 mmol) as starting materials. Yield: 775 mg (83%). Anal. Calcd for $C_{32}H_{25}Br_2MoN_3O_3P_2$: C, 47.03; H, 3.08; N, 5.14. Found: C, 46.95; H, 3.12; N, 5.01. ^1H NMR (δ, acetone-d_6, 20 °C): 8.70 (s, 2H, N*H*), 7.59 (m, 5H, Ph), 7.47 (m, 5H, Ph), 7.16 (t, J = 7.2 Hz, 1H, py), 7.01 (m, 5H, Ph), 6.85 (m, 5H, Ph), 6.56 (d, J = 7.8 Hz, 2H, py). $^{31}P\{^1H\}$ NMR (δ, acetone-d_6, 20 °C): 125.3. IR (ATR, cm^{-1}): 2040 (ν_{CO}), 1975 (ν_{CO}), 1875 (ν_{CO}).

[Mo(PNP-*i*Pr)(CO)$_3$Br]Br (4b). This complex was prepared analogously to **3a** with $Mo(CO)_6$ (500 mg, 1.89 mmol) and PNP-*i*Pr (**1b**; 678 mg, 1.98 mmol) as starting materials. Yield: 965 mg (75%). Anal. Calcd for $C_{20}H_{33}Br_2MoN_3O_3P_2$: C, 35.26; H, 4.88; N, 6.17. Found: C, 35.13; H, 4.92; N, 6.20. ^1H NMR (δ, $CDCl_3$, 20 °C): 9.08 (s, 2H, N*H*), 7.24 (d, J = 9.9 Hz, 2H, py), 7.10 (t, J = 7.4 Hz, 1H, py), 3.55 (m, 2H, $CH(CH_3)_2$), 2.96 (m, 2H, $CH(CH_3)_2$). 1.44 (m, 24H, $CH(CH_3)_2$). $^{13}C\{^1H\}$ NMR (δ, $CDCl_3$, 20 °C): 234.6 (t, J = 7.2 Hz, *C*O), 218.3 (t, J = 11.5 Hz, *C*O), 175.1 (s, py), 175.0 (s, py), 160.0 (t, J = 4.9 Hz, py), 142.1 (s, py), 102.7 (s, py), 30.8 (d, J = 12.8 Hz, $CH(CH_3)_2$), 30.6 (d, J = 14.9 Hz, $CH(CH_3)_2$), 30.3 (d, J = 12.4 Hz, $CH(CH_3)_2$), 30.1 (d, J = 11.6 Hz, $CH(CH_3)_2$), 19.4 (s, $CH(CH_3)_2$), 19.3 (s, $CH(CH_3)_2$), 19.1 (s, $CH(CH_3)_2$), 18.1 (s, $CH(CH_3)_2$). $^{31}P\{^1H\}$ NMR (δ, $CDCl_3$, 20 °C): 126.7. IR (ATR, cm^{-1}): 2030 (ν_{CO}), 1967 (ν_{CO}), 1936 (ν_{CO}).

[W(PNP-Ph)(CO)$_3$] (5a). A solution of **3a** (200 mg, 0.22 mmol) in THF (15 mL) was stirred in the presence of NaHg (10%) (16 mg, 0.66 mmol) for 8 h at room temperature. The solvent was then removed under reduced pressure. The residue was redissolved in acetone (10 mL), and the solution was filtered through Celite. After removal of the solvent under reduced pressure, a yellow solid was obtained, which was washed twice with diethyl ether (10 mL) and dried under vacuum. Yield: 140 mg (85%). Anal. Calcd for $C_{32}H_{25}N_3O_3P_2W$: C, 51.57; H, 3.38; N, 5.64. Found: C, 51.63; H, 3.41; N, 5.50. ^1H NMR (δ, acetone-d_6, 20 °C): 7.64 (t, J = 8.6 Hz, 1H, py), 7.44 (bs, 8H, Ph), 7.30 (m, 12H, Ph), 6.43 (d, J = 7.6 Hz, 2H, py), 5.93 (d, J = 8.9 Hz, 2H, N*H*). $^{13}C\{^1H\}$ NMR (δ, acetone-d_6, 20 °C): 206.0 (t, J = 4.6 Hz, *C*O), 196.6 (t, J = 9.1 Hz, *C*O), 159.6 (d, J = 4.7 Hz, py), 159.3 (d, J = 5.5 Hz, py), 142.1 (s, py), 132.0 (s, Ph), 131.0 (d, J = 12.4 Hz, Ph), 129.1 (d, J = 11.5 Hz, Ph), 127.9 (d, J = 6.6 Hz, Ph), 102.0 (d, J = 10.7 Hz, py). $^{31}P\{^1H\}$ NMR (δ, acetone-d_6, 20 °C): 100.2 (s, J_{W-P} = 327 Hz). IR (ATR, cm^{-1}): 1955 (ν_{CO}), 1847 (ν_{CO}), 1759 (ν_{CO}).

[W(PNP-*i*Pr)(CO)$_3$] (5b). This complex was prepared analogously to **5a** with **3b** (500 mg, 0.65 mmol) and NaHg (45 mg, 1.95 mmol) as starting materials. Yield: 315 mg (80%). Anal. Calcd for $C_{20}H_{33}N_3O_3P_2W$: C, 39.43; H, 5.46; N, 6.90. Found: C, 39.51; H, 5.42; N, 6.84. ^1H NMR (δ, CD_2Cl_2, 20 °C): 7.15 (t, J = 8.2 Hz, 1H, py), 6.15 (d, J = 7.9 Hz, 2H, py), 5.50 (bs, 2H, N*H*), 2.40 (m, 4H, $CH(CH_3)_2$), 1.24 (m, 24H, $CH(CH_3)_2$). $^{13}C\{^1H\}$ NMR (δ, CD_2Cl_2, 20 °C): 221.1 (t, J = 2.0 Hz, *C*O), 210.6 (t, J = 7.1 Hz, *C*O), 162.5 (t, J = 8.5 Hz, py), 137.1 (s, py), 96.6 (t, J = 3.1 Hz, py), 32.60 (t, J = 12.8 Hz, $CH(CH_3)_2$), 18.5 (t, J = 1.7 Hz, $CH(CH_3)_2$), 18.1 (t, J = 2.9 Hz, $CH(CH_3)_2$). $^{31}P\{^1H\}$ NMR (δ, CD_2Cl_2, 20 °C): 128.5 (s, J_{W-P} = 315 Hz). IR (ATR, cm^{-1}): 1929 (ν_{CO}), 1805 (ν_{CO}), 1784 (ν_{CO}).

[W(PNP-*t*Bu)(CO)$_3$] (5c). This complex was prepared analogously to **5a** with **3c** (350 mg, 0.42 mmol) and NaHg (30 mg, 1.27 mmol) as starting materials. Yield: 215 mg (77%). Anal. Calcd for $C_{24}H_{41}N_3O_3P_2W$: C, 43.32; H, 6.21; N, 6.32. Found: C, 43.23; H, 6.42; N, 6.48. ^1H NMR (δ, CD_2Cl_2, 20 °C): 7.37 (bs, 2H, N*H*), 7.18 (t, J = 8.0 Hz, 1H, py), 6.29 (d, J = 7.5 Hz, 2H, py), 1.41 (t, J = 5.6 Hz, 36H, $C(CH_3)_3$). $^{13}C\{^1H\}$ NMR (δ, acetone-d_6, 20 °C): 224.7 (t, J = 6.4 Hz,*C*O), 219.4 (t, J = 7.0 Hz, *C*O), 162.6 (d, J = 6.7 Hz, py), 137.8 (s, py), 97.1 (s, py), 40.7 (t, J = 7.5 Hz, $C(CH_3)_3$), 25.8 (d, J = 7.3 Hz, $C(CH_3)_3$). $^{31}P\{^1H\}$ NMR (δ, CD_2Cl_2, 20 °C): 147.2 (s, J_{W-P} = 329 Hz). IR (ATR, cm^{-1}): 1914 (ν_{CO}), 1799 (ν_{CO}), 1759 (ν_{CO}).

Alternative Synthesis of [Mo(PNP-*i*Pr)(CO)$_3$] (2b). This complex was prepared analogously to **5a** with **4b** (88 mg, 0.13 mmol) and NaHg (9 mg, 0.39 mmol) as starting materials. Yield: 61 mg (90%). All spectral data for **2a** are identical with those of the authentic sample reported previously.[13]

[Mo(PNP-Ph)(CO)$_3$H]BF$_4$ (7a). To a solution of **2a** (200 mg, 0.30 mmol) in CH_2Cl_2 (10 mL) was added HBF_4 ((46 μL, 0.45 mmol, 54% solution in Et_2O) at room temperature. After the solution was stirred overnight, a pale yellow precipitate was formed, which was collected on a glass frit, washed with diethyl ether, and dried under vacuum. Yield: 193 mg (85%). Anal. Calcd for $C_{32}H_{26}BF_4MoN_3O_3P_2$: C, 51.57; H, 3.52; N, 5.64. Found: C, 51.66; H, 3.59; N, 5.70. ^1H NMR (δ, acetone-d_6, −60 °C): 9.25 (s, 2H, N*H*), 8.23 (m, 13H, Ph, py), 7.93 (m, 8H, Ph), 6.99 (d, J = 8.0 Hz, 2H, py), −3.78 (dd, $^2J_{HP}$ = 21.6 Hz, $^2J_{HP}$ = 48.5 Hz, 1H, Mo*H*). $^{13}C\{^1H\}$ NMR (δ, CD_2Cl_2, 20 °C): 212.7 (t, J = 11.2 Hz, *C*O), 203.2 (t, J = 8.4 Hz, *C*O), 158.4 (d, J = 6.1 Hz, py), 158.1 (d, J = 8.3 Hz, py), 141.6 (s, py), 135.3 (s, py), 134.5 (d, J = 55.6 Hz, Ph), 131.8 (s, Ph), 130.7 (d, J = 13.7 Hz, Ph), 129.0 (d, J = 11.1 Hz, Ph), 102.2 (d, J = 8.3 Hz, py). $^{31}P\{^1H\}$ NMR (δ, acetone-d_6, −60 °C): 111.5 (d, $^2J_{PP}$ = 88.4 Hz), 97.8 (d, $^2J_{PP}$ = 88.4 Hz). IR (ATR, cm^{-1}): 2042 (ν_{CO}), 1940 (ν_{CO}), 1937 (ν_{CO}).

[Mo(PNP-*i*Pr)(CO)$_3$H]BF$_4$ (7b). This complex was prepared analogously to **7a** with **2b** (200 mg, 0.38 mmol) and HBF_4 (78 μL, 0.58 mmol) as starting materials. Yield: 200 mg (87%). Anal. Calcd for $C_{20}H_{34}BF_4MoN_3O_3P_2$: C, 39.43; H, 5.63; N, 6.90. Found: C, 39.53; H, 5.71; N, 6.99. ^1H NMR (δ, acetone-d_6, −60 °C): 8.86 (d, J = 41.2 Hz, 2H, N*H*), 8.00 (t, J = 8.2 Hz, 1H, py), 6.95 (d, J = 2.91 Hz, 1H, py), 6.92 (d, J = 2.91 Hz, 1H, py), 3.27 (m, 4H, $CH(CH_3)_2$), 1.83 (m, 24H, $CH(CH_3)_2$), −4.98 (dd, $^2J_{HP}$ = 36.7 Hz, $^2J_{HP}$ = 51.0 Hz, 1H, Mo*H*). $^{13}C\{^1H\}$ NMR (δ, CD_2Cl_2, 20 °C): 212.3 (t, J = 11.3 Hz, *C*O), 205.8 (t, J = 9.0 Hz, *C*O), 159.8 (d, J = 3.9 Hz, py), 159.7 (d, J = 3.9 Hz, py), 141.5 (s, py), 100.5 (d, J = 7.5 Hz, py), 31.5 (d, J = 29.5 Hz, $CH(CH_3)_2$), 17.8 (d, J = 2.3 Hz, $CH(CH_3)_2$). $^{31}P\{^1H\}$ NMR (δ, acetone-d_6, −60 °C): 142.3 (d, $^2J_{PP}$ = 90.4 Hz), 121.4 (d, $^2J_{PP}$ = 90.4 Hz). IR (ATR, cm^{-1}): 2035 (ν_{CO}), 1923 (ν_{CO}), 1920 (ν_{CO}).

[Mo(PNP-*t*Bu)(CO)$_3$H]BF$_4$ (7c). This complex was prepared analogously to **7a** with **2c** (240 mg, 0.42 mmol) and HBF_4 (85 μL, 0.62 mmol) as starting materials. Yield: 243 mg (87%). Anal. Calcd for $C_{24}H_{42}BF_4MoN_3O_3P_2$: C, 43.33; H, 6.36; N, 6.32. Found: C, 43.43; H, 6.42; N, 6.28. ^1H NMR (δ, acetone-d_6, −60 °C): 8.06 (bs, 2H, N*H*), 7.62 (t, J = 8.3 Hz, 1H, py), 6.62 (d, J = 7.9 Hz, 2H, py), 1.82 (d, J = 5.8 Hz, 18H, $C(CH_3)_3$), 1.80 (d, J = 6.5 Hz, 18H, $C(CH_3)_3$), −4.34 (dd, $^2J_{HP}$ = 20.7 Hz, $^2J_{HP}$ = 47.8 Hz, 1H, Mo*H*). $^{13}C\{^1H\}$ NMR (δ, acetone-d_6, 20 °C): 213.7 (t, J = 12.1 Hz, *C*O), 209.5 (t, J = 9.4 Hz, *C*O), 160 (d, J = 7.0 Hz, py), 141.8 (s, py), 137.9 (s, py), 101.5 (d, J = 6.5 Hz, py), 97.3 (s, py), 41.2 (d, J = 15.8 Hz, $C(CH_3)_3$), 24.8 (d, J = 7.1 Hz, $C(CH_3)_3$). $^{31}P\{^1H\}$ NMR (δ, acetone-d_6, −60 °C): 158.8 (d, $^2J_{PP}$ = 81.5 Hz), 142.8 (d, $^2J_{PP}$ = 81.5 Hz). IR (ATR, cm^{-1}): 2019 (ν_{CO}), 1937 (ν_{CO}), 1916 (ν_{CO}).

[Mo(PNP^{Me}-*i*Pr)(CO)$_3$H]BF$_4$ (7d). This complex was prepared analogously to **7a** with **2d** (67 mg, 0.11 mmol) and HBF_4 (23 μL, 0.17 mmol) as starting materials. Yield: 63 mg (90%). Anal. Calcd for $C_{22}H_{38}BF_4MoN_3O_3P_2$: C, 41.46; H, 6.01; N, 6.59. Found: C, 41.55; H, 6.12; N, 6.47. ^1H NMR (δ, acetone-d_6, −60 °C): 7.93 (t, J = 8.2 Hz, 1H, py), 6.65 (d, J = 8.2 Hz, 2H, py), 3.41 (s, 6H, $N(CH_3)$), 3.25 (m, 4H, $CH(CH_3)_2$), 1.24 (d, J = 7.00 Hz, 6H, $CH(CH_3)_2$), 1.22 (d, J = 7.80 Hz, 12H, $CH(CH_3)_2$), 1.16 (d, J = 7.00 Hz, 6H, $CH(CH_3)_2$), −5.49 (dd, $^2J_{HP}$ = 20.9 Hz, $^2J_{HP}$ = 49.3 Hz, 1H, Mo*H*). $^{13}C\{^1H\}$ NMR (δ, CD_2Cl_2, 20 °C): 210.8 (t, J = 10.8 Hz, *C*O), 205.4 (t, J = 9.5 Hz, *C*O), 161 (t, J = 5.2 Hz, py), 141.9 (s, py), 100.7 (s, py), 35.3 (s, NCH_3), 32.3 (d, J = 24.9 Hz, $CH(CH_3)_2$), 19.3 (d, J = 7.6 Hz, $CH(CH_3)_2$), 17.9 (s, $CH(CH_3)_2$). $^{31}P\{^1H\}$ NMR (δ, acetone-d_6, −60 °C): 166.1 (d, $^2J_{PP}$ = 85.4 Hz), 147.7 (d, $^2J_{PP}$ = 85.4 Hz). IR (ATR, cm^{-1}): 2028 (ν_{CO}), 1928 (ν_{CO}), 1910 (ν_{CO}).

[W(PNP-Ph)(CO)$_3$H]BF$_4$ (8a). This complex was prepared analogously to **7a** with **5a** (210 mg, 0.28 mmol) and HBF_4 (58 μL, 0.42 mmol) as starting materials. Yield: 186 mg (80%). Anal. Calcd for $C_{32}H_{26}BF_4N_3O_3P_2W$: C, 46.13; H, 3.15; N, 5.04. Found: C, 46.23; H,

dx.doi.org/10.1021/om400254k | *Organometallics* 2013, 32, 3042−3052

Table 2. Details for the Crystal Structure Determinations of Compounds 3a·CH_3OH, 4b, 2d, 5b·THF·$^1/_2C_6H_{14}$, 5c·THF, 7a, 7d·CH_2Cl_2, and 8a

	3a·CH_3OH	4b	2d	5b·THF·$^1/_2C_6H_{14}$
formula	$C_{33}H_{29}Br_2N_3O_4P_2W$	$C_{20}H_{33}Br_2MoN_3O_3P_2$	$C_{22}H_{37}MoN_3O_3P_2$	$C_{27}H_{48}N_3O_4P_2W$
fw	937.20	681.19	549.43	724.47
cryst size, mm	0.16 × 0.06 × 0.05	0.59 × 0.20 × 0.18	0.24 × 0.14 × 0.10	0.50 × 0.40 × 0.20
color, shape	orange prism	yellow plate	yellow prism	yellow plate
cryst syst	triclinic	monoclinic	orthorhombic	monoclinic
space group	$P\bar{1}$ (No. 2)	$C2/c$ (No. 15)	$Pnma$ (No. 62)	$P2_1/c$ (No. 14)
a, Å	10.1741(6)	29.6913(15)	18.6552(5)	10.1399(10)
b, Å	13.1580(7)	10.7919(5)	12.1772(3)	15.5053(18)
c, Å	14.1040(8)	16.7764(8)	10.9035(2)	20.036(2)
α, deg	99.456(3)	90	90	90
β, deg	95.412(3)	97.954(1)	90	94.485(5)
γ, deg	104.306(3)	90	90	90
V, Å^3	1786.63(17)	5323.9(4)	2476.93(10)	3140.5(6)
T, K	296(2)	173(2)	100(2)	100(2)
Z	2	8	4	4
ρ_{calcd}, g cm^{-3}	1.742	1.700	1.473	1.532
μ(Mo Kα), mm^{-1}	5.598	3.640	0.687	3.815
F(000)	908	2720	1144	1468
abs corr	multiscan, 0.77−0.56	multiscan, 0.50−0.32	multiscan, 0.93−0.83	multiscan, 0.75−0.46
θ range, deg	1.96−30.00	2.30−30.00	2.18−30.07	1.66−30.00
no. of rflns measd	46633	36362	20758	77629
R_{int}	0.060	0.022	0.033	0.042
no. of unique rflns	10399	7732	3770	9124
no. of rflns with $I > 2\sigma(I)$	7880	6562	3328	6686
no. of params/restraints	393/6	294/96	167/0	335/75
R1 ($I > 2\sigma(I)$)[a]	0.0385	0.0273	0.0217	0.0398
R1 (all data)	0.0625	0.0351	0.0276	0.0689
wR2 ($I > 2\sigma(I)$)	0.0822	0.0693	0.0507	0.0805
wR2 (all data)	0.0884	0.0734	0.0534	0.0907
min/max diff Fourier peaks, e Å^{-3}	−1.39/1.56	−1.01/0.97	−0.32/0.43	−1.80/1.85
	5c·THF	**7a**	**7d**·CH_2Cl_2	**8a**
formula	$C_{28}H_{49}N_3O_4P_2W$	$C_{32}H_{26}BF_4MoN_3O_3P_2$	$C_{23}H_{40}BCl_2F_4MoN_3O_3P_2$	$C_{32}H_{26}BF_4N_3O_3P_2W$
fw	737.48	745.25	722.17	833.16
cryst size, mm	0.30 × 0.17 × 0.15	0.42 × 0.35 × 0.28	0.32 × 0.30 × 0.14	0.24 × 0.08 × 0.06
color, shape	yellow block	yellow block	yellow plate	yellow column
cryst syst	monoclinic	orthorhombic	monoclinic	orthorhombic
space group	$P2_1/n$ (No. 14)	$Pbca$ (No. 61)	$P2_1/n$ (No. 14)	$Pbca$ (No. 61)
a, Å	8.9480(2)	17.4696(5)	8.4324(3)	17.5150(4)
b, Å	16.2069(4)	15.5290(4)	23.4895(7)	15.5022(3)
c, Å	21.6874(5)	23.3940(6)	16.2384(5)	23.3387(5)
α, deg	90	90	90	90
β, deg	95.539(1)	90	104.815(2)	90
γ, deg	90	90	90	90
V, Å^3	3130.41(13)	6346.5(3)	3109.46(17)	6336.9(2)
T, K	100(2)	100(2)	100(2)	100(2)
Z	4	8	4	8
ρ_{calcd}, g cm^{-3}	1.565	1.560	1.543	1.747
μ(Mo Kα), mm^{-1}	3.828	0.576	0.751	3.809
F(000)	1496	3008	1480	3264
abs corr	multiscan, 0.60−0.51	multiscan, 0.85−0.78	multiscan, 0.75−0.63	multiscan, 0.75−0.56
θ range, deg	1.89−30.00	1.96−30.00	2.17−30.00	1.96−30.00
no. of rflns measd	59364	147535	52608	103531
R_{int}	0.023	0.030	0.030	0.032
no. of unique rflns	9120	9239	9052	9225
no. of rflns with $I > 2\sigma(I)$	8540	8380	8280	8120
no. of params/restraints	355/0	440/0	366/0	440/0
R1 ($I > 2\sigma(I)$)[a]	0.0202	0.0252	0.0216	0.0200
R1 (all data)	0.0226	0.0302	0.0253	0.0260
wR2 ($I > 2\sigma(I)$)	0.0470	0.0595	0.0504	0.0385

dx.doi.org/10.1021/om400254k | *Organometallics* 2013, 32, 3042−3052

Table 2. continued

	5c·THF	7a	7d·CH_2Cl_2	8a
wR2 (all data)	0.0479	0.0636	0.0525	0.0406
min/max diff Fourier peaks, e Å^{-3}	−1.03/1.40	−0.71/0.50	−0.43/0.45	−0.87/0.74

[a] $R1 = \sum||F_o| - |F_c||/\sum|F_o|$; $wR2 = \{\sum[w(F_o^2 - F_c^2)^2]/\sum[w(F_o^2)^2]\}^{1/2}$.

3.12; N, 5.20. ^{1}H NMR (δ, acetone-d_6, −60 °C): 9.74 (bs, 2H, N*H*), 8.15 (s, 8H, Ph), 8.25 (t, J = 8.4 Hz, 1H, py), 8.15 (m, 8H, Ph), 7.94 (m, 12H, Ph), 7.04 (d, J = 8.0 Hz, 2H, py), −3.43 (dd, $^2J_{HP}$ = 22.4 Hz, $^2J_{HP}$ = 53.8 Hz 1H, W*H*). ^{13}C{^{1}H} NMR (δ, acetone-d_6, 20 °C): 205.9 (t, J = 9.7 Hz, CO), 196.6 (t, J = 8.7 Hz, CO), 159.5 (d, J = 5.9 Hz, py), 159.3 (d, J = 5.9 Hz, py), 142.1 (s, py), 132.0 (s, py), 130.9 (d, J = 13.0 Hz, Ph), 129.5 (d, J = 13.7 Hz, Ph), 129.1 (d, J = 12.1 Hz, Ph), 127.9 (d, J = 4.6 Hz, Ph), 102.0 (d, J = 9.4 Hz, py). ^{31}P{^{1}H} NMR (δ,acetone-d_6, −60 °C): 95.5 (d, $^2J_{PP}$ = 85.9 Hz), 84.8 (d, $^2J_{PP}$ = 85.9 Hz). IR (ATR, cm^{-1}): 2038 (ν_{CO}), 1963 (ν_{CO}), 1918 (ν_{CO}).

[W(PNP-*i*Pr)(CO)$_3$H]BF$_4$ (8b). This complex was prepared analogously to **8a** with **5b** (200 mg, 0.33 mmol) and HBF_4 (20 μL, 0.49 mmol) as starting materials. Yield: 207 mg (90%). Anal. Calcd for $C_{20}H_{34}BF_4N_3O_3P_2W$: C, 34.46; H, 4.92; N, 6.03. Found: C, 34.55; H, 5.02; N, 6.10. ^{1}H NMR (δ, CD_2Cl_2, 20 °C): 8.47 (bs, 2H, N*H*), 7.50 (t, J = 8.5 Hz, 1H, py), 6.67 (d, J = 7.7 Hz, 2H, py), 2.41 (m, 4H, C*H*(CH$_3$)$_2$), 1.30 (m, 28H, CH(C*H*$_3$)$_2$), −4.83 (dd, $^2J_{HP}$ = 23.3 Hz, $^2J_{HP}$ = 54.7 Hz, 1H, W*H*). ^{13}C{^{1}H} NMR (δ, CD_2Cl_2, 20 °C): 205.5 (t, J = 8.5 Hz, CO), 198.0 (t, J = 8.1 Hz, CO), 160.1 (d, J = 3.9 Hz, py), 141.6 (s, py), 100.4 (d, J = 6.4 Hz, py), 31.9 (d, J = 25.5 Hz, *C*H(CH$_3$)$_2$), 18.0 (d, J = 4.2 Hz, CH(*C*H$_3$)$_2$). ^{31}P{^{1}H} NMR (δ, CD_2Cl_2, 20 °C): 125.9 (d, $^2J_{PP}$ = 80.0 Hz), 108.6 (d, $^2J_{PP}$ = 80.0 Hz). IR (ATR, cm^{-1}): 2027 (ν_{CO}), 1910 (ν_{CO}), 1906 (ν_{CO}).

[W(PNP-*t*Bu)(CO)$_3$H]BF$_4$ (8c). This complex was prepared analogously to **8a** with **5c** (200 mg, 0.30 mmol) and HBF_4 (18 μL, 0.45 mmol) as starting materials. Yield: 207 mg (90%). Anal. Calcd for $C_{24}H_{42}BF_4N_3O_3P_2W$: C, 38.27; H, 5.62; N, 5.58. Found: C, 38.29; H, 5.52; N, 5.52. ^{1}H NMR (δ, acetone-d_6, 20 °C): 8.00 (bs, 2H, N*H*), 7.60 (t, J = 6.7 Hz, 1H, py), 6.75 (d, J = 8.3 Hz, 2H, py), 1.59 (s, 18H, C(C*H*$_3$)$_3$), 1.53 (s, 18H, C(C*H*$_3$)$_3$). −4.16 (dd, $^2J_{HP}$ = 37.8 Hz, $^2J_{HP}$ = 50.8 Hz, 1H, W*H*). ^{31}P{^{1}H} NMR (δ, CD_2Cl_2, 20 °C): 141.1 (d, $^2J_{PP}$ = 83.6 Hz), 126.8 (d, $^2J_{PP}$ = 83.6 Hz). IR (ATR, cm^{-1}): 2021 (ν_{CO}), 1934 (ν_{CO}), 1897 (ν_{CO}).

X-ray Structure Determination. Single crystals of the complexes **3a**, **4b**, **2d**, **5b**,**c**, **7a**,**d**, and **8a** suitable for X-ray diffraction were mainly obtained by the solvent/antisolvent liquid−liquid diffusion method at room temperature using CH_2Cl_2/diethyl ether (**4b**, **2d**, **7a**,**d**, **8a**) or THF/n-hexane (**5b**,**c**), while **3a** was crystallized from methanol at −20 °C. The crystals of **3a**, **5b**,**c**, and **7d** were solvates (**3a**·CH_3OH, **5b**·THF·$^1/_2$hexane, **5c**·THF, **7d**·CH_2Cl_2). X-ray diffraction data were collected at T = 100 K on a Bruker Kappa APEX-2 CCD area detector diffractometer using graphite-monochromated Mo Kα radiation (λ = 0.71073 Å) and φ- and ω-scan frames covering complete spheres of the reciprocal space with θ_{max} = 30°. Corrections for absorption and $\lambda/2$ effects were applied using the program SADABS.[29] After structure solution with the program SHELXS97 refinement on F^2 was carried out with the program SHELXL97.[30] Non-hydrogen atoms were refined anisotropically. Most hydrogen atoms were placed in calculated positions and thereafter treated as riding. Crystal data are reported in Table 2, and detailed structural data are given in CIF format in the Supporting Information. Variata are as follows. The solid-state structure of **3a** (**3a**·CH_3OH) contained methanol and eventually some water disordered in a large oval infinite channel along the *a* axis embodying also the free bromide anions. The contribution of this solvent to the structure factors was removed with the procedure SQUEEZE of the program PLATON.[31] This structure shows also a Br by CO and a complementary CO by Br substitution disorder (equatorial C32−O3 by Br1′ and axial Br1 by C32′ and O3′ in 86:14 proportion). The crystal structure of **5b** contains an ordered THF and a disordered *n*-hexane solvent molecule, the latter across a center of inversion; the solid is therefore **5b**·THF·$^1/_2C_6H_{14}$. The contribution of the *n*-hexane solvent molecule to the structure factors was removed with the procedure SQUEEZE of the program PLATON. **5b** has also an orientation-disordered isopropyl group. The hydride complexes **7a** and **8a** form an isostructural pair, [Mo/W(PNP-Ph)(CO)$_3$H]BF_4, space group *Pbca*, with very similar unit cell dimensions, bond lengths, and bond angles. Both structures show a disorder of the equatorial CO group (C32−O3) and the hydride H atom (H1), which appear in two approximately equivalent positions left and right of the plane bisecting the complexes perpendicular to the pyridine ring. Due to the very good quality of the diffraction data of both complexes and due to good separations of the respective atom positions, it was possible to refine the approximately half-occupied positions of the hydride H atoms without restraints. The left/right ratio of the population parameter of CO and H in the molybdenum complex **7a** is 0.540(3)/0.460(3) and in the tungsten complex **8a** is 0.586(4)/0.414(4) (for C32, O3, H1/C32′, O3′, H1′; cf. Figures 7 and 9, which depict only the dominant nonprimed part). In contrast, the analogous molybdenum hydrido carbonyl complex **7d**·CH_2Cl_2 was perfectly ordered and gave on refinement with high-quality diffraction data a hydride position in very good agreement with complexes **7a** and **8a**, fully supporting the split atom refinements of these two crystal structures.

Computational Details. All calculations were performed using the GAUSSIAN 09 software package[32] on the Phoenix Linux Cluster of the Vienna University of Technology and the B3LYP functional[33] without symmetry constraints. The optimized geometries were obtained with the Stuttgart/Dresden ECP (SDD) basis set[34] to describe the electrons of the tungsten and molybdenum atoms. For all other atoms a standard 6-31g** basis set was employed.[35] All geometries were optimized without symmetry constraints. Frequency calculations were performed to confirm the nature of the stationary points, yielding one imaginary frequency for the transition states and none for the minima. Each transition state was further confirmed by following its vibrational mode downhill on both sides and obtaining the minima presented on the energy profiles. All energies reported are Gibbs free energies and thus contain zero-point, thermal, and entropy effects at 298 K and 1 atm pressure. A natural population analysis (NPA)[36] and the resulting Wiberg indices[27] were used to study the electronic structure and bonding of the optimized species. The NPA analysis was performed with the NBO 5.0 program.[37]

■ ASSOCIATED CONTENT

Supporting Information

CIF files giving complete crystallographic data and technical details for complexes **3a**, **4b**, **2d**, **5b**,**c**, **7a**,**d**, and **8a**. This material is available free of charge via the Internet at http://pubs.acs.org.

■ AUTHOR INFORMATION

Corresponding Author

*E-mail for K.K.: kkirch@mail.tuwien.ac.at.

Notes

The authors declare no competing financial interest.

■ ACKNOWLEDGMENTS

Financial support by the Austrian Science Fund (FWF) (Project No. P24202-N17) and by Fundação para a Ciência e Tecnologia, FCT (PEst-OE/QUI/UI0100/2011), is gratefully acknowledged

REFERENCES

(1) Dahloff, W. V.; Nelson, S. M. *J. Chem. Soc. A* **1971**, 2184.

(2) (a) Vasapollo, G.; Giannoccaro, P.; Nobile, C. F.; Sacco, A. *Inorg. Chim. Acta* **1981**, *48*, 125. (b) Steffey, B. D.; Miedaner, A.; Maciejewski-Farmer, M. L.; Bernatis, P. R.; Herring, A. M.; Allured, V. S.; Carperos, V.; DuBois, D. L. *Organometallics* **1994**, *13*, 4844. (c) Hahn, C.; Sieler, J.; Taube, R. *Chem. Ber.* **1997**, *130*, 939. (d) Hahn, C.; Vitagliano, A.; Giordano, F.; Taube, R. *Organometallics* **1998**, *17*, 2060. (e) Hahn, C.; Spiegler, M.; Herdtweck, E.; Taube, R. *Eur. J. Inorg. Chem.* **1999**, 435.

(3) Jiang, Q.; Van Plew, D.; Murtuza, S.; Zhang, X. *Tetrahedron Lett.* **1996**, *37*, 797.

(4) (a) Andreocci, M. V.; Mattogno, G.; Zanoni, R.; Giannoccaro, P.; Vasapollo, G. *Inorg. Chim. Acta* **1982**, *63*, 225. (b) Sacco, A.; Vasapollo, G.; Nobile, C.; Piergiovanni, A.; Pellinghelli, M. A.; Lanfranchi, M. *J. Organomet. Chem.* **1988**, *356*, 397. (c) Abbenhuis, R. A. T. M.; del Rio, I.; Bergshoef, M. M.; Boersma, J.; Veldman, N.; Spek, A. L.; van Koten, G. *Inorg. Chem.* **1998**, *37*, 1749.

(5) (a) Rahmouni, N.; Osborn, J. A.; De Cian, A.; Fisher, J.; Ezzamarty, A. *Organometallics* **1998**, *17*, 2470. (b) Sablong, R.; Newton, C.; Dierkes, P.; Osborn, J. A. *Tetrahedron Lett.* **1996**, *37*, 4933. (c) Sablong, R.; Osborn, J. A. *Tetrahedron Lett.* **1996**, *37*, 4937. (d) Barloy, L.; Ku, S. Y.; Osborn, J. A.; De Cian, A.; Fischer, J. *Polyhedron* **1997**, *16*, 291.

(6) (a) Zhang, J.; Leitus, G.; Ben-David, Y.; Milstein, D. *J. Am. Chem. Soc.* **2005**, *127*, 10840. (b) Zhang, J.; Gandelman, M.; Shimon, L. J. W.; Rozenberg, H.; Milstein, D. *Organometallics* **2004**, *23*, 4026. (c) Hermann, D.; Gandelman, M.; Rozenberg, H.; Shimon, L. J. W.; Milstein, D. *Organometallics* **2002**, *21*, 812.

(7) Gibson, D. H.; Pariya, C.; Mashuta, M. S. *Organometallics* **2004**, *23*, 2510.

(8) Katayama, H.; Wada, C.; Taniguchi, K.; Ozawa, F. *Organometallics* **2002**, *21*, 3285.

(9) Jia, G.; Lee, H. M.; Williams, I. D.; Lau, C. P.; Chen, Y. *Organometallics* **1997**, *16*, 3941.

(10) Müller, G.; Klinga, M.; Leskelä, M.; Rieger, B. *Z. Anorg. Allg. Chem.* **2002**, *628*, 2839.

(11) Ansell, J.; Wills, M. *Chem. Soc. Rev.* **2002**, *31*, 259.

(12) (a) Schirmer, W.; Flörke, U.; Haupt, H.-J. *Z. Anorg. Allg. Chem.* **1987**, *545*, 83. (b) Schirmer, W.; Flörke, U.; Haupt, H.-J. *Z. Anorg. Allg. Chem.* **1989**, *574*, 239.

(13) Benito-Garagorri, D.; Becker, E.; Wiedermann, J.; Lackner, W.; Pollak, M.; Mereiter, K.; Kisala, J.; Kirchner, K. *Organometallics* **2006**, *25*, 1900.

(14) (a) Benito-Garagorri, D.; Puchberger, M.; Mereiter, K.; Kirchner, K. *Angew. Chem., Int. Ed.* **2008**, *47*, 9142; *Angew. Chem.* **2008**, *120*, 9282. (b) Benito-Garagorri, D.; Alves, L. G.; Puchberger, M.; Mereiter, K.; Veiros, L. F.; Calhorda, M. J.; Carvalho, M. D.; Ferreira, L. P.; Godinho, M.; Kirchner, K. *Organometallics* **2009**, *28*, 6902. (c) Benito-Garagorri, D.; Alves, L. G.; Veiros, L. F.; Standfest-Hauser, C. M.; Tanaka, S.; Mereiter, K.; Kirchner, K. *Organometallics* **2010**, *29*, 4923.

(15) (a) Alves, L. G.; Dazinger, G.; Veiros, L. F.; Kirchner, K. *Eur. J. Inorg. Chem.* **2010**, 3160. (b) Benito-Garagorri, D.; Wiedermann, J.; Pollak, M.; Mereiter, K.; Kirchner, K. *Organometallics* **2007**, *26*, 217.

(16) Benito-Garagorri, D.; Mereiter, K.; Kirchner, K. *Eur. J. Inorg. Chem.* **2006**, 4374.

(17) Lang, H.-F.; Fanwick, P. E.; Walton, R. A. *Inorg. Chim. Acta* **2002**, *392*, 1.

(18) (a) Kinoshita, E.; Arashiba, K.; Kuriyama, S.; Miyake, Y.; Shimazaki, R.; Nakanishi, H.; Nishibayashi, Y. *Organometallics* **2012**, *31*, 8437. (b) Arashiba, A.; Sasaki, K.; Kuriyama, S.; Miyake, Y.; Nakanishi, H.; Nishibayashi, Y. *Organometallics* **2012**, *31*, 2035. (c) Arashiba, K.; Miyake, Y.; Nishibayashi, Y. *Nat. Chemistry* **2011**, *3*, 120.

(19) Wingard, L. A.; White, P. S.; Templeton, J. L. *Dalton Trans.* **2012**, *41*, 11438.

(20) For examples of molybdenum and tungsten hydridocarbonyl complexes, see: (a) Burchell, R. P. L.; Sirsch, P.; Decken, A.; McGrady, G. S. *Dalton Trans.* **2009**, 5851. (b) Namorado, S.; Cui, J.; de Azevedo, C. G.; Lemos, M. A.; Duarte, M. T.; Ascenso, J. R.; Dias, A. R.; Martins, A. M. *Eur. J. Inorg. Chem.* **2007**, 1103. (c) Shafiq, F.; Szaldza, D. J.; Creutz, C.; Bullock, R. M. *Organometallics* **2000**, *19*, 824. (d) Calvo, M.; Gomez-Sal, P.; Manzanero, A.; Royo, P. *Polyhedron* **1998**, *17*, 1081. (e) Brammer, L.; Zhao, D.; Bullock, R. M.; McMullan, R. K. *Inorg. Chem.* **1993**, *32*, 4819. (f) Protasiewicz, J. D.; Theopold, K. H. *J. Am. Chem. Soc.* **1993**, *115*, 5559. (g) Caffyn, A. J. M.; Feng, S. G.; Dierdorf, A.; Gamble, A. S.; Eldredge, P. A.; Vossen, M. R.; White, P. S.; Templeton, J. L. *Organometallics* **1991**, *10*, 2842.

(21) (a) Cotton, A. F.; Falvello, L. R.; Meadows, J. H. *Inorg. Chem.* **1984**, *24*, 514. (b) Boyden, J. A.; Colton, R. *Aust. J. Chem.* **1968**, *21*, 2567.

(22) For pincers with non-meridional coordination geometries see: Adams, J. J.; Arulsamy, N.; Roddick, D. M. *Organometallics* **2011**, *30*, 697.

(23) Curtis, M. D.; Shiu, K.-B. *Inorg. Chem.* **1985**, *24*, 1213.

(24) Baker, P. K.; Al-Jahdali, M.; Meehan, M. M. *J. Organomet. Chem.* **2002**, *648*, 99. (b) Baker, P. K.; Drew, M. G. B.; Moore, D. S. *J. Organomet. Chem.* **2002**, *663*, 45.

(25) (a) Hoffmann, R.; Beier, B. F.; Muetterties, E. L.; Rossi, A. R. *Inorg. Chem.* **1977**, *16*, 511. (b) Thompson, H. B.; Bartell, L. S. *Inorg. Chem.* **1968**, *7*, 488.

(26) Parr, R. G.; Yang, W. In *Density Functional Theory of Atoms and Molecules*; Oxford University Press: New York, 1989.

(27) (a) Wiberg, K. B. *Tetrahedron* **1968**, *24*, 1083. (b) Wiberg indices are electronic parameters related to the electron density between atoms. They can be obtained from a natural population analysis and provide an indication of the bond strength.

(28) Perrin, D. D.; Armarego, W. L. F. *Purification of Laboratory Chemicals*, 3rd ed.; Pergamon: New York, 1988.

(29) Bruker programs: *APEX2, version 2009.9-0*; *SAINT, version 7.68 A*; *SADABS, version 2008/1*; *SHELXTL, version 2008/4*, Bruker AXS Inc., Madison, WI, 2009.

(30) Sheldrick, G. M. *Acta Crystallogr.* **2008**, *A64*, 112−122.

(31) Spek, A. L. *J. Appl. Crystallogr.* **2003**, *36*, 7−13.

(32) Frisch, M. J. et al.. *Gaussian 09, Revision A.02*; Gaussian, Inc., Wallingford, CT, 2009.

(33) (a) Becke, A. D. *J. Chem. Phys.* **1993**, *98*, 5648. (b) Miehlich, B.; Savin, A.; Stoll, H.; Preuss, H. *Chem. Phys. Lett.* **1989**, *157*, 200. (c) Lee, C.; Yang, W.; Parr, G. *Phys. Rev. B* **1988**, *37*, 785.

(34) (a) Haeusermann, U.; Dolg, M.; Stoll, H.; Preuss, H. *Mol. Phys.* **1993**, *78*, 1211. (b) Kuechle, W.; Dolg, M.; Stoll, H.; Preuss, H. *J. Chem. Phys.* **1994**, *100*, 7535. (c) Leininger, T.; Nicklass, A.; Stoll, H.; Dolg, M.; Schwerdtfeger, P. *J. Chem. Phys.* **1996**, *105*, 1052.

(35) (a) McLean, A. D.; Chandler, G. S. *J. Chem. Phys.* **1980**, *72*, 5639. (b) Krishnan, R.; Binkley, J. S.; Seeger, R.; Pople, J. A. *J. Chem. Phys.* **1980**, *72*, 650. (c) Wachters, A. J. H. *Chem. Phys.* **1970**, *52*, 1033. (d) Hay, P. J. *J. Chem. Phys.* **1977**, *66*, 4377. (e) Raghavachari, K.; Trucks, G. W. *J. Chem. Phys.* **1989**, *91*, 1062. (f) Binning, R. C., Jr.; Curtiss, L. A. *J. Comput. Chem.* **1990**, *11*, 1206. (g) McGrath, M. P.; Radom, L. *J. Chem. Phys.* **1991**, *94*, 511.

(36) (a) Carpenter, J. E.; Weinhold, F. *J. Mol. Struct. (THEOCHEM)* **1988**, *169*, 41. (b) Carpenter, J. E. Ph.D. Thesis, University of Wisconsin, Madison, WI, 1987. (c) Foster, J. P.; Weinhold, F. *J. Am. Chem. Soc.* **1980**, *102*, 7211. (d) Reed, A. E.; Weinhold, F. *J. Chem. Phys.* **1983**, *78*, 4066. (e) Reed, A. E.; Weinhold, F. *J. Chem. Phys.* **1985**, *83*, 1736. (f) Reed, A. E.; Weinstock, R. B.; Weinhold, F. *J. Chem. Phys.* **1985**, *83*, 735. (g) Reed, A. E.; Curtiss, L. A.; Weinhold, F. *Chem. Rev.* **1988**, *88*, 899−926. (h) Weinhold, F.; Carpenter, J. E. *The Structure of Small Molecules and Ions*; Plenum: New York, 1988; p 227.

(37) Glendening, E. D.; Badenhoop, J. K.; Reed, A. E.; Carpenter, J. E.; Bohmann, J. A.; Morales, C. M.; Weinhold, F. *NBO 5.0*; Theoretical Chemistry Institute, University of Wisconsin, Madison, WI, 2001.